



Origin and physicochemical behaviour of atmospheric PM . in cities located in the area of the Nord-Pas-de-Calais region, France

Adib Kfoury

► To cite this version:

Adib Kfoury. Origin and physicochemical behaviour of atmospheric PM . in cities located in the area of the Nord-Pas-de-Calais region, France. Other. Université du Littoral Côte d'Opale, 2013. English. NNT : 2013DUNK0403 . tel-01804650

HAL Id: tel-01804650

<https://theses.hal.science/tel-01804650>

Submitted on 1 Jun 2018

HAL is a multi-disciplinary open access archive for the deposit and dissemination of scientific research documents, whether they are published or not. The documents may come from teaching and research institutions in France or abroad, or from public or private research centers.

L'archive ouverte pluridisciplinaire **HAL**, est destinée au dépôt et à la diffusion de documents scientifiques de niveau recherche, publiés ou non, émanant des établissements d'enseignement et de recherche français ou étrangers, des laboratoires publics ou privés.

THÈSE

présentée à

L'UNIVERSITÉ DU LITTORAL CÔTE D'OPALE

en vue de l'obtention du titre de

DOCTEUR DE L'UNIVERSITÉDiscipline : **CHIMIE**

par

Adib KFOURY**« Origine et physicochimie des particules atmosphériques PM_{2.5} dans des villes du littoral de la région Nord-Pas-de-Calais »****« Origin and physicochemical behaviour of atmospheric PM_{2.5} in cities located in the littoral area of the Nord-Pas-de-Calais region, France »****Soutenue le 30 Mai 2013 devant la Commission d'Examen***Membres du Jury :***P. SHIRALI****Président du Jury****N. SALIBA****Rapporteur****I. FERNÁNDEZ-OLMO****Rapporteur****O. FAVEZ****Examineur****G. DELMAIRE****Examineur****F. LEDOUX****Encadrant de Thèse****D. COURCOT****Directeur de Thèse**

Acknowledgments

I would like to address my gratitude to Pr. Dominique COURCOT and Dr. Frédéric LEDOUX. Thanks to both of you I was able to accomplish this work in the best possible conditions.

Pr. COURCOT you were an excellent director during this project, starting with your scientific critique all the way to the human character that you showed towards me during this thesis. I will not forget how much you stood beside me, simplifying the difficulties that we encountered along the way, and helping me to overcome them.

Dr. LEDOUX you were also present all the time helping me in the job at hand, which I find to be extremely important and rare for an assistant director. I wasn't expecting to find you available like that whenever I needed you, and I cannot thank you enough for it.

I would like to thank Pr. Pirouz SHIRALI, the director of our laboratory and president of my PhD thesis jury: you have set an example on how to be modest and give attention to all the research body that you direct. I thank you for your kindness and the will to give endlessly especially when it concerns your students.

This PhD has been financed by the Syndicat Mixte de la Côte d'Opale (SMCO) to which I present my deepest gratitude. I address many thanks to the members of the jury: Pr. Najat SALIBA, Pr. Ignacio FERNÁNDEZ OLMO, Dr. Olivier FAVEZ and Dr. Gilles DELMAIRE, especially those who traveled from their home countries to France.

In addition, the success of this work was also related to the teams implicated in every aspect of it. I will start with the Centre Commun des Mesures – Dunkerque, in which I analyzed my collected samples. Within this team, I would like to thank Habiba NOUALI, Dr. Fabrice CASIER, Dorothee DEWAELE, who allowed me to use their materials and stood beside me until I finished all my analysis during the master and the PhD projects.

In the same time, I would like to express my gratitude to Dr. Francine CASIER, Dr. Saâd BOUHSINA and Amaury KASPROWIAK who helped me in the samples analysis.

I am also grateful for the creators and users of the WNMf modeling algorithm in both the “Laboratoire d'Informatique, Signal et Image de la Côte d'Opale - LISIC” and “Unité de Chimie Environnementale et Interactions sur le Vivant - UCEIV”: Dr. Gilles ROUSSEL, Dr. Gilles DELMAIRE and Dr. Dany HLEIS: without your previous work on the WNMf, the final section of this PhD project could not be accomplished successfully.

I also would like to thank Atmo-NPdC who allowed us to use their monitoring station locale in Saint-Omer.

My arrival to France was made possible through a convention between the University of Balamand and the Université du Littoral Côte d'Opale. Within this context, I would like to thank Pr. Antoine ABOUKAIS and Pr. Edmond ABI-AAD from the ULCO. I am proud to call you friends before colleagues.

I specifically want to thank Pr. ABOUKAIS: you represent an exceptional and successful Lebanese personality, as well as the father figure for the students working in the laboratory. I also accept with great honors all the advices you gave to me during my research project, and I will never forget that you welcomed me in your own house the first day I arrived to France.

From UoB, I would like to thank all the teachers implicated in the environmental sciences master program. During my master studies in the university, I encountered many extraordinary people who helped me all the way to my graduation with an excellence award, and I thank them all.

I specifically thank Dean ATTIEH: your warm welcome goes back all the way to the beginning in 2007. I am so proud of calling you a teacher and a dear friend. I also bow in front of your friendly character that you manage to conserve while passing from Chairmen to Dean of the Faculty of Sciences.

Dr. NADER: I cannot describe how much you have impacted my life scientifically and personally. I would like to thank you for allowing me to handle huge responsibilities, and for showing me how to be a leader. You will always be my mentor in several ways and I am honored to be counted as your student.

I address an additional gratitude to Dr. El MASRI: you have showed me the way to properly communicate scientific knowledge with the non-scientific community. I can say, without any doubts, that you have one of the best communication skills that I have ever seen. In many ways, I still owe you a lot for what you have taught me.

Finally, I would like to thank my laboratory colleagues that helped me in their own way to cope with the pressure resulting from excessive work. I will not cite any names to prevent omitting anyone...

I owe all my achievements to my family who stood closely beside me all the time. I cite my mother Antoinette, sisters (Ghada and Samar) and fiancée (Jennifer).

I dedicate the last words of appreciation to my father's soul: *thanks to you I managed to succeed this much in my life, a success that will never be complete because I cannot enjoy it with you anymore.*

I express my sincere gratitude to all the persons who I forgot to mention.

GENERAL CONTENTS

I. GENERAL INTRODUCTION	3
II. CHAPTER I - Literature and background studies	
II.1. Introduction	12
II.2. Atmospheric Particulate Matter – Aerosol	12
II.3. Emissions flux of PM in the Atmosphere	19
II.4. Review on international and national air quality standards	31
II.5. Background on fine PM studies	35
II.6. The situation in the Nord-Pas-de-Calais (NPdC) region	46
II.7. Hypothesis and objectives	53
II.8. Works cited	55
III. CHAPTER II - Materials and methods used for sampling and analysis	
II.1. Introduction	65
II.2. Sampling sites	65
II.3. Materials used for sampling	69
II.4. Analysis of inorganic components and total carbon	74
II.5. Sampling protocol validation	81
II.6. Works cited	86
IV. CHAPTER III – Concentrations trends and statistical analysis of Major Elements (ME), Soluble Ions (SI), and Total Carbon (TC)	
III.1. Introduction	92
III.2. Meteorology in the “Littoral Côte d’Opale” coastline	92
III.3. Meteorology encountered during the sampling campaigns	94
III.4. Average concentrations and contributions to PM _{2.5}	106
III.5. Average concentrations comparison at a European scale	112
III.6. Chronological evolution of ME, SI and TC	121
III.7. Analysis of above limit peaks of PM _{2.5}	134
III.8. Concentration’s evolution by wind sector	153
III.9. Discussion of the results	162
III.10. Conclusion	167
III.11. Works Cited	169

V. CHAPTER IV - Concentrations trends, statistical analysis and source identification of Trace Elements (TE)	
IV.1. Introduction	175
IV.2. Elemental average concentrations and contributions	175
IV.3. Average TE concentrations comparison on the European scale	180
IV.4. Industrial Impact analysis	186
IV.5. Crustal Enrichment Factor analysis	188
IV.6. Global TE correlations study	191
IV.7. Concentration's evolution by wind sector	196
IV.8. Conclusion	215
IV.9. Works Cited	216
VI. CHAPTER V - Identification of sources profiles and contributions using WNMF receptor modeling	
V.1. Introduction	223
V.2. Early development and use of receptor modeling	224
V.3. Comparison between receptor models	225
V.4. Matrix factorization methods	227
V.5. Application of weighted NMF for source apportionment	230
V.6. Weighted NMF operating conditions	236
V.7. Verification of calculations' reliability	238
V.8. NMF calculated sources' profiles (matrix F)	245
V.9. Sources' contributions (matrix G)	250
V.10. Conclusion	267
V.11. Works Cited	269
VII. GENERAL CONCLUSION	271
VIII. APPENDICES	276

General Introduction

Atmospheric pollution is considered to have one of the most dangerous impacts on human health, especially in large cities. In addition to gaseous compounds (volatile organic compounds, sulfur dioxide, nitrogen oxides and ozone), suspended particles constitute the most important atmospheric pollutants. This particulate matter, consistently present in the atmosphere, can originate from natural sources (marine aerosols, soil erosion, volcanic eruptions, biogenic particles...etc.) as well as from anthropogenic ones (road traffic, industrial emissions...etc.) which are very significant in heavily populated regions.

Atmospheric suspended particles are suspected to have an impact on human health on one hand and to influence the chemistry of the troposphere on the other. The human health risks can be explained by the fact that the micrometer diameter of the particles, and sub-micrometer in a lot of cases, cause irritations of the respiratory tract and organs after deep penetration through inhalation. In addition, if the considered aerosol contains toxic components (transition metals, metalloids, and polycyclic aromatic hydrocarbons), other dangerous consequences will emerge in case these toxic species interact with respiratory organs tissues.

Globally, the air quality was enhanced during the past decades in most industrialized countries. The European directive 1999/30/CE of April 22nd 1999 defines the annual average limit values for PM₁₀ in ambient air, which has been 40 µg/m³ since January 1st 2005.

However, this directive indicated that all European states should take measures in order to identify the principal sources of particles in the regions that exhibit above limit values, as well as to take sufficient measures to decrease the particle diffusion in an attempt to secure a cleaner ambient air, thus limiting health problems. Despite these efforts, many European Union states like Italy, Austria, Greece, Spain, Belgium, France...etc, have exhibited episodes of above limit concentrations of atmospheric particles since a couple of years ago.

The Nord-Pas-de-Calais region is included in the French zones exhibiting high PM₁₀ levels frequently registered by official air quality monitoring stations of the “Réseau agréé de Surveillance de Qualité de l’Air”, in particular during the winter season and the beginning of spring, which is also reproduced in other French regions as well (Ile de France, Rhône Alpes). For these reasons, at the beginning of 2011, the European Committee launched a litigation procedure against France for the disrespect of the legislation. On the national level, there is an urgent need to understand the reasons behind these high particulate levels as well as the need

to gather as much scientific data as possible in order to provide answers needed on the national and European level.

In parallel, the legislation on PM_{2.5} limit values issued under directive 2008/50/EC have evolved since 2010, and is defined to an annual limit value of 25 µg/m³ starting the 1st of January 2015. In addition, we can also remind that a long term quality objective equals to 10 µg/m³ (annual average) is defined for a sufficient human health and environmental protection all together.

Nowadays, few studies have been conducted on the exposure levels to fine particles in cities of the Nord-Pas-de-Calais region. Other than the concentration measurements realized by official monitoring networks, there are no additional knowledge on the chemical composition of PM_{2.5} in the region, despite the fact that the exposition to road transport, domestic activities and/or industrial activities emissions is between the highest.

Within the scope of this thesis, we propose the study of the chemical composition and origin of PM_{2.5} in moderately sized cities, located near the littoral facade of the Nord-Pas-de-Calais region (Dunkerque, Boulogne-sur-Mer and Saint-Omer). In fact, few studies have been conducted in the urban-industrial zone of Dunkerque, and no study has revealed the chemical composition of PM_{2.5} in other cities like Boulogne-sur-Mer (coastal city) and Saint-Omer (inland: 40 km distance from the coastline).

The main objectives of this work aims at:

- i. Acquiring a better knowledge on the chemical composition of PM_{2.5} (ionic species, metallic major and trace elements, and total carbon).
- ii. Identifying the different sources of PM_{2.5} emission.
- iii. Conducting a geographical and chronological record of the composition of particles, and compare the exposure level from one site to the other.
- iv. Evaluating the contributions of natural and anthropogenic sources separately to the PM_{2.5} concentration.

Therefore, this thesis report is divided into five chapters.

The first chapter presents the generalities on atmospheric particles. It particularly aims at exposing different aerosols sources and their physicochemical characteristics. The chapter also focuses on the emissions of particles into the atmosphere on a global, European and French scale, while highlighting the small size fractions of these particles. In addition, a review on the international and French atmospheric particles limit values is realized, followed

by the analysis of the evolution of this science with emphasis on the chemical composition and anthropogenic sources of particles including the most important industrial emissions composition which can be found in the literature. Afterwards, a section on air quality in the Nord-Pas-de-Calais region and the exposition of the main objectives of this study will conclude this chapter.

The second chapter describes in details the methodology that is used in order to achieve the objectives mentioned at the end of the first chapter. It begins with a detailed description of the sampling sites, which includes the geographical locations as well as the most important nearby influences including natural and anthropogenic sources of emissions. Furthermore, the equipments used in this study are also detailed in this chapter. It encloses the sampling materials (filters and samplers) in addition to the analytical techniques used to determine the chemical species concentrations in the atmosphere. These techniques are ICP-MS, ICP-AES and CHNS-O micro analyzer for an important list of elements and total carbon analysis, and ion chromatography for water soluble ions quantification. Finally, the chapter ends with a meticulous description of the customized sampling protocol used for the collect of the particles.

The third chapter begins with a description on the recorded meteorology during the sampling campaigns, including temperatures, wind activities and precipitations. This step is followed by the first presentation of the chemical analysis results. This latter is depicted in a first step in a comparison of average concentrations of major elements, ions and total carbon. These average concentrations are compared between the sampling sites as well as to other studies in Europe. In addition, the chronological evolution of the different chemical species was conducted, and included the same groups mentioned earlier. Another important section of this chapter follows and revolves around the identification and detailed analysis of above limit values episodes of $PM_{2.5}$. However, the chapter content at this stage includes an emphasis on the evolution of each major chemical species by wind sector in a concentration rose analysis section, which allowed the analysis of the concentration variation by wind sector and concluded the chapter.

Following the third chapter, a deeper investigation on the trace elements chemical trends constitutes the subject of chapter four. In this latter, the trace metals concentrations are analyzed in the form of averages and compared between the sites for each campaign, but also to other average concentrations found in European studies. However, in order to understand the impact of anthropogenic sources, an industrial impact and crustal enrichment factor

analysis followed the comparison section. To this section is added another type of analysis that includes a correlation study between some elements, which points at some possible anthropogenic sources of emissions. The correlation analysis is followed by a study of concentrations evolution by wind sector, which included two important subsections. The first is a concentration rose analysis by campaign, which showed the principal sectors under which we observed high concentrations. However, the second part included another correlation study, using some selected samples that are under a specific anthropogenic influence. At the end of this last section, elemental ratios are proposed to trace the influence of some industrial PM_{2.5} sources.

Finally, the collected information on the chemical composition of the PM_{2.5} samples are modeled using a non-negative matrix factorization based method detailed in the fifth chapter. A description of the modeling techniques begins the chapter, which is then followed by a comparison between the modeling methods in order to attest our final choice. The latter relied on a weighted non-negative matrix factorization (NMF) method developed with the collaboration of the “Laboratoire d’Informatique, Signal et Image de la Côte d’Opale” (LISIC). The developed NMF is fed by the chemical data provided by the chemical analysis in order to uncover the main emission profiles and their respective contributions in each collected sample. The chapter contains details about the operating conditions of NMF modeling used in this study as well as a detailed verification of the output reliability. Afterwards, the calculated profiles and contributions are discussed extensively to uncover many sources of particles emission in each site, as well as long distance influences between some of the sampling sites.

CHAPTER I:

Literature and background studies

TABLE OF CONTENTS

I.1. Introduction.....	12
I.2. Atmospheric Particulate Matter - Aerosol	12
I.2.1. Size classification of PM.....	13
I.2.2. Origins of PM.....	15
I.2.2.1. Naturally Emitted Aerosols	16
I.2.2.1.1. Mineral dust	16
I.2.2.1.2. Sea salts.....	16
I.2.2.1.3. Volcanic ash.....	16
I.2.2.1.4. Biogenic aerosols	16
I.2.2.2. Anthropogenic Aerosols	17
I.2.2.2.1. Secondary anthropogenic aerosol	17
I.2.2.2.2. Carbonaceous particles	17
I.2.2.2.3. Biomass burning	17
I.2.2.2.4. Secondary Inorganic Aerosols (SIA)	18
I.3. Emissions flux of PM in the atmosphere	19
I.3.1. Global situation	19
I.3.2. European anthropogenic emissions	20
I.3.2.1. TSP, PM ₁₀ , and PM _{2.5} emissions.....	20
I.3.2.2. Metals emissions	21
I.3.2.3. Anthropogenic emissions by sector	22
I.3.2.3.1. TSP emissions by sector	22
I.3.2.3.2. PM ₁₀ emissions by sector	23
I.3.2.3.3. PM _{2.5} emissions by sector	24
I.3.2.3.4. Anthropogenic emissions for “non-road transport” and “agriculture” sectors.....	25
I.3.3. French anthropogenic emissions	26
I.3.3.1. TSP, PM ₁₀ , and PM _{2.5} emissions.....	26
I.3.3.2. Metals emissions	27
I.3.3.3. Anthropogenic emissions by sector	28
I.3.3.3.1. TSP emissions by sector	28
I.3.3.3.2. PM ₁₀ emissions by sector	29
I.3.3.3.3. PM _{2.5} emissions by sector	30
I.4. Review on international and national air quality standards	31
I.4.1. PM ₁₀ limit values.....	31
I.4.2. PM _{2.5} limit values	32
I.4.3. Metals guideline values	33
I.5. Background on fine PM studies.....	35
I.5.1. Early studies	35
I.5.2. Chemical composition and sources of fine PM.....	36
I.5.2.1. Sources of metals.....	36
I.5.2.1.1. Crustal.....	37
I.5.2.1.2. Traffic exhaust emissions.....	37
I.5.2.1.3. Traffic non-exhaust emissions	37
I.5.2.1.4. Oil-fuel combustion	38
I.5.2.1.5. Coal combustion	38
I.5.2.1.6. Long range transport (LRT).....	39
I.5.2.1.7. Biomass combustion	39
I.5.2.1.8. Industry	39
I.5.2.1.8.i. Steel works	39
I.5.2.1.8.ii. Petro-chemistry.....	40
I.5.2.1.8.iii. Metallurgy and Pigment industry	40
I.5.2.1.8.iv. Cement industry.....	40
I.5.2.1.8.v. Glassmaking industry.....	41
I.5.2.1.9. Ships, ship yards, and harbor	41
I.5.2.2. Sources and contribution of ions in PM _{2.5}	41

I.5.2.2.1.	Sea spray	41
I.5.2.2.2.	Traffic related ions	42
I.5.2.2.3.	Secondary inorganic aerosols	42
I.5.2.3.	Sources of carbon	43
I.5.3.	Health effects of fine PM inhalation	44
I.6.	The situation in the Nord-Pas de Calais (NPdC) region	46
I.6.1.	Emissions of PM in NPdC	47
I.6.2.	Air quality in the NPdC region	49
I.6.2.1.	PM level.....	49
I.6.2.2.	PM daily limit exceedance	50
I.6.2.3.	Physicochemical characteristics of PM and its origins.....	51
I.7.	Hypothesis and objectives	53
I.8.	Works Cited.....	55

LIST OF FIGURES

Figure 1: Schematic representation of aerosols size distribution in relation with formation mechanisms (Whitby & Cantrell, 1976).....	15
Figure 2: Flow chart of possible formation reactions of different nitrates and sulfates chemical species; taken from (Arruti, et al., 2011) who reproduced it from (Matsumoto & Tanaka, 1996), (Alastuey, et al., 2004), (Pakkanen, 1996), and (Hewitt & Jackson, 2005) which represent (a), (b), (c), and (d) respectively.	18
Figure 3: Anthropogenic emissions trends of TSP, PM ₁₀ , and PM _{2.5} in Europe from 1990 to 2010 in Kt (EEA(a), 2012).....	20
Figure 4: Anthropogenic emissions trends of Cu, Pb and Zn in Europe between 1990 and 2010 in Kt (EEA(a), 2012).....	21
Figure 5: Anthropogenic emissions trends of As, Cd, Cr, Se, and Ni in Europe between 1990 and 2010 in Kt (EEA(a), 2012).....	22
Figure 6: Emissions trends of TSP by sector in Europe between 1990 and 2010 in Kt (EEA(a), 2012)	23
Figure 7: Emissions trends of TSP emitted from “waste” and “solvent and product use” sectors in Europe between 1990 and 2010 in tonnes (EEA(a), 2012).....	23
Figure 8: Emissions trends for PM ₁₀ by sector in Europe between 1990 and 2010 in Kt (EEA(a), 2012).....	24
Figure 9: Emissions trends of PM ₁₀ emitted from “waste” and “solvent and product use” sectors in Europe between 1990 and 2010 in tonnes (EEA(a), 2012).....	24
Figure 10: Emissions trends for PM _{2.5} by sector in Europe between 1990 and 2010 in Kt (EEA(a), 2012)	25
Figure 11: Emissions trends of PM _{2.5} emitted from “waste” and “solvent and product use” sectors in Europe between 1990 and 2010 in tonnes (EEA(a), 2012).....	25
Figure 12: Emissions trends emitted from the “non-road transport” sector in Europe between 1990 and 2010 in tonnes (EEA(a), 2012).....	26
Figure 13: Emissions trends emitted from the “agriculture” sector in Europe between 1990 and 2010 in tonnes (EEA(a), 2012).....	26
Figure 14: Anthropogenic emissions trends of TSP, PM ₁₀ , and PM _{2.5} in France from 1990 to 2010 in Kt (EEA(a), 2012).....	27
Figure 15: Anthropogenic emissions of Cu and Zn in France between 1990 and 2010 in Kt (EEA(a), 2012)	27
Figure 16: Anthropogenic emissions of As, Cd, and Pb in France between 1990 and 2010 in Kt (EEA(a), 2012)	28
Figure 17: Anthropogenic emissions of Cr, Se, and Ni in France between 1990 and 2010 in Kt (EEA(a), 2012)	28
Figure 18: Emissions trends for TSP emitted from: road transport, commercial/institutional and household, industrial processes, and agriculture sectors; in France between 1990 and 2010 in tonnes (EEA(a), 2012).....	29
Figure 19: Emissions trends for TSP emitted from: energy production and distribution, energy use in industry, non-road transportation, solvent and product use, and waste sectors; in France between 1990 and 2010 in tonnes (EEA(a), 2012).....	29
Figure 20: Emissions trends for PM ₁₀ emitted from: energy production and distribution, commercial-institutional and households, road transportation, industrial processes, and agriculture sectors; in France between 1990 and 2010 in tonnes (EEA(a), 2012)	30
Figure 21: Emissions trends for PM ₁₀ emitted from: energy use in industry, non-road transportation, solvent and product use, and waste sectors; in France between 1990 and 2010 in tonnes (EEA(a), 2012).....	30
Figure 22: Emissions trends for PM _{2.5} emitted from: energy production and distribution, commercial-institutional and households, road transportation, and industrial processes sectors; in France between 1990 and 2010 in tonnes (EEA(a), 2012).....	31
Figure 23: Emissions trends for PM _{2.5} emitted from: energy use in industry, non-road transportation, solvent and product use, agriculture, and waste sectors; in France between 1990 and 2010 in tonnes (EEA(a), 2012).	31
Figure 24: Summary of the major adverse health effects of PM inhalation on the human body (Aphekom, 2011)	46
Figure 25: Map of France (upper right corner) and the “Nord Pas de Calais” region; reproduced from (CarteFrance, 2012) and (Dalet, 2012)	47
Figure 26: Declared industrial PM emissions trend from 2004 till 2010 in the NPdC region (DREAL, 2011)....	48
Figure 27: Some of the industrial dust emissions in the NPdC department; SRD = Société de Raffinerie de Dunkerque, Al Dk = Rio Tinto Dunkerque, EDF = Electricité De France (Bouchain), Cargill SAS (Haubourdin), E.ON – Central (Hornaing), Arc International (Arques); source (DREAL, 2011)	49
Figure 28: Annual mean concentration of PM ₁₀ in Dunkerque, Boulogne-sur-Mer, Saint-Omer, Bethune, Lille, and in µg/m ³ ; source (Ministère de l’Écologie, 2012).....	50
Figure 29: Map of the regions (in red) representing more than 35 days of PM ₁₀ daily limit (50 µg/m ³) exceedance between 2007 and 2009 in France (Source: LCSQA)	50

LIST OF TABLES

Table 1: Particles flux estimation in the atmosphere (Delmas, et al., 2007)	19
Table 2: Guideline values for metals in the Atmosphere	34

I.1.Introduction

In this chapter, we will restate the terminology used in the science of atmospheric particles, starting by the basic definitions of particulate matter (PM). The origins, physical and chemical characteristics, and the evolution of PM in the atmosphere will be discussed as well, with emphasis on the fine particle fraction under study (diameter < 2.5 μm). In addition, European and French emissions of PM, the latest standards for particulate matter (PM) pollution released by the European Parliament as well as those recommended by the World Health Organization (WHO) and the United States Environmental Protection Agency (USEPA) will be reviewed. On the other hand, emphasis will be laid upon the chemical composition of PM and the link between this latter and the sources of emissions that was found in some of the oldest scientific publications that we were able to acquire until the latest in 2012. The importance of tracking PM sources, origins and chemical composition resides within the health effects of PM inhalation, especially on the respiratory tract and organs; therefore, this subject will be included in this section as well. Finally, the situation in the region of the study will be investigated.

I.2.Atmospheric Particulate Matter - Aerosol

By definition, an aerosol is a general term that technically refers to a suspension of fine solid particles or liquid droplets in a gas. This term refers to atmospheric particles and their gaseous environment. It is commonly used by researchers who work in the fields of atmospheric dynamics and climate. However, researchers who study atmospheric pollution levels and their respective health impacts use the term “particulates” instead. This explains the fact that the air associated to the particles when talking about aerosols is nothing but a transport vector of these particles in the air and into the respiratory tract (Villenave, et al., 2012).

These particles can be directly emitted into the atmosphere by natural and anthropogenic sources, and are called “primary aerosols”. On the other hand, some particles can be generated by gas-to-particle conversion processes, thus they are called “secondary aerosols”. More definitions will come along as we move into subdivisions that can be related to the size and to the chemical composition of atmospheric PM.

I.2.1. Size classification of PM

The interest in PM is majorly related to its effect on the respiratory tract and organs, and therefore is linked to the penetration capacity when inhaling. Consequently, smaller particle diameter means deeper penetration. The importance of PM size doesn't stop at health effects only, but it also stretches to environmental pollution, effects on climate and visibility. Therefore, studying the characteristics of the different size fractions of PM comes in first, in order to understand the sources of emissions and level of impacts.

Before boarding the subject of size distribution, we should specify that the diameter of the particles discussed herein will be the “equivalent aerodynamic diameter” (D_{ae}) instead of Stokes or volume equivalent diameters. The reason behind this differentiation is the facts that we consider that atmospheric particles do not necessarily have well-defined spherical, cubic, elliptical, or other shapes. Therefore we define the diameter of an atmospheric particle (regardless of its shape) in the atmosphere as equal to the diameter of a spherical one that has the same terminal velocity considering a density of 1 g/cm^3 , and hence is called “equivalent aerodynamic diameter”. For example, an atmospheric particle with $D_{ae} = 2.5 \text{ }\mu\text{m}$ is defined as a particle that have the same terminal velocity of a spherical shaped particle (density = 1 g/cm^3) with a $2.5 \text{ }\mu\text{m}$ diameter. Generally, the size of atmospheric PM is strongly related to their generation mode and atmospheric conditions. For that reason, the D_{ae} value range can stretch from a few angstroms (\AA) up to a hundred micrometers.

Between inhalable PM, the size ranges that are mostly studied are the ones discussed hereafter. Total suspended particles (or TSP) represent all atmospheric suspended particles enclosing a D_{ae} range from few nano-meters to more than a hundred micrometers.

Within the TSP class, there are many subclasses of PM used in the literature. In general, recent classification of particles is based on their D_{ae} only, when other methods link D_{ae} with formation mechanisms (Whitby & Cantrell, 1976).

The first classification method, based on the size, divides atmospheric PM into three subclasses:

- “Coarse” fraction with a diameter that exceeds $2.5 \text{ }\mu\text{m}$. The inhalable part of this fraction includes a D_{ae} range between 2.5 and $10 \text{ }\mu\text{m}$ ($\text{PM}_{10-2.5}$).
- “Fine” fraction particles with an aerodynamic diameter between 0.1 and $2.5 \text{ }\mu\text{m}$ ($\text{PM}_{2.5-0.1}$). Human activities are known to contribute in the largest part of this fraction of PM that is characterized by its deep penetrating capacity when inhaled.

- “Nano” fraction is the one having a D_{ae} that ranges between 0.03 and less than 0.1 μm . It is either generated by anthropogenic activities (mostly combustion) or by natural events (oxidation of natural terpenes emitting secondary organic aerosol). This fraction is important from a public health point of view since it gets into alveolar tissue and can diffuse rapidly in the blood stream.

The second classification method takes in consideration the formation mechanisms, and also shows other ranges of PM that are illustrated in Figure 1. We notice that this distribution is consisted from three ranges starting from:

- 1) The *Nucleation* range or *Aitken nuclei* range that regroups all PM with an aerodynamic diameter less or equal to approximately 0.1 μm . This class represents particles formed by gas-to-particle conversion mechanisms or coagulation of primary particles.
- 2) The *Accumulation* range that includes PM with a D_{ae} between 0.1 and 2.5 μm . Particles of this class are formed in the beginning by vapor condensation on Aitken particles, or a coagulation of this latter to form particles with greater diameter.
- 3) The *Coarse* range regroups particles with an aerodynamic diameter exceeding 2.5 μm . It regroups natural but also anthropogenic direct particles emissions.

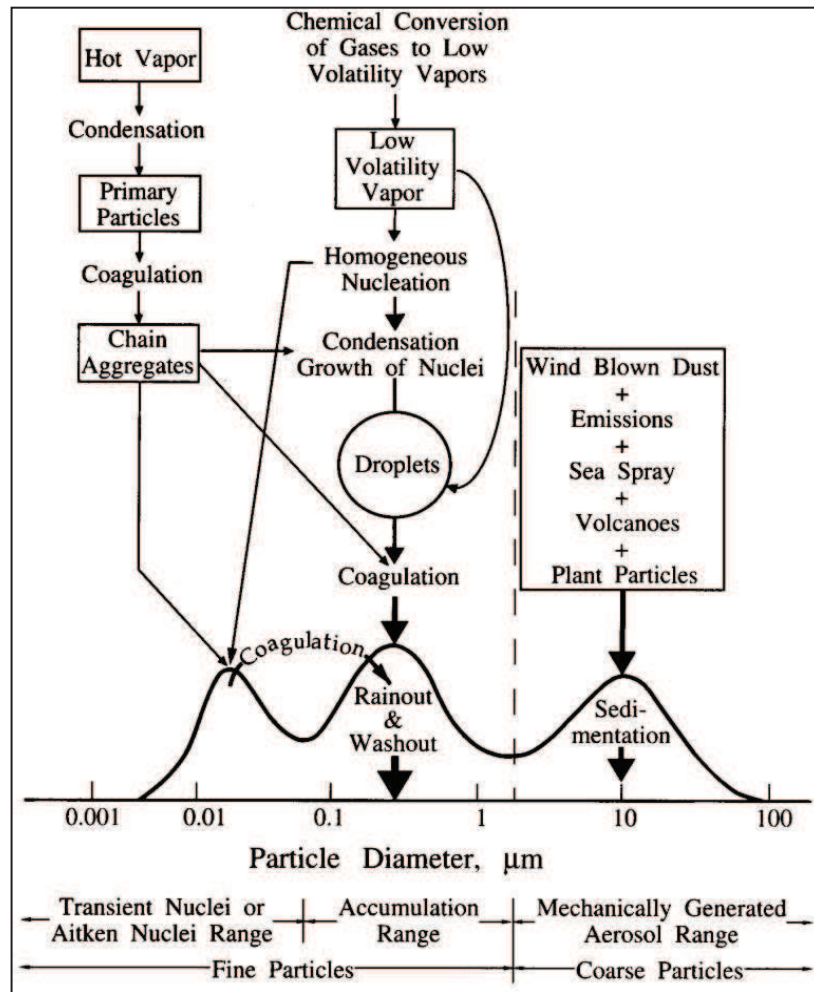


Figure 1: Schematic representation of aerosols size distribution in relation with formation mechanisms (Whitby & Cantrell, 1976)

The *Aitken nuclei* range particles has a relatively short suspension time in the atmosphere due to their rapid transformation to give larger particles. However, the *Accumulation* range is characterized by the longest suspension time in the atmosphere when compared to *Aitken* and *Coarse*, and it accounts for most of the aerosols surface area and constitutes an important part of the aerosol mass. The last range is characterized by a rapid sedimentation of particles due to its large size. In this project, the particle size under study will include the *Accumulation* range and a part of the *Aitken* nuclei: D_{ae} between 0.03 and 2.5 μm ($\text{PM}_{2.5-0.03}$).

I.2.2. Origins of PM

Generally atmospheric PM can be generated from natural sources (terrestrial dust, volcanic action, sea spray, reactions between natural gaseous emissions), but also from human

activities: industrial processes, fuel combustion, transportation and non-industrial fugitive sources (roadway dust, construction, etc).

I.2.2.1. Naturally Emitted Aerosols

I.2.2.1.1. Mineral dust

Terrestrial dust (also known as soil dust) is naturally generated by Aeolian erosion of soil surfaces, which generates and suspends dust, when wind speed exceeds 3 m/sec (Masclet & Cachier, 1998). The main species found in soil dust are quartz, calcite, gypsum, aluminosilicates and some iron oxides. The proportions of these components vary from one study site to another, due to the difference in the soil chemical composition around the world (Wedepohl, 1995). Gravitational settling and wet deposition are the major removal processes for mineral dust from the atmosphere (Seinfeld & Pandis, 2006).

I.2.2.1.2. Sea salts

Sea salts are produced by oceanic spray (Blanchard & Woodcock, 1957). Waves movement generates salt water droplets that are emitted into the atmosphere by the “bubbling” phenomenon. These droplets are dried up in the atmosphere to give solid salts, which chemical composition is very close to that of sea water, and is listed hereafter by order of decreasing weight percentage (wt %): chlorine, sodium, sea salt-sulfates (ss-SO_4^{2-}), magnesium, calcium and potassium. Sea salt-sulfates represent the sulfate load in marine aerosols. Sulfur is found majorly in the form of dimethylsulphide ($\text{DMS} = (\text{CH}_3)_2\text{S}$) in sea water and sulfates are generated by the oxidation of the latter which is emitted from algae. It is important to distinguish between these sulfates and the ones emitted from different anthropogenic sources in the atmosphere called non sea salt-sulfates (nss-SO_4^{2-}).

I.2.2.1.3. Volcanic ash

Volcanic ash is emitted into the atmosphere occasionally with the occurrence of a volcanic eruption (Hidy, 1984) and (Andrea, 1995), like the eruption of Eyjafjöl (Iceland) in 2010. This type of PM can be found loaded with silicon, metals, and sulfates resulting from gas to particle conversion mechanisms.

I.2.2.1.4. Biogenic aerosols

Biogenic organic aerosols can be directly emitted into the atmosphere as pollen, spores, and plant fragments. These constituents are usually found concentrated in the coarse fraction of PM (Seinfeld & Pandis, 2006). It can also be generated by atmospheric oxidation or

condensation of gaseous hydrocarbons emitted from plants such as terpenoids, like isoprene and other species (Masclet & Cachier, 1998). In this case, these particles are included within the secondary organic aerosol (SOA) group.

I.2.2.2. Anthropogenic Aerosols

Anthropogenic aerosols can be encountered as primary aerosols or/and secondary aerosols, and are related to human activities (industrial and domestic). The chemical composition includes a large variety of elements, like carbon in the form of “soot” and/or debris from wheel abrasion, lead, iron, zinc, copper, vanadium, etc. In addition, these aerosols can contain toxic and carcinogenic substances such as PAHs in small but significant quantities.

I.2.2.2.1. Secondary anthropogenic aerosol

Secondary anthropogenic aerosols are produced with the condensation of vapors emitted into the atmosphere on the surface of the particles coupled usually to a photochemical oxidation. For that reason they are called “conversion aerosols”, and are characterized by their relatively small size. Its chemical composition varies depending on the origins of emissions and on the climatic conditions. However, these particles contain a substantial load of sulfates, nitrates, organic matter, and a variety of metal oxides (Masclet & Cachier, 1998).

I.2.2.2.2. Carbonaceous particles

One of the most important primary anthropogenic aerosols is carbonaceous particles. These particles contain black carbon “BC” (also known as elemental carbon “EC”), and organic materials (Seinfeld & Pandis, 2006). Elemental carbon can be produced only by combustion processes, and is solely primary, whereas organic compounds can be emitted directly with the carbon rich particle in a primary fashion, or are adsorbed on the surface of carbon particles, or transformed to particles in the atmosphere to form secondary particles. The carbon content of both elemental carbon fraction and organic is called the “total carbon”.

I.2.2.2.3. Biomass burning

Another type of anthropogenic aerosols is the one produced by biomass burning, which is defined here as the intentional burning of land, for example: tropical vegetation burning, savanna burning in the dry season, etc. The quantity and type of emissions from this kind of combustion is related to vegetation types, moisture content, ambient temperature, humidity, and wind speed. However, CO₂, CO, NO_x, CH₄, organic PM, are the most important chemical substances present in this type of emissions (Seinfeld & Pandis, 2006).

I.2.2.2.4. Secondary Inorganic Aerosols (SIA)

This atmospheric PM profile is specifically important since it allows tracing local and distant human activities. Figure 2 summarizes the chemical reactions that leads to the chemical species encountered in SIA. These latter are majorly composed of ions, namely: nitrates, sulfates, and ammonium; but still contains other chemical species including metals (Figure 2). The origin of this type of aerosols is anthropogenic through sulfur and nitrogen oxides emissions, interacting with natural emissions of ammonia and metals in a relatively high humidity medium. Recent studies show that the industrial and land transportation sectors are the main sources of SO_2 and NO_x emissions respectively, whereas ammonia emission in Europe is essentially linked to agricultural activities.

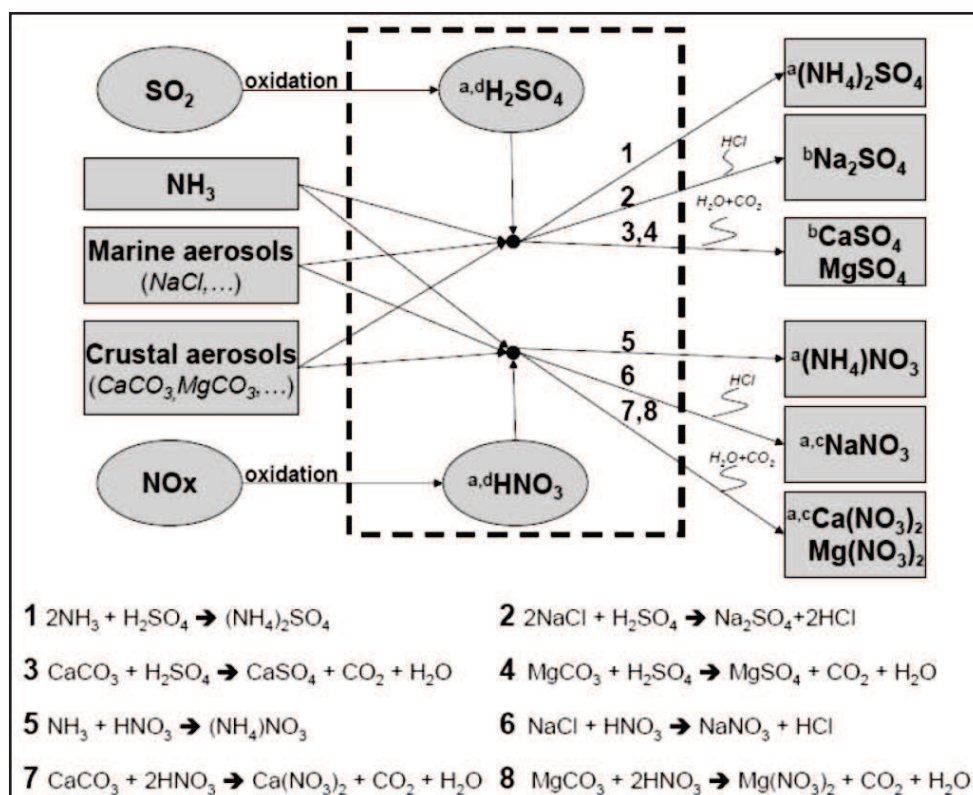


Figure 2: Flow chart of possible formation reactions of different nitrates and sulfates chemical species; taken from (Arruti, et al., 2011) who reproduced it from (Matsumoto & Tanaka, 1996), (Alastuey, et al., 2004), (Pakkanen, 1996), and (Hewitt & Jackson, 2005) which represent (a), (b), (c), and (d) respectively.

I.3. Emissions flux of PM in the atmosphere

I.3.1. Global situation

On a global scale, emissions for both primary and secondary particles can be estimated in the atmosphere depending on their anthropogenic or natural sources. By looking at Table 1, global natural emissions of PM account for about 90% of the total flux, whereas anthropogenic PM account for the remaining 10% of the PM mass emitted yearly in the atmosphere of the planet.

Table 1: Particles flux estimation in the atmosphere (Delmas, et al., 2007)

Origin		Sources	Flux (Mt.yr ⁻¹)	
			Averaged estimation	Min. & Max. estimation
Natural	Primary	Mineral dust	1500	1000-3000
		Sea salt	1300	1000-10000
		Volcanic ash	33	4-10000
		Biogenic debris	50	26-80
	Secondary	Biogenic sulfates	90	80-150
		Volcanic sulfates	12	5-60
		Secondary organic aerosols	55	40-200
		Nitrates	22	15-50
		Total	3060	2170-23540
	Anthropogenic	Primary	Soot	20
Industrial dust			100	40-130
Secondary		Biomass combustion	80	60-160
		Anthropogenic sulfates	140	170-250
		Anthropogenic nitrates	36	25-65
		Organic aerosols	10	0,5-25
Total		390	300-710	

(Mt=10⁶ tonnes)

This difference between natural and human induced emissions is essentially caused by the natural emissions of sea salts and mineral dust. However, the relatively small participation of human activities in global PM emissions (~10%) should not be taken lightly, since it is mainly in the fine particles range. It is persistent in the atmosphere of heavily populated areas from which it was mostly emitted in the first place. In the case of large cities, the proportions between natural and anthropogenic particles are strongly different, leading in some cases to an inversion of the tendencies. Furthermore, its chemical composition can cause adverse health

effects due to the organic component as well as the transition metals that can lay down many risks on human health.

This discussion about the emission inventories for global PM emissions aimed to grasp a general idea about the amount of PM emitted into the atmosphere. However, detailed study of the emission trends of specific PM sizes such as PM_{10} and $PM_{2.5}$, as well as metals emissions in Europe and in France will follow in the forthcoming part.

I.3.2. European anthropogenic emissions

The data used in this section is extracted from the European Environment Agency (EEA(a), 2012). It will be used to discuss emission trends, from 1990 to 2010, around Europe for TSP, PM_{10} , $PM_{2.5}$ and some metals. This first analysis on global European emissions will be followed by a detailed analysis on some chosen sectors emissions, all anthropogenic, for the same period. The chosen sectors are: energy production and distribution, energy use in industry, road transport, non-road transport, commercial/institutional and household, industrial processes, agriculture, waste, and solvent/product use.

I.3.2.1. TSP, PM_{10} , and $PM_{2.5}$ emissions

Figure 3 shows the evolution of anthropogenic emissions in Europe for the major three size classes of particles: TSP, PM_{10} , and $PM_{2.5}$.

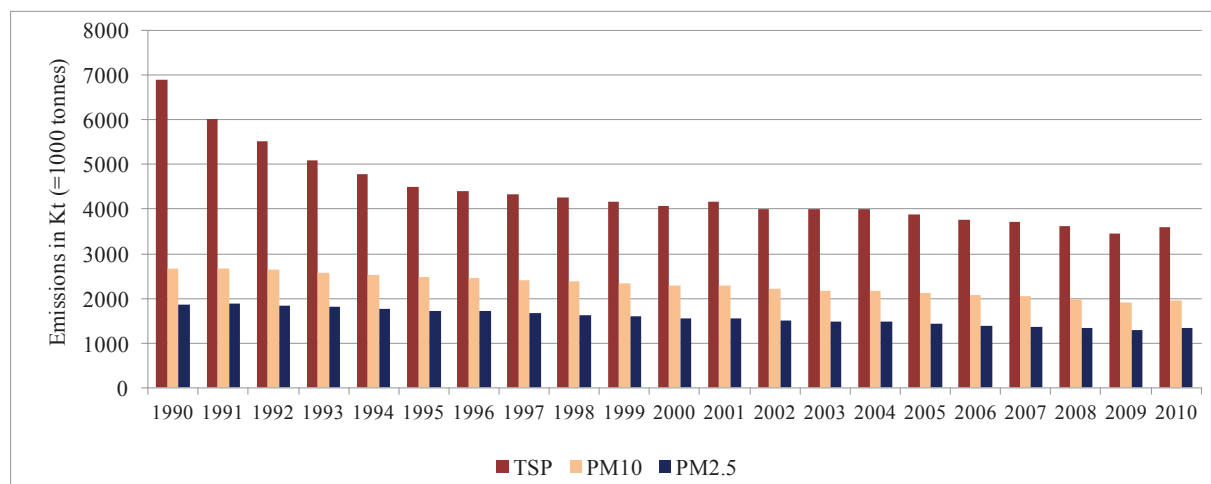


Figure 3: Anthropogenic emissions trends of TSP, PM_{10} , and $PM_{2.5}$ in Europe from 1990 to 2010 in Kt (EEA(a), 2012)

A reduction in the emissions can be observed for the three classes of PM from 1990 till 2010. However, TSP emissions decreased significantly between the 90's and 2010 value when compared to PM_{10} and $PM_{2.5}$ who conserved a moderate decrease for that same period.

We can also notice that in all cases, $PM_{2.5}$ accounted for more than 66% of PM_{10} which proves the extent of human activities contribution in the load of these specific fine particles on the European level.

I.3.2.2. Metals emissions

We emphasize on the importance of tracing these emissions specifically for As, Cd, Cr, Ni, and Pb which all have limit values defined by the World Health Organization (WHO), United States Environmental Protection Agency (US EPA), and the European Union (EU). Metallic emissions in Europe were retrieved from EEA (EEA(a), 2012) for the following metals: As, Cd, Cr, Se, Ni, Cu, Pb, and Zn. The trends are illustrated in Figure 4 and Figure 5.

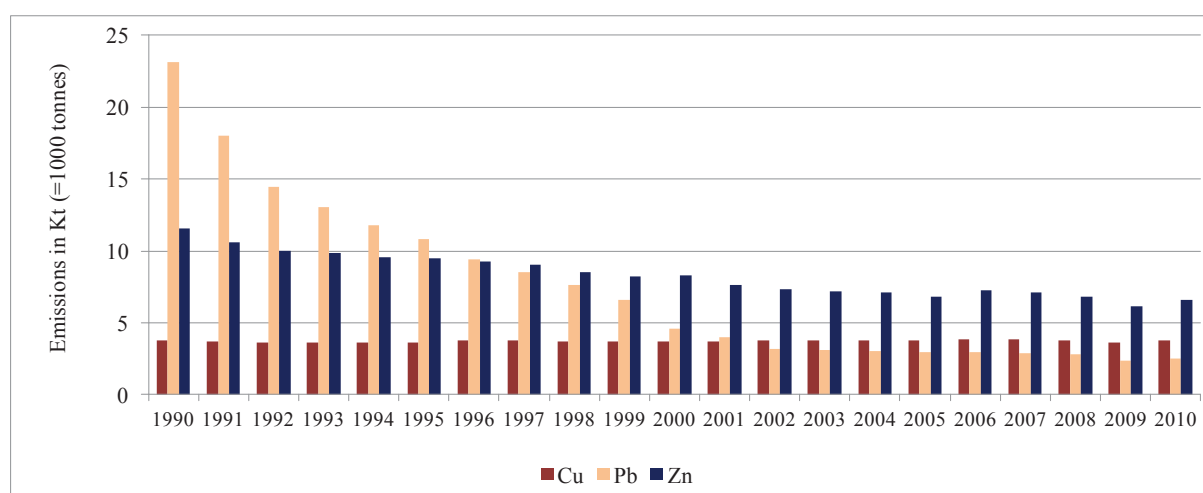


Figure 4: Anthropogenic emissions trends of Cu, Pb and Zn in Europe between 1990 and 2010 in Kt (EEA(a), 2012)

By looking at Figure 4 we can conclude that Pb emissions decreased drastically between 1990 and 2000 linked mainly to the introduction of unleaded gasoline, after which Pb emissions conserved a constant emissions level in Europe, whereas Zn kept on decreasing all the way till 2010. Cu emissions oscillated around 3.7 Kt from 1990 till 2010, with some recent years (3.85 Kt in 2006) having higher values when compared to the 90's.

As, Cd, Ni and Cr levels have decreased in that same time period (Figure 5). Se was adopting almost the same pattern as Cu, with some recent values slightly exceeding older levels for this metal.

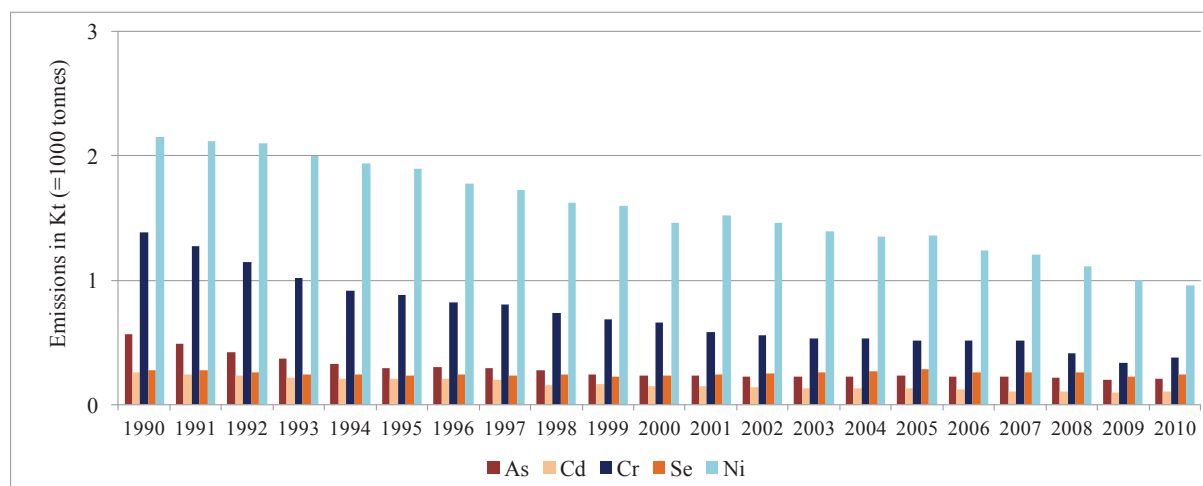


Figure 5: Anthropogenic emissions trends of As, Cd, Cr, Se, and Ni in Europe between 1990 and 2010 in Kt (EEA(a), 2012)

Global anthropogenic emissions trends in Europe evolved with a descending pattern for most of the studied metals. However, a closer look is essential to uncover which sector had a high participation in the emissions of PM and metals, which will be discussed hereafter.

I.3.2.3. Anthropogenic emissions by sector

In this section, we will be analyzing the emissions trend from 1990 to 2010 for PM and metals by activity sector. The sectors under study will be: energy production and distribution, energy use in industry, road transport, non-road transport, commercial/institutional and household, industrial processes, agriculture, waste, and solvent/product use. In each part of the following analysis will include all sectors except the “agriculture” and “Non road transportation” sectors which will be detailed separately due to the difference in the scale of emissions.

I.3.2.3.1. TSP emissions by sector

Emissions of TSP are found different from one sector to another. TSP emissions had decreasing trends for all the studied sectors except “commercial / institutional and household” and “solvent and product use” (Figure 6 and Figure 7). Furthermore, a remarkable decrease was found in the case of “energy production and distribution” when it reached a value of 237.1 Kt in 2010, which is almost 1/8th the value of 1990.

As for the “waste” sector, the figures conserved certain stability in the emission loads of TSP until 2005. After which, it was followed by a significant decrease that remained constant till 2010.

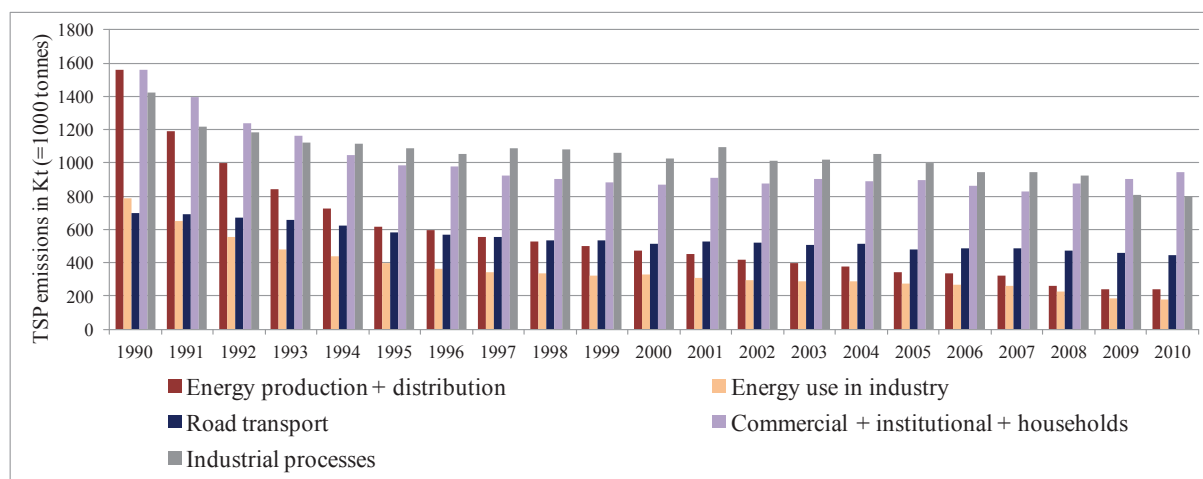


Figure 6: Emissions trends of TSP by sector in Europe between 1990 and 2010 in Kt (EEA(a), 2012)

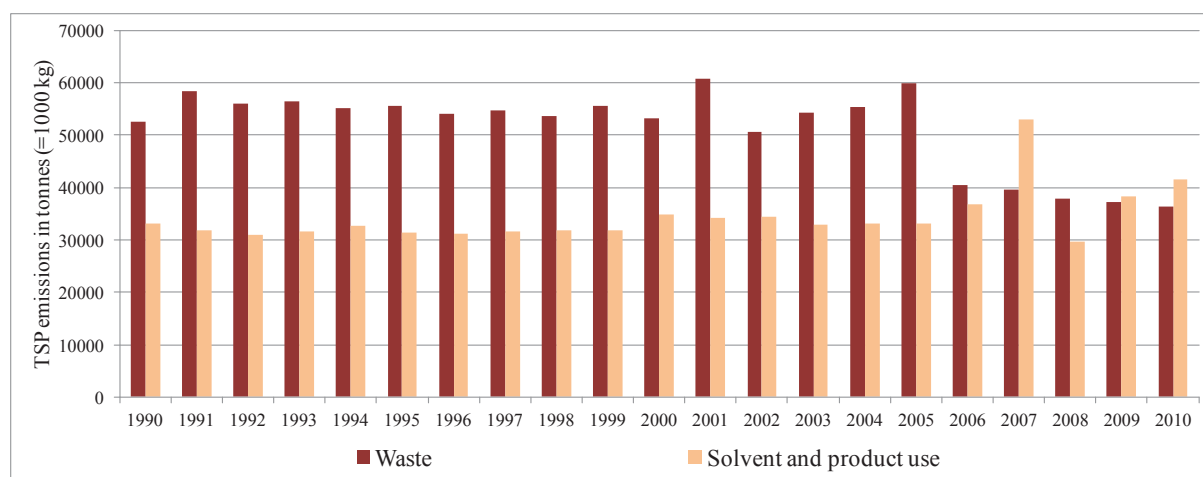


Figure 7: Emissions trends of TSP emitted from “waste” and “solvent and product use” sectors in Europe between 1990 and 2010 in tonnes (EEA(a), 2012)

I.3.2.3.2. PM₁₀ emissions by sector

In this part, PM₁₀ anthropogenic emissions data by sector were illustrated in Figure 8 and Figure 9.

The emissions in this case showed decreasing trends except in the case of “commercial-institutional and household” sector only. In this latter, a recent increase in the emissions can be observed between 2007 and 2010. PM₁₀ emission trends are found having a similar pattern with those for TSP in the case of the “waste” sector, whereas “solvent and product use” emissions fluctuated between 20 and 25 Kt, with a recent decrease noticed in the 2007-2010 period.

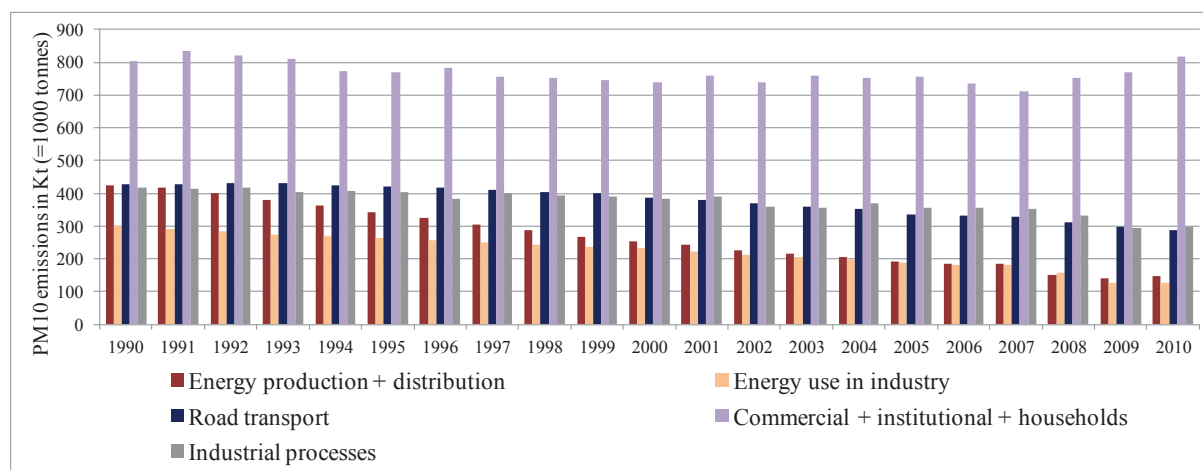


Figure 8: Emissions trends for PM₁₀ by sector in Europe between 1990 and 2010 in Kt (EEA(a), 2012)

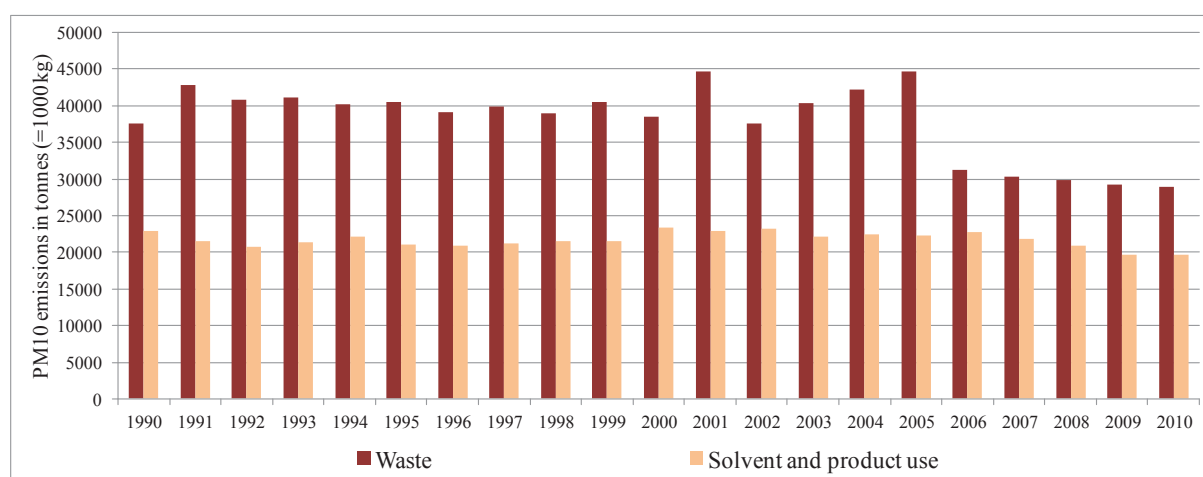


Figure 9: Emissions trends of PM₁₀ emitted from “waste” and “solvent and product use” sectors in Europe between 1990 and 2010 in tonnes (EEA(a), 2012)

I.3.2.3.3. PM_{2.5} emissions by sector

Data on the emissions of PM_{2.5} by sector are illustrated in Figure 10 and Figure 11. The trends show a similar pattern than the one observed in the case of PM₁₀ in all the above discussed sectors. This shows that these two size fractions are highly related to human activities, as well as related to each other. By comparing PM₁₀ to PM_{2.5} data, especially for the “road transport” sector, we can notice that PM_{2.5} anthropogenic emissions constitute a significant part of PM₁₀ emissions, which can be related to combustion emissions of fine particles.

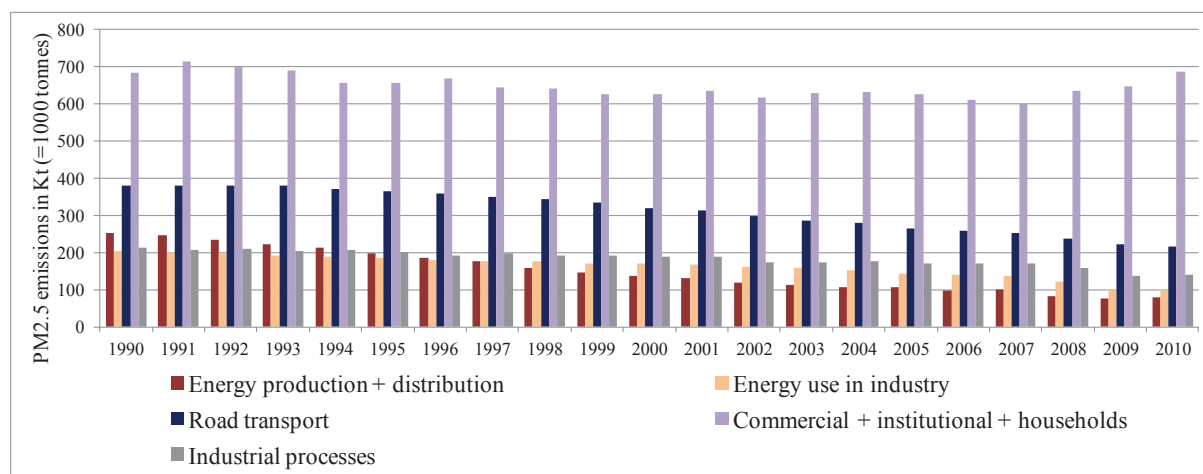


Figure 10: Emissions trends for PM_{2.5} by sector in Europe between 1990 and 2010 in Kt (EEA(a), 2012)

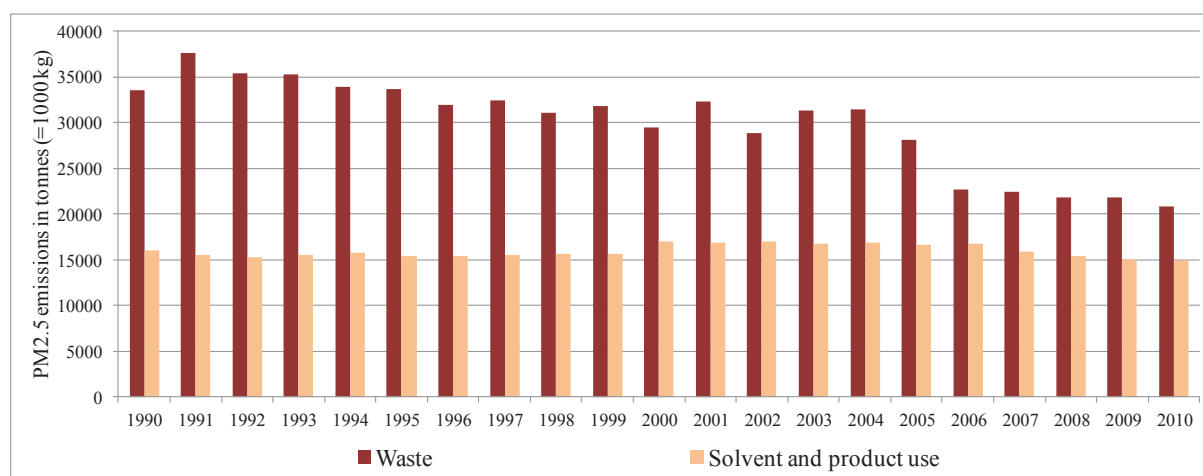


Figure 11: Emissions trends of PM_{2.5} emitted from “waste” and “solvent and product use” sectors in Europe between 1990 and 2010 in tonnes (EEA(a), 2012)

I.3.2.3.4. Anthropogenic emissions for “non-road transport” and “agriculture” sectors

TSP, PM₁₀, and PM_{2.5} anthropogenic emissions show similar patterns when studying “non-road transport” emissions, with a relative decrease between 2008 and 2010 (Figure 12). Furthermore, PM_{2.5} contributes significantly to PM₁₀ (about 90%) and TSP (about 70%) levels. This proves the extent of human activities, especially combustion processes (see I.3.2.3.3), in the variations of these emissions. An opposite example can be found in the “agriculture” sector emissions (Figure 13). In this case, TSP and PM₁₀ were found to have an increasing trend, whereas PM_{2.5} showed a relative decrease when approaching 2010.

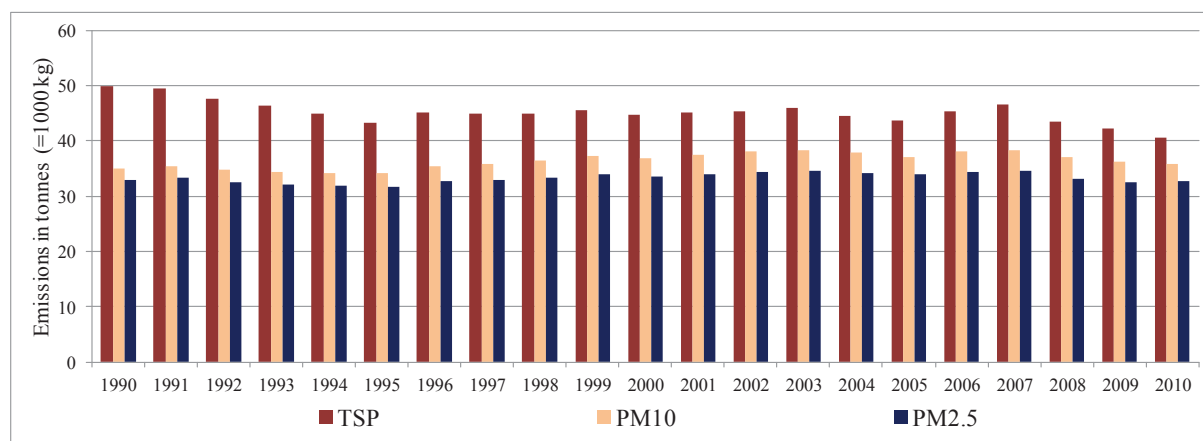


Figure 12: Emissions trends emitted from the “non-road transport” sector in Europe between 1990 and 2010 in tonnes (EEA(a), 2012)

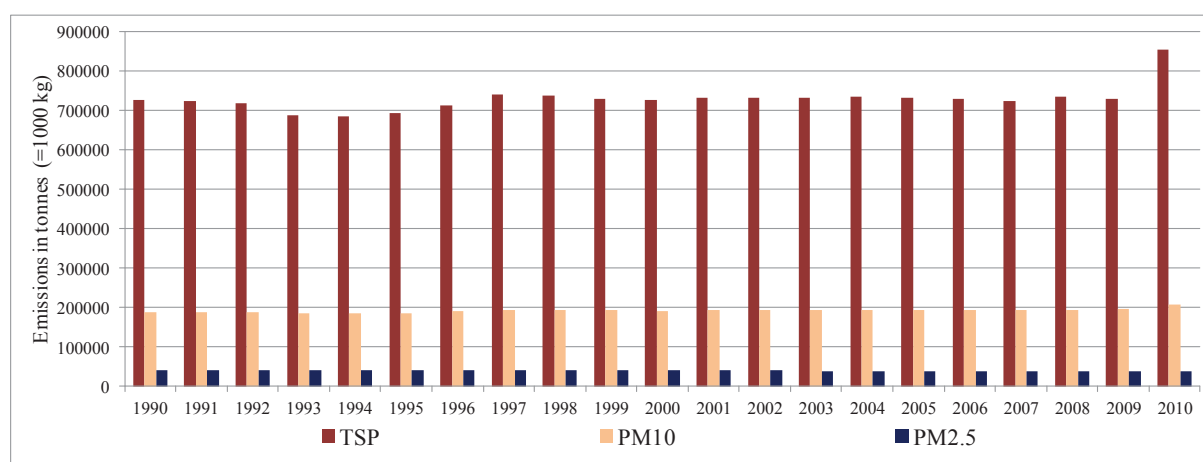


Figure 13: Emissions trends emitted from the “agriculture” sector in Europe between 1990 and 2010 in tonnes (EEA(a), 2012)

I.3.3. French anthropogenic emissions

For this section, the data was extracted from the EEA (EEA(a), 2012). On the European level, a decreasing pattern was adopted by most anthropogenic emissions in general, with some exceptions in certain sectors. However, since this project is conducted in France, it is necessary to study the evolution of the anthropogenic emissions on the national level, and compare it to the European situation in order to uncover any changes on the local scale. The same list of sectors that was previously studied will also be included in this following analysis.

I.3.3.1. TSP, PM₁₀, and PM_{2.5} emissions

The evolution of anthropogenic emissions for the three major classes of PM is similar to that of the European situation for PM₁₀ and PM_{2.5} emissions (Figure 14). On the other hand, TSP decreased less severely in France when compared to Europe in general.

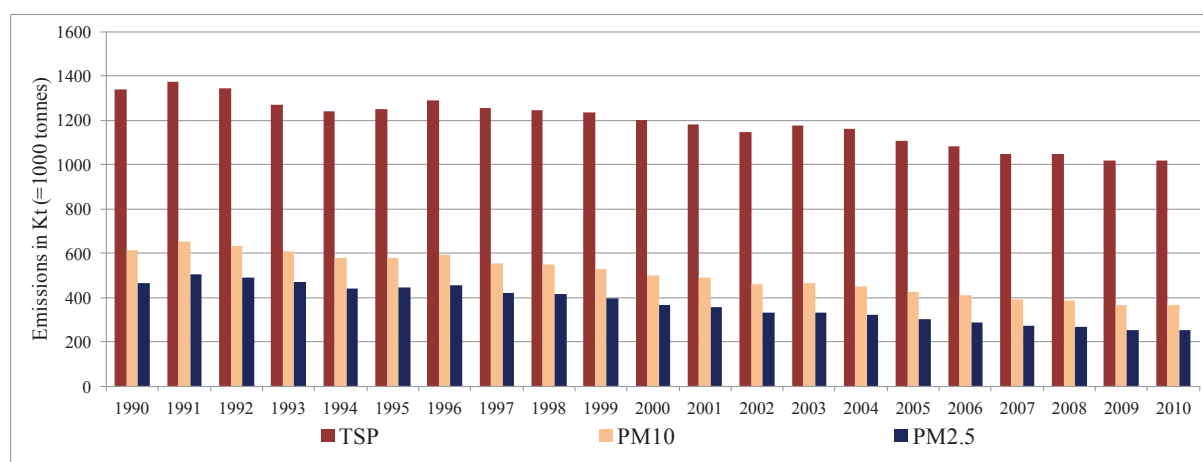


Figure 14: Anthropogenic emissions trends of TSP, PM₁₀, and PM_{2.5} in France from 1990 to 2010 in Kt (EEA(a), 2012)

I.3.3.2. Metals emissions

Metals anthropogenic emissions in France are illustrated in Figure 15, Figure 16 and Figure 17. Cu and Zn emissions decreased considerably to 1.9% and 11.7% in 2010 respectively.

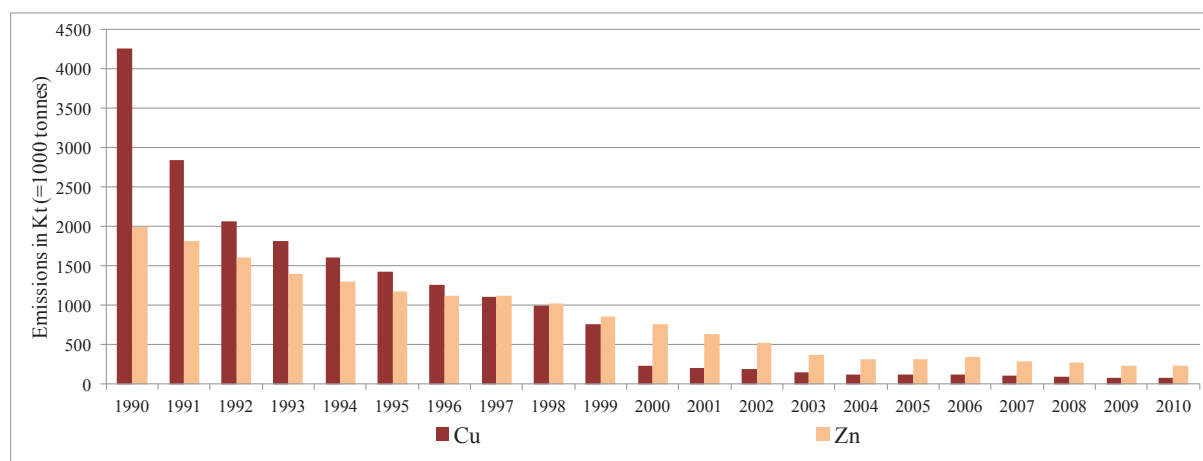


Figure 15: Anthropogenic emissions of Cu and Zn in France between 1990 and 2010 in Kt (EEA(a), 2012)

On the other hand, As, Cd, Cr emissions decreased in a moderated fashion, when compared to Ni and Pb (Figure 16 and Figure 17). These latter decreased more gradually till 2010. Finally, Se emissions showed almost stable levels between 1990 and 2010 (Figure 17).

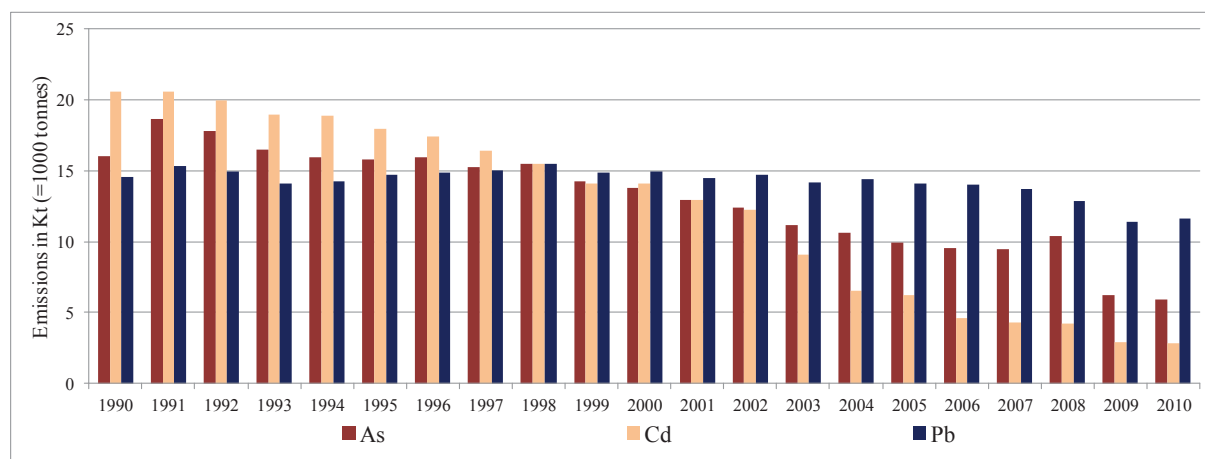


Figure 16: Anthropogenic emissions of As, Cd, and Pb in France between 1990 and 2010 in Kt (EEA(a), 2012)

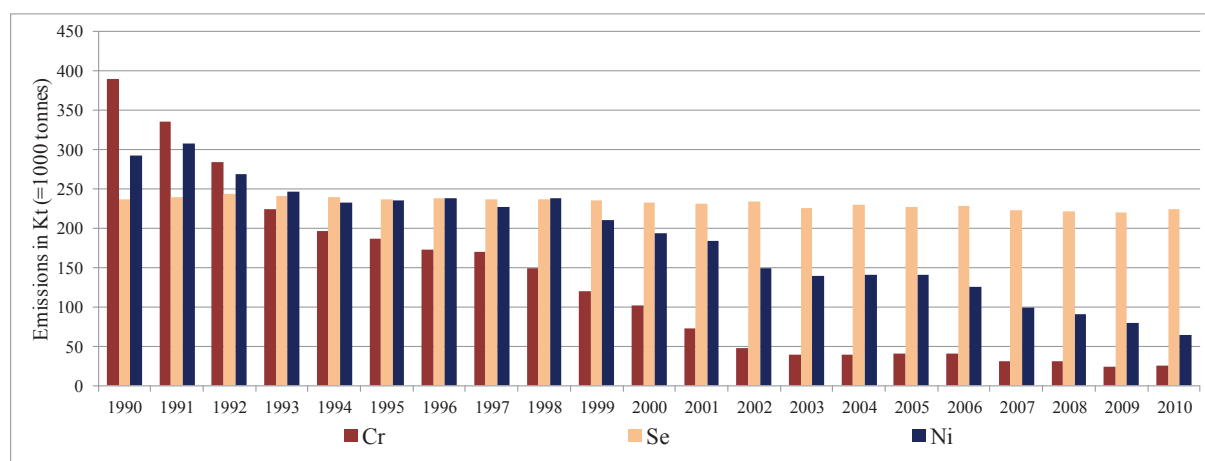


Figure 17: Anthropogenic emissions of Cr, Se, and Ni in France between 1990 and 2010 in Kt (EEA(a), 2012)

I.3.3.3. Anthropogenic emissions by sector

I.3.3.3.1. TSP emissions by sector

Based on the difference in the scale of emissions, the sectors were divided into two groups. The first group includes: road transport, commercial/institutional and household, industrial processes, and agriculture. And the second regroups: energy production and distribution, energy use in industry, non-road transportation, solvent and product use, and finally the waste sector. All gathered data are illustrated in Figure 18 and Figure 19.

Recent TSP emissions in France are found low when compared to older values related to all sectors except “agriculture” and “solvent and product use”. Agriculture emissions show

that TSP levels increased in 2009 – 2010 to match 1998 and 1991 values (Figure 18), whereas the “solvent and product use” TSP emissions increased above the 1990 value (Figure 19).

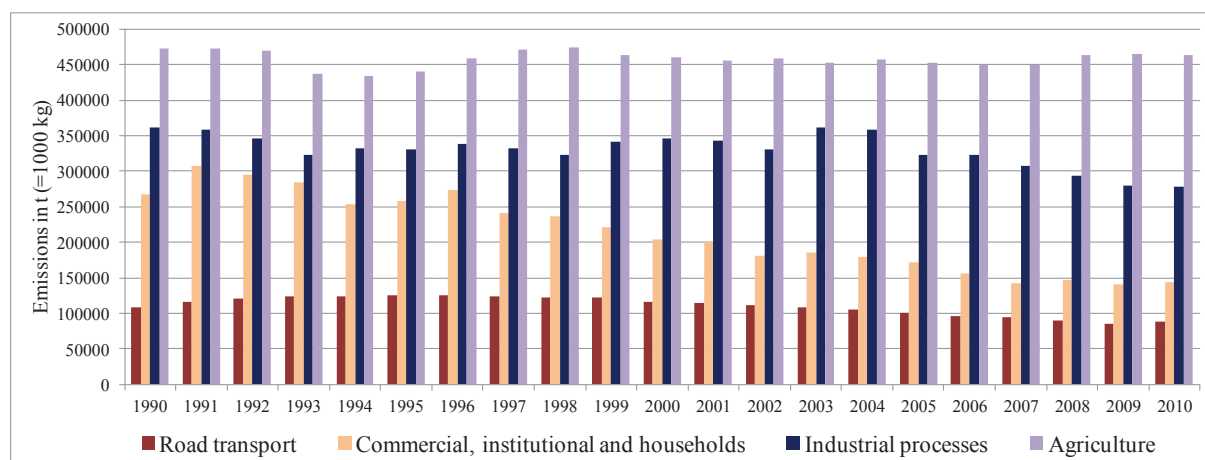


Figure 18: Emissions trends for TSP emitted from: road transport, commercial/institutional and household, industrial processes, and agriculture sectors; in France between 1990 and 2010 in tonnes (EEA(a), 2012)

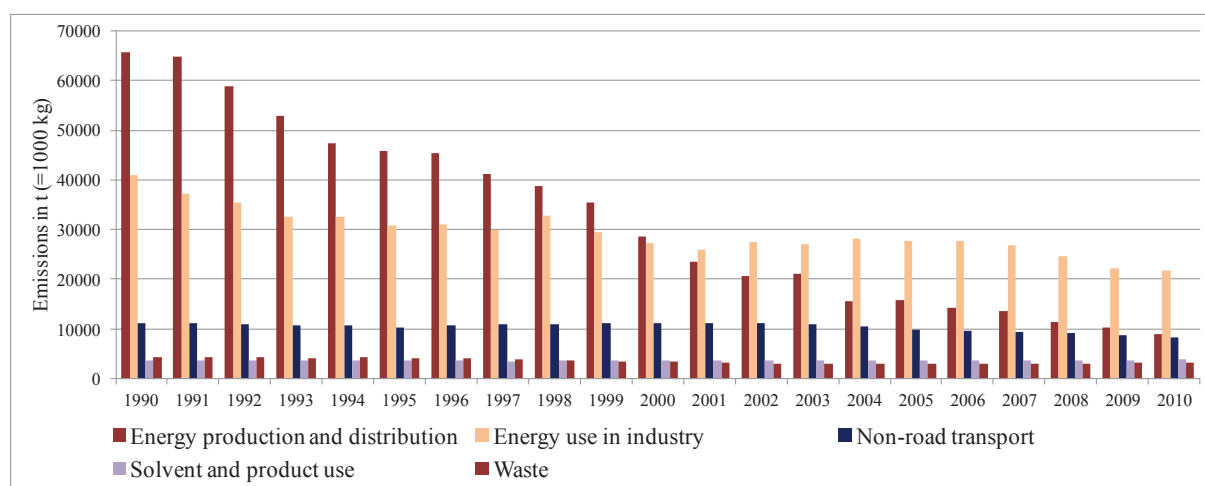


Figure 19: Emissions trends for TSP emitted from: energy production and distribution, energy use in industry, non-road transportation, solvent and product use, and waste sectors; in France between 1990 and 2010 in tonnes (EEA(a), 2012)

I.3.3.3.2. PM₁₀ emissions by sector

Emissions trends of PM₁₀ in France show a moderate decrease in all analyzed sectors (Figure 20 and Figure 21) except for “solvent and product use”. This latter emissions exhibited a slight increase in 1990 to get to the highest (2701 tonnes) in 2010.

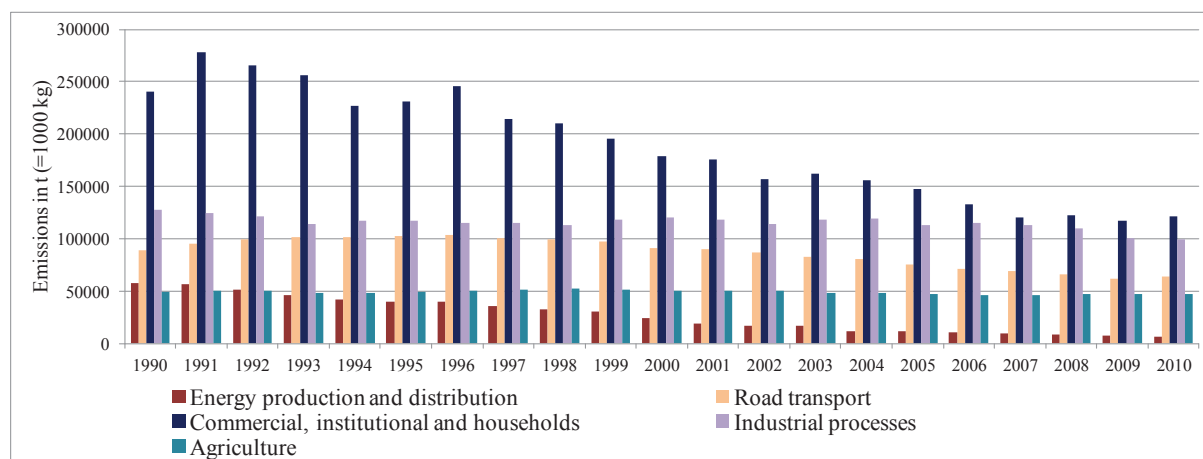


Figure 20: Emissions trends for PM₁₀ emitted from: energy production and distribution, commercial-institutional and households, road transportation, industrial processes, and agriculture sectors; in France between 1990 and 2010 in tonnes (EEA(a), 2012)

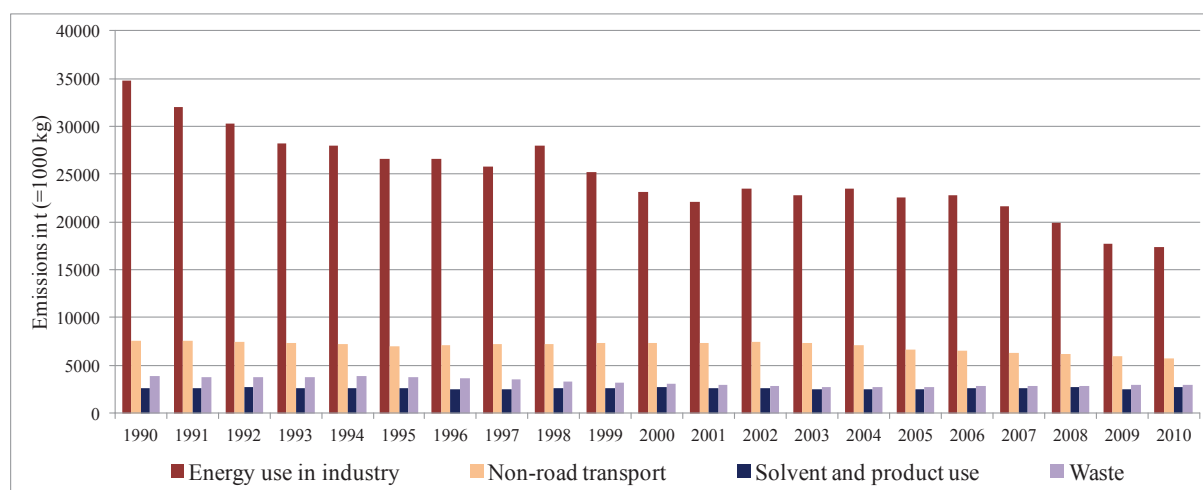


Figure 21: Emissions trends for PM₁₀ emitted from: energy use in industry, non-road transportation, solvent and product use, and waste sectors; in France between 1990 and 2010 in tonnes (EEA(a), 2012)

I.3.3.3.3. PM_{2.5} emissions by sector

Figure 22 and Figure 23 summarize the emissions trends of PM_{2.5} for all concerned sectors from 1990 to 2010. The evolution of these emissions shows a decrease in all sectors emissions since the 90's except for the case of “solvent and product use” sector. This latter trends revealed an increase in the emissions between 2008 (1361 tonnes) and 2010 (1382 tonnes).

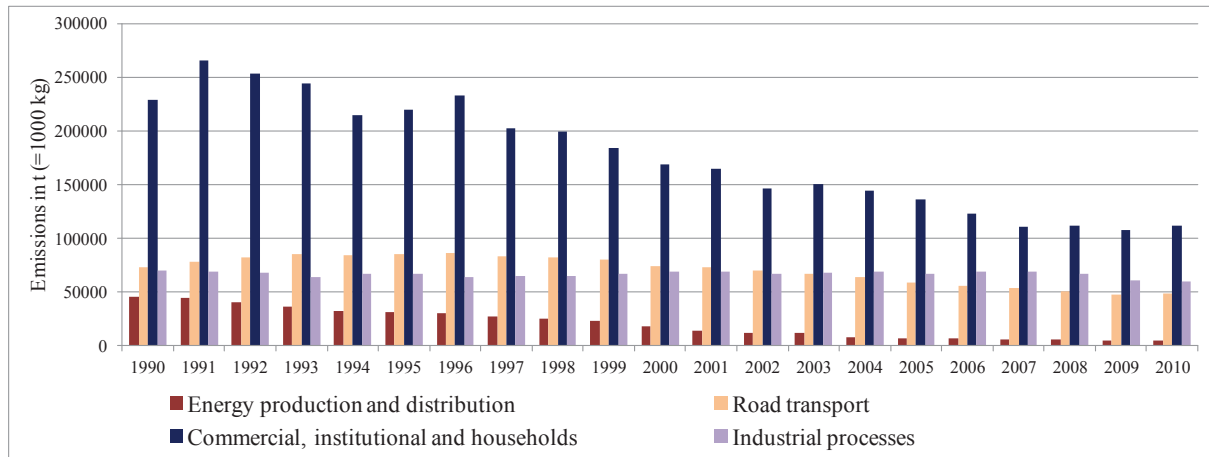


Figure 22: Emissions trends for PM_{2.5} emitted from: energy production and distribution, commercial-institutional and households, road transportation, and industrial processes sectors; in France between 1990 and 2010 in tonnes (EEA(a), 2012)

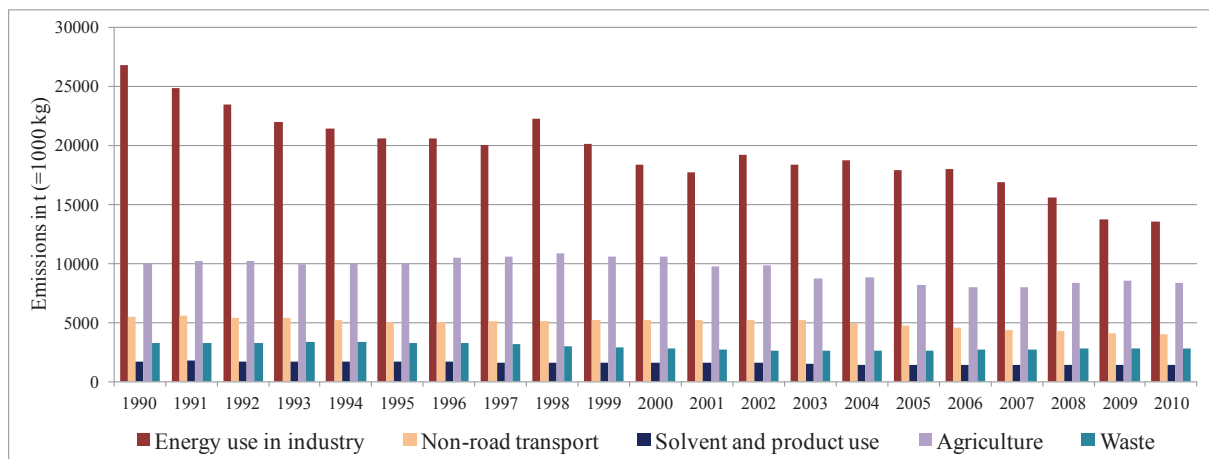


Figure 23: Emissions trends for PM_{2.5} emitted from: energy use in industry, non-road transportation, solvent and product use, agriculture, and waste sectors; in France between 1990 and 2010 in tonnes (EEA(a), 2012)

I.4.Review on international and national air quality standards

I.4.1. PM₁₀ limit values

The limit values for this size fraction of atmospheric PM are defined at the European level, but also by the US EPA and WHO. In this latter, PM₁₀ limit was set at 20 $\mu\text{g}/\text{m}^3$ as an annual mean value, and 50 $\mu\text{g}/\text{m}^3$ for the 24 hours mean value (WHO, 2006). On the other hand, the US EPA has set PM₁₀ limit values to 50 and 150 $\mu\text{g}/\text{m}^3$ for the annual and daily (24 hours average) limits respectively.

PM₁₀ limit values were also defined in Europe to 40 and 50 $\mu\text{g}/\text{m}^3$ as annual and 24 hours average respectively without crossing the 35 daily exceedance limit. These regulations

are already enforced since January 2005 (Directive-2005/0183) in Europe as well as in France. However, the limit values set by the European directive for ambient air PM₁₀ are being exceeded in France to an extent where the European Union obligated France to face the EU justice court for not respecting the limit values of PM₁₀ in 2011 (Collet, 2011).

France is not the only country that exceeds these limits. In 2010, about 21% of the urban population in the European Union was exposed to PM₁₀ levels that exceed the limit value. The frequency of exposure to above limit values varied between 18% and 41% in 2001. These variations reflected the changes caused by meteorological conditions (EEA(b), 2012).

I.4.2. PM_{2.5} limit values

PM_{2.5} limit values are set and enforced in the USA. Historically, the determination of limit values for this size range of PM evolved from high values to lower ones, after coupling assessments on human health problems linked to the exposure to these particles. For example, the United States National Ambient Air Quality Standards (NAAQS) changed the limit value for PM_{2.5} (24 hour) from 65 µg/m³ (1997) to 35 µg/m³ (2006). However, their annual average value was stabilized to 15 µg/m³ (USEPA, 2012).

The World Health Organization (WHO) followed the US EPA steps and had many interim targets for PM_{2.5} annual mean concentrations (35, 25, and 15 µg/m³) as well as for the 24-hour concentrations (75, 50, and 37.5 µg/m³), before settling with 10 and 25 µg/m³ as guideline values for PM_{2.5} annual and 24-hour concentrations respectively (WHO, 2006).

As for the European Union, the Directive “2008/50/EC” published the targets values and limit values for PM_{2.5} (Directive-2008/50/EC, 2008). In the latter, PM_{2.5} annual average limit values of 25 µg/m³ and 20 µg/m³ were defined as objectives to be met in January, 2015 and 2020 respectively.

In the year 2010, French legislation on suspended PM was modified to consider PM sizes below 10 µm. Hence, since 2010, PM_{2.5} levels are being monitored in regions populated by more than 100 000 inhabitants. The monitoring sites in those regions are located in an urban background location.

Many PM_{2.5} limit values were converted from the European to the French legislation (Decree-n°2010-1250, 2010). Thus a target value was set at 25 µg/m³, which should be met in 2015. Meanwhile, the limit value will evolve yearly following a decreasing order. In 2010, the value was set at 29 µg/m³, then 28 µg/m³ in 2011, 27 µg/m³ in 2012, and 26 µg/m³ for 2013 and 2014.

Based on annual reports on air quality in France between 2007 and 2011, the annual averages of $PM_{2.5}$ is found to range between 15 and 25 $\mu g/m^3$ in some French regions (MEDDTL, 2010). Few exceeding limit values were identified in large cities such as Lyon and Paris in 2009. Furthermore, a seasonal variation of the particles concentrations was identified: the highest levels were recorded under dry anticyclone weather conditions that usually favor pollutants accumulation. Such episodes are encountered particularly during winter and the beginning of spring seasons.

More concerns about the respect of limit values of PM in the ambient air have been raised in France in which limit values for PM_{10} are regularly being broken; therefore the question remains: what about the levels and sources of $PM_{2.5}$ in the NPdC region? Furthermore, our project will deal with the chemical composition of $PM_{2.5}$, including an extended list of metal species from which some have guidelines values. These guidelines will be discussed in the forthcoming section.

I.4.3. Metals guideline values

Current atmospheric standards for metals are of a great importance to this work, since it will be used to evaluate the results and compare them to international and national standards. The WHO, EPA, EU, and the French government addressed the problem regarding the concentrations of certain inorganic pollutants in the atmosphere, specifically some elements that have observable adverse health effects and are emitted from anthropogenic activities. Guidelines values were set for these elements: As, Cd, Cr, Pb, Mn, Ni, and V.

The adverse health effects of these metals are detailed in the Air quality guidelines for Europe (WHO, 2000), in which “As” is found to increase incidence of lung cancer in occupationally exposed groups, and therefore is considered carcinogenic. “Cd” and “Cd-compounds” are classed as Group 1 human carcinogens. Its inhalation is found to cause renal alterations as well. On the other hand, “Cr” represents a different case, where “Cr (III)” is an essential element for humans and animals, so the problem resides in the load of “Cr (VI)” in the environment. This latter is found to be toxic and carcinogenic.

Furthermore, “Pb” can cause nerve problems in adults, hearing impairment and disturb Vitamin-D metabolism in children. Smaller age groups are found to be more sensitive to this metal, like children whose cerebral system can be specifically affected. On the other hand, some exposure tests on animals proved that Pb loads alters hearing functions and the ability to comprehend. However, it is extremely difficult to prove that the same effects exist in humans. Nevertheless, researches have proven through epidemiological studies on school children that

the exposition to Pb resulted in developmental (psychomotor system) or intellectual troubles as well as behavioral problems. In this latter, the observed consequences were hyperactivity, lack of concentration, and impulsivity (INSERM, 1999).

In the case of “Mn”, its accumulation can cause pneumonitis, pneumonia, reproductive dysfunction, and even neurotoxicity (at a low-level exposure). However, “Ni” can increase the risk of lung and nasal cancer. This was observed under exposure within Ni refining industries. In the mean time, “V” contamination is found to be highly related to the inhaled dose. An exposure to low doses can cause irritations of the upper respiratory tract, which is considered as minor effects when compared to chronic bronchitis and pneumonitis that can result from exposure to high concentrations (WHO, 2000).

As for the guidelines values, Table 2 summarizes the available data taken from different sources. However, few terms need to be defined like “Exposure LV”, which means the exposure limit value (measured per day) not to be exceeded. Another used term is “Target”, which herein means the annual average objective to be attained for a better air quality.

Table 2: Guideline values for metals in the Atmosphere

	Annual average ^(a,c)	Exposure LV ^(a)	3 months average ^(b)	Target (>2012) ^(c)
As	-	-	-	6 ng/m ³
Cd	-	5 ng/m ³	-	5 ng/m ³
Cr	-	-	-	-
Pb	500 ng/m ³ ^(c)	-	150 ng/m ³	250 ng/m ³
Mn	150 ng/m ³ ^(a)	-	-	-
Ni	-	-	-	20 ng/m ³
V	-	< 1000 ng/m ³	-	-

^a (WHO, 2000)

^b (USEPA, 2012)

^c (MEEDDAT, 2008)

A closer look at Table 2 shows that a large list of elements is missing as well as implemented limit values for As, Cr, and V. This last case can be explained by the difficulties that researchers encounter when defining thresholds for adverse health effects (WHO, 2000).

The remaining trace elements that are not on the list constitute a large list, and highlight the importance of our work, in which we will be able to monitor elements concentration range and their sources.

I.5. Background on fine PM studies

In this section, we will inspect some of the works that we could find and that deal with the subject of atmospheric PM pollution. The early studies on the fine fraction of PM were mostly conducted to unfold the formation related to direct emissions or gas-to-particles conversion processes. In the 90's period, more focus was laid on the chemical composition in relation with the formation mechanisms of fine PM. In the same period, a lot of attention was given to the toxicology of fine PM and on the sources of emissions through biological and chemical testing. The evolution of fine particles studies continued in the same upward direction from 2000 till recently, with more emphasis on the chemical composition as a source tracer, but also on the smaller fractions like: fine, ultra-fine, and nano particles. Therefore in the following section, we will discuss the advancements in fine PM research.

I.5.1. Early studies

Between the 70's and 80's period, most research subjects concerning atmospheric PM revolved around the formation mechanisms, penetration in the respiratory tract, industrial emissions analysis, early toxicity studies and chemical composition. Within the research axis of understanding the formation of PM, a lot of studies went to analyze the chemical composition of fine and ultrafine particles.

Bricard et al, in 1977 worked on the formation of new ultrafine particles from gases in a search to better understand the nucleation mode of particles considering the presence of SO₂ and NO₂ (Bricard, et al., 1977). In the same period more work was conducted also on the formation of particles through nucleation processes (Yue, 1979). On the other hand, the health effects of the deposition of ultrafine PM in the lungs was being studied in that period by (Boffa, et al., 1977) which is one of the oldest articles that we found on the inhalation effects of particles, and emphasized the importance of studying the toxicity of PM.

Deeper chemical investigations can be found in the studies conducted in the 80's, especially some works conducted with the objective of tracing elements that are problematic such as Mn (Davis, et al., 1988), and "Pb, V, Ni, Mn and Fe" ((Paul, et al., 1983) and (John & George, 1983)). Toxicity issues had also been discussed in that period, such as the carcinogenicity of atmospheric Benzo-a-Pyren studied by Perera (Perera, 1981).

I.5.2. Chemical composition and sources of fine PM

Additional interests in the chemical composition of the fine fraction of PM started in the 90's. The issues of formation and evolution of these PM in the atmosphere, the emissions sources and toxicity were extensively studied during this period.

The formation of particles in the atmosphere was the subject of many studies ((Bigg, 1997);(James & Alan, 1999); and (Liisa, 1999)), when others worked on the changes in the chemical composition of these particles (Veli-Matti, et al., 1998) with aging mechanisms (Kotzick & Niessner, 1999). On the other hand, the use of mathematical modeling started to emerge in that period in order to understand particles emissions using positive matrix factorization (Kaarle, et al., 1996). Also, receptor modeling was used in Germany to distinguish between three sources of PM_{2.5} emissions: road dust, secondary aerosols, and vehicle combustion (Pohlmann, et al., 1999).

The sources of PM emissions were the subject of many studies, from which transport related emissions were highlighted as an important source of particles ((Antonio, et al., 1998) and (Lidia, et al., 1999)). Furthermore, wood combustion particles characteristics were studied in (Gaegauf, et al., 1997), who found that combustion air supply plays an essential role in the amount of PAHs emissions.

Studies on the inorganic chemical composition of fine PM fractions were also available in that period. Some of these studies were conducted in big cities in the US (Huges & Cass, 1998) and in China (Guor-Cheng, et al., 1999). In this latter, PM₁₀ bound heavy metals concentrations were found higher during the day when compared to the night time. Also, PM_{2.5} was found to be the major part of day time PM₁₀, and they were found in high concentration in a suburban area compared to a rural one. On the other hand more investigation on the metallic content of PM_{2.2} was conducted in the Los Angeles area (Huges & Cass, 1998), in which Fe concentration was found to be most prominent, followed by K, Na, Ti, Zn and Cr.

The analysis of a detailed chemical composition of fine PM is very important when searching for sources and their impacts. Metals, ions, and carbon contents uncovered in recent studies on fine PM will be detailed hereafter in order to explain the variety of anthropogenic contribution in fine PM loads.

I.5.2.1.Sources of metals

Metallic compositions of fine PM is highly related to nearby as well as distant sources. Metals cocktail within this fraction of aerosols can present a quantitative and mostly a

qualitative variety. These fluctuations are mostly linked to the emissions of metals from anthropogenic sources. Therefore, quantitative variations of elements in PM can be explained once the source of emissions is identified. However, this last task is complicated, especially when the studied region presents a mixture of many anthropogenic sources. The difficult section in such studies is to be able to determine which metal or group of metals is resulting from which activity, knowing that in most cases, different human activities enrich PM with similar metals. Therefore, the variations in metals concentrations in PM_{2.5} based on their origins of emissions will be discussed in this section using results from studies conducted around Europe.

I.5.2.1.1. Crustal

Also known as mineral dust (see section I.2.2.1.1), crustal particles can be emitted directly with wind suspending soil minerals into the air, or from anthropogenic activities re-suspending this sediment from the ground. Many elements can be considered as tracers of mineral dust, from which: Al, Ca, Fe, Si, Ti and Mg were categorized as soil dust elements ((Wu, et al., 2007); (Ilacqua, et al., 2007)). However, each study has to follow other sources contributions, which might have common tracers with the previously mentioned elements. In some studies, Al and Si oxides correlations pointed at this type of fine dust particles (Gotschi, et al., 2005), but also Ti and Ca may be considered tracers if found correlated (Cyrys, et al., 2003).

I.5.2.1.2. Traffic exhaust emissions

In traffic exhaust emissions, carbon content is always found important along with other metals that are considered as tracers of direct exhaust emissions. Between these metals: Cu, K, Mn, Zn, Pb, Ba, Sb, Br, As, V, and Cd are mostly used to trace traffic direct emissions ((Moloi, et al., 2002); (Mazzei, et al., 2008); (Beslic, et al., 2008); (Ilacqua, et al., 2007)). One problem in determining the tracers for traffic emissions is the fact that one element can correlate with many others, displaying different scenarios of anthropogenic contribution. In some studies, long range transport (LRT) traffic emissions were identified in fine PM, in which As, Cl, K, S, and EC were well correlated (Ilacqua, et al., 2007).

I.5.2.1.3. Traffic non-exhaust emissions

Under this category we regroup brakes of vehicles and tyre road wear, and also re-suspended dust particles (see section I.5.2.1.1). In the first group, Cu – Cd correlations seems to be a commonly used tracers for brakes of vehicles emissions ((Beslic, et al., 2008) and

(Rajsic, et al., 2008)). However, Fe can also be considered as a tracer (Vallius, et al., 2003) along with Ba and Mn (Birmili, et al., 2006) of brakes emissions. Furthermore, Sb – Cu correlations were used to identify brake linings in Spain (Moreno, et al., 2006) and in the United Kingdom (Gietl, et al., 2010), whereas Cr – Cu correlations were used for the same purpose in a study conducted in Amsterdam (Boogaard, et al., 2011).

On the other hand, tyres road abrasion can be traced by following Zn correlations (Vallius, et al., 2003), or Ba – Mn correlations (Moreno, et al., 2006). In fact, high Zn concentrations in the tyres can be explained since the element is introduced in the vulcanization process during tyres manufacturing.

Finally, traffic related re-suspended dust particles were traced using Zn to Mn and Al to Fe correlations (Rajsic, et al., 2008). Another example can be found in (Vallius, et al., 2003), in which a correlation between Fe and Mn concentrations was found to be a tracer of crustal traffic re-suspended dust. Also Cu, Zn, and Fe correlations pointed at traffic emissions (Vallius, et al., 2005) as well as Sb, Cu, Fe, and Zn correlations can be used as specific tracers of traffic emissions ((Pakkanen, et al., 2001); (Strak, et al., 2011); and (Salvador, et al., 2012)).

I.5.2.1.4. Oil-fuel combustion

For this source of emissions, studies seem to have some sort of a consensus on the use of Ni – V correlations to uncover this contribution source ((Cyrys, et al., 2003); (Ilacqua, et al., 2007) and (Mazzei, et al., 2008)). On the other hand, heavy oil combustion can be identified by linking SO₂ emissions to Ni and V (Vallius, et al., 2003). In some cases however, Ni was associated to Mo and Co in PM_{2.5} to point at oil combustion source of PM emissions (Pakkanen, et al., 2001).

I.5.2.1.5. Coal combustion

Arsenic was found to be one common element that is mostly used to trace coal combustion. It can also be correlated to Hg (Freitas, et al., 2005), to Se to trace residential coal combustion (Salvador, et al., 2012), to Cd and Pb (Schleicher, et al., 2011), or even to a list of metals: Cd, Bi, Tl, K, Zn, and Pb, to trace aged coal combustion aerosols (Pakkanen, et al., 2001). In other studies, unique metals in PM can be used as tracers of coal combustion process, like “S” (Cyrys, et al., 2003) and “Se” (Ilacqua, et al., 2007) for example.

I.5.2.1.6. Long range transport (LRT)

Even though this origin of PM can be identified by studying ionic composition of the particles, complementary methods can still be used to uncover this source. For example, a combination of metals was studied by Ilacqua (Ilacqua, et al., 2007), in which LRT combined with traffic sources was identified by the presence of As, Zn, Pb and K. Finally, a correlation between Pb, Sb, and Cd was used to identify LRT sources in (Pakkanen, et al., 2001).

I.5.2.1.7. Biomass combustion

Tracing the biomass combustion emissions using metals concentrations is more difficult since one major metal is used in order to identify biomass or wood combustion: K. The problem reside within the use of this element to trace many other sources as well, especially industrial combustions and works, which will be discussed later. Potassium was used as marker of biomass combustion in Helsinki (Ilacqua, et al., 2007) and in Estonia (Orru, et al., 2010) as well. Furthermore, it can be used also to trace wood combustion emissions (Vallius, et al., 2003). Finally, to be able to better determine wood or biomass combustion sources, we must consider organic species (like organic carbon “OC”) as well as the presence of high K content in PM. Also, between the different organic components, levoglucosan has been proved to be a suitable marker for biomass combustion in PM (Favez, et al., 2009).

I.5.2.1.8. Industry

Industrial emissions tracing can be one of the most challenging tasks when studying PM sources in the environment. The problem is within the complexity of separating the many different origins of industrial emissions. In an industrial complex, many activities may load the atmosphere with PM that has a close chemical composition, especially heavy metals combinations. For example, Pb and Cr correlations were used to trace industrial gasoline and oil refinery sources ((Gotschi, et al., 2005) and (Rajsic, et al., 2008)). In Madrid, industrial activities were identified by the presence of Cr, Ni, Pb, and Zn (Salvador, et al., 2012). In some cases, a combination of many elements (Zn, Mn, K, and Fe) with gases measurements (SO₂) can be used to trace industrial and incineration activities (Vallius, et al., 2005).

We will discuss hereafter examples about tracing some industrial activities that are contributing significantly to PM loads:

I.5.2.1.8.i. Steel works

In tracing steel works emissions, (Oravisjarvi, et al., 2003) found that K can be used to trace sintering works, Zn to trace smelting, and Cu for mechanical works. On the other hand:

Pb, Zn, Mn, Cd, and As were found to constitute a signature for steel works activities in Spain (Moreno, et al., 2006).

Also by combining the chemical composition of PM_{2.5} in the vicinity of a steel plant along with Factor Analysis-Multiple Linear Regression model (FA-MLR), (Oravisjarvi, et al., 2003) have found that Ca, Cd, K, Na, Pb and Cl were correlated. Therefore, they can be used as tracers for sintering works. The same reasoning was used to trace the influence of steelmaking plant emissions by using Co, Fe, Li, Mn, Zn and F as tracers.

On the other hand, (Dall'Osto, et al., 2008) studied the size distributions and the chemical characterization of PM in a region affected by a large integrated steelworks. They confirmed the presence of Fe, Pb, Zn and Ni when being under industrial influences, and the concentration of these metals in the micron and sub-micron modes.

Furthermore, SEM-EDX technique was used to uncover iron-rich spherical particles loads in blast furnaces and steel making plant emissions ((Moreno, et al., 2006) and (Hleis, et al., 2013)). This feature can also be used to trace industrial activities as well.

Finally, coke plants emissions seems to be signed by OC, EC, SO₄²⁻, As, and Se ((Weitkamp, et al., 2005) and (Jiun-Horng, et al., 2007)).

1.5.2.1.8.ii. Petro-chemistry

Nickel can be used to trace this source of PM (Freitas, et al., 2005). In addition to Ni, other metals can be used together to trace petrochemical PM emissions, such as V, Pb, Zn, Cr, and Co (Moreno, et al., 2006).

1.5.2.1.8.iii. Metallurgy and Pigment industry

Metallurgic activities were found to increase the concentrations of As, Cu, Pb, and Zn in PM_{2.5} in Spain, whereas Cr, Mo, Ni, and Co along with As and Cu constituted a fingerprint for pigment industry (Moreno, et al., 2006), as well as Ti which is concentrated in the primary product of pigment industries.

1.5.2.1.8.iv. Cement industry

On the influence of the cement industry, Al, Si, Ca, SO₄²⁻, K, Mg, and Sr can be considered as highly associated in atmospheric PM originated from cement factories (Santacatalina, et al., 2010). Nevertheless, the abundance of mineral species in this profile makes the separation between cement production and re-suspended soil dust a very difficult task. On the other hand, (Gutierrez-Cañas, et al., 2005) proceeded by studying emissions raw feed enrichment factor, and found that Cd, Pb, As, Cu, Sb, and Tl were mostly enriched

compared to clinker raw feed. The same study explained the existence of a difference in metals emissions from this type of industrial activity related to solid fuel conversion processes.

I.5.2.1.8.v. Glassmaking industry

Particulate matter emissions from this type of industries contain numerous elements. A first group includes Al, Ti, Ca, Mg, Fe, Mn, Sr, Rb and Ba, which are concentrated in the ore used to produce glass ((Rampazzo, et al., 2008) and (Mantovan, et al., 2003)). Other elements can also be emitted from other levels within the production line, especially after using specific elements for product composition improvement and/or for coloring (Li, Zn, Ag, Se, Cd, Sb and Pb). After Mantovan (Mantovan, et al., 2003), As, Se and Cd can serve as a “finger print” of the glassmaking factory in Murano (Italy).

I.5.2.1.9. Ships, ship yards, and harbor

Up to our knowledge, few studies dealt with the emissions from shipping transportation and/or harbor activities. Ship yard activities were traced by (Moloi, et al., 2002) using Ca – Ni correlations. In Helsinki (Finland), a combination of black carbon (BC), Zn, K, Ni, and V were used to identify oil combustion and ships emissions (Pakkanen, et al., 2001). It seems that Ni and V are commonly used to trace heavy oil combustion and ships activities that might include oil combustion emissions itself. Finally, Fe, Ni, V, Ca, and Ba were linked to use of petrol and/or oils (Moldanová, et al., 2009).

I.5.2.2. Sources and contribution of ions in PM_{2.5}

Ionic composition plays a major role in defining the anthropogenic contributions in the load of fine PM_{2.5}, but also to the chemical composition of these particles. In many studies around the world, soluble metals and other ions were analyzed to uncover natural and human contributions in PM emissions. Between the different ions present in the aerosols, Cl⁻, Na⁺, Mg²⁺, SO₄²⁻, NO₃⁻, and NH₄⁺ constitute the most important species in terms of abundance and significance in tracing natural and pollution activities described hereafter.

I.5.2.2.1. Sea spray

As defined in section I.2.2.1.2, sea salts are generated by oceanic spray, and therefore are considered as natural aerosols. Many studies identified sea salt within sampled particles by studying Na and Cl correlations. Some studies added Mg ((Pakkanen, et al., 2001) and (Salvador, et al., 2012)) or Mg and K (Ilacqua, et al., 2007).

Within this category of aerosols we can distinguish between “fresh sea salt” and “aged sea salt”. The first type is directly emitted from the sea, in which ions such as sea- SO_4^{2-} , Na^+ , Cl^- , Mg^{2+} , K^+ and Br^- are concentrated in the aerosol with proportions similar to the ones found in sea water. However, once fresh sea salt passes over a polluted region, the relatively acidic atmosphere created by the anthropogenic emissions (such as HNO_3 and H_2SO_4) in the atmosphere of the region will force a reaction between these acidic species and the sea salt. This reaction results in the decrease in the concentrations of Cl^- and Br^- , which will be transformed into gaseous HCl and HBr (Delmas, et al., 2007). On the other hand, the reaction will increase anions such as NO_3^- and SO_4^{2-} in this secondary aerosol, also known in that phase as “aged sea salt”.

I.5.2.2.2. Traffic related ions

In the use of ions to determine contributions, NO_3^- ions were found to point at traffic sources (Gotschi, et al., 2005). Ionic loads can also result from distant sources and get to specific sites with LRT. Within this category, non-sea SO_4^{2-} ions constitute a signature for traffic-LRT (Oravisjarvi, et al., 2003). In another study, ion rich LRT aerosols were identified in a rural environment with an important SO_4^{2-} and NH_4^+ load (Pakkanen, et al., 2001).

I.5.2.2.3. Secondary inorganic aerosols

Secondary inorganic aerosols were identified in Spain, where SO_4^{2-} , NH_4^+ , and V constituted the secondary sulfates aerosols (Salvador, et al., 2012). In this same study, secondary nitrates were found to be constituted mainly by NO_3^- and NH_4^+ ions. Also, within the category of secondary sulfates, non-sea SO_4^{2-} are found abundant and can point at regional sources of pollution (Vallius, et al., 2005).

Finally, the contribution of ions in fine $\text{PM}_{2.5}$ mass can fluctuate depending on the sources, but it is always found exceeding that of metals. For example, SO_4^{2-} and NO_3^- combined to Na^+ and NH_4^+ was found to contribute in about 70% of $\text{PM}_{2.5}$ (Yin & Harrison, 2008). On the other hand, a 47% contribution of $\text{SO}_4^{2-} / \text{NO}_3^- / \text{NH}_4^+$ in $\text{PM}_{2.15}$ was found to be generated from diesel traffic emissions (Hitzenberger, et al., 2006). Also, many studies proved that ionic loads in fine PM are not exclusively generated locally, but mostly on a regional level. In some cases rural sites may have higher levels than distant light traffic sites in the same region. Researchers have found that $\text{SO}_4^{2-} / \text{NO}_3^- / \text{NH}_4^+$ proportion in fine PM had increased from 36%, to 38%, and rose to 42% in “light-traffic”, “traffic-industrial”, and rural site respectively (Pateraki, et al., 2012). The reason behind the elevation of ions levels at the rural site was linked to regional pollution sources instead of the local sources. Furthermore,

SO_4^{2-} , NH_4^+ , and K^+ ions were found to constitute over 85% of $\text{PM}_{2.5}$ in Lecce, southern Italy (Perrone, et al., 2011). Thus we can conclude the importance of surveying ionic species concentrations in $\text{PM}_{2.5}$ to be able to explain the load of particles as well as to trace local and distant source emissions. Its importance doesn't close down at this level, but it expands to the fact that these chemical forms constitute a major part of fine PM, as discussed earlier in this section, when compared to metals whose contribution in the PM mass is found relatively smaller.

I.5.2.3.Sources of carbon

The carbon content is divided between two major types: organic carbon (OC) and elemental carbon (EC). The latter is also known as black carbon or soot. The sum of OC and EC content in PM gives the total carbon content (TC). EC and OC can be emitted directly and simultaneously into the atmosphere from combustion sources, whereas OC can have other origins such as photochemical reaction of gaseous precursors in the atmosphere. The variations between TC, OC, and EC in relation to the influence of pollution sources will be discussed hereafter.

TC content in $\text{PM}_{2.5}$ fluctuates depending on nearby sources of pollution. It can vary from 23% to 37% in some cases (Yin & Harrison, 2008). In Lecce, southern Italy, TC made about 29% (with a max getting to 50% in some samples) of $\text{PM}_{2.5}$ (Perrone, et al., 2011). In this same study, OC and EC concentrations ranged between 2 - 13 $\mu\text{g}/\text{m}^3$ and 0.4 - 5 $\mu\text{g}/\text{m}^3$ respectively. Furthermore, EC and OC contents were investigated in 6 European cities in 2006 (Sillanpaa, et al., 2006) to find that these components constituted the major load of chemicals in $\text{PM}_{2.5}$, with OC always having the highest contribution when compared to EC: 31% (OC) to 9% (EC) in Duisburg; 54% (OC) to 5.7% (EC) in Prague; 23% (OC) to 5.4% (EC) in Amsterdam; 46% (OC) to 8.4% (EC) in Helsinki; 21% (OC) to 7.6% (EC) in Barcelona; 35% (OC) to 6.6% (EC) in Athens (Sillanpaa, et al., 2006).

OC can be found more concentrated than EC in $\text{PM}_{2.5}$ when sampling is located next to a traffic site. This was verified in (Pateraki, et al., 2012), where three types of sites was studied: light traffic, traffic and industry, and a distant control site. In this latter, OC and EC contents were 11% and 4% respectively, showing that at the less influenced site OC was higher than EC. However, at the light traffic site, OC and EC were found to constitute 18% and 3%, which verifies the effect of traffic on OC concentrations. However, the second site influenced by industrial emissions as well as traffic, EC concentrations rose to almost match

the OC content (OC = 17% and EC = 15%) showing that traffic emissions contributed in OC when industrial emissions raised EC concentrations.

In another study, a comparison between diesel and gasoline traffic was studied (Hitzenberger, et al., 2006). Diesel traffic was found to increase EC/TC ratio when compared to gasoline traffic ratio.

Finally, a mixture of combustion emissions can also be identified using carbon concentrations. For example, good EC correlations with Zn, K, V, and Ni pointed at local traffic and ships emissions contributions in Helsinki (Pakkanen, et al., 2001).

I.5.3. Health effects of fine PM inhalation

Studies about the health effects of PM inhalation focused on many adverse effects from which asthma, increase in lung cell permeability, oxidative stress on DNA, and cardiovascular / respiratory / cerebrovascular diseases were the most important. Furthermore, and as discussed earlier in section I.4.3, the effects of inhalation can also lead to the appearance of chronic diseases such as cancer. On the other hand, focus has also been given to the inhalation mode of particles, mostly to outdoor and indoor exposure scenarios.

London smog in 1952 marked a starting point of the interest in the relationship between pollution and health effects. Afterwards, researches on the health impacts of particles inhalation increased significantly specially in the 90's. Important associations were found between PM₁₀, black smoke, and sulfate concentrations and the prevalence of symptoms of the lower respiratory tract in children living in Netherlands (Saskia, et al., 1999). On the other hand, severe inflammatory responses and extensive lung injuries were observed in mouse lung as a response to the soluble fraction of collected ultrafine particles (Ian, et al., 1999). Furthermore, investigations on the effect of traffic related emissions were conducted to find that cough, wheeze, runny nose, and doctor diagnosed asthma were significantly reported for children living within 100 m from a freeway (Patricia, et al., 1997). In addition, carbon black particles toxicity on rodent lung epithelial cells was found increasing with the increase in the total surface and the decrease in the size of carbon particles (Murphy, et al., 1999).

On the exposure to fine PM, outdoor personal exposure was linked to the transportation mode in use. Passengers in cars and buses were found to be more exposed to high concentrations of PM compared to cyclers and people walking on sidewalks (Kaur & Nieuwenhuijsen, 2009), to conclude that the location and duration of exposure is a factor to be considered. Furthermore, indoor versus outdoor exposure to PM was studied in (Buonanno, et al., 2011). In this study, females were more exposed to PM while cooking,

when men were exposed in working time, and finally children were mostly exposed to emissions from transportation traffic.

Combustion related PM exposure were associated to respiratory mortality (PM_{2.5}), and cardiovascular and cerebrovascular mortality (PM₁). Furthermore, red-ox metals content of this fine PM contributed in the oxidative stress of human cells (Perez, et al., 2009).

Traffic exposure and effects of traffic emitted particles were extensively studied. On this subject, traffic exhaust was found to induce DNA oxidative stress, and was verified using 8-hydroxydesoxyguanosine (8-OHdG) as a tracer for the effects of such emissions (Lai, et al., 2005). Furthermore, emissions from combustion in vehicles were found to increase the risk of asthma in children (up to 14 years of age). Concentrations of PM_{2.5}, EC and OC, and SO₄²⁻ increased the risk of asthma by 6%, 7.4%, and 2.1% respectively in that age group (Anderson, et al., 2001). Also, Zn and S rich PM emitted with tire debris were found to alter the morphology and proliferation of alveolar cell line A549, accumulate in human liver cell line HepG2, and cause malformations in *X. Laevis* frog embryos (Gualtieri, et al., 2005).

Respiratory and cardiovascular diseases were found linearly linked to exposure of elderly people to LRT – PM₁₀, whereas pediatric asthma was associated to the exposure to NO and accumulation mode PM emitted mainly from traffic (Andersen, et al., 2008). Another example on traffic effects can be observed in Spain, where a linear relationship was found between PM_{2.5}, NO, circulatory problems, heart disease, and cardiovascular problems (Maté, et al., 2010). Also, the inhalation of smoke was found to increase the levels of Clara Cell protein CC16, which is an indicator of lung cell permeability (Timonen, et al., 2004).

On a global European level, a recent study on the effects of fine PM was conducted in 25 European cities. In its summary report (Aphekom, 2011), many results were illustrated on the effects of reducing PM_{2.5} emissions, exposure to PM_{2.5}, and SO₂ emissions on population health and the economy in Europe. This works outcome showed that a decrease to a level of 10 µg/m³ in PM_{2.5} concentration (WHO annual mean; see section I.4.2) could add up to 22 months of life expectancy for adults older than 30 years of age, depending on the city in which they are mostly exposed. On the other hand, exceeding the WHO guideline for this size fraction will eventually lead to 19000 deaths, 15000 of which from cardiovascular diseases, and about €31.5 billion in health and related costs. The study also showed the positive feedback of sulfur reduction in fuels in 20 cities, in which 2200 premature deaths valued at €192 million were prevented. And finally, the report summarized the effects of PM inhalation on the human body (Figure 24).

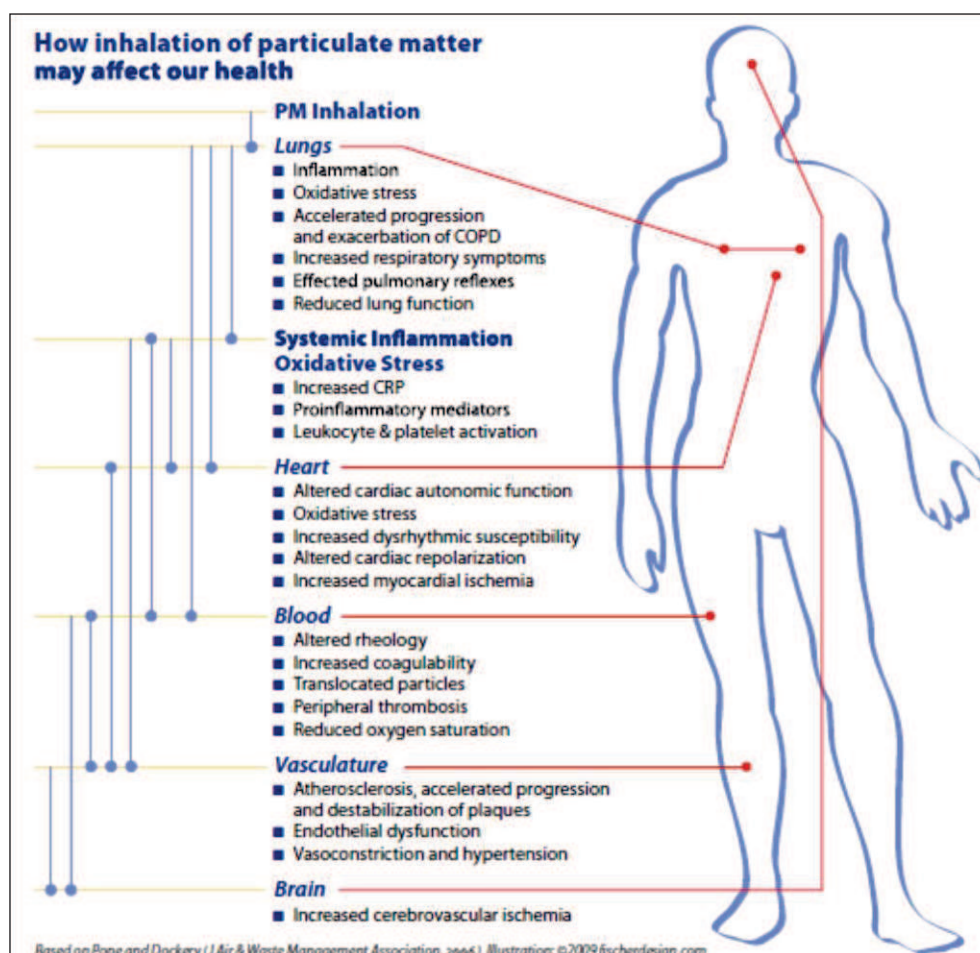


Figure 24: Summary of the major adverse health effects of PM inhalation on the human body (Aphekom, 2011)

I.6.The situation in the Nord-Pas de Calais (NPdC) region

The NPdC region (12414 km²), which is concerned by this study is located on the northern coastline border of France (Figure 25). The coastal side of the region stretches between two regional seas: English Channel and North-Sea. The coastal side of this area is called the “Littoral Côte d’Opale”, and the whole region is known for its high industrial and agricultural activities, but also for the high urbanization characterized by a dense population (ATMO, 2010). Its location close to the sea makes winter temperatures relatively acceptable, with a high average of wind velocity. This climatic condition favors pollutants dispersion, except when sea breeze occurs, during which pollutants accumulate above the coastal zone.

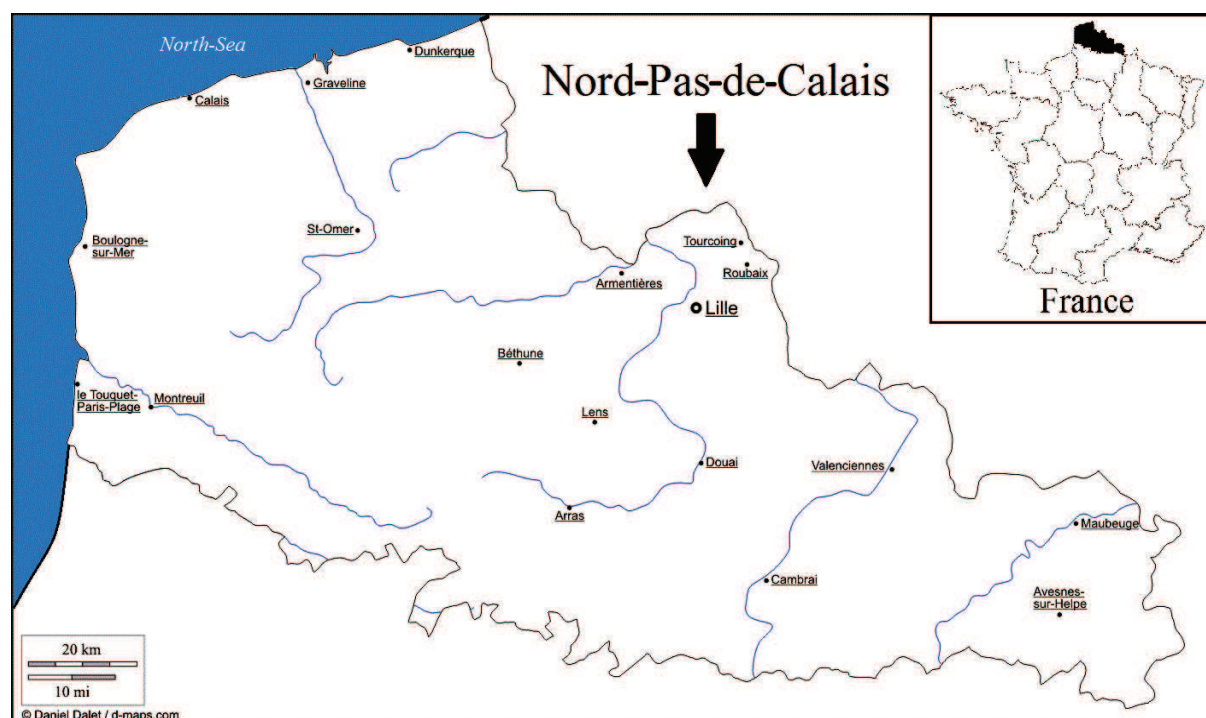


Figure 25: Map of France (upper right corner) and the “Nord Pas de Calais” region; reproduced from (CarteFrance, 2012) and (Dalet, 2012)

Furthermore, the region is considered to have one of the highest transportation activities including on-road and maritime. This high urbanization, industrialization, and geo-strategic trading location of the region lead to important loads of pollutants emitted by these different activities, from which we are interested mostly in atmospheric PM. This upload resulted in the submission of about 835 establishments to pollution taxes known as: *Taxe générale sur les Activités Polluantes* (TGAP). Furthermore, 43 establishments were classified as having high threshold and 34 as low threshold of pollution release, the majority of which are located in Dunkerque (one of the most industrialized site in France), Calais, and an ancient mining basin (ATMO, 2011).

Finally, transportation routes, high activity areas, and cities represent about 13% of the NPdC terrain surface, which proportionally is the most urbanized region (8.3%) when compared to the rest of France (ATMO, 2011).

I.6.1. Emissions of PM in NPdC

In this section we will discuss the emissions of particles from anthropogenic sources in the NPdC region, with emphasis on recent data, as well as on the emissions in different cities within the region, particularly: Dunkerque, Boulogne-sur-Mer and Saint-Omer. These three

cities are the main focus of this study, and are subjected to different kinds of pollution sources.

The declared total industrial dust emissions in the NPdC region represented in Figure 26 shows a gradual decrease in the scale of emissions between 2004 and 2009, after which we can observe a light increase.

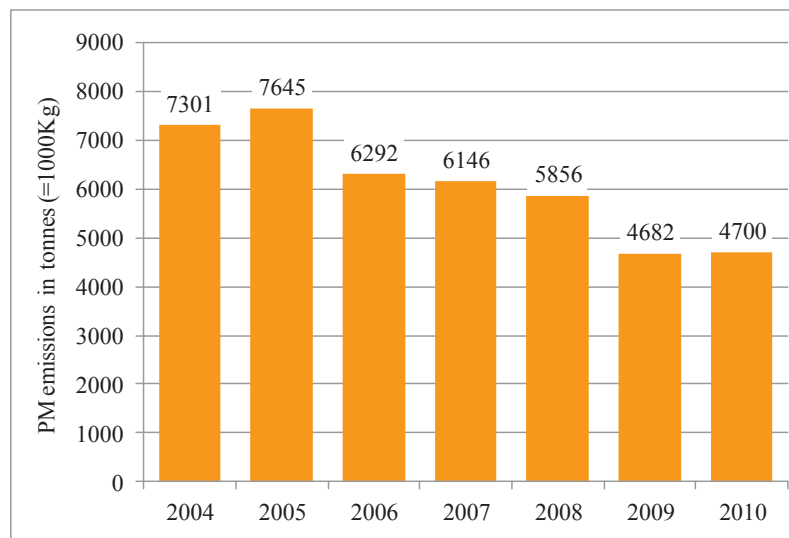


Figure 26: Declared industrial PM emissions trend from 2004 till 2010 in the NPdC region (DREAL, 2011)

Dust emissions from different industrial sectors prove the magnitude of the industrial emissions contributions in the NPdC, and specifically in the industrialized site of Dunkerque. Figure 27 shows dust emissions evolution for each of the most important industries in NPdC. By analyzing the chart, we notice that the emissions are relatively decreasing for ArcelorMittal and EDF, when it is fluctuating around a stable level for SRD and Al Dk. In addition, we should note that Arcelor Mittal, SRD, and Al Dk are all located in Dunkerque. This proves the importance of Dunkerque's site as a first choice for air quality study.

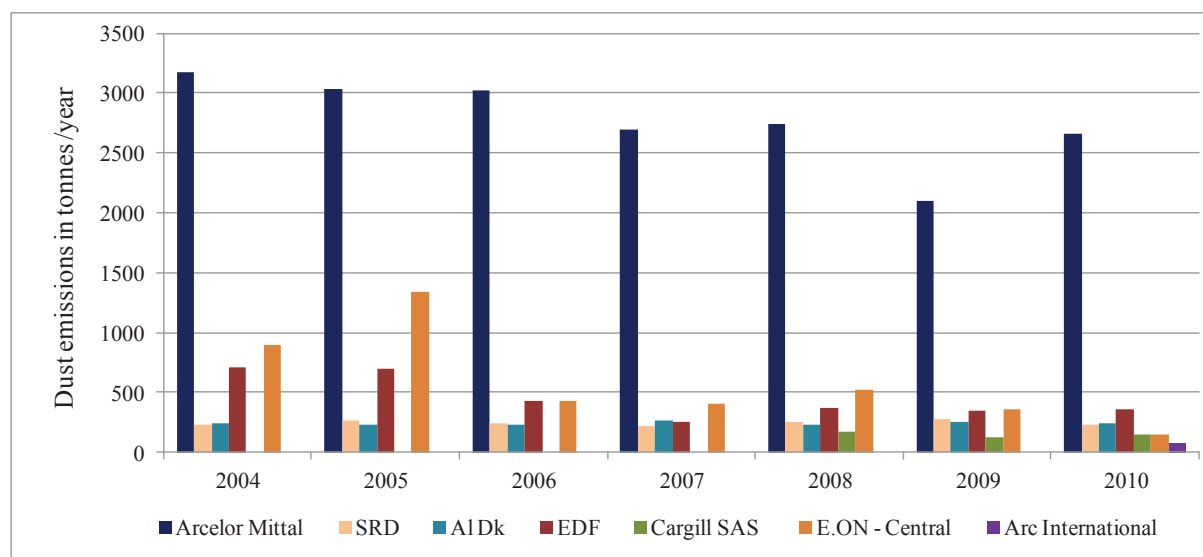


Figure 27: Some of the industrial dust emissions in the NPdC department; SRD = Société de Raffinerie de Dunkerque, Al Dk = Rio Tinto Dunkerque, EDF = Electricité De France (Bouchain), Cargill SAS (Haubourdin), E.ON – Central (Hornaing), Arc International (Arques); source (DREAL, 2011)

I.6.2. Air quality in the NPdC region

I.6.2.1. PM level

Annual mean concentrations trend for some urban and industrial-urban cities within the NPdC region were acquired (Ministère de l'Écologie, 2012) for a period stretching between 2002 and 2009, and were illustrated in Figure 28. Between the studied cities, we chose the following: Dunkerque, Boulogne-sur-Mer, Saint-Omer, Bethune and Lille (see Figure 25). The first three represent the sites that are the subject of this study, whereas “Bethune” is an inland rural site less influenced by pollution sources and is similar to “Saint-Omer”, and finally “Lille” is the most urbanized city between the others in the NPdC region.

Dunkerque is found to have the highest PM_{10} mean concentration between the other cities except in 2009, when “Lille” and “Saint-Omer” had higher values. Dunkerque is a highly industrialized site, which explains the elevation in the PM_{10} mean concentrations over the years to pass over the levels at “Lille”, which is largely more urbanized than “Dunkerque”. However, the decrease in 2009 might be related to world economic crisis that highly affected the industrial sector. The lack of data in “Saint-Omer” before 2006 makes us wonder about its comparison to “Bethune” and “Boulogne-sur-Mer”. However, the data collected in 2007, 2008 and 2009 shows that the city is more concentrated in PM_{10} when compared to the other two. Finally, Boulogne-sur-Mer annual mean decreased significantly between 2007 and 2009.

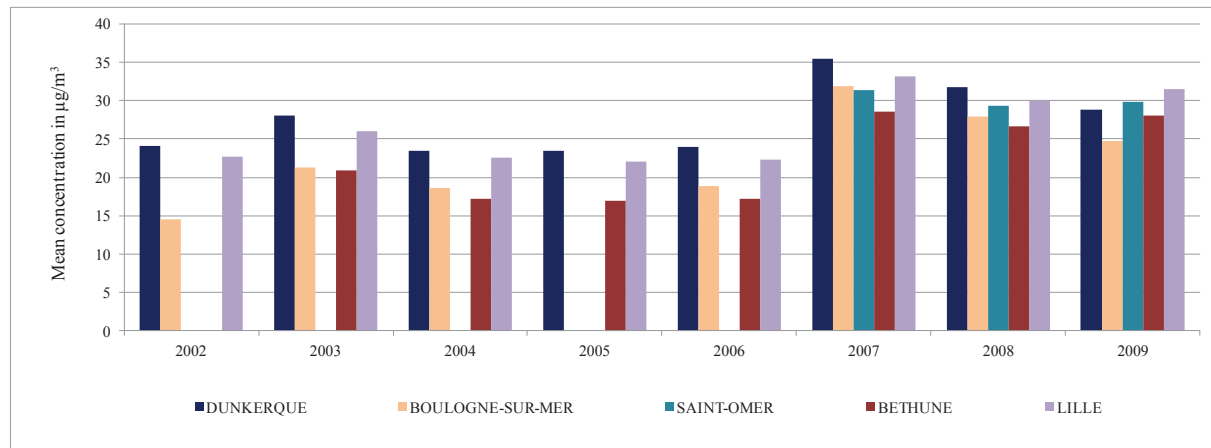


Figure 28: Annual mean concentration of PM₁₀ in Dunkerque, Boulogne-sur-Mer, Saint-Omer, Bethune, Lille, and in µg/m³; source (Ministère de l'Écologie, 2012)

In January 2007, a new PM₁₀ measuring methodology was adopted and installed in different air monitoring networks. This modification aimed at adjusting the French monitoring results to match the criteria defined in the European method by considering the amount of volatile compounds for the concentration measurements. The change affected daily and annual concentrations that were found higher. This increase stands behind the elevation beyond limit values.

I.6.2.2. PM daily limit exceedance

In France, the daily PM₁₀ limit value (50 µg/m³) was the subject of intensive monitoring in the past few years. It has been noticed that the 35 days of exceedance per year allowed were exceeded in many French regions like Ile de France, Rhone-Alpes, Alsace, Provence Alpes Côte d'Azur and Nord Pas de Calais (Figure 29).

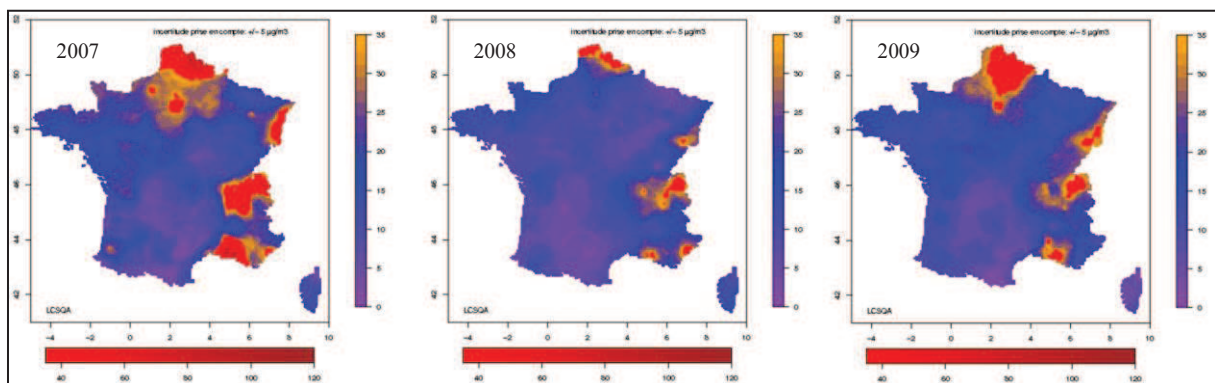


Figure 29: Map of the regions (in red) representing more than 35 days of PM₁₀ daily limit (50 µg/m³) exceedance between 2007 and 2009 in France (Source: LCSQA)

The situation was relatively alleviated in 2010, which can be partially explained by the meteorological conditions that favored atmospheric particles dispersion.

However, exceedance episodes were identified on a regional level in NPdC, from which 14 days of particulate pollution have lead to raise the alarm of the “procédure d’information et de recommandation (PIR)”. In 2011, a total of 35 days of PIR were detected during winter and the beginning of spring.

I.6.2.3. Physicochemical characteristics of PM and its origins

The “Littoral Côte d’Opale” region is highly industrial as well as urbanized, therefore is influenced by many atmospheric PM pollution sources. The emissions of these PM can originate from different sectors such as residential, industrial, transport, natural... etc, but also natural emissions which are mostly emitted by sea spray due to the coastal aspect of the region. Many studies have been conducted in the region in order to uncover the chemical composition of these emissions, but also to understand their possible toxicity on humans.

These studies were conducted majorly within the research strategy of the “Institut de Recherches en Environnement Industriel” (IRENI), which constitutes a multidisciplinary research program that is focused on the study of air quality by following three major research axes:

- Air quality: metrology, modeling and remediation
- Health effects of atmospheric pollution
- Legislative and socio-economic impacts

All these actions are conducted by scientists related to many higher education establishments of the NPdC region: Université de Lille 1, Université de Lille 2, Université d’Artois, Université du Littoral Côte d’Opale and École des Mines de Douai.

On the chemical composition of PM in the “Littoral Côte d’Opale” region, (Ledoux, et al., 2002) and (Ledoux, et al., 2006) studied the chemical properties of paramagnetic Fe^{3+} and Mn^{2+} in aerosols collected in Wimereux and Boulogne-sur-Mer respectively. The latest showed that paramagnetic species concentrations increased with wind coming from the continental sector. On the other hand, more focus was given to the city of Dunkerque due to the multiple pollution sources present in and around the city. Hence, using Electronic Paramagnetic Resonance (EPR), Fe^{3+} ions were found in agglomerated form within aerosols coming from the industrial wind sector. In the same time, the study evidenced that agglomerated iron was found within the coarse PM fraction compared to the iron clusters found in the fine fraction (Ledoux, et al., 2004). Atmospheric aerosols concentrations in

Dunkerque were found higher in winter when compared to summer (Ledoux, et al., 2006). Furthermore, metals such as Al, Ba, Fe, Pb, and Ti were found highly concentrated with winds originating from the industrial sector in the summer and with urban wind sector in the winter. In the same study, it was found that 27% of iron was mainly resulting from industrial activities, whereas Zn high concentrations originated from a continental sector. Finally, LRT aerosols were found to highly contribute in the loads of SO_4^{2-} , NO_3^- , and NH_4^+ .

Other studies were directed towards uncovering specific tracers of steelmaking ((Lamaison, 2006) and (Hleis, 2010)). Moreover, these studies focused on the physicochemical characteristics of samples collected at the sources of emissions as well as in the ambient air under the same sources sectors. In addition, the evaluation of the impacts of these industrial emissions on ambient air levels of PM was evaluated using receptor modeling namely: positive matrix factorization (Lamaison, 2006) and non-negative matrix factorization (Hleis, 2010). These studies uncovered a moderate contribution of industrial sources in the levels of PM_{10} . On the other hand, the modeling proved that the loads of certain metals (Fe, Mn, Pb and Cd) are majorly resulting from industrial contributions.

In addition, (Cazier, et al., 2011) found that $\text{PM}_{2.5}$ collected in Dunkerque were loaded with Zn that is originated from nearby industries and tyre wear, but also with Mn from Fe-Mn production site nearby, Ca in CaCO_3 form, and Mg-K from crustal and marine sources.

The toxicity of airborne $\text{PM}_{2.5}$ was studied in Dunkerque to find that industrial and motor traffic related PM increased oxidative stress and inflammatory responses on L132 epithelial lung cells (Garçon, et al., 2006). On the other hand, reactive oxygen species as well as protein secretion of inflammatory mediators were increased due to the exposure of BEAS-2B human bronchial cells to $\text{PM}_{2.5}$ collected in Dunkerque. These reactive oxygen species point at an increase in oxidative damage and bronchial inflammation respectively (Dergham, et al., 2012).

I.7.Hypothesis and objectives

The NPdC region is a section of the French zones exhibiting high levels of suspended particles which are regularly recorded by official air monitoring network stations. On the other hand, the recorded atmospheric levels of PM₁₀ show that concentrations increased above the limit values many times since 2007, in particular during the winter season and at the beginning of spring. This seasonal increase was also observed in other regions in France, such as in Ile de France and Rhône-Alpes. For these reasons, at the beginning of 2011, the European Committee ranked France in a contentious situation due to the disrespect of the environmental legislation concerning the daily average limit value. In addition to the European context, there is an increasing need to understand the reason behind these above limit values levels on the French national level. Therefore, it is necessary to assemble enough scientific data in order to provide answers for the questions raised on both national and European levels.

In parallel, the legislation on the limit values of PM_{2.5} (Directive-2008/50/EC) evolved since 2010 and will be roofed to 25 µg/m³ in January 1st, 2015. In addition, we remind that an objective of 10 µg/m³ (annual mean) is under scope as a long term atmospheric level to be attained for an adequate protection of human health.

Until now, few studies had been conducted on the exposition level to fine PM in NPdC cities. Furthermore, the continuous monitoring of PM_{2.5} concentration trends is not yet matched by chemical analysis. Hence, a real deficiency in the knowledge on the chemical composition of this fraction is factual, especially in the region where the exposition to regular road traffic, domestic or industrial emissions is the most prominent.

In this study, we intend to study the chemical composition and origins of PM_{2.5} in average sized cities located next to the littoral facade of the region (Dunkerque, Boulogne-sur-Mer and Saint-Omer). In fact, up to our knowledge, no studies were conducted on the chemical composition and origins of PM_{2.5} in this region especially in Boulogne-sur-Mer (coastal) and in Saint-Omer (40 km inland) except some studies in Dunkerque.

There are many reasons standing behind our choice of these three cities:

- Dunkerque is an urban-industrial site that could be influenced by urban, industrial and marine sectors.
- Boulogne-sur-Mer represents a urban background coastal city that is subjected to a main marine influence, but does not include any industrial PM emitters.

- Saint-Omer is an urban center located inland and could be influenced by marine wind intrusions similarly to the first two sites. The city encloses an industrial site and is surrounded by vast agricultural lands.

The principal objectives of this work aim at:

- Acquiring knowledge on the chemical composition of $PM_{2.5}$, like ionic species, major metallic and trace elements and carbonic fraction.
- Identifying different particles sources of emissions
- Constructing spatial/chronological trends of PM composition and comparing the levels of exposition from one city to another.
- Evaluating the contribution of natural versus anthropogenic levels in the load of atmospheric suspended $PM_{2.5}$.

In order to accomplish these objectives, this study was divided into three successive actions performed following this sequence:

- 1) Sampling of $PM_{2.5}$ in three cities of the NPdC region: Dunkerque, Boulogne-sur-Mer and Saint-Omer. In details, two mid-daily sampling campaigns (winter and spring) will be realized, each of which in two sites simultaneously:
 - a. Winter campaign: will be achieved in Dunkerque and Boulogne-sur-Mer
 - b. Spring campaign: will be achieved in Dunkerque and Saint-Omer
- 2) Detailed chemical characterization of the samples, with a focus on ionic species, major elements, trace elements and total carbon. The variations interpretations, including spatial/chronological trends, will be achieved taking into account the meteorological conditions as well as the air masses origins.
- 3) Identification of emissions sources by means of receptor modeling: a method based on a non-negative matrix factorization principle. This latter was developed by Dr G. Delmaire and Dr G. Roussel (LISIC, ULCO), who are experts in signal analysis and with which the UCEIV laboratory collaborates to offer its expertise in the environmental approach as well as the chemical tracing of the sources. This type of models is widely used in source apportionment studies. On one hand, it identifies emissions source profiles and quantifies the contributions of these profiles.

I.8. Works Cited

- Alastuey, A., Querol, X., Rodriguez, S., Plana, F., Lopez-Soler, A., Ruiz, C., & Mantilla, E. (2004). Monitoring of atmospheric particulate matter around sources of secondary inorganic aerosol. *Atmospheric Environment*, 38(30), 4979-4992.
- Andersen, Z. J., Wahlin, P., Raaschou-Nielsen, O., Ketzel, M., Scheike, T., & Loft, S. (2008). Size distribution and total number concentration of ultrafine and accumulation mode particles and hospital admissions in children and the elderly in Copenhagen, Denmark. *Occup Environ Med*, 65, 458-466.
- Anderson, H. R., Bremner, S. A., Atkinson, R. W., Harrison, R. M., & Walters, S. (2001). Particulate matter and daily mortality and hospital admissions in the west midlands conurbation of the United Kingdom: associations with fine and coarse particles, black smoke and sulphate. *Occup Environ Med*, 58, 504-510.
- Andrea, M. (1995). *Climatic effects of changing atmospheric aerosol levels. Future climates of the world: a modelling perspective*. (Elsevier, Ed.) A. Henderson-Sellers.
- Antonio, M. H., Thomas, K. W., & Robert, H. A. (1998). On-road emissions of particulate polycyclic aromatic hydrocarbons and black carbon from gasoline and diesel vehicles. *Environmental Science and Technology*, 32(4).
- Aphekcom. (2011). *Summary report of the Aphekcom project 2008-2011*. Aphekcom.
- Arruti, A., Fernandez-Olmo, I., & Irabien, A. (2011). Regional evaluation of particulate matter composition in an Atlantic coastal area (Cantabria region, northern Spain): spatial variations in different urban and rural environments. *Atmospheric research*, 101, 280-293.
- ATMO, N. (2010). *Synthese - Bilan Annuel*. Atmo NPdC.
- ATMO, N. (2011). *Synthese - Bilan Annuel*. ATMO.
- Beslic, I., Sega, K., Cackovic, M., Klaic, Z. B., & Bajic, A. (2008). Relationship between 4-day air mass back trajectories and metallic components in PM10 and PM2.5 particle fractions in Zagreb air, Croatia. *Bull Environ Contam Toxicol*, 80, 270-273.
- Bigg, E. (1997). A mechanism for the formation of new particles in the atmosphere. *Atmospheric Research*, 43, 129-137.
- Birmili, W., Allen, A. G., Bary, F., & Harrison, R. M. (2006). Trace metal concentrations and water solubility in size-fractionated atmospheric particles and influence of road traffic. *Environ. Sci. Technol.*, 40, 1144-1153.
- Blanchard, D., & Woodcock, A. (1957). Bubble formation and modification in the sea and its meteorological significance. *Tellus*, 9, 145-159.
- Boffa, C., Berra, A., & Rubino, G. (1977). Deposition in the lungs of ultrafine particles. *Annali del l'Istituto Superiore di Sanita*, 13(1-2), 161-176.
- Boogaard, H., Kos, G. P., Weijers, E. P., Janssen, N. A., Fischer, P. H., van der Zee, S. C., . . . Hoek, G. (2011). Contrast in air pollution components between major streets and background locations: Particulate matter mass, black carbon, elemental composition, nitrogen oxide and ultrafine particle number. *Atmospheric Environment*, 45, 650-658.
- Bricard, J., Cabane, M., & Madelaine, G. (1977). Formation of atmospheric ultrafine particles and ions. *Journal of Colloid and Interface Science*, 58(1), 113-124.
- Buonanno, G., Giovinco, G., Morawska, L., & Stabile, L. (2011). Tracheobronchial and alveolar dose of submicrometer particles for different population age groups in Italy. *Atmospheric Environment*, 45, 6216-6224.
- CarteFrance. (2012, September 13). Retrieved from CarteFrance web site: <http://www.cartesfrance.fr/geographie/fond-cartes-france/fond-carte-region.html>

- Cazier, F., Dewaele, D., Delbende, A., Nouali, H., Garçon, G., Verdin, A., . . . Shirali, P. (2011). Sampling analysis and characterization of particles in the atmosphere of rural, urban and industrial areas. *Procedia Environmental Sciences*, 4, 218–227.
- Collet, P. (2011). PM10 : la France poursuivie en justice par l'UE pour non-respect des normes de qualité de l'air. (S. COGITERRA, Ed.) *Actu-Environnement*. Retrieved from <http://www.actu-environnement.com/ae/news/depassements-normes-pollution-air-france-cjeu-12597.php4>
- Cyrys, J., Stolzel, M., Heinrich, J., Kreyling, W., Menzel, N., Wittmaack, K., . . . Wichmann, H.-E. (2003). Elemental composition and sources of fine and ultrafine ambient particles in Erfurt, Germany. *The Science of the Total Environment*, 305, 143-156.
- Dalet, D. (2012, September 13). *d-maps.com cartes gratuites*. Retrieved from d-maps.com: <http://d-maps.com>
- Dall'Osto, M., Booth, M., Smith, W., Fisher, R., & Harrison, R. (2008). A study of the size distributions and the chemical characterization of airborne particles in the vicinity of a large integrated steelworks. *Aerosol Science and Technology*, 42(12), 981-991.
- Davis, D., Hsiao, K., Ingels, R., & Shikiya, J. (1988). Origins of manganese in air particulates in California. *JAPCA*, 38(9), 1152-1157.
- Decree-n°2010-1250. (2010). *Decree-n°2010-1250*. French State Council.
- Delmas, R., Mégie, G., & Peuch, V.-H. (2007). *Physique et chimie de l'atmosphère*. Belin.
- Dergham, M., Lepers, C., Verdin, A., Billet, S., Cazier, F., Courcot, D., . . . Garçon, G. (2012). Prooxidant and proinflammatory potency of air pollution particulate matter (PM2.5–0.3) produced in rural, urban, or industrial surroundings in human bronchial epithelial cells (BEAS-2B). *Chem. Res. Toxicol.*, 25, 904–919.
- Directive-2005/0183. (2005). *Directive 2005/0183*. Official Journal of the European Union.
- Directive-2008/50/EC. (2008). *Directive 2008/50/EC*. Official Journal of the European Union.
- DREAL. (2011). *L'industrie au regard de l'environnement en Nord Pas de Calais - Les chiffres clés*. Retrieved September 14, 2012
- EEA(a). (2012). *Air pollutant emissions data viewer (LRTAP Convention)*. Retrieved June 2012, from European Environment Agency: www.eea.europa.eu
- EEA(b). (2012). *Air quality in Europe — 2012 report*. Luxembourg: Office for Official Publications of the European Union, 2012.
- E-PRTR. (2012, September 14). *The European Pollutant Release and Transfer Register*. Retrieved from E-PRTR: <http://prtr.ec.europa.eu/TimeSeriesPollutantReleases.aspx>
- Favez, O., Cachier, H., Sciar, J., Sarda-Estève, R., & Martinon, L. (2009). Evidence for a significant contribution of wood burning aerosols to PM2.5 during the winter season in Paris, France. *Atmospheric Environment*, 43, 3640–3644.
- Freitas, M., Farinha, M. M., Ventura, M. G., Almeida, S. M., Reis, M. A., & Pacheco, A. M. (2005). Gravimetric and chemical features of airborne PM10 and PM2.5 in mainland Portugal. *Environmental Monitoring and Assessment*, 109, 81-95.
- Gaegauf, C., Hueglin, C., Kunzel, S., & Burtscher, H. (1997). Characterization of wood combustion particles: morphology, mobility, and photoelectric activity. *Environmental Science and Technology*, 31(12), 3439–3447.
- Garçon, G., Dagher, Z., Zerimech, F., Ledoux, F., Courcot, D., Aboukais, A., . . . Shirali, P. (2006). Dunkerque city air pollution particulate matter-induced cytotoxicity, oxidative stress and inflammation in human epithelial lung cells (L132) in culture. *Toxicology in Vitro*, 20, 519–528.
- Gietl, J. K., Lawrence, R., Thorpe, A. J., & Harrison, R. M. (2010). Identification of brake wear particles and derivation of a quantitative tracer for brake dust at a major road. *Atmospheric Environment*, 44, 141-146.

- Gotschi, T., Hazenkamp-von Arx, M. E., Heinrich, J., Bono, R., Burney, P., Forsberg, B., . . . Villani, S. (2005). Elemental composition and reflectance of ambient fine particles at 21 European locations. *Atmospheric Environment*, 39, 5947-5958.
- Gualtieri, M., Andrioletti, M., Mantecca, P., Vismara, C., & Camatini, M. (2005). Impact of tire debris on in vitro and in vivo systems. *Particle and Fibre Toxicology*.
- Guor-Cheng, F., Cheng-Nan, C., Yuh-Shen, W., Peter Pi-Cheng, F., Ding-Guor, Y., & Chia-Chium, C. (1999). Characterization of chemical species in PM_{2.5} and PM₁₀ aerosols in suburban and rural sites of central Taiwan. *The Science of the Total Environment*, 234, 203-212.
- Gutierrez-Cañas, C., Legarreta, J., Larrion, M., Vega, J. R., García, E., & Astarloa, S. (2005). Source signature and HM's Enrichment in PM_{2.5} Emission from Clinker Production. *In the Proc. of The Air & Waste Management Association's 98th Annual Conference & Exhibition*. Minneapolis.
- Hewitt, C., & Jackson, A. (2005). *Handbook of Atmospheric Science: Principles and Application* (1 ed.). Blackwell publishing.
- Hidy, G. M. (1984). *Aerosols, an industrial and environmental science*. Academic Press.
- Hitzenberger, R., Ctyroky, P., Berner, A., Tursic, J., Podkrajsek, B., & Grgic, I. (2006). Size distribution of black (BC) and total carbon (TC) in Vienna and Ljubljana. *Chemosphere*, 65, 2106-2113.
- Hleis, D. (2010). *Evaluation de la contribution d'émissions sidérurgiques à la teneur en particules en suspension dans l'atmosphère à une échelle locale*. Thèse de l'Université du Littoral Cote d'Opale.
- Hleis, D., Fernández-Olmo, I., Ledoux, F., Kfoury, A., Courcot, L., Desmonts, T., & Courcot, D. (2013). Chemical profile identification of fugitive and confined particle emissions from an integrated iron and steelmaking plant. *Journal of Hazardous Materials*, 250–251, 246–255.
- Huges, L. S., & Cass, G. R. (1998). Physical and chemical caraterisation of atmospheric ultrafine particles in the Los Angeles area. *Environmental Science and Technology*, 32(9).
- Ian, A. Y., Heather, P., & Renaud, V. (1999). Pulmonary toxicity of an atmospheric particulate sample is due to the soluble fraction. *Toxicology and Applied Pharmacology*, 157, 43-50.
- Ilacqua, V., Hänninen, O., Saarel, K., Katsouyanni, K., Künzli, N., & Jantunen, M. (2007). Source apportionment of population representative samples of PM_{2.5} in three European cities using structural equation modelling. *Science of the Total Environment*, 384, 77-92.
- INSERM. (1999). *Plomb dans l'environnement: quels risques pour la santé ?* Les Éditions INSERM.
- James, I. C., & Alan, B. R. (1999). A density functional theory study of the hydrates of NH₃-H₂SO₄ and its implications for the formation of new atmospheric particles. *J. Phys. Chem. A*, 103, 2801-2811.
- Jiun-Horng, T., Kuo-Hsiung, L., Chih-Yu, C., Jian-Yuan, D., Ching-Guan, C., & Hung-Lung, C. (2007). Chemical constituents in particulate emissions from an integrated iron and steel facility. *Journal of Hazardous Materials*, 147, 111–119.
- John, S. D., & George, T. D. (1983). Mass and elemental composition of fine and coarse particles in six U.S. cities. *Journal of the Air Pollution Control Association*, 33(12), 1162-1171.
- Kaarle, H., Markku, K., Pasi, A., Kirsti, L., Reijo, V., & Kari, H. (1996). The investigations of aerosol particle formation in urban background area of Helsinki. *Atmospheric Research*, 41, 281-298.

- Kaur, S., & Nieuwenhuijsen, M. (2009). Determinants of personal exposure to PM_{2.5}, ultrafine particle counts, and CO in a transport microenvironment. *Environ. Sci. Technol.*, 43, 4737-4743.
- Kotzick, R., & Niessner, R. (1999). The effects of aging processes on critical supersaturation ratios of ultrafine carbon aerosols. *Atmospheric Environment*, 33, 2669-2677.
- Lai, C.-H., Liou, S.-H., Lin, H.-C., Shih, T.-S., Tsai, P.-J., Chen, J.-S., . . . Strickland, P. T. (2005). Exposure to traffic exhausts and oxidative DNA damage. *Occup Environ Med*, 62, 216-222.
- Lamaison, L. (2006). *Characterisation des particules atmosphériques et identification de leurs sources dans une atmosphère urbaine sous influence industrielle*. Thèse de l'Université des Sciences & Technologies de Lille.
- Ledoux, F., Courcot, L., Courcot, D., Aboukais, A., & Puskaric, E. (2006). A summer and winter apportionment of particulate matter at urban and rural areas in northern France. *Atmospheric Research*, 82, 633-642.
- Ledoux, F., Laversin, H., Courcot, D., Courcot, L., Zhilinskaya, E., Puskaric, E., & Aboukais, A. (2006). Characterization of iron and manganese species in atmospheric aerosols from anthropogenic sources. *Atmospheric Research*, 82, 622-632.
- Ledoux, F., Zhilinskaya, E. A., Courcot, D., Aboukais, A., & Puskaric, E. (2004). EPR investigation of iron in size segregated atmospheric aerosols collected at Dunkerque, Northern France. *Atmospheric Environment*, 38, 1201-1210.
- Ledoux, F., Zhilinskaya, E., Bouhsina, S., Courcot, L., Bertho, M.-L., Aboukais, A., & Puskaric, E. (2002). EPR investigations of Mn²⁺, Fe³⁺ ions and carbonaceous radicals in atmospheric particulate aerosols during their transport over the eastern coast of the English Channel. *Atmospheric Environment*, 36, 939-947.
- Lidia, M., Stephen, T., Dale, G., Chris, G., & Esther, R. (1999). A study of the horizontal and vertical profile of submicrometer particles in relation to a busy road. *Atmospheric Environment*, 33, 1261-1274.
- Liisa, P. (1999). Effects of the increased UV radiation and biogenic VOC emissions on ultrafine sulphate aerosol formation. *Journal of Aerosol Science*, 30(3), 355-367.
- Mantovan, I., Rado, N., Rampazzo, G., & Visin, F. (2003). Correlations among inorganic elements in particulate matter (PM₁₀) in urban area of Venezia-Mestre. *Annali di Chimica*, 93, 421-428.
- Masclat, P., & Cachier, H. (1998). Atmospheric particles: Physicochemical characteristics. *Analisis magazine*, 26(9).
- Maté, T., Guaita, R., Pichiule, M., Linares, C., & Díaz, J. (2010). Short-term effect of fine particulate matter (PM_{2.5}) on daily mortality due to diseases of the circulatory system in Madrid (Spain). *Science of the Total Environment*, 408, 5750-5757.
- Matsumoto, K., & Tanaka, H. (1996). Formation and dissociation of atmospheric particulate nitrate and chloride: an approach based on phase equilibrium. *Atmospheric Environment*, 30, 639-648.
- Mazzei, F., D'Alessandro, A., Lucarelli, F., Nava, S., Prati, P., Valli, G., & Vecchi, R. (2008). Characterization of particulate matter sources in an urban environment. *Science of the total Environment*, 401, 81-89.
- MEDDTL. (2010). *Bilan de la qualité de l'air en France en 2010: et des principales tendances observées au court de la période 2000-2010*. Ministère de l'Ecologie, du Développement Durable, des Transports et du Logement.
- MEEDDAT. (2008). *Ministère de l'Ecologie, de l'Energie, du Développement Durable, et de l'Amenagement du Territoire - Décret n° 2008-1152 du 7 Novembre 2008 relatif à la qualité de l'air*. Paris: Journal Officiel de la République Française. Retrieved

- September 12, 2012, from
<http://www.legifrance.gouv.fr/affichTexte.do?cidTexte=JORFTEXT000019735657>
 Ministère de l'Écologie, d. D. (2012, September 14). *Observations et Statistiques*. Retrieved from Ministère de l'Écologie, du Développement Durable et de l'Énergie - Commissariat général au Développement durable:
<http://www.stats.environnement.developpement-durable.gouv.fr/Eider/tables.do#>
- Moldanová, J., Fridella, E., Popovicheva, O., Tishkova, V., Faccineto, A., & Focsa, C. (2009). Characterisation of particulate matter and gaseous emissions from a large ship diesel engine. *Atmospheric Environment*, 43(16), 2632-2641.
- Moloi, K., Chimidza, S., Selin Lindgren, E., Viksna, A., & Standzenieks, P. (2002). Black carbon, mass and elemental measurements of airborne particles in the village of Serowe, Botswana. *Atmospheric Environment*, 36, 2447-2457.
- Moreno, T., Querol, X., Alastuey, A., Viana, M., Salvador, P., Sanchez de la Campa, A., . . . Gibbons, W. (2006). Variations in atmospheric PM trace metal content in Spanish towns: Illustrating the chemical complexity of the inorganic urban aerosol cocktail. *Atmospheric Environment*, 40, 6791-6803.
- Murphy, S. A., Bérubé, K. A., & Richards, R. J. (1999). Bioreactivity of carbon black and diesel exhaust particles to primary Clara and type II epithelial cell cultures. *Occupational Environmental Medicine*, 56, 813-819.
- Oravisjarvi, K., Timonen, K., Wiikinkoski, T., Ruuskanen, A., Heinanen, K., & Ruuskanen, J. (2003). Source contributions to PM_{2.5} particles in the urban air of a town situated close to a steel works. *Atmospheric Environment*, 37, 1013-1022.
- Orru, H., Kimmel, V., Kikas, Ü., Soon, A., Künzli, N., Schins, R. P., . . . Forsberg, B. (2010). Elemental composition and oxidative properties of PM_{2.5} in Estonia in relation to origin of air masses — results from the ECRHS II in Tartu. *Science of the Total Environment*, 408, 1515-1522.
- Pakkanen, T. (1996). Study of formation of coarse particle nitrate aerosol. *Atmospheric Environment*, 30, 2475-2482.
- Pakkanen, T. A., Loukkola, K., Korhonen, C. H., Aurela, M., Makela, T., Hillamo, R. E., . . . Maenhaut, W. (2001). Sources and chemical composition of atmospheric fine and coarse particles in the Helsinki area. *Atmospheric Environment*, 35, 5381-5391.
- Pateraki, S., Assimakopoulos, V., Bougiatioti, A., Kouvarakis, G., Mihalopoulos, N., & Vasilakos, C. (2012). Carbonaceous and ionic compositional patterns of fine particles over an urban Mediterranean area. *Science of the Total Environment*, 424, 251-263.
- Patricia, v. V., Mirjam, K., Jeroen, d. H., Nicole, J., Hendrik, H., & Bert, B. (1997). Motor Vehicle Exhaust and Chronic Respiratory Symptoms in Children Living near Freeways. *Environmental Research*, 74, 122-132.
- Paul, L. J., Joan, D. M., Thomas, A., Robert, F., Arthur, G., Ronald, H., . . . Nathan, R. M. (1983). The new jersey project on airborne toxic elements and organic substances (ATEOS): a summary of the 1981 summer and 1982 winter studies. *Journal of the Air Pollution Control Association*, 33(7), 649-657.
- Perera, F. (1981). Carcinogenicity of airborne fine particulate benzo(a)pyrene: an appraisal of the evidence and the need for control. *Environmental Health Perspectives*, 42, 163-185.
- Perez, L., Medina-Ramon, M., Kunzli, N., Alastuey, A., Pey, J., Perez, N., . . . Sunyer, J. (2009). Size fractionate particulate matter, vehicle traffic, and case-specific daily mortality in Barcelona, Spain. *Environ. Sci. Technol.*, 4707-4714.
- Perrone, M., Piazzalunga, A., Prato, M., & Carofalo, I. (2011). Composition of fine and coarse particles in a coastal site of the central Mediterranean: Carbonaceous species contributions. *Atmospheric Environment*, 45, 7470-7477.

- Pohlmann, G., Koch, W., Theisen, M., & Niebner, R. (1999). Receptor modelling of urban aerosol. *Journal of Aerosol Science*, 30(I), S763-S764.
- Rajsic, S., Mijic, Z., Tasic, M., Radenkovic, M., & Joksic, J. (2008). Evaluation of the levels and sources of trace elements in urban particulate matter. *Environmental Chemistry Letter*, 6, 95-100.
- Rampazzo, G., Masiol, M., Visin, F., Rampado, E., & Pavoni, B. (2008). Geochemical characterization of PM₁₀ emitted by glass factories in Murano, Venice (Italy). *Chemosphere*, 71(11), 2068-2075.
- Salvador, P., Artíñano, B., Viana, M., Alastuey, A., & Querol, X. (2012). Evaluation of the changes in the Madrid metropolitan area influencing air quality: Analysis of 1999-2008 temporal trend of particulate matter. *Atmospheric Environment*, 57, 175-185.
- Santacatalina, M., Reche, C., Minguillón, M., Escrig, A., Sanfelix, V., Carrat, A., . . . Querol, X. (2010). Impact of fugitive emissions in ambient PM levels and composition: A case study in Southeast Spain. *Science of The Total Environment*, 408(21), 4999-5009.
- Saskia, v. d., Gerard, H., H Marike, B., Jan, S. P., Joop, v. W., & Bert, B. (1999). Acute effects of urban air pollution on respiratory health of children with and without chronic respiratory symptoms. *Occupational Environmental Medicine*, 56, 802-812.
- Schleicher, N. J., Norra, S., Chai, F., Chen, Y., Wang, S., Cen, K., . . . Stüben, D. (2011). Temporal variability of trace metal mobility of urban particulate matter from Beijing - A contribution to health impact assessments of aerosols. *Atmospheric Environment*, 45, 7248-7265.
- Seinfeld, J. H., & Pandis, S. N. (2006). Atmospheric chemistry and physics: from air pollution to climate change - 2nd Edition. United States of America: John Wiley & Sons, Inc.
- Sillanpaa, M., Hillamo, R., Saarikoski, S., Frey, A., Pennanen, A., Makkonen, U., . . . Salonen, R. O. (2006). Chemical composition and mass closure of particulate matter at six urban sites in Europe. *Atmospheric Environment*, 40, S212-S223.
- Strak, M., Steenhof, M., Godri, K. J., Gosens, I., Mudway, I. S., Cassee, F. R., . . . Janssen, N. A. (2011). Variation in characteristics of ambient particulate matter at eight locations in the Netherlands - The RAPTES project. *Atmospheric Environment*, 45, 4442-4453.
- Timonen, K. L., Hoek, G., Heinrich, J., Bernard, A., Brunekreef, B., de Hartog, J., . . . Pekkanen, J. (2004). Daily variation in fine and ultrafine particulate air pollution and urinary concentrations of lung Clara cell protein CC16. *Occup Environ Med*, 61, 908-914.
- USEPA. (2012). *National Ambient Air Quality Standards*. Retrieved June 2012, from United States Environment Protection Agency: <http://www.epa.gov/air/criteria.html>
- Vallius, M., Janssen, N., Heinrich, J., Hoek, G., Ruuskanen, J., Cyrys, J., . . . Pekkanen, J. (2005). Sources and elemental composition of ambient PM_{2.5} in three European cities. *Science of the Total Environment*, 337, 147-162.
- Vallius, M., Lanki, T., Tiittanen, P., Koistinen, K., Ruuskanen, J., & Pekkanen, J. (2003). Source apportionment of urban ambient PM_{2.5} in two successive measurement campaigns in Helsinki, Finland. *Atmospheric Environment*, 37, 615-623.
- Veli-Matti, K., Kimmo, T., Risto, H., & Tuomo, P. (1998). Substitution of chloride in sea-salt particles by inorganic and organic anions. *Journal of Aerosol Science*, 29(8), 929-942.
- Villenave, E., Aymoz, G., Beekmann, M., Baeza-Squiban, A., & Colosio, J. (2012). Air pollution by particulate matter: connecting stakeholders and scientific advances. *Pollution Atmospherique, Numero Special*.
- Wedepohl, H. K. (1995). The composition of the continental crust. *Geochimica et Cosmochimica Acta*, 59(7), 1217-1232.
- Weitkamp, E. A., Lipsky, E. M., Pancras, P. J., Ondov, J. M., Polidori, A., Turpin, B. J., & Robinson, A. L. (2005). Fine particle emission profile for a large coke production

- facility based on highly time-resolved fence line measurements. *Atmospheric Environment*, 39, 6719–6733.
- Whitby, K. T., & Cantrell, B. (1976). Fine particles. *Proc. Int. Confe. Environmental Sensing and Assessment*. Las Vegas: Institute of Electrical and Electronic Engineers.
- WHO. (2000). *Air quality guidelines for Europe - 2nd Edition*. WHO regional publications. European series ; No. 91.
- WHO. (2006). *Air quality guidelines - Global update 2005*. World Health Organization.
- Wu, C.-f., Larson, T. V., Wu, S.-y., Williamson, J., Westberg, H. H., & Liu, S. L.-J. (2007). Source apportionment of PM_{2.5} and selected hazardous air pollutants in Seattle. *Science of the Total Environment*, 386, 42-52.
- Yin, J., & Harrison, R. M. (2008). Pragmatic mass closure study for PM_{1.0}, PM_{2.5} and PM₁₀ at roadside, urban background and rural sites. *Atmospheric Environment*, 42, 980-988.
- Yue, G. C. (1979). The formation of ultrafine aerosols through nucleation on ions process. *Journal of Aerosol Science*, 10(2), 186-187.

CHAPTER II:

Materials and Methods used for Sampling and Analysis

TABLE OF CONTENTS

II.1.	Introduction	65
II.2.	Sampling sites	65
II.2.1.	Dunkerque	66
II.2.2.	Boulogne-sur-Mer	67
II.2.3.	Saint-Omer	68
II.3.	Materials used for sampling	69
II.3.1.	DIGITEL® High Volume Sampler DA-80	69
II.3.2.	Sampling filters	71
II.3.2.1.	Cellulose filters contamination reduction	71
II.3.2.2.	Quartz fiber filters contamination reduction	72
II.3.3.	Meteorological, PM ₁₀ and PM _{2.5} data acquisition	72
II.3.4.	Filters preparation before sampling	72
II.4.	Analysis of inorganic components and total carbon	74
II.4.1.	Inductively Coupled Plasma-Mass Spectrometer (ICP-MS)	74
II.4.1.1.	Samples preparations	74
II.4.1.2.	ICP-MS principles and characteristics	74
II.4.2.	Inductively Coupled Plasma-Atomic Emission Spectroscopy (ICP-AES) ..	76
II.4.3.	CHNS-O Analyzer	77
II.4.3.1.	Samples preparations	77
II.4.3.2.	CHNS-O Analyzer principles and characteristics	78
II.4.4.	Ion Chromatography (IC)	79
II.4.4.1.	Samples preparations	79
II.4.4.2.	Ion chromatography principles and characteristics	79
II.4.5.	Analysis of certified standards	80
II.5.	Sampling protocol validation	81
II.5.1.	Methodology	81
II.5.2.	Results	83
II.6.	Works Cited	86

LIST OF FIGURES

Figure 1 Satellite imagery showing the three sampling sites cities locations	66
Figure 2: Satellite imagery showing “Lamartine” sampling site and the major PM sources influences	67
Figure 3: Satellite imagery showing “Musée” sampling site and the major PM sources influences	68
Figure 4: Satellite imagery showing “Ribot” sampling site and the major PM sources influences	69
Figure 5 (A) HVS DA-80 in its field housing (B) Longitudinal section of the PM _{2.5} sampling head used with the DA-80 for sampling, the air passing in the bottom section (red arrow) holds PM _{2.5} only.	70
Figure 6 Photo of the DA-80 high volume sampler location in Dunkerque showing the stabilizing metallic grid on the floor holding about 150 kg of cement.	71
Figure 7 Filter preparation using quartz fiber filter (a) glued using an adhesive tape (b) to a cellulose fiber filter (c)	73
Figure 8 Example of a sample taken using the DA-80 the darker side represents the quartz semi-filter when the other lighter one is the cellulose semi-filter adhesive tape can be seen in the middle.	73
Figure 9 Atmospheric concentrations (ng m ⁻³) calculated using the mixed quartz-cellulose fiber filters versus atmospheric concentration determined using the whole cellulose filter for a selection of elements	85

LIST OF TABLES

Table 1 List of the elements analyzed by ICP-MS, their calibration ranges and detection limits	75
Table 2 List of elements analyzed by ICP-AES, their calibration ranges and detection limits	77
Table 3 Calibration range for TC analysis	78
Table 4 Detection limits (DL) found for the analyzed ions	80
Table 5 Summary of NIST SRM-1648 analysis using ICP-MS and ICP-AES	80
Table 6 Summary of soil (certificate 133317) and cystine (certificate 134139) total carbon analysis	81
Table 7 Summary of NIST SRM-1648 certified anions analysis	81
Table 8 Trace elements contents in QMA quartz fiber filter (in ng/g of filter)	82
Table 9 Mass of Cu sampled on the cellulose part and on the quartz fiber part of the mixed filter and corresponding air volume passing through	84

II.1.Introduction

This chapter includes a detailed explanation of the materials and methods used in this study in order to achieve the objectives mentioned in chapter I. It begins with a description of the Nord-Pas-de-Calais region as well as the chosen sampling sites for this study.

A second section will follow, and includes explanations on the used sampling materials, details on the functioning of the high volume sampler, the used sampling filters and the acquisition of meteorological data.

The third section of this chapter revolves around the analysis materials and procedures that were used in order to determine the chemical composition of the collected PM_{2.5} samples. In total, four different methods were used for the quantification of a large list of chemical species in the collected samples. The chapter will be concluded by the sampling protocol validation experiment.

II.2.Sampling sites

Our project scope is to study PM_{2.5} levels and origins in the Nord-Pas-de-Calais (NPdC) region. The logical choice was to select a group of cities located at a certain distance from each other and subjected to a combination of pollution sources including similar and different types.

The main site under focus in this work is located in Dunkerque (about 222417 inhabitants), followed by another site in Boulogne-sur-Mer (about 118932 inhabitants) and a third in Saint-Omer (about 64000 inhabitants), and finally all three sites can be found illustrated in Figure 1.



Figure 1 □ Satellite imagery showing the three sampling sites cities locations

Our sampling strategy consists of a simultaneous sampling of $PM_{2.5}$ at two sites for comparison. Therefore, we divided our sampling campaign into two parts □ the first one was conducted in winter (from November 16th to December 31st 2010) between Dunkerque and Boulogne-sur-Mer, when the second one was realized in spring (from March 10th to April 30th 2011) between Dunkerque and Saint-Omer. Further details on each site characteristics are discussed hereafter.

II.2.1. Dunkerque

This city is heavily industrialized and located on the coastline of the north of France, and is limited by the French-Belgian border from the east. However, the sampling site is located within the city center, next to the “Lamartine” university building of the Université du Littoral Côte d’Opale (Lat. □ 51.036323 □ Lon. □ 2.379408). The sampling site was chosen specifically in a way that allows us to sample under the effects of urban and industrial emissions (Figure 2). In summary, depending on the wind direction, this sampling site can be subjected to a possible influence of a mixture of PM sources □ the urban sector extends on a wide range (60 □ 290 □) in some sectors of which appears an Electric steel plant (30 □ 70 □) and an integrated steel works (260 □ 290 □) influences. Finally, the northern sector represents the marine sector influence.



Figure 2 □ Satellite imagery showing “Lamartine” sampling site and the major □M sources influences

Our sampling point □as located at 10m elevation from the ground level. It □as installed on the rooftop of the “Lamartine” building to prevent sampling of any punctual events localized at the street ground level.

II.2.2. Boulogne-sur-Mer

The second sampling point is located in Boulogne-sur-Mer city and called “Musée” (Lat. □50.723461 □ Lon. □1.608783). Boulogne-sur-Mer is a coastal fishing and touristic site located at about 70 to 80 km south-□est of Dunkerque (Figure 3).

The marine influence through sea salt emissions can affect the site from almost all directions e□cept the SE sector. Direct marine emissions can arrive to the sampling location from the nearby marine sector (180 □45 □). In addition, seaport activities can also influence the city from the □estern side (250 □310 □). Ho□ever, emissions influence from Dunkerque’s industrial-urban site is a possibility that cannot be discarded. Thus, NE air masses can hold marine, urban-industrial and continental types of emissions. Furthermore, the 70 □180 □sector can be a source of continental air mass from inland Europe. Finally, the remaining 180 □250 □

sector □inds can hold urban-marine mixed influences. The sampling point in Boulogne-sur-Mer is located at 7m from the ground level to prevent the sampling of any promptly produced local emissions.

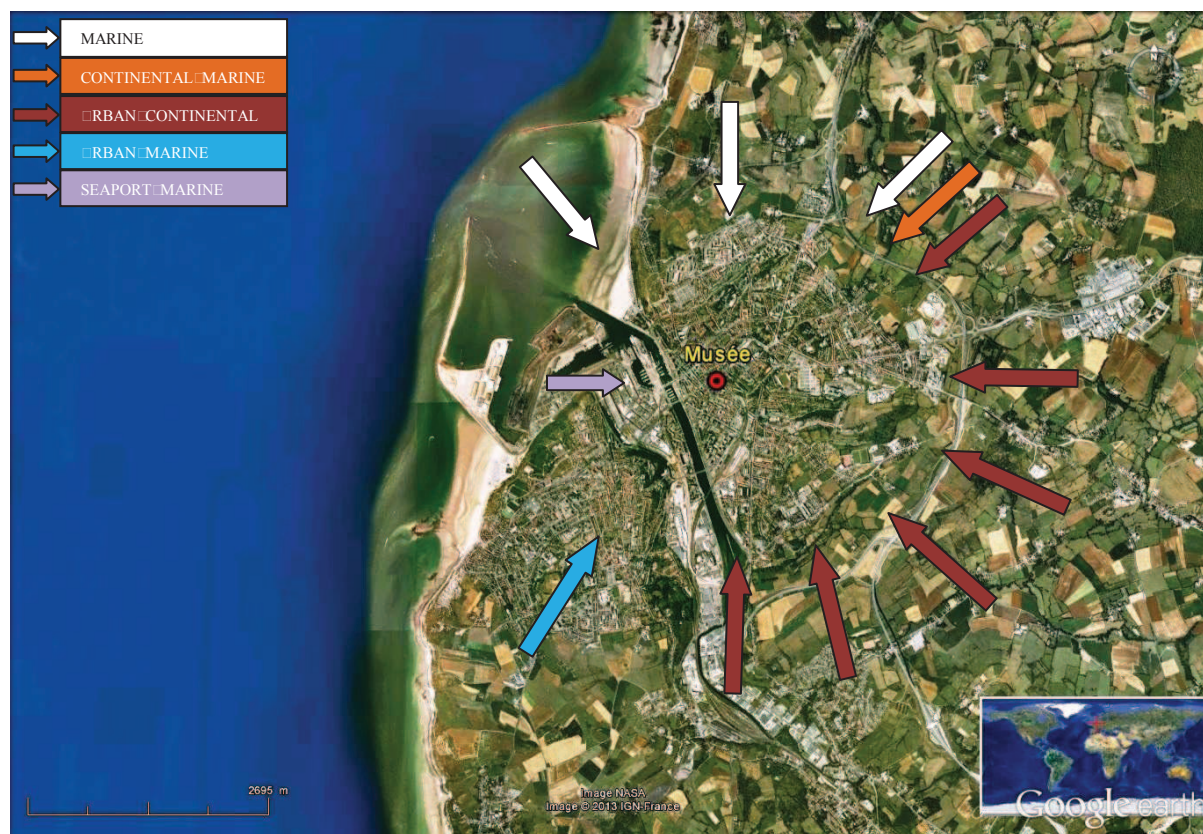


Figure 3 □ Satellite imagery showing “Musée” sampling site and the major □M sources influences

II.2.3. Saint-Omer

This site □as specifically chosen due to its inland position. It exhibits different conditions than the first t□o sites. The main influences are the urban-continental and urban-marine mixed types that can affect the site from the 30□220□ and 220□30□ sectors respectively, as illustrated in Figure 4. Dunkerque’s urban-industrial site might also affect the city from the NE sector (10□30□) by a marine-industrial mixed type of PM. However, a local light industrial source of PM emissions located in the city of Arques can be considered as an additional source, □hich did not exist in the first t□o sampling sites. The industry is represented by a glass factory located in the south eastern side of the city (120□150□). Our sampling location □ithin the city □as located in the city center (Lat.□50.747825□Lon.□2.258617), on the top of a shed used by the French air quality monitoring group (Atmo), and

is situated in the perimeter of “Lycée Ribot”. The sampler □as installed on the roof of the shed at about 7 m from the ground ne□t to a moderately busy street.

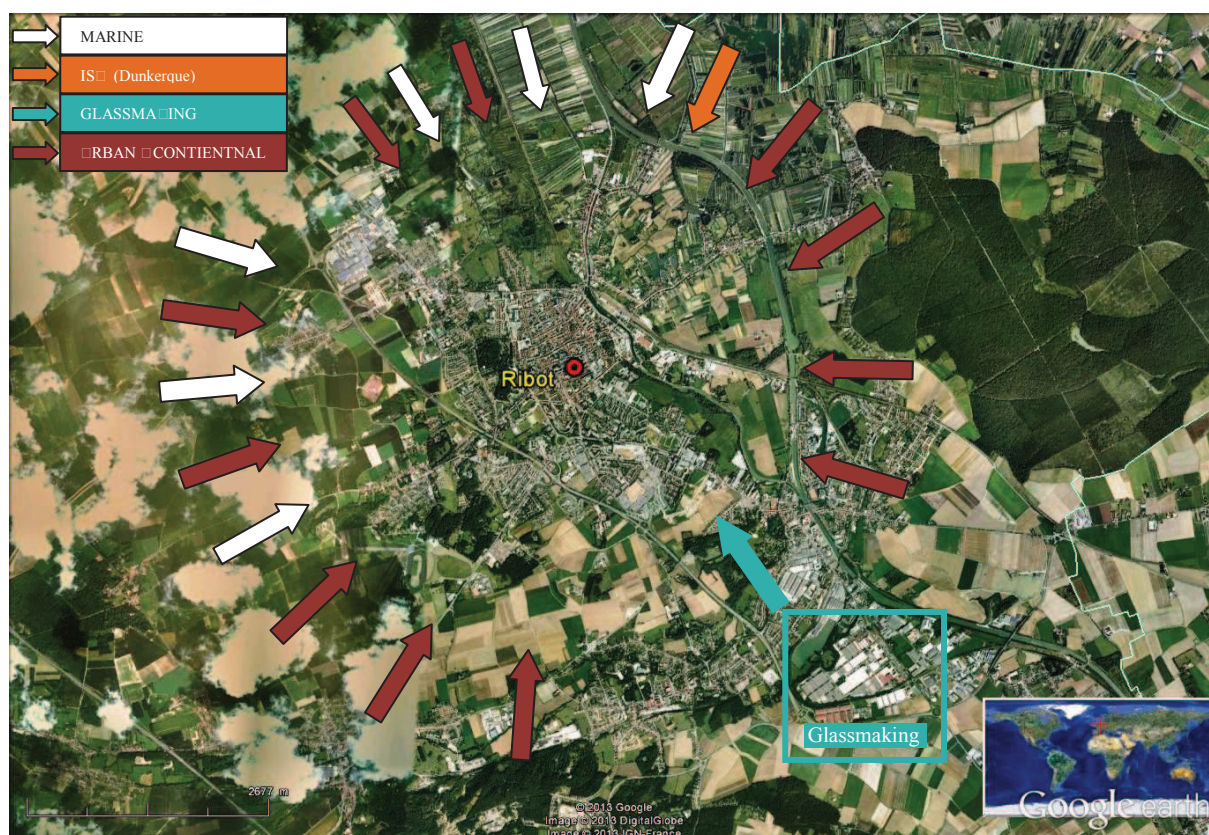


Figure 4: Satellite imagery showing “Ribot” sampling site and the major □M sources influences

II.3. Materials used for sampling

II.3.1. DIGITEL® High Volume Sampler DA-80

The sampling at each site □as realized using an automatic High-Volume Sampler (HVS) made by DIGITEL® □the DA-80 (Figure 5-(A)). The sampler is equipped □ith field housing for additional protection in the field, and is characterized by an automatic filter changer, a precision flo□ meter coupled to a photoelectric cell (flo□ rate sensor) that regulates the turbine suction po□er by monitoring a floater in the flo□ meter. The sampler is also equipped □ith thermal resistances to regulate the inside temperature of the machine as □ell as the sampling head in □hich the separation of the PM sizes occurs. Heating is used in the machine to prevent any possible malfunction resulting from freezing □hen temperatures drop belo□ zero.

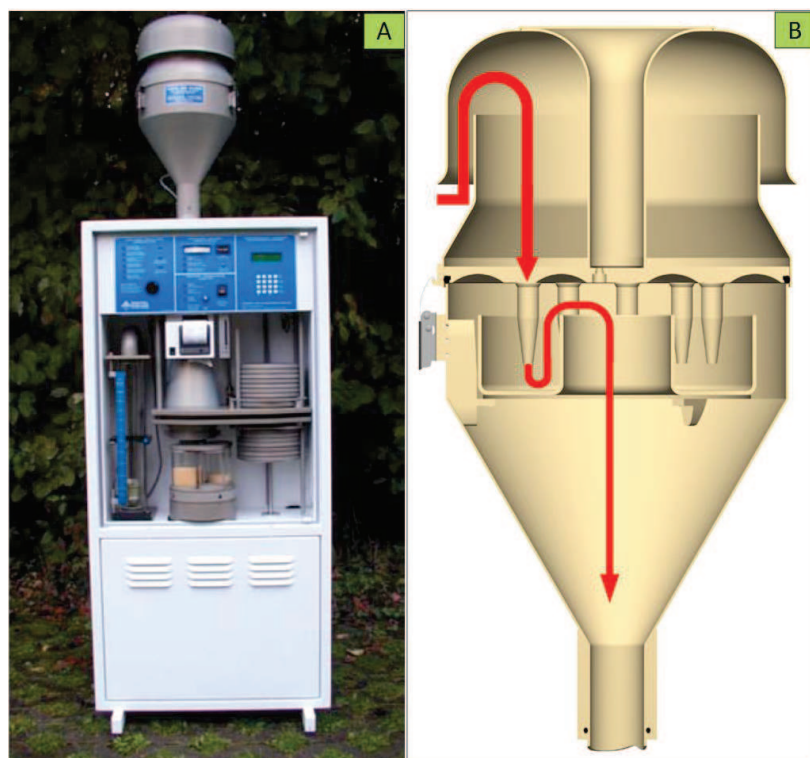


Figure 5 □ (A) □ DA-80 in its field housing □ (B) □ longitudinal section of the PM_{2.5} sampling head used with the DA-80 for sampling the air passing in the bottom section □ red arrow □ holds PM_{2.5} only.

During sampling, a PM_{2.5} impactor (Figure 5-(B)) □as placed on the top of the vacuum tract of the DA-80. The head has a cut-off diameter of 2.5 □m, □hich allo□s only PM_{2.5} ($D_{ae} \leq 2.5 \mu\text{m}$) to pass through the system into the filters under 30 m³/h vacuum at 15□C, 1013 hPa. The receptacle of the head □as covered □ith a thin layer of Do□ Corning® high vacuum grease to keep undesired larger particles from rebounding inside the tract.

Finally, the DA80 is also capable of recording outside temperatures and atmospheric pressure in addition to sampling data such as date, sampling start and end time, air flo□ correction coefficients, pressure correction coefficients, and most importantly the real sampling volume taking into account sampling temperature and pressure. Metallic grids □ere used to stabilize the DA-80 that □as firmly attached to. The grids held about 150 kg (15 □ 10 kg) of cement blocks made specifically to maintain a stable position □hen sub□ected to heavy □inds (Figure 6).



Figure 6 Photo of the A8 big volume sampler location in Dunkerque showing the stabilizing metallic grid on the floor holding about 15 kg of cement.

II.3.2. Sampling filters

The choice of filters was linked to the objectives of the project. It is highly related to the analytical procedure and the chemical species that are aimed at in this work which include a list of elements, water soluble ions and total carbon. Therefore, we were forced to consider two main filters matrices: cellulose and quartz fiber filters. The first type is used for elements and ions analysis, when the other is typically used for carbon quantification. However, cellulose based samples cannot be used for carbon analysis since the carbon loaded matrix of the filter will bias our results. On the other hand, we found through chemical analysis that unashed quartz fiber filters have high contents of metals incrustated within the fibers (see Table 8 in section II.5), and hence are not ashable with acids. Therefore, we were obliged to use both types of filters simultaneously for sampling.

II.3.2.1. Cellulose filters contamination reduction

Unashed Whatman® 41 cellulose filters (150 mm) have significant concentrations of many elements (up to 15 µg/g in the case of Fe for example). These filters need to be ashed before sampling and therefore were treated as described by (Ledoux, et al., 2006) for Fe analysis. Filters are submerged in 0.5M HCl and 0.5M HNO₃ for 24h, then rinsed with ultrapure water (MilliQ®, Millipore® resistivity 18.2 MΩ.cm). Then, filters are dried under a laminar flow hood (Class 100, US Federal Standard 209a), and hermetically kept in cleaned

Petri dishes and stored in a freezer (-20°C). This treatment lowers the Fe contamination under 0.1 µg per filter, and contents of all other metals are lower than the detection limits.

II.3.2.2. Quartz fiber filters contamination reduction

Whatman® QMA quartz microfiber filters (150 mm) were sealed inside handmade aluminum foil pouches, one pouch for each filter. After opening one side of the pouches, filters were heated up to 450°C in a closed oven for 48 hours in order to decrease carbon content to below the detection limit. Afterwards, each filter was conserved inside its original pouch until sampling.

II.3.3. Meteorological, PM₁₀ and PM_{2.5} data acquisition

Meteorological data included rainfall occurrence and quantity as well as wind directions, speed and gusts were acquired from Météo France (Convention LCO Météo France). The stations in which the data was recorded are located in Dunkerque (station n° 59183001), Boulogne-sur-Mer (station n° 62160001) and Radinghem (station n° 62685001). This latter is an inland station located next to our site in Saint-Omer.

As for the PM_{2.5} hourly average concentrations (in µg m⁻³), the data was retrieved from website of Atmo-NPdc (<http://www.atmo-npdc.fr>), which can be found in the information section on daily recording. We should note that PM_{2.5} data was available only for Dunkerque, whereas PM₁₀ was retrieved for all three sites.

II.3.4. Filters preparation before sampling

Our objectives force us to consider Whatman® 41 cellulose filters and Whatman® QMA quartz microfiber filters as substrates for PM sampling. Consequently, we found that combining the two types in one filter can be used as a support for sampling. This filter is constituted of half cellulose filter glued using an adhesive tape to a half quartz fiber filter. This resolves the analytical problem by giving us one half of a filter as cellulose for elemental and soluble ions analysis and the other as quartz fiber for carbon quantification (Figure 7).

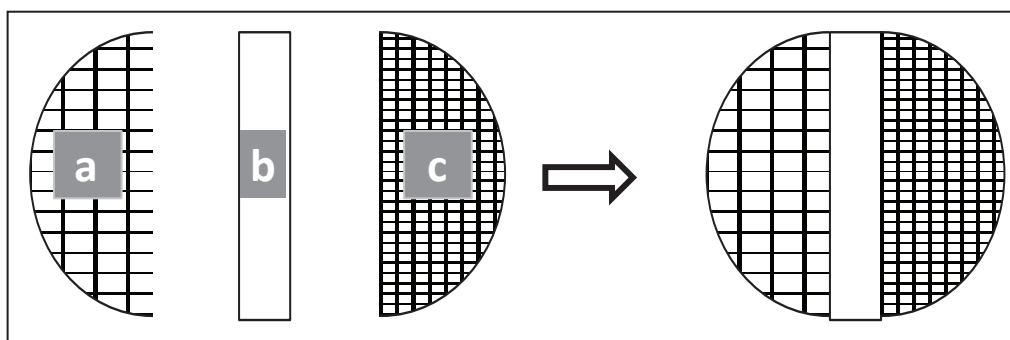


Figure 7 Filter preparation using quartz fiber filter (a) glued using an adhesive tape (b) to a cellulose fiber filter (c)

This mixture resolved the analytical issue but conversely created another problem that concerns the volume of air flow through each part of the filter. Usually, when sampling occurs using a homogeneous filter (one type of fiber), PM deposition is considered to be uniform on the filter's surface because air is passing regularly through the surface. This fact could not be adopted in our study since the filter is made from two different matrices, and obviously one side will have higher flow than the other as can be clearly seen in one of our samples. Furthermore, the collected particles are deposited on the surface of the quartz fiber filter, but they penetrate deeply into the fibers of the cellulose filter (Figure 8).



Figure 8 Sample of a sample taken using the A8. The darker side represents the quartz semi-filter and the other lighter one is the cellulose semi-filter. Adhesive tape can be seen in the middle.

One consequence of this difference in air flows is the accumulation of PM on one side more than the other, which will eventually lead to an under- or over-estimation of the concentrations depending on the analyzed chemical species.

Finally, in order to fix this problem, we proposed a method that has been validated and described in section II.5.

II.4. Analysis of inorganic components and total carbon

In this work, an important list of chemical species was analyzed which includes the following elements □ Ag, Al, As, Ba, Bi, TC, Ca, Cd, Co, Cr, Cu, Fe, □, Mg, Mn, Na, Nb, Ni, P, Pb, Rb, Sb, Sc, Sn, Sr, Te, Ti, Tl, V and □n. In addition, the following list of water soluble ions was also analyzed □ NH_4^+ , Cl^- , NO_3^- and SO_4^{2-} . The analysis of the elements was realized using Inductively Coupled Plasma-Mass spectrometry (ICP-MS) and Inductively Coupled Plasma Atomic Emission spectroscopy (ICP-AES), whereas the analysis of total carbon was achieved using a CHNS □ microanalysis. Finally, the water soluble ions were quantified using ion chromatography. These techniques, along with their respective analytical conditions are detailed in the upcoming sections.

II.4.1. Inductively Coupled Plasma-Mass Spectrometer (ICP-MS)

This method was used in our study in order to quantify a list of elements that is usually found in trace amounts in the atmosphere. It requires dissolution of the collected particles in order to be introduced in the analyzer in liquid form.

II.4.1.1. Samples preparations

Using a scalpel blade, approximately 250 mg (about 18th) of each sampled cellulose and quartz fiber filter were cut and placed into a PTFE flask, then digested with 5.5 mL of $\text{HNO}_3/\text{HF}/\text{HClO}_4$ (4 □ 0.5 v/v/v, Suprapur®, Merck®) at 120 °C for 4h. The acids were then evaporated at 170 °C for 4h using heating wells, and ultrapure water was added to the residue and heated at 90 °C for 1h. In order to perform this digestion, we used a *DigiPREP MS*® digestion kit that allows the digestion of 48 samples simultaneously.

Finally, the cooled solution was diluted with MilliQ® water up to 10 mL added with 0.2 □ of nitric acid and filtered on PTFE membrane (0.45 □m) prior to analysis.

II.4.1.2. ICP-MS principles and characteristics

Metals analysis was realized using inductively coupled plasma-mass spectrometer (ICP-MS) coupled with a collision reaction cell to minimize polyatomic interferences during the measurements. The analysis begins with the sample injection in the analyzer, and then the solution containing the elements passes through a nebulizer which transforms it into fine

droplets and injects it in the plasma torch in a flow of argon gas. The argon gas is burned with the droplets at 8000°C which is sufficient to ionize all the atoms in the sample by eliminating one peripheral electron from each. Inside the torch, the sample goes through different phases □ liquid, solid, gas, atom then ion. The latter enters a quadrupole unit that separates in a fraction of a second the ions depending on their mass to charge ratio (m/z). Hence, each ion quits the quadrupole at a certain specific time. Finally, the concentration relative to each element that hits the detector is proportional to its quantity in the sample and is measured by the mass spectrometer in counts per second.

Many polyatomic species such as ArC^+ , ArO^+ , $NaAr^+$, $CaAr^+$, and $MgAr^+$ can disrupt the measurements due to the fact that they have the same m/z ratio than that of other analyzed elements. For that reason, we usually break polyatomic species by using the following collision gases □ helium, hydrogen and air. These gases are injected one at a time in a Collision Reaction Cell (CRC) located between the plasma torch and the mass spectrometer. This section of the instrumentation is also known as Collision Reaction Interface (CRI). The gas collides with polyatomic species, breaks them and continues its path. Collision gases selection is based on their efficiency from a thermodynamic point of view, and also on the atomic mass. Smaller masses reduce the loss of sensitivity due to atoms dispersion during the collisions. Table 1 illustrates the characteristics of our ICP-MS method.

Table 1 □ List of the elements analyzed by ICP-MS □ their calibration ranges and detection limits

Element	Atomic mass	Collision gas	Calibration range ppb	Detection limit ppb
Sc	45	Air	0.2 - 0.5 - 1 - 2 - 5 - 10	0.084
Ti	49	Air	0.2 - 0.5 - 1 - 2 - 5 - 10 - 20 - 50	0.055
V	51	Helium	0.2 - 0.5 - 1 - 2 - 5 - 10 - 20	0.005
Cr	52	Helium	0.2 - 0.5 - 1 - 2 - 5 - 10 - 20	0.006
Mn	55	Helium	0.2 - 0.5 - 1 - 2 - 5 - 10 - 20 - 50	0.006
Co	59	Air	0.2 - 0.5 - 1 - 2 - 5 - 10 - 20	0.059
Ni	60	Helium	0.2 - 0.5 - 1 - 2 - 5 - 10 - 20	0.032
Cu	65	Helium	0.2 - 0.5 - 1 - 2 - 5 - 10 - 20 - 50	0.039
As	75	Air	0.2 - 0.5 - 1 - 2 - 5 - 10	0.162
Se	77	Air	0.2 - 0.5 - 1 - 2 - 5	0.221
Rb	85	Air	0.2 - 0.5 - 1 - 2 - 5	0.059
Nb	93	Air	0.2 - 0.5 - 1 - 2 - 5	0.087
Ag	107	Air	0.2 - 0.5 - 1 - 2 - 5 - 10	0.077
Cd	110	Air	0.2 - 0.5 - 1 - 2 - 5 - 10	0.038
Sn	118	Air	0.2 - 0.5 - 1 - 2 - 5 - 10	0.105
Sb	121	Air	0.2 - 0.5 - 1 - 2 - 5 - 10	0.112
Te	128	Air	0.2 - 0.5 - 1 - 2 - 5 - 10	0.084
Tl	205	Air	0.2 - 0.5 - 1 - 2 - 5 - 10	0.121
Pb	208	Air	0.2 - 0.5 - 1 - 2 - 5 - 10 - 20 - 50	0.072
Bi	209	Air	0.2 - 0.5 - 1 - 2 - 5 - 10 - 20	0.145

For the analysis □e used a Varian® 820-MS, □ith a Collision Reaction Interface (CRI) in □hich □e used helium as collision gas in addition to air used to quantify elements □ith minimum polyatomic interferences. Data treatment □as realized using Varian® ICP-MS e□pert v2.1 b105 soft□are.

Standard solutions for ICP-MS calibration □ere prepared from a multi-element solution (10 ppm). The dilutions □ere achieved using MilliQ® ultra pure □ater, and the volumes □ere measured by □eighting the flasks at each addition to obtain higher precision. Calibration solutions □ere also acidified □ith 0.2□ HNO₃ Suprapur®.

The Detection Limits (DL) calculated for the studied elements given in Table 1 are equal to three times the standard deviation value calculated from 10 blank solution measurements. All the considered elements gave above DL concentration values, e□cept Se □hich □as al□ays belo□ DL.

II.4.2. Inductively Coupled Plasma-Atomic Emission Spectroscopy (ICP-AES)

ICP-AES □as used to quantify some elements that are usually found in moderate to high concentrations in the atmosphere and hence do not require any additional sensitivity in the detection procedure. Our ICP-AES instrument is the iCAP 6000 Series from Thermo SCIENTIFIC®. The functioning mode of the instrument is similar to the ICP-MS Varian® 820-MS described above, but the chemical species detection is different.

The samples should be introduced in the analyzer in liquid form. Therefore, the same solutions obtained after samples mineralization (see section II.4.1.1) □ere analyzed □ith this technique. Each sample is in□ected and then sprayed □ith a nebulizer inside a plasma torch □here the elements of the sample change phases starting from liquid, passing through solid and gas, and ending in an e□cited atom form. Instantly after the transformation, the e□cited atom □ill return to its initial non-e□cited status and emit a ray that is characteristically linked to the atom. The group of rays emitted from the e□cited atoms is transferred inside a dispersive system and then diverged to separate each ray by its □avelength. The diverged rays are redirected to face a plate formed by photomultiplier that increase the □avelengths intensity and transform it into electric signals corresponding to each element. The electric signals are captured and pro□ected as peaks that are proportional to the corresponding elements concentrations. The electric signal treatment □as realized by Thermo® iTEVA-Control Center v 2.5.0.84.

One inconvenience can be encountered □hen using this method is the presence of many energy levels for atomic e□citation□thus one atom can emit many rays (having different

wavelengths) while going back to non-excited status depending on which high energy level he is found at after excitation. The selection of rays was based on the capacity of these latter to give the highest intensity for each element and on the minimum interferences between them. The list of elements quantified using this technique, along with the respective analytical conditions are illustrated in (Table 2). In the case of Fe, Mg and Na, the concentration was the average concentration found between the two highest intensity rays. The instrument used for the analysis can also detect emitted rays using two modes: radial detection and direct axial detection. The latter is the most sensible between the two methods, and hence it is selected for our analysis.

Table 2 List of elements analyzed by ICP-AES, their calibration ranges and detection limits

Element	Wavelengths nm	Calibration range ppb	Detection limit ppb
Al	1670	50 - 100 - 250 - 500 - 1000 - 2000 - 5000	4
Ba	4554	0.5 - 1 - 2.5 - 5 - 10 - 20 - 50	0.4
Ca	3933	50 - 100 - 250 - 500 - 1000 - 2000 - 5000	29
Fe	2382 - 2599	50 - 100 - 250 - 500 - 1000 - 2000 - 5000	21
	7698	50 - 100 - 250 - 500 - 1000 - 2000 - 5000	15
Mg	2795 - 2802	50 - 100 - 250 - 500 - 1000 - 2000 - 5000	13
Na	5889 - 5895	50 - 100 - 250 - 500 - 1000 - 2000 - 5000	33
P	1782	5 - 10 - 25 - 50 - 100 - 200 - 500	3
Sr	4077	0.5 - 1 - 2.5 - 5 - 10 - 20 - 50	0.2
Zn	2138	5 - 10 - 25 - 50 - 100 - 200 - 500	2

II.4.3. CHNS-O Analyzer

QMA quartz fiber filters were used for total carbon analysis. For this latter, we used a FLASH 2000 Organic Elemental Analyzer from Fisher Scientific®. The analyzer is equipped with two chromatography columns: one for C, H, N and S analysis, whereas the other is for O detection.

II.4.3.1. Samples preparations

Approximately 30 mg of each QMA quartz fiber filter was weighed using a Mettler Toledo® microbalance with a 0.01 mg precision. This weighed fraction of the filter is enclosed in two (25 × 25 mm) Thermo Scientific® tin foils using laboratory tweezers. The samples are then arranged in an automatic sampler that is piloted by the analyzer software (Thermo Scientific® Eager Experience version 1.2).

II.4.3.2. C₁₈S₁₈ Analyzer principles and characteristics

The quartz reactive column is composed of a combustion area at the top, which is a few centimeters of empty space that is heated up to 900°C to allow the combustion of the introduced sample. Afterwards, a 10 mm layer of quartz wool separates between the combustion zone and a few centimeters layer of copper oxide granules. This latter is separated from copper metallic bars (up to 10 cm) by another 10 mm layer of quartz wool. At the end of the copper bars, another 25 mm of quartz wool are laying on the bottom of the column. A constant helium flow passes through the column and plays the role of carrier gas.

The sample enclosed in tin foils is introduced into the heated combustion side of the column where tin rapidly atomize, thus increasing the temperature around the sample up to 1800°C approximately. This reaction occurs in the heated combustion area at the top of the column. At this high temperature, all carbon content of the sample in the capsules is atomized. Total released carbon is then oxidized into CO₂ after passing through the oxidation section formed by copper oxide granules. The excessive oxygen is captured in the copper bars which are the reduction section of the column. Then CO₂ passes with helium gas vector into a gas chromatography column (used for the separation of C, H, N, and S), to continue afterwards into the detector—a katharometer. The detection at this level is measured by the difference in the thermal conductivity between the carrier gas and the formed CO₂.

Calibration of the analyzer was realized using soil (2.29% carbon) and cystine (C₆H₁₂NO₄S₂ 30.05% carbon) certified reference materials. The calibration details are summarized in Table 3. The DL for TC analysis was calculated using the standard deviation (SD) equation applied on 10 measurements of Tin paper blanks TC content—DL = 3 × SD. The DL of our analyzer was 0.00367 mg of carbon, which is verified to be lower than the contents of all analyzed samples in this study.

Table 3—Calibration range for C analysis

Soil	C content %g	Cystine	C %g
Standard 1	4	Standard 1	19
Standard 2	8	Standard 2	60
Standard 3	14	Standard 3	138
Standard 4	20	Standard 4	155
Standard 5	23	Standard 5	256

II.4.4. Ion Chromatography (IC)

II.4.4.1. Samples preparations

Anions and cations were extracted from a piece of the cellulose filter (about 16th) that is sliced using a scalpel blade, then weighed and placed in the bottom of a beaker and covered with a small quantity of Milli-Q® ultrapure water (2 to 3 mL). The beaker is placed in an ultrasonic bath for 15 min, and the leachate containing the ions is filtered using a syringe coupled to a Sartorius® cellulose acetate membrane (porosity 0.45 µm). The leachate is then placed in a polyethylene flask. The filter was submerged again in few milliliters of ultrapure water Milli-Q® before undergoing another ultrasonic bath and filtration. The same procedure was repeated three times successively. The final volume of the gathered extracted solutions in the flask is finally adjusted up to 20 mL by adding ultrapure water, and the resulting solution is conserved in the fridge at 4°C until analysis.

II.4.4.2. Ion chromatography principles and characteristics

Simultaneous analysis of water soluble anions (F^- , Cl^- , NO_3^- , PO_4^{3-} and SO_4^{2-}) and ammonium (NH_4^+) was realized using a Dionex® D100® coupled to a Dionex® ICS 900® ion chromatography column, after water leaching of a part of the collected cellulose filter.. The information given by the conductivity meter was treated using CHROMELEON® software.

For anion analysis, a solution made from Na_2CO_3 and $NaHCO_3$ (3.5 mM and 1 mM respectively) is used as mobile phase. It passes in the chromatographic column in a 1.2 mL/min solution flow. An electrochemical suppressor is used to decrease the mobile phase signal. On the other hand, an initial anion stock solution of 500 mg/L was prepared using EMS®RE® MERC® NaF, NaCl, $NaNO_3$, Na_3PO_4 and Na_2SO_4 salts. The calibration range covered a range between 0.5 and 100 ppm including 1, 2.5, 5, 10, 25 and 50 ppm.

A solution of methane sulfonic acid (CH_3SO_3H , 20 mM) is used as mobile phase in the soluble anions analysis, in a 1.2 mL/min eluent flow. An electrochemical suppressor is also used to neutralize the conductivity of this mobile phase. Calibration of the anion column was realized using a stock solution (500 mg/L) prepared from NH_4Cl salt from EMS®RE® MERC®. The etalon covered the same concentration range used for anions analysis.

Finally, a succession of blanks analysis enabled us to estimate the detection limit of our analyzers for both anions and cations. This detection limit was calculated for each ion based on the standard deviation of the results of 10 ultra pure water Milli-Q® blank samples following the same equation used for TC detection limit: $DL = 3 \times SD$. The results showed

that F^- and PO_4^{3-} ions could not be detected, whereas for the rest of the ions the DL are summarized in Table 4.

Table 4 Detection limits found for the analyzed ions

Ions	NO_3^-	NO_2^-	Cl^-	SO_4^{2-}	PO_4^{3-}	S^{2-}
DL (ppm)	0.00296	ND*	0.00296	0.00008	ND*	0.00009

*ND: not detected

II.4.5. Analysis of certified standards

In order to validate our sample preparation procedure as well as the reliability of our measuring technique, we analyzed a certified urban particulate matter sample (NIST SRM-1648) using ICP-MS, ICP-AES and Ion Chromatography, as well as soil (Thermo Scientific® certificate 133317) and cystine (Thermo Scientific® certificate 134139) reference materials using the CHNS-O analyzer.

Using the same method described in section II.4.1.1, our SRM-1648 certified dust sample was digested and prepared for elemental analysis for a selection of elements. Table 5 shows the details about this analysis, in which the recovered values proved to be highly acceptable.

Table 5 Summary of NIST SRM-1648 analysis using ICP-MS and ICP-AES

Elements	Analyzer	Obtained values		Certified values		Recovery
			SD		SD	
Al	ICP-AES	3,437	$\pm 0,127$	3,42	$\pm 0,11$	101
Ba	ICP-AES	0,071	$\pm 0,002$	0,074	-	96
Ca	ICP-AES	5,956	$\pm 0,190$	-	-	-
Fe	ICP-AES	3,894	$\pm 0,030$	3,91	$\pm 0,10$	100
K	ICP-AES	1,032	$\pm 0,002$	1,05	$\pm 0,01$	98
Mg	ICP-AES	0,781	$\pm 0,023$	0,800	$\pm 0,014$	98
Na	ICP-AES	0,406	$\pm 0,014$	0,425	$\pm 0,002$	96
Sr	ICP-AES	0,021	$\pm 0,001$	-	-	-
Zn	ICP-AES	0,436	$\pm 0,006$	0,476	$\pm 0,014$	92
Cu	ICP-MS	0,059	$\pm 0,001$	0,061	-	97
Mn	ICP-MS	0,081	$\pm 0,003$	0,079	-	103
Ti	ICP-MS	0,392	$\pm 0,006$	0,400	-	98
Pb	ICP-MS	0,692	$\pm 0,007$	0,655	$\pm 0,008$	106
V	ICP-MS	0.015	± 0.002	0.014	± 0.0003	104

On the other hand, TC certified soil and cystine samples were also analyzed using our CHNS-O analyzer. Soil dust and cystine crystals were weighed and enclosed in tin capsules

before analysis, following the same protocol used for our samples analysis. The results summarized in Table 6 show very good recovered values, which prove that our analysis conditions are optimal.

Table 6 □ Summary of soil □ certificate 133317 □ and cystine □ certificate 134139 □ total carbon analysis

Reference	Measured [mg]	SD	Certified [mg]	Recovered [%]
Soil TC	0.01092	± 0.00026	0.01086	101
Cystine TC	0.06451	± 0.00122	0.06437	100

Finally, the SRM-1648 was also used to validate our water soluble anions analysis protocol. From the certified material, 2.2 mg of particles were deposited on a cellulose filter. The latter was treated with ultrapure water following the protocol described in section II.4.4.1. The solution was analyzed for Cl^- and SO_4^{2-} contents, and the results are summarized in Table 7. Nitrates and ammonium contents could not be analyzed because the SRM-1648 certifies a total nitrogen percentage only.

Table 7 □ Summary of □ IS □ S □ M □ 1648 certified anions analysis

Ion	Measured [%]	SD (%)	Certified [%]	Recovered [%]
Cl^-	0.47	± 0.02	0.45	104
SO_4^{2-}	14.1	± 0.5	15 [*]	94

*Certified to 5% as "S", converted to 15% as SO_4^{2-}

II.5. Sampling protocol validation

In the previous section, we described the reasons behind the use of a dual type of filters combined in one for our sampling campaign. The use of this montage will eventually lead to a difference in PM deposition on each half of the filter. The turbine used in our DA-80 creates a stable flow in the sampling system, which will be divided unequally between the cellulose and quartz fiber part.

II.5.1. Methodology

In order to correct for this PM deposition difference, we were obliged to find a method that allows us to calculate the exact volume that passes through each half of the filter. The idea was to determine the mass of a reference element that has been collected on each of the two parts of the filter (quartz fiber and cellulose) □ the collected mass is directly proportional

to the volume of filtered air. The reference element must be present in low quantities in both ashed cellulose and glass fiber filters, but also relatively abundant in the PM in order to better determine how the PM is distributed between the two parts of the filter.

Ashed cellulose filter blank values are found very low all trace metals contents are below the DL (see section II.3.2.1). This is not the case for the QMA quartz fiber filters which contain a large variety of trace metals (Table 8). Among those, the choice of the reference element is guided by considering its high abundance in the atmosphere compared to its filter content. For example, Ag, Bi, Co and Nb showed interesting low contents in the filter but they exist in trace concentrations in ambient air. Consequently, Cu was selected as the reference element.

Table 8 Trace elements contents in QMA quartz fiber filter in ng/g of filter

Element	ng/g
Ag	34
As	261
Bi	119
Cd	128
Co	40
Cr	1050
Cu	162
Mn	724
Nb	53
Ni	302
Pb	375
Rb	409
Sb	458
Sc	798
Sn	211

After chemical analysis of each part of the filter, we quantified the masses of Cu sampled in the cellulose part (Cu_{cell}) and in the quartz fiber part (Cu_{QMA}) of the mixed filters. Thus, the total mass of collected Cu (Cu_{tot}) is the sum of Cu_{cell} + Cu_{QMA} , and is directly linked to the total sampled air volume. In these conditions, the volume of air passing through the cellulose part of the mixed filter (V_{cell}) is equal to

$$V_{cell} = \frac{Cu_{cell} (ng)}{Cu_{tot} (ng)} \times V_{tot} \quad \text{Equation 11}$$

Similarly, the volume of air passing through the QMA quartz fiber part is given by

$$V_{QMA} = \frac{Cu_{QMA} (ng)}{Cu_{tot} (ng)} \times V_{tot} \quad \text{Equation 2}$$

The calculated V_{cell} is used to determine elements and water soluble ions atmospheric concentrations quantified from the cellulose half of the filter, whereas V_{QMA} is used to determine the atmospheric TC concentrations which are measured using the glass fiber half of our mixed filter.

II.5.2. Results

In order to validate the proposed methodology, a sampling campaign was realized using two DA-80 samplers in parallel for a period of seven days, beginning from 05/12/2010 till 05/19/2010. One of the samplers was loaded with 15 washed cellulose filters (see section II.3.2.1) and the second sampler was loaded with 15 of our laboratory made mixed quartz-cellulose fiber filters (see section II.3.4). The two samplers were placed next to each other in Dunkerque's site and launched at the same time for the same sampling period. Two samples of $PM_{2.5}$ per day (12 hours each) were collected for a total of 14 samples that can be used to validate the protocol.

Atmospheric concentration values obtained using the mixed quartz-cellulose filter according to the previously described methodology, will be compared to the atmospheric concentration values obtained using the whole cellulose filter considered as reference.

The quantification of the Cu masses in the cellulose and QMA parts of the mixed filters shows different concentrations as illustrated in Table 9. This proves and confirms that the volumes penetrating through each section of the filter are not equal. The application of Equation (1) and Equation (2) allowed the determination of the filtered air volume through each part V_{cell} and V_{QMA} (Table 9). This last result shows that V_{cell} and V_{QMA} are not only different when compared to each other, but also not equal between the samples. The difference can be explained by the fact that the surface of each part of the mixed filter is never exactly equal to the other. Sometimes we can have more cellulose surface than QMA in one filter, when in contrary we can sometimes have larger QMA surface than cellulose in another.

Table 9 Mass of Cu sampled on the cellulose part and on the quartz fiber part of the mixed filter and corresponding air volume passing through

Dates	Cu _{cell} [ng]	Cu _{MA} [ng]	V _{tot} [m ³]	Cu _{tot} [ng]	V _{cell} [m ³]	V _{MA} [m ³]
05/12/2010 (00-12)	56	122	333	178	105	228
05/12/2010 (12-24)	37	77	333	114	109	224
05/13/2010 (00-12)	246	246	333	492	166	167
05/13/2010 (12-24)	181	244	329	425	140	189
05/14/2010 (00-12)	145	136	331	281	171	161
05/14/2010 (12-24)	101	101	327	201	164	163
05/15/2010 (00-12)	194	206	329	400	160	170
05/15/2010 (12-24)	100	116	330	215	153	177
05/16/2010 (00-12)	58	73	332	131	147	186
05/16/2010 (12-24)	183	167	330	350	173	157
05/17/2010 (00-12)	180	198	332	378	158	174
05/17/2010 (12-24)	209	293	326	502	136	190
05/18/2010 (00-12)	211	236	326	447	154	172
05/18/2010 (12-24)	124	147	325	271	149	176
05/19/2010 (00-12)	118	72	327	190	204	123

Finally, we compared the atmospheric elemental concentrations (in ng m⁻³) determined from the mixed filter using V_{cell} with the ones found by analyzing a part of the complete cellulose filter sample using V_{tot}. Figure 9 illustrates this comparison for some of the less abundant elements which quantification is the most problematic. The figure shows that the atmospheric concentrations obtained using the mixed filter are very close to those found using the whole cellulose filter. The recovery appears to be between 89% for Bi and Sn and 106% for Ag, which is very acceptable considering that studied elements are present at very low concentration values. Thus, we can conclude that the methodology proposed here allows a precise estimation of the elemental atmospheric concentrations using mixed quartz-cellulose filters and Cu as reference element. The sampling protocol is then fully validated.

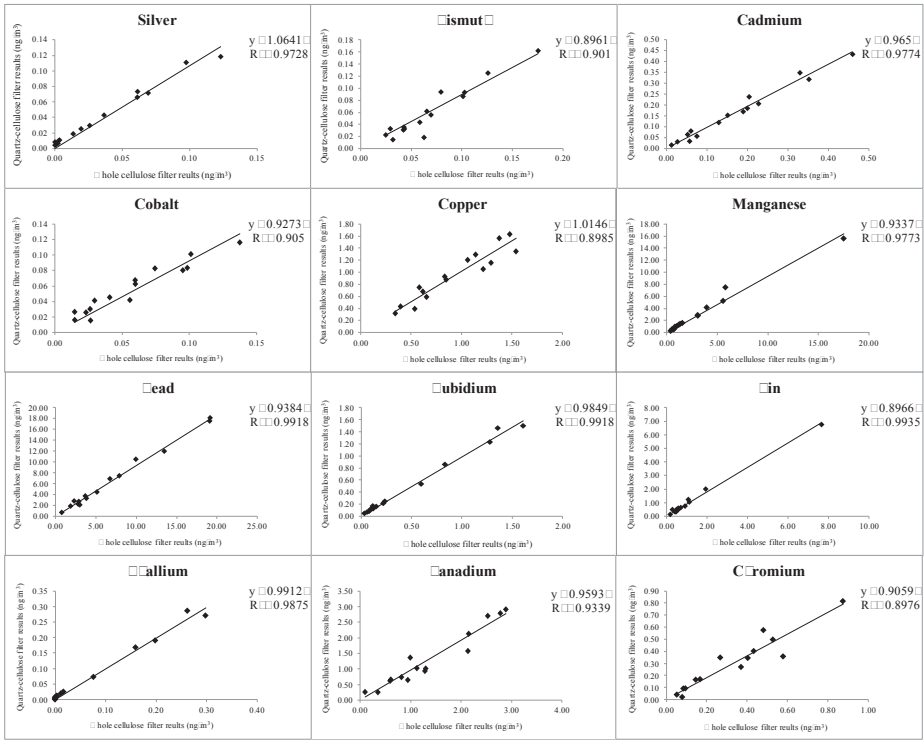


Figure 9 Atmospheric concentrations (ng m⁻³) calculated using teflon-coated quartz-cellulose fiber filters versus atmospheric concentration determined using teflon-coated cellulose filter for a selection of elements

II.6. Works Cited

Ledoux, F., Laversin, H., Courcot, D., Courcot, L., Zhilinskaya, E., Puskaric, E., Aboukaïs, A. (2006). Characterization of iron and manganese species in atmospheric aerosols from anthropogenic sources. *Atmospheric Research*, 82, 622–632.

CHAPTER III □

Concentrations trends and statistical
analysis of Major Elements (ME),
Soluble Ions (SI), and Total Carbon
(TC)

TABLE OF CONTENTS

III.1.	Introduction	92
III.2.	Meteorology in the “Littoral Côte d’Opale” coastline.....	92
III.3.	Meteorology encountered during the sampling campaigns.....	94
III.3.1.	inter campaign.....	95
III.3.1.1.	ind, precipitation and temperature conditions in Dunkerque	95
III.3.1.2.	ind, precipitation and temperature conditions in Boulogne-sur-Mer	98
III.3.2.	Spring campaign	100
III.3.2.1.	ind, precipitation and temperature conditions in Dunkerque	101
III.3.2.2.	ind, precipitation and temperature conditions in Saint-Omer	103
III.4.	Average concentrations and contributions to $PM_{2.5}$.....	106
III.4.1.	inter campaign averages comparison	106
III.4.2.	Spring campaign averages comparison.....	109
III.5.	Average concentrations comparison at a European scale	112
III.5.1.	Location and characteristics of the comparison sites.....	112
III.5.2.	Comparison of ME, SI, and TC average concentrations.....	115
III.5.2.1.	Marine major elements	117
III.5.2.2.	SIA major ions	118
III.5.2.2.1.	Nitrates.....	119
III.5.2.2.2.	Sulfates.....	119
III.5.2.2.3.	Ammonium	119
III.5.2.3.	Total Carbon (TC)	119
III.5.2.4.	Other ME metals.....	120
III.6.	Diurnal evolution of ME, SI and TC	121
III.6.1.	inter campaign.....	122
III.6.1.1.	Sea salts diurnal evolution	122
III.6.1.2.	Fe and Nss-Ca diurnal evolution.....	123
III.6.1.3.	Al and Nss-Mg diurnal evolution	125
III.6.1.4.	TC and Nss-TC diurnal evolution	126
III.6.1.5.	SIA diurnal evolution.....	128
III.6.2.	Spring campaign	129
III.6.2.1.	Sea salts diurnal evolution	129
III.6.2.2.	Fe and Nss-Ca diurnal evolution.....	130
III.6.2.3.	Al and Nss-Mg diurnal evolution	131
III.6.2.4.	TC and Nss-TC diurnal evolution	132
III.6.2.5.	SIA diurnal evolution.....	133
III.7.	Analysis of above limit peaks of $PM_{2.5}$.....	134
III.7.1.	Identification of above limit-value peaks of $PM_{2.5}$	134
III.7.1.1.	inter campaign above limit-value peaks.....	135
III.7.1.2.	Spring campaign above limit-value peaks	137
III.7.2.	Detailed analysis of above limit peaks of $PM_{2.5}$	139
III.7.2.1.	$PM_{2.5}$ inter campaign episodes.....	139
III.7.2.1.1.	General observation	139
III.7.2.1.2.	Detailed interpretation of $PM_{2.5}$ above limit values for the inter campaign	141
III.7.2.2.	$PM_{2.5}$ spring campaign episodes	146
III.7.2.2.1.	General observations.....	146
III.7.2.2.2.	Detailed interpretation of above limit values for the inter campaign	148
III.8.	Concentration evolution by wind sector.....	153
III.8.1.	inter campaign.....	155
III.8.1.1.	Major marine element origins.....	155
III.8.1.2.	SIA major ions origins	156
III.8.1.3.	Combustion elements origins-TC and	156
III.8.1.4.	Fe, Ca, and Al origins	157
III.8.2.	Spring campaign	158
III.8.2.1.	Major marine element origins.....	158
III.8.2.2.	SIA major ions origins	159
III.8.2.3.	Combustion elements origins-TC and	160

III.8.2.4.	Fe, Ca, and Al origins	161
III.9.	Discussion of the results	162
III.10.	Conclusion	167
III.11.	Works Cited	169

LIST OF FIGURES

Figure 1 Temperatures and rainfall monthly average variations for the NPdC region from 1981 to 2010	94
Figure 2 Wind rose at Dunkerque during the winter campaign (data source Météo France)	96
Figure 3 Variation of precipitation (in mm) by wind sector of 45° in relation to wind speed at Dunkerque during the winter campaign (data source Météo France)	97
Figure 4 Evolution of 00h-12h and 12h-24h temperatures (in °C) at Dunkerque during the winter campaign ...	97
Figure 5 Wind rose in Boulogne-sur-Mer during the winter campaign (data source Météo France)	98
Figure 6 Variation of precipitation (in mm) by wind sector of 45° in relation to wind speed at Boulogne-sur-Mer during the winter campaign (data source Météo France)	99
Figure 7 Evolution of 00h-12h and 12h-24h temperatures (in °C) at Boulogne-sur-Mer during the winter campaign	100
Figure 8 Wind rose at Dunkerque during the spring campaign (data source Météo France)	101
Figure 9 Variation of precipitation (in mm) by wind sector of 45° in relation to wind speed at Dunkerque during the spring campaign (Source Météo France)	102
Figure 10 Evolution of 00h-12h and 12h-24h temperatures (in °C) at Dunkerque during the spring campaign	103
Figure 11 Wind rose at Saint-Omer during the spring campaign (data source Météo France)	104
Figure 12 Variation of precipitation (in mm) by wind sector of 45° in relation to wind speed at Saint-Omer during the spring campaign (Source Météo France)	104
Figure 13 Evolution of temperatures (in °C) at Saint-Omer during the spring campaign	105
Figure 14 SI and TC average concentrations at Dunkerque and Boulogne-sur-Mer	108
Figure 15 ME and TE average concentrations at Dunkerque and Boulogne-sur-Mer	108
Figure 16 SI and TC average concentrations at Dunkerque and Saint-Omer	111
Figure 17 ME and TE average concentrations at Dunkerque and Saint-Omer	111
Figure 18 Comparison sites location on the European map (modified from (Dalet, 2012))	113
Figure 19 Diurnal evolution of sea salts concentrations ($\text{ng}\cdot\text{m}^{-3}$) in Dunkerque and Boulogne-sur-Mer during the winter campaign	123
Figure 20 Diurnal evolution of Fe and Nss-Ca concentrations in Dunkerque and Boulogne-sur-Mer during the winter campaign	124
Figure 21 Diurnal evolution of Al and Nss-Mg concentrations in Dunkerque and Boulogne-sur-Mer during the winter campaign	126
Figure 22 Diurnal evolution of TC and Nss- Cl concentrations in Dunkerque and Boulogne-sur-Mer during the winter campaign	127
Figure 23 Diurnal evolution of SIA , NH_4^+ , NO_3^- and SO_4^{2-} concentrations in Dunkerque and Boulogne-sur-Mer during the winter campaign	128
Figure 24 Diurnal evolution of sea salts concentrations in Dunkerque and Saint-Omer during the spring campaign	130
Figure 25 Diurnal evolution of Fe and Nss-Ca concentrations in Dunkerque and Saint-Omer during the spring campaign	131
Figure 26 Diurnal evolution of Al and Nss-Mg concentrations in Dunkerque and Saint-Omer during the spring campaign	132
Figure 27 Diurnal evolution of TC and Nss- Cl concentrations in Dunkerque and Saint-Omer during the spring campaign	133
Figure 28 Diurnal evolution of SIA concentrations in Dunkerque and Saint-Omer during the spring campaign	134
Figure 29 Evolution of Atmo PM_{10} and $\text{PM}_{2.5}$ recorded data and the total analyzed species in Dunkerque and Boulogne-sur-Mer during the winter campaign (red lines limit values of $25\text{ }\mu\text{g}\cdot\text{m}^{-3}$ ($\text{PM}_{2.5}$) and $50\text{ }\mu\text{g}\cdot\text{m}^{-3}$ (PM_{10}))	136
Figure 30 Evolution of Atmo PM_{10} and $\text{PM}_{2.5}$ recorded data and the total analyzed species in Dunkerque and Saint-Omer during the spring campaign (red lines limit values of $25\text{ }\mu\text{g}\cdot\text{m}^{-3}$ ($\text{PM}_{2.5}$) and $50\text{ }\mu\text{g}\cdot\text{m}^{-3}$ (PM_{10})) ..	138
Figure 31 Chemical composition of selected $\text{PM}_{2.5}$ samples exhibiting above limit value peaks in Dunkerque and Boulogne-sur-Mer during the winter campaign	140
Figure 32 Diurnal evolution of the temperature, $\text{PM}_{2.5}$ level, TC, SIA and Al concentrations ($\text{ng}\cdot\text{m}^{-3}$) in $\text{PM}_{2.5}$ during winter	142
Figure 33 Air mass backward trajectories drawn using HYSPLIT (Draxler & Rolph, 2012) for three selected samples (November 28 th , December 7 th and 29 th 2010) in Dunkerque (above three) and Boulogne-sur-Mer (below) Height 100m AGL, Duration 48 hrs, Start 100 °TC, Vertical motion isobaric, Neutrality trajectory every 2 hrs, Mass trajectories 6	143
Figure 34 Chemical composition of $\text{PM}_{2.5}$ above limit value samples in Dunkerque and Saint-Omer during the spring campaign	147

Figure 35 Diurnal evolution of the temperature, PM _{2.5} level, TC, SIA and Al concentrations (ng·m ⁻³) in PM _{2.5} during spring	149
Figure 36 Air mass backward trajectories drawn using HYSPLIT (Draxler & Rolph, 2012) for three selected samples (March 15 th , April 16 th and 24 th 2011) in Dunkerque (above three) and Saint-Omer (below) Height 100m AGL, Duration 48 hrs, Start 100 mTC, Vertical motion isobaric, Ne trajectory every 2 hrs, Mass trajectories 6	150
Figure 37 Major marine elements concentration roses for Dunkerque and Boulogne-sur-Mer during the winter campaign	155
Figure 38 SIA major ions concentration roses for Dunkerque and Boulogne-sur-Mer during the winter campaign	156
Figure 39 TC and Σ concentration roses for Dunkerque and Boulogne-sur-Mer during the winter campaign ..	157
Figure 40 Fe, Ca, and Al concentration roses for Dunkerque and Boulogne-sur-Mer during the winter campaign	158
Figure 41 Sea salt elements concentration roses for Dunkerque and Saint-Omer during the spring campaign ..	159
Figure 42 SIA species concentration roses for Dunkerque and Saint Omer during the spring campaign	160
Figure 43 TC and Σ concentration roses for Dunkerque and Saint-Omer during the spring campaign	161
Figure 44 Fe, Ca, and Al concentration roses for Dunkerque and Saint-Omer during the spring campaign	162

LIST OF TABLES

Table 1 Classification of the encountered wind speeds during our sampling campaigns	94
Table 2 Average concentrations of ME, TE, SI, and TC found in PM _{2.5} collected in Dunkerque and Boulogne-sur-Mer during the winter campaign (in ng·m ⁻³)	107
Table 3 Average concentrations of ME, TE, SI, and TC found in PM _{2.5} collected in Dunkerque and Saint-Omer during the spring campaign (in ng·m ⁻³)	110
Table 4 Characteristics of the comparison sites chosen from different European locations	114
Table 5 Arithmetic average concentrations (in ng·m ⁻³) comparison between our region and Europe	116
Table 6 Percentage of average sea salt and non sea salt fractions within sea salt components in winter	122
Table 7 Percentage of average sea salt and non sea salt fractions within sea salt components in spring	129
Table 8 Example of concentration roses calculations	154

III.1. Introduction

Tracing metals, ions and total carbon sources is found to be of a great importance as highlighted in Chapter I. Following the detailed explanation about the sampling and analytical method in chapter II, we present and discuss the results herein. The encountered meteorological conditions will be detailed for each of the studied sites Dunkerque, Boulogne-sur-Mer, and Saint-Omer. The result interpretations will incorporate four chemical species groups

- Major Elements (ME) including Al, Ca, Fe, Si, Mg and Na
- Trace Elements (TE) which group Ag, As, Ba, Bi, Cd, Co, Cr, Cu, Mn, Nb, Ni, P, Pb, Rb, Sb, Sc, Sn, Sr, Te, Ti, Tl, V and Zn
- Soluble Ions (SI) which assemble NH_4^+ , Cl^- , NO_3^- and SO_4^{2-}
- Total Carbon (TC) which includes both Organic “OC” and Elemental Carbon “EC”.

However, in this chapter, TE elements will be considered all together as a global trace elements concentration. The detailed analysis of this group will be achieved in Chapter IV.

An inter-site comparison between the average concentrations found in each site of simultaneous sampling will be included in this chapter. Also the average concentrations found for the above mentioned list of elements will be compared to other results found in other studies conducted in specific sites in Europe. Furthermore, a diurnal evolution of each chemical species in ME, TC, and SI will be studied and compared within each site. And finally, a study of chemical species enrichment in relation to wind directions will be conducted using concentration roses.

III.2. Meteorology in the “Littoral Côte d’Opale” coastline

The typical climate of this region is oceanic temperate, with modest seasonal variations and almost regular precipitation at the end of the year, between mid autumn and till the end of winter.

Wind flues can hit the region from all four sides, with each direction presenting its own characteristics and can influence local weather

- Under a western flu, the region is found situated on the axis of atmospheric depression circulation coming from the Atlantic Ocean. In this case, wind speed can be found high if not stormy, followed by precipitation (high humidity).

- Under a southern flow, air masses that pass over France can reach to the region. These air masses are found to heat ambient air in winter and can drastically increase temperatures in summer causing heat waves. In this case, the region can sometimes be considered as one of the hottest spots in France, with temperatures reaching 30°C, even on the coastline.
- Northern flow winds are usually coming from the North Sea. These flows represent typical northern cold air masses. In this case, temperatures are found at their lowest levels, which might lead to hail or snow fallout in the region during winter season.
- A dry and sunny weather can be observed in spring and summer seasons under eastern flow, but it can also lead to a glacial weather during winter with a cloudless sky.

Furthermore, the dominant winds are from the NE and SW sector in general with different properties. Wind blowing from the NE sector comes along with anticyclone conditions. Typically, the weather is found to be stable, without precipitation, and with low wind speed leading in most cases to the accumulation of pollutants in the atmosphere. On the other hand, winds from the SW sector are linked to atmospheric depression conditions. They are usually characterized by high wind velocity and abundant precipitation that leads to a rapid dispersion and rainout and/or washout of atmospheric pollutants respectively.

Monthly mean temperatures and rainfall accumulation data retrieved from www.lameteo.org database for the past 30 years (1981-2010) are illustrated in Figure 1. Saint-Omer data were not available.

The trend shows that the lowest recorded temperature (about 5°C) occurs during January-February and the highest was encountered during July-August (around 18°C). Furthermore, rainfall monthly accumulations were the highest during October and November.

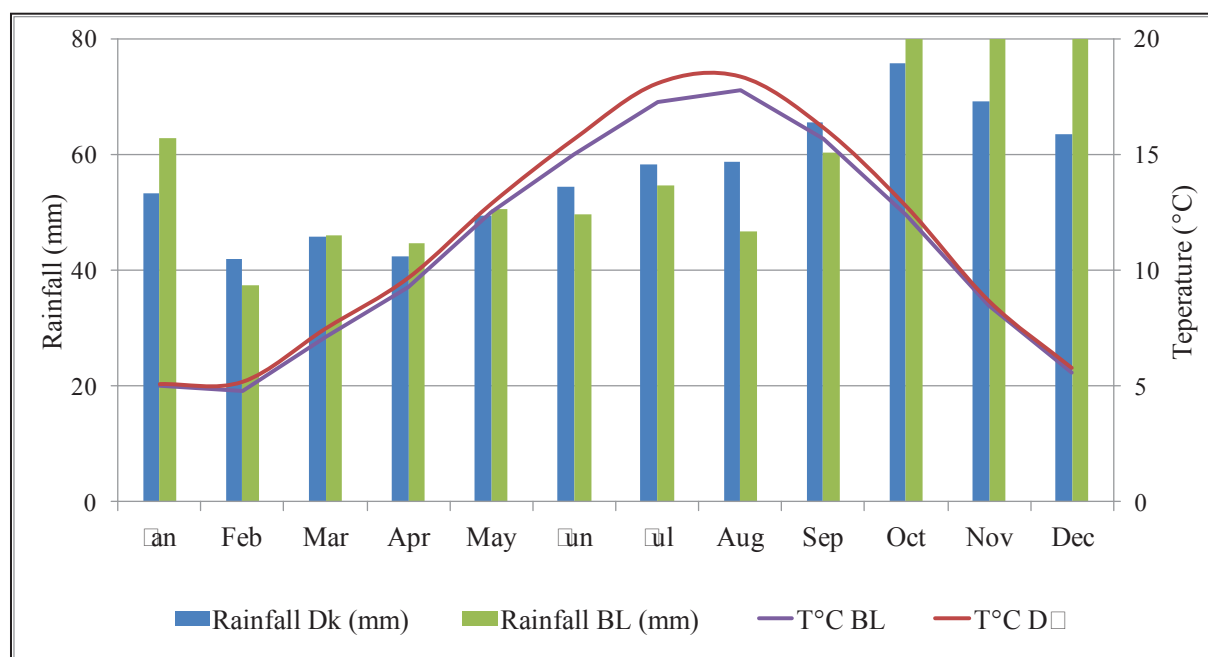


Figure 1 Temperatures and rainfall monthly average variations for the Dk region from 1981 to 2011

This glimpse on the regional climate resumes only a generalized on the Littoral Cote d'Opale weather, which reflects the climatic situation of the NPdC region. However, local differences may be found when we focus on a specific time period or on a specific site. Therefore the following section will expose the meteorology observed during the sampling periods.

III.3. Meteorology encountered during the sampling campaigns

During the sampling periods, wind velocity and direction, precipitation, and temperature measurements were retrieved from Météo France and from our onsite weather stations, and used to draw wind roses, precipitation trends and temperature trends for the sampling sites. Wind velocities were divided into four major classes illustrated in Table 1.

Table 1 Classification of the encountered wind speeds during our sampling campaigns

Wind speed	Velocity in m/s	Rank in Beaufort scale	Description
High	> 8	5 to 8	Fresh breeze to fresh gale
Moderate	4 to 8	3 to 4	Gentle to moderate breeze
Low	2 to 4	2 to 3	Light to gentle breeze
Very low	< 2	0 to 1	Calm to light air

For very low speed winds, wind velocity is extremely low and therefore a specific wind direction cannot be defined. As for precipitation, its accumulation (sum of precipitation heights recorded in mm) will be discussed per wind sector (45° each).

Finally, temperature trends retrieved from the DA80 automatic sampler will be presented in the form of trend lines for each site per campaign. These graphs will display temperature evolution during two daily periods—the first one from 00h to 12h (midnight – noon) and the second from 12h - 24h (noon – midnight).

III.3.1. Winter campaign

Sampling during the winter campaign was held in Dunkerque (from 11/18/2010 to 12/31/2010) and Boulogne-Sur-Mer (from 11/16/2010 to 12/28/2010) simultaneously. A total of 81 and 86 samples were taken at Dunkerque and Boulogne-sur-Mer respectively.

This campaign was characterized by rainfall accumulation of 69 mm (Dunkerque) and 49 mm (Boulogne-sur-Mer) during the sampling period. When compared to the usual rainfall recorded at these sites, the results are found below the historical averages calculated for the same period, which were 98 and 123 mm for Dunkerque and Boulogne-sur-Mer respectively (www.lameteo.org). Furthermore, the average temperatures were 1°C (Dunkerque) and 2°C (Boulogne-sur-Mer) and are much lower than 7 °C which is usually found at these sites (www.lameteo.org).

During this first sampling campaign, precipitation and temperature were found different than the usual averages of the region: the climate was colder and dryer. Therefore, in the following sections we will detail our recorded meteorological conditions at the sampling sites.

III.3.1.1. Wind, precipitation and temperature conditions in Dunkerque

A closer look at Dunkerque's winter wind rose (Figure 2) shows that most frequent wind directions were E, followed by S, NE and NW. An examination of wind velocity shows that high speed wind came from all previously mentioned sectors with a frequency of 22%. Furthermore, moderate speed wind (4 to 8 m/s) was recorded coming from E, S and NW sectors (48% frequency). Finally, low speed wind was found coming from S and E directions (25% frequency), when very low speed wind was almost absent in Dunkerque during this campaign (5% frequency). We should note that the recording shows only NE winds, which does not accord with the usually expected NE and SW dominant wind tendencies.

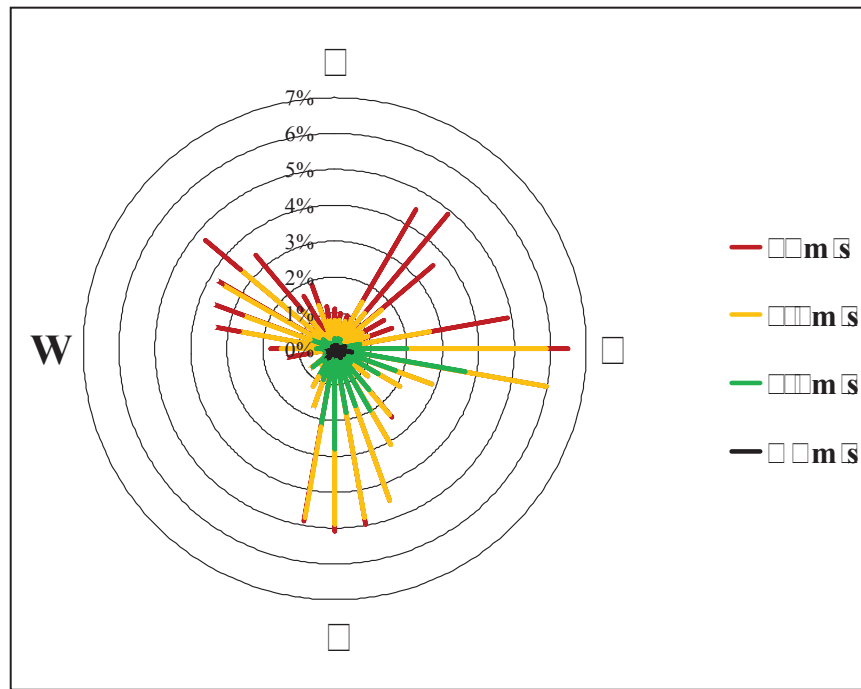


Figure 3 Wind rose at Dunkerque during the inter campaign data source
to France

On the other hand, total precipitation in Dunkerque during this period was 69 mm. Figure 3 illustrates in details the evolution of precipitation in relation to wind direction. We can distinguish that rain was poured heavily with winds coming from directions between W and NE ($270^\circ - 0^\circ - 45^\circ$). Furthermore, winds from the S to W ($180^\circ - 270^\circ$) directions contributed in less rainfall than the previously described sectors. The lowest rainfall quantity can be observed with E to S winds ($90^\circ - 180^\circ$).

However, a comparison between wind speed and rainfall concludes that high speed winds are not necessarily related to precipitation in this period.

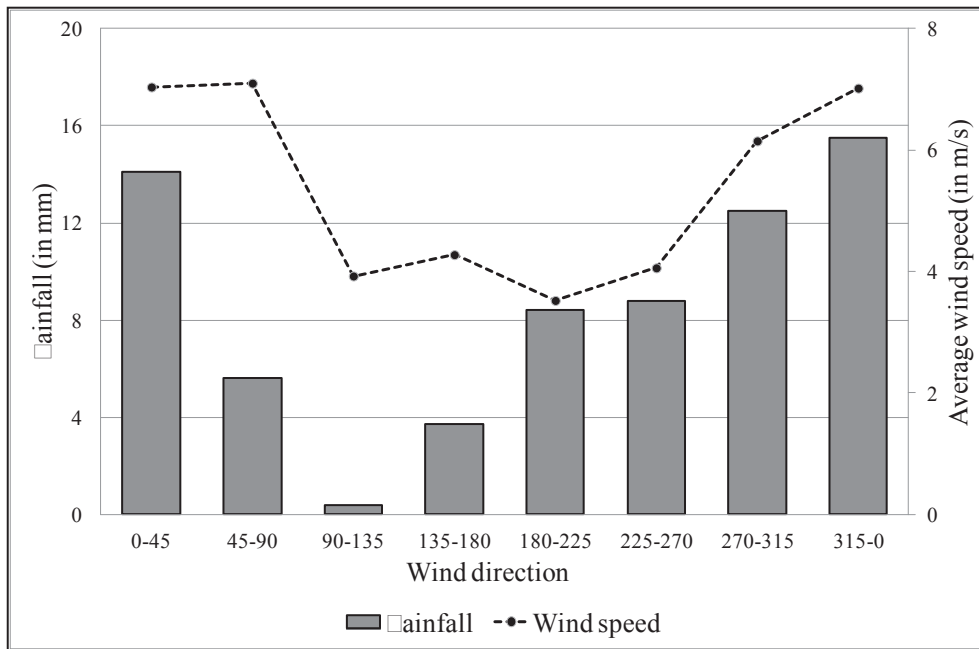


Figure 3 Variation of precipitation in mm and wind speed in relation to wind direction at Dunkerque during the inter campaign data source to France

Temperature fluctuations in Dunkerque in this period were ranging from 8 to -8°C (Figure 4). These trends prove that our campaign was conducted under real winter weather conditions. In addition, snow episodes were recorded for this period between November 26th - December 2nd and December 17th - 19th of 2010. These dates are marked by subzero temperatures.

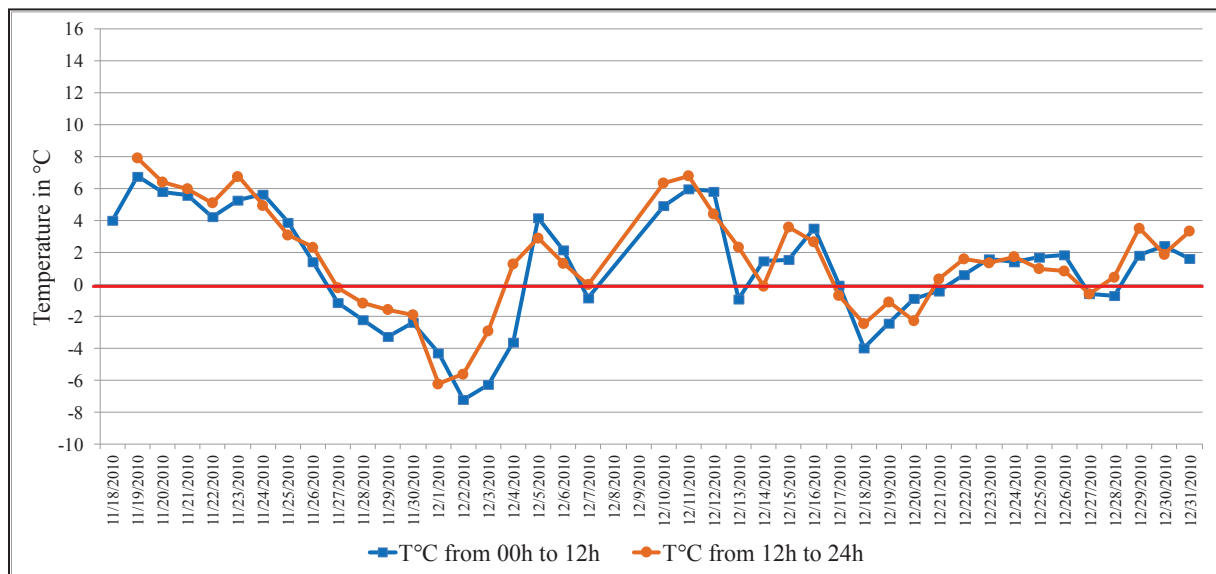


Figure 4 Evolution of maximum and 1-hour temperatures in °C at Dunkerque during the inter campaign

Local variations show slightly higher temperatures in the 12h-24h period when compared to 00h-12h ones. Normally, higher differences should be expressed between the two periods, but the observed small differences can be explained by the proximity of the coastal city to the sea, which moderate extreme temperatures variations in the 24 hours period.

III.3.1. Wind, precipitation and temperature conditions in Boulogne-sur-Mer

Boulogne-sur-Mer wind rose (Figure 5) shows that wind originated mainly from the NE-E, SE-S and NW-N sectors. High speed wind (7% frequency) comes mainly from the N and W directions, whereas moderate speed wind originates from the E-NE (52%), S-SE and N-NW sectors. Low speed wind was also recorded coming from the E-NE and S-SE sectors in much smaller frequencies (31%). Finally, very low speed (stagnant) wind was encountered in 10% of the period.

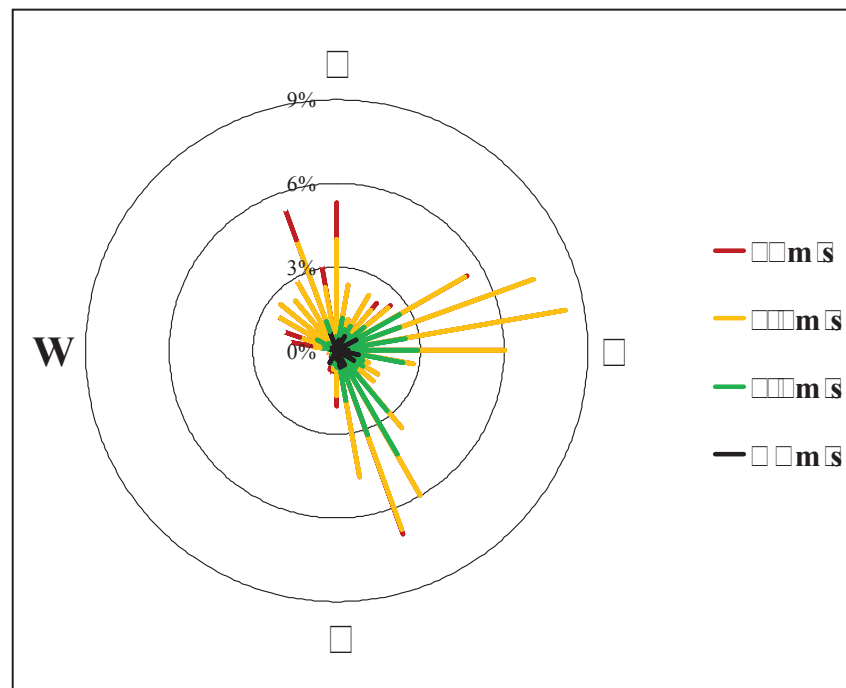
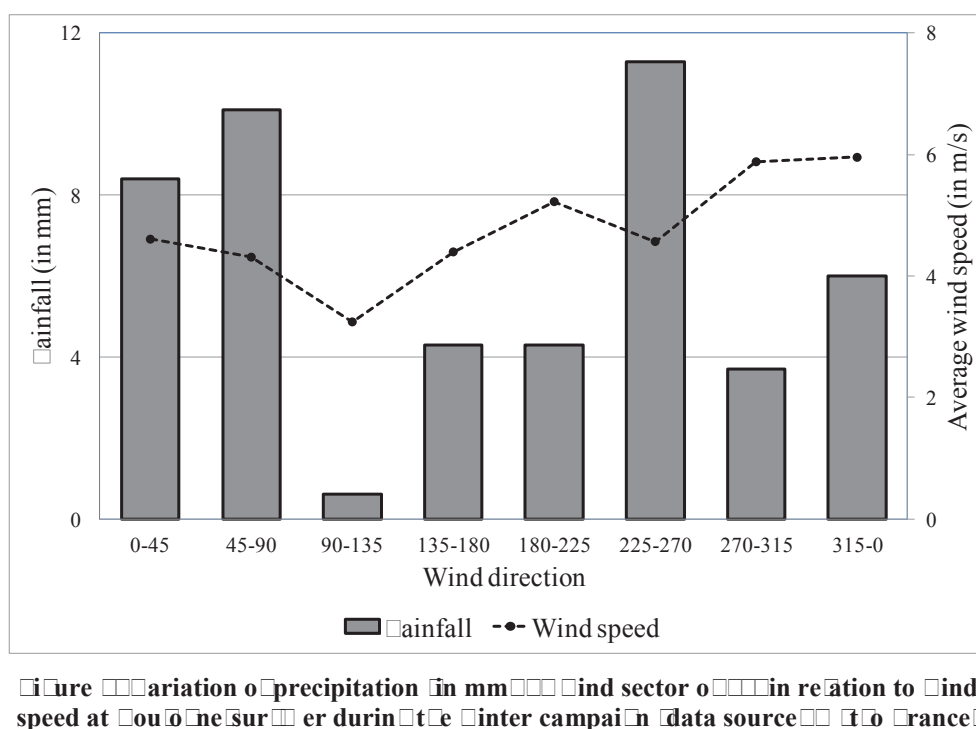


Figure 5 Wind rose in Boulogne-sur-Mer during the inter campaign data source: Météo France

Precipitation recordings show that rainy weather was not linked to a specific wind speed at this site (Figure 6). Furthermore, rainfall quantity was found higher when associated to winds between N and E sectors ($0^\circ - 90^\circ$) from one side, and between SW and W sectors ($225^\circ - 270^\circ$) on the other. For the rest of the wind sectors, fluctuations in rainfall ranged

between 4 and 6 mm, except for the E-SE sector in which precipitation levels are negligible. Finally, rainfall trend in Boulogne-sur-Mer is found slightly different than in Dunkerque.



Temperature fluctuations at Boulogne-sur-Mer were found similar to those found in Dunkerque for this period (Figure 7). The range was limited to a maximum of 8°C and a minimum of -6°C and constant slightly higher temperatures were also observed in the 12h-24h period when compared to 00h-12h ones. As found for Dunkerque, snow episodes were observed at Boulogne-sur-Mer between November 29th – December 4th and December 16th – 25th of 2010.

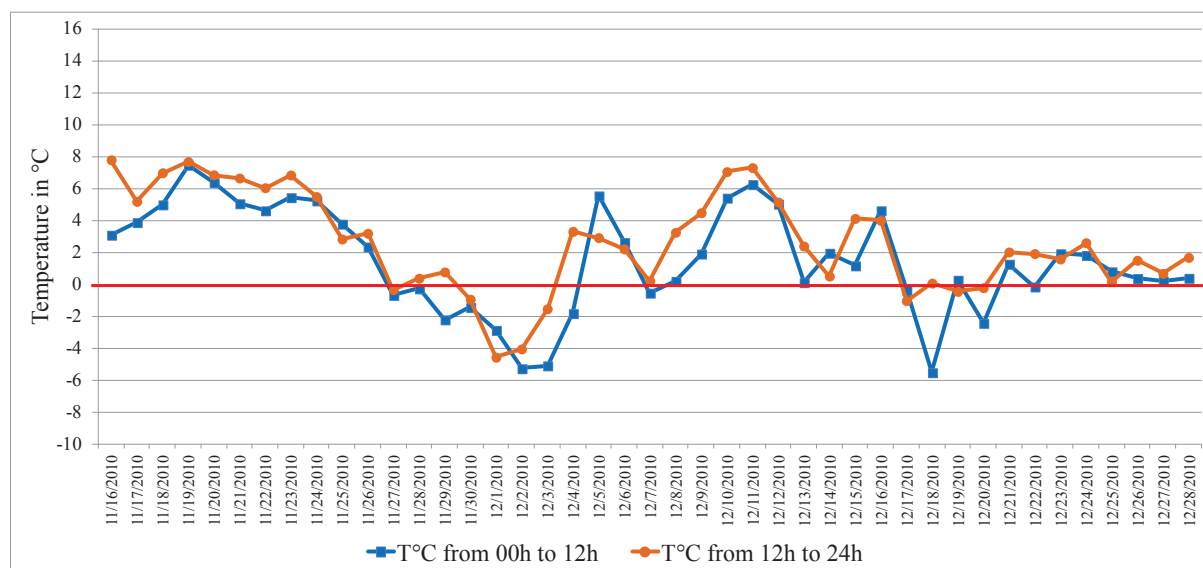


Figure 3.1 Evolution of Dunkerque and Boulogne-sur-Mer temperatures in Dunkerque and Boulogne-sur-Mer during the winter campaign

To resume all, we found that the winter campaign (11/18/2010 –12/31/2010) is characterized by:

- Low temperatures: the values were 1°C in Dunkerque and 2°C in Boulogne-sur-Mer, which are much less than the 7°C average found at these sites for the past 30 years.
- Dominating wind directions of NW, NE and S were recorded instead of the usually dominating NE and SW sectors.
- Precipitation levels were also below the usual seasonal trend, but also marked with snowing events.

III.3.2.Spring campaign

Sampling during the spring campaign was conducted simultaneously at Dunkerque (from 03/12/2011 to 04/30/2011) and at Saint-Émer (from 03/10/2011 to 04/30/2011), to collect a total of 97 and 104 samples respectively. Local recorded rainfall during this period was 19 and 28 mm for Dunkerque and Saint-Émer respectively, which are much below the 67 mm average found for the Nord region for the same period (between 1981 and 2010).

On the other hand, average temperatures during this campaign were 11°C in Dunkerque and Saint-Émer, which are higher than the 8°C found as an average for the Nord region in previous years. In addition, no snowing events are usually recorded during this period of the year, which was also the case during our sampling period. Finally, we conclude that during our spring sampling campaign, the climate was dryer and warmer than the usual.

III.3.1. Wind, precipitation and temperature conditions in Dunkerque

Dunkerque was mostly subjected to wind coming from directions ranging between N-NE and E-NE, and few winds coming from the S and SW sectors (Figure 8). These winds were mostly of moderate speed (46%) followed by low speed (30%), very low speed (15%), and high speed type (9%). This latter was frequently blowing from the NE direction.

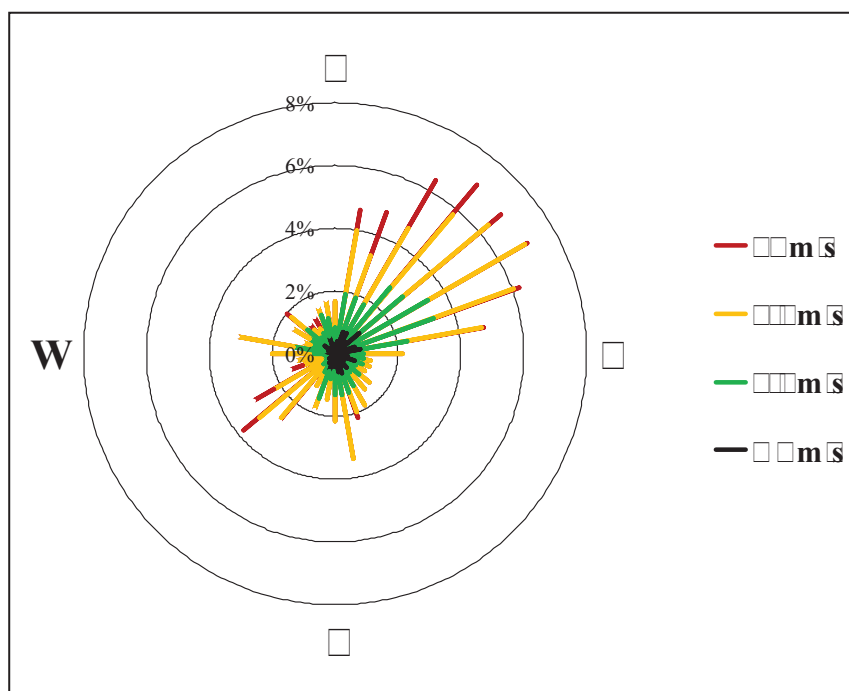


Figure 8 Wind rose at Dunkerque during the spring campaign. Data source: Météo France.

An illustration of the variations in rainfall and wind speed by sector of 45° can be found in Figure 9, in which we can notice that rainfall occurred mostly with winds from the NW to NE sectors ($315^\circ - 0^\circ - 45^\circ$). In the rest of the sectors, precipitation was very low and did not increase much beyond 2 mm with $180^\circ - 225^\circ$ winds, proving that we were sampling under a relatively dry weather.

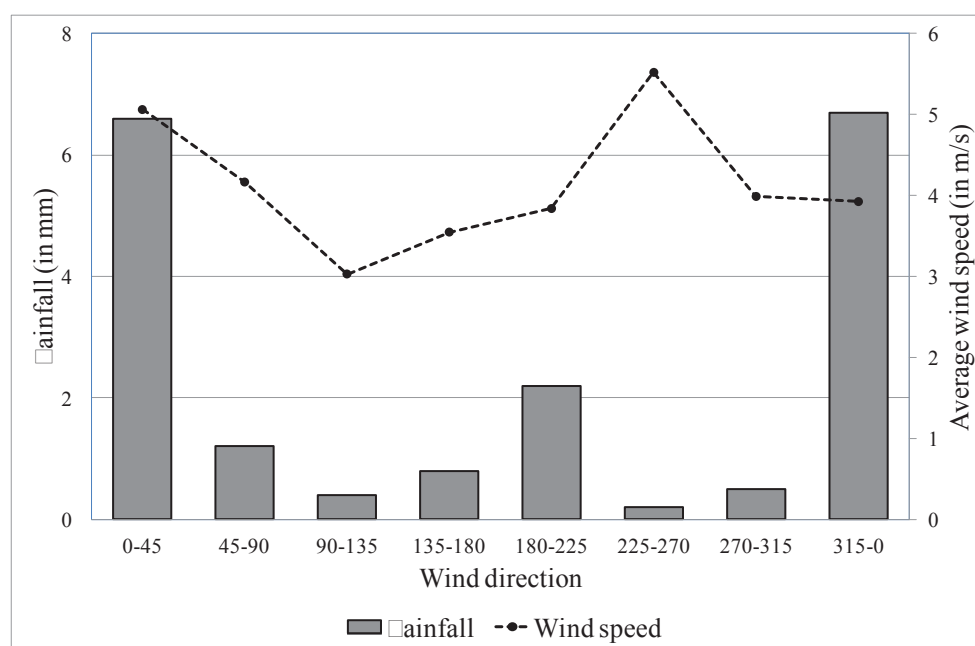


Figure 10: Variation of precipitation in mm by wind sector and average wind speed at Dunkerque during the spring campaign. Source: Météo France.

On the other hand, temperatures were found to be extremely fluctuating in this period (Figure 10), from low levels at the beginning, to higher ones before the end of the campaign. Globally, temperatures measured at the sampling site ranged between 0°C and 23°C, with an average found to be close to 10°C. These fluctuations show that we were able to sample under different weather conditions: winter to spring conditions in the beginning, typical spring weather, and summer weather (between 04/19 and 04/22/2011). The difference between the cold (00h-12h) and the warm (12h-24h) period of the day were clearly expressed in the recordings when compared to the winter campaign daily temperature fluctuations.

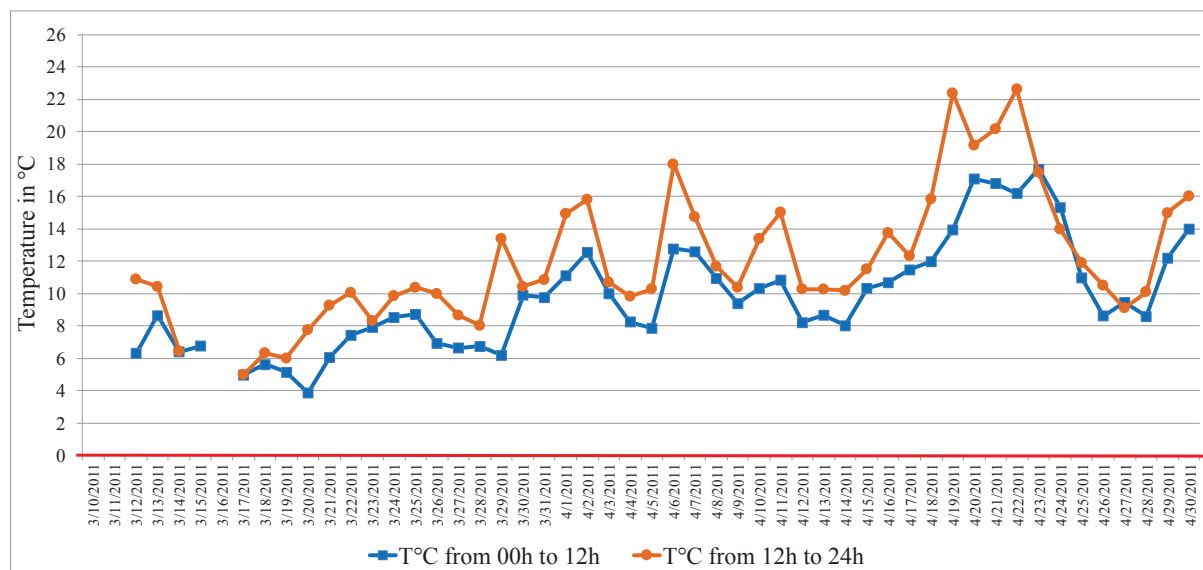


Figure 1 Evolution of 12h and 24h temperatures in °C at Dunkerque during the spring campaign

III.3. Wind, precipitation and temperature conditions in Saint-mer

In Saint-mer, the dominant wind was blowing essentially from the NE and SW directions (Figure 11). The highest frequency (38%) was found for low speed, followed by moderate speed (32%), very low (27%) and finally high speed (3%). However, the difference between Saint-mer and the rest of the sites is found in the frequency of very low speed winds: 27% versus 5% to 15% respectively. This last observation emphasizes the fact that in Saint-mer we sampled for a significant amount of time under major stagnant atmospheric condition.

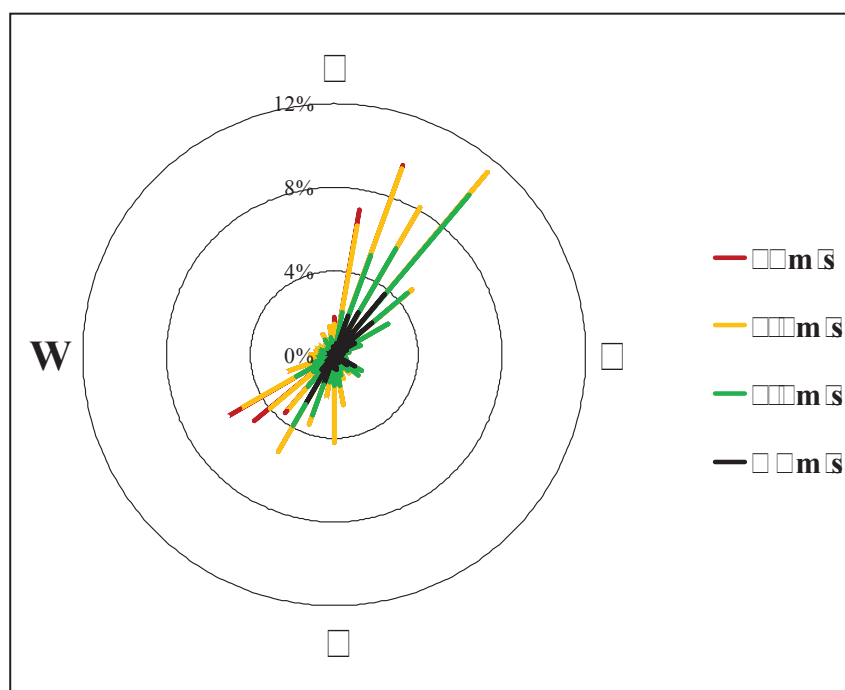


Figure 11 Wind rose at Aintamer during the spring campaign data source is from France

On the other hand, precipitation is found to be highly associated to winds coming from the S-W quarter ($180^{\circ} - 270^{\circ}$), whereas N sector winds did not carry the same load of rain (about 3.5 mm). The rest of the sectors rainfall was found negligible (Figure 12).

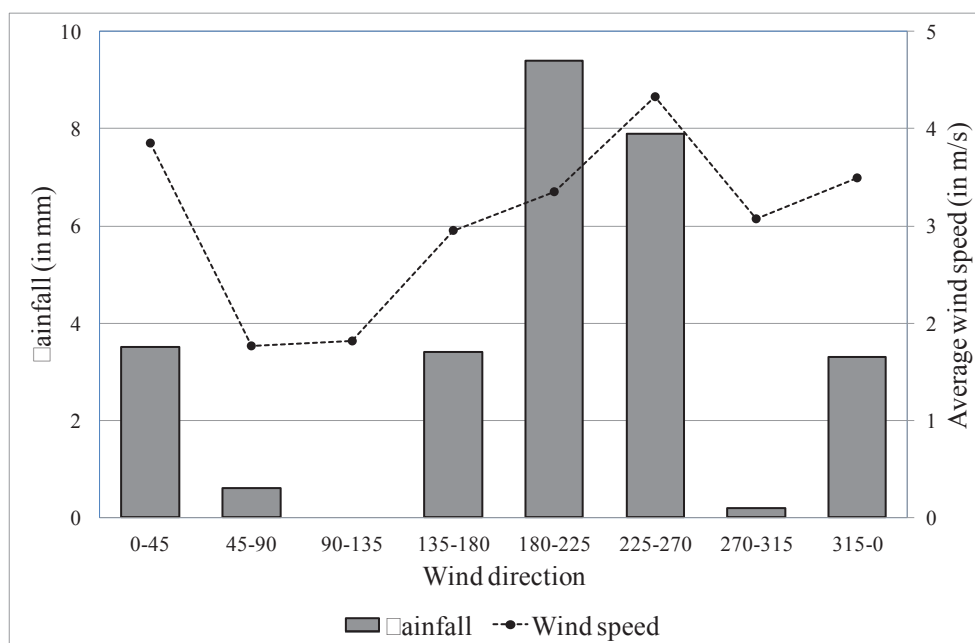


Figure 12 Variation of precipitation (in mm) by wind sector of Aintamer in relation to wind speed at Aintamer during the spring campaign data source is from France

Finally, temperatures at Saint-Émer are found to be relatively higher than those recorded at Dunkerque for the same period (Figure 13). The 12h-24h temperatures fluctuated between 6°C and 24°C , and in the same time the 00h-12h temperatures were fluctuating between 2°C and 16°C . On the other hand, a resemblance between Saint-Émer and Dunkerque temperature trends can be noticed at the level of the separation between cold (00h-12h) and warm period (12h-24h) of the day, during which the separation was amplified at Saint-Émer. This difference can be related to the fact that Saint-Émer is an inland site, and cannot benefit from the effect of the sea in moderating the variations of daily temperatures.

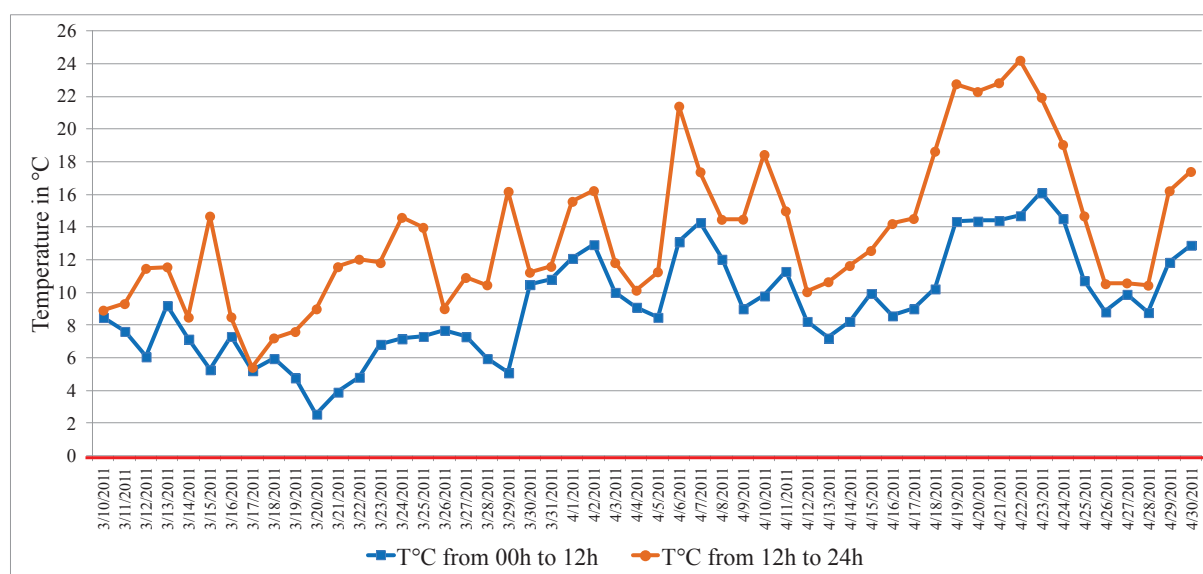


Figure 13 Evolution of temperatures in °C at Saint-Émer during the spring campaign

To resume all, we found that the spring campaign (03/10/2011 – 04/30/2011) is characterized by:

- High temperatures: 10°C in Dunkerque and 11°C in Saint-Émer, which are higher than the average found for these sites for the past 30 years (8°C). Furthermore, temperatures higher than 20°C were recorded during the second half of the campaign, which occurred under clear sky sunny days.
- A NE dominant wind direction associated with dry atmosphere, but also SW winds sometimes accompanied by some rainfall. These situations are almost in accordance with the usual seasonal observations.

III.3.3.era.e concentrations and contriutions to .

Ambient air $\text{PM}_{2.5}$ samples taken from Dunkerque, Boulogne-sur-Mer and Saint-omer during winter and spring campaigns were analyzed for ME, SI and TC content following the analytical methodology described in Chapter II. After the gathering of analytical data, a comparison between the results of sites will be realized as a first step to understand the trends of the analyzed chemical species within the region. Furthermore, in order to understand the difference in the level of our ions and elements concentrations with those found in nearby countries, a comparison with other sites chosen from the European continent will take place in the forthcoming section.

III.4.1. Winter campaign averages comparison

The results of the chemical analysis of the collected samples in Dunkerque and Boulogne-sur-Mer are illustrated in Table 2. We should note that between the TE group, TI concentration in Dunkerque's winter campaign from the first sample until 12/13/2012 (44 samples) could not be acquired due to technical reasons.

$\text{PM}_{2.5}$ mass fluctuations recorded by the air quality surveillance network of Atmo were retrieved from the "bulletin quotidien" page within the network web site (<http://www.atmo-npdc.fr>). A $\text{PM}_{2.5}$ average concentration of 24860 ng/m^3 was calculated for Dunkerque's winter campaign using Atmo data. It is found close to the limit value of $25 \text{ } \mu\text{g/m}^3$ (24 hours average) defined by the W (W, 2006) and the European Union (target value for 2015). In the case of Atmo, the measurements were taken by weighting procedures. However, our total analyzed $\text{PM}_{2.5}$ average concentration is lower than the one found with Atmo data. Our total is the sum of all the analyzed chemical species and doesn't consider other elements like oxygen concentrations, knowing that a lot of elements are found in oxide forms in the particles. Therefore, the difference between the two resides within the measurement and calculation method. We should also note that $\text{PM}_{2.5}$ monitoring stations are not installed at Boulogne-sur-Mer and Saint-omer. Instead Atmo monitors PM_{10} at those sites.

On the other hand, total $\text{PM}_{2.5}$ chemical species average concentration is found higher for Dunkerque than Boulogne-sur-Mer. ME average concentration in Dunkerque shows different levels, ranging from low values like 17.8 ng/m^3 found in the case of Al to very high ones such as TC concentration of 6198 ng/m^3 . However, Na is found to have the highest average between major metals, followed by Cu, Fe, Ca, Mg and Al.

Table 10: Average concentrations of $\text{PM}_{2.5}$, PM_{10} , SI , and TC found in PM_{10} collected in Dunkerque and Boulogne-sur-Mer during the inter campaign in nm^3

$\text{PM}_{2.5}$ (our study)	Dunkerque		Boulogne-sur-Mer	
	$\mu\text{g m}^{-3}$	SD	$\mu\text{g m}^{-3}$	SD
Al	17.8	± 12	0.1	13.1 ± 7.1
Ca	49.5	± 33.3	0.3	43.5 ± 26.8
Fe	92.9	± 96.1	0.5	52.6 ± 50.5
Mg	132	± 73.4	0.8	123 ± 75
Mg	34.2	± 38.2	0.2	24.5 ± 25.5
Na	237	± 267	1.3	202 ± 179
TE	84.9	± 102	0.5	50.3 ± 47
N_4^{+}	1914	± 1008	10.9	1706 ± 892
Cl^-	580	± 309	3.3	558 ± 279
N_3^-	5707	± 4734	32.5	5872 ± 4338
S_4^{2-}	2521	± 1779	14.3	2449 ± 1726
TC	6198	± 4175	35.3	5625 ± 3688
Total analyzed	17568		100	16719
$\text{PM}_{2.5}$ (Atmo)*	24860		-	

*Source: <http://www.atmo-npdc.fr>

The total contribution of ME in the total average accounted for about 3.2% compared to the 3.3% contribution coming from Cl^- only. The latter is the less concentrated ion within the SI group, proving the extent of ions contribution (61.1%) compared to the remaining elements in the load of $\text{PM}_{2.5}$. On the other hand, average TC accounted for 35.3% of total analyzed $\text{PM}_{2.5}$, and represents the highest average when compared individually to the other analyzed components.

As for Boulogne-sur-Mer, the results show that ME represent the same tendencies as the ones found in Dunkerque, with Na levels being higher than Cl^- , followed by Fe, Ca, Mg and Al. In the case of SI, the contribution in the total analyzed $\text{PM}_{2.5}$ average was also high (63.2%), when in the same time TC contribution decreased to 33.6% when compared to Dunkerque, leaving N_3^- with the highest contribution (35.1%). Also, TE average in Boulogne-sur-Mer is found to be low when compared to Dunkerque's average.

The average concentrations of SI, TC, ME and TE between Dunkerque and Boulogne-sur-Mer are compared herein (Figure 14 and Figure 15) in order to examine the variations in the chemical composition from one sampling site to another in the region.

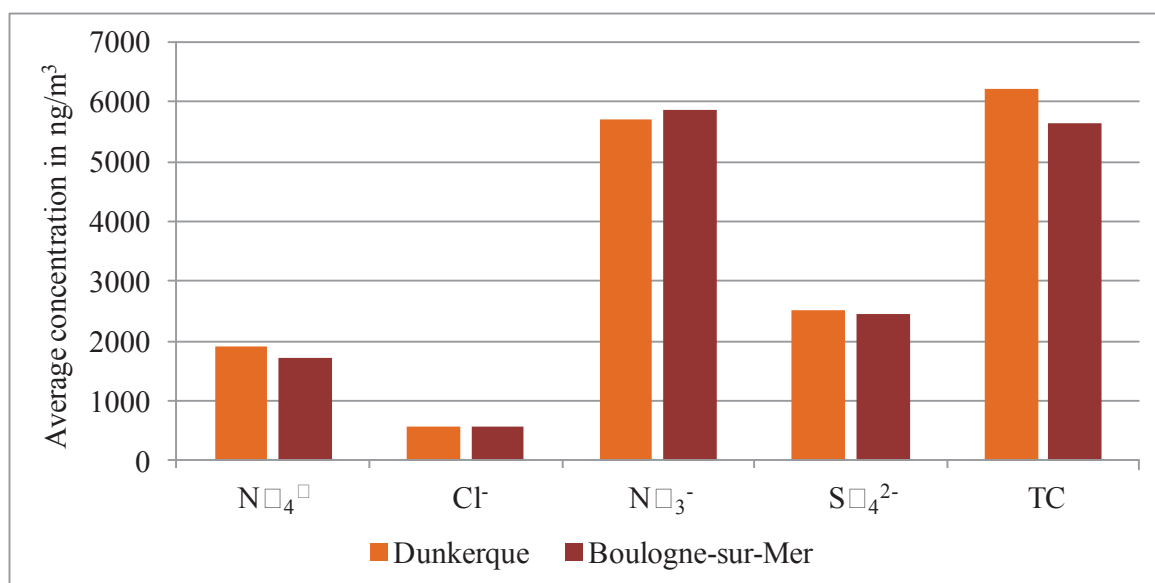


Figure 14 and average concentrations at Dunkerque and Boulogne-sur-Mer

For SI and TC, the values representing Dunkerque are found slightly higher than the ones representing Boulogne-sur-Mer for all the compared species except N_3^- (Figure 14).

Furthermore, the comparison of ME and TE averages illustrated in Figure 15 shows a similarity with the ones observed above. Dunkerque's values for all major metals were always found higher than in Boulogne-sur-Mer except Fe. We can also notice that in Dunkerque, Fe and TE levels were almost 2 and 1.5 fold higher than their respective levels in Boulogne-sur-Mer.

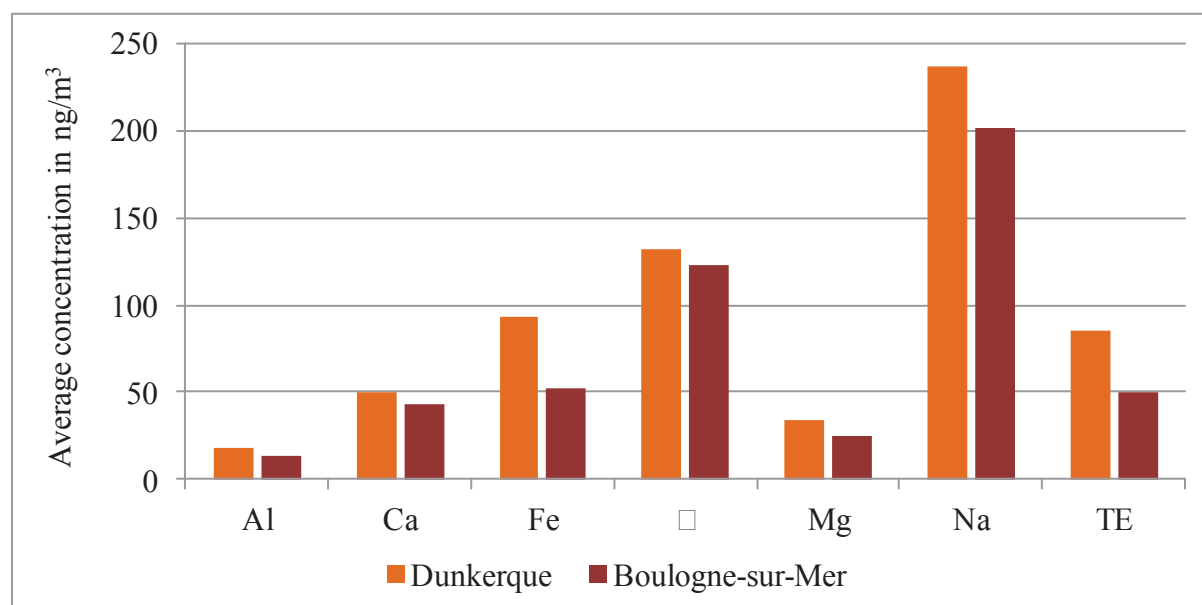


Figure 15 and average concentrations at Dunkerque and Boulogne-sur-Mer

For the winter campaign, the comparison between the concentrations of major components of $\Sigma M_{2.5}$ in Dunkerque and Boulogne-sur-Mer showed that:

- ME concentrations were comparable between the two sites with few exceptions.
- Highest concentrations were reserved to TC (5625-6198 ng/m³) and NO_3^- (5707-5872 ng/m³), followed by SO_4^{2-} (2449-2521 ng/m³) and NO_4^+ (1706-1914 ng/m³). The sum of these four species accounted for about 93% of the total analyzed species in $\Sigma M_{2.5}$.
- Fe, Ca, Al and Mg elements tend to be in higher concentrations in Dunkerque than in Boulogne-sur-Mer.

III.4.2.Spring campaign averages comparison

Table 3 summarizes the average concentrations of the analyzed chemical species in the samples taken from Dunkerque and Saint-omer during the spring campaign. We notice that total $\Sigma M_{2.5}$ chemical species average concentration is found slightly higher at Saint-omer.

When compared to the winter campaign, Dunkerque's spring values for ME show a decrease in the levels of Σ from 136 to 98.9 ng/m³. The succession during the spring campaign in decreasing order of metals average concentrations in Dunkerque becomes: Na, Fe, Σ , Ca, Mg and Al. Furthermore, SI contribution in fine $\Sigma M_{2.5}$ at Dunkerque was found to be 75.6%, with major nitrate ($\approx 50\%$) content. As for TE, the atmospheric average concentration is found higher than during the winter season, whereas TC values decreased from 6198 ng/m³ in winter to 4727 ng/m³ in spring. These differences will be extensively discussed in section III.6.

In the case of Saint-omer, average concentrations between ME elements have similar trends than the ones observed in Boulogne-sur-Mer during winter, with $Na > Fe > Ca > Mg > Al$. In addition, SI accounted for 74.6% of $\Sigma M_{2.5}$ load on average, which is comparable to the value found in Dunkerque (75.6%) for the same period. TC exhibited a different scenario in this campaign since its average contribution in fine ΣM rose to 23% in Saint-omer when compared to the 21.3% found in Dunkerque. It can be recalled that average contributions values for TC in the winter campaign were 33.6% (5625 ng/m³) and 35.3% (6198 ng/m³) in Boulogne-sur-Mer and Dunkerque respectively.

Table 3: Average concentrations of Al, Ca, Fe, and Na found in μg collected in Dunkerque and Saint-mer during the spring campaign in ng m^{-3}

	Dunkerque		Saint-mer		
<i>PM_{2.5} (our study)</i>	μg	<i>SD</i>	μg	<i>SD</i>	μg
Al	27.8	± 18.0	0.1	21.8	± 14.7
Ca	65.1	± 42.1	0.3	51.0	± 29.3
Fe	101	± 174	0.5	52.1	± 41.8
Na	98.9	± 68.6	0.4	107	± 67
Mg	42.2	± 56.9	0.2	25.2	± 31.5
TE	240	± 362	1.1	186	± 265
TE	100	± 160	0.5	76	± 75
NO_4^-	2306	± 1261	10.4	4466	± 2943
Cl^-	543	± 351	2.4	508	± 405
NO_3^-	11064	± 9470	49.9	9066	± 7598
SO_4^{2-}	2854	± 1528	12.9	2826	± 1751
TC	4727	± 2363	21.3	5205	± 2733
Total analyzed	22169		100.0	22591	100.0
<i>PM_{2.5} (Atmo)*</i>	33125			-	

*Source: <http://www.atmo-npdc.fr>

Finally, just like in the case of the first campaign, a significant difference was found between our total analyzed $\text{PM}_{2.5}$ and the measured $\text{PM}_{2.5}$ mass by Atmo. This latter exceeds the daily limit value of $25 \mu\text{g}/\text{m}^3$ defined by the WHO (WHO, 2006) and $28 \mu\text{g}/\text{m}^3$ defined as limit value for 2011 in France.

Further investigations on the trends of Atmo $\text{PM}_{2.5}$ (for Dunkerque) and PM_{10} (for Dunkerque, Boulogne-sur-Mer and Saint-mer) during the two sampling periods will be detailed later in this chapter.

The comparison of SI and TC between the two sites exhibited a different scene than the one we observed in the winter campaign (Figure 16). Some ions were found at the same level in the two sites (Cl^- and SO_4^{2-}), whereas NO_4^- and TC were higher at the inland site of Saint-mer, and only NO_3^- was found higher in Dunkerque.

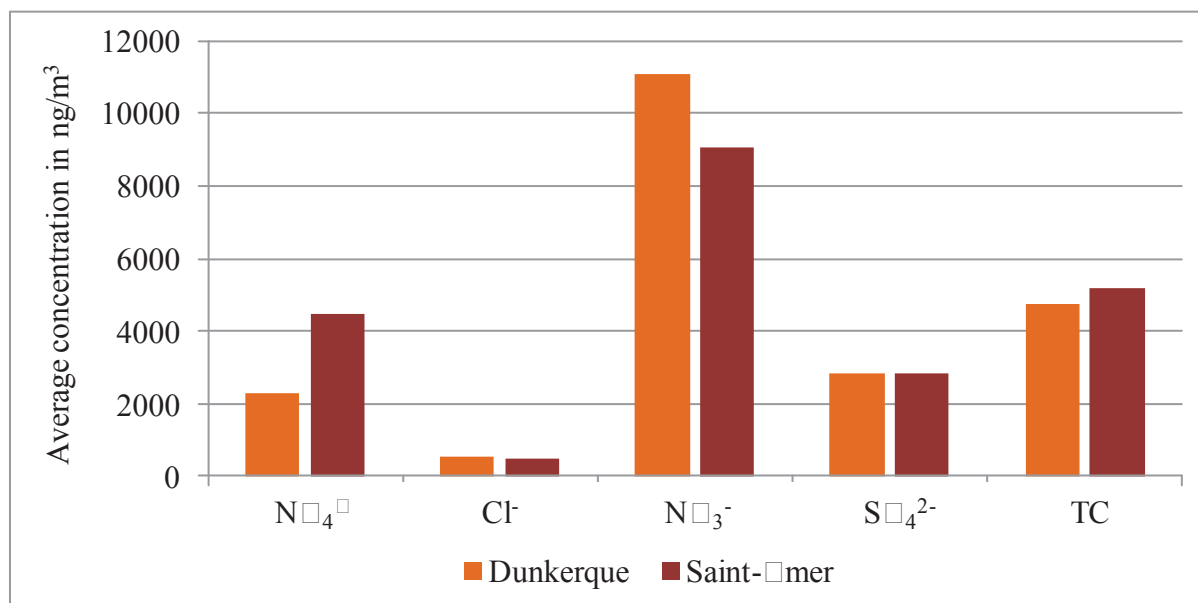


Figure 17 and average concentrations at Dunkerque and Saint-mer

The comparison of ME concentrations between the two sites of the spring campaign revealed higher values for Dunkerque except in the case of Cl^- , for which Saint-mer average concentration was found higher (Figure 17). In particular, Fe levels were doubled at the coastal industrialized site, where in the same time TE value was about 25% higher in Dunkerque.

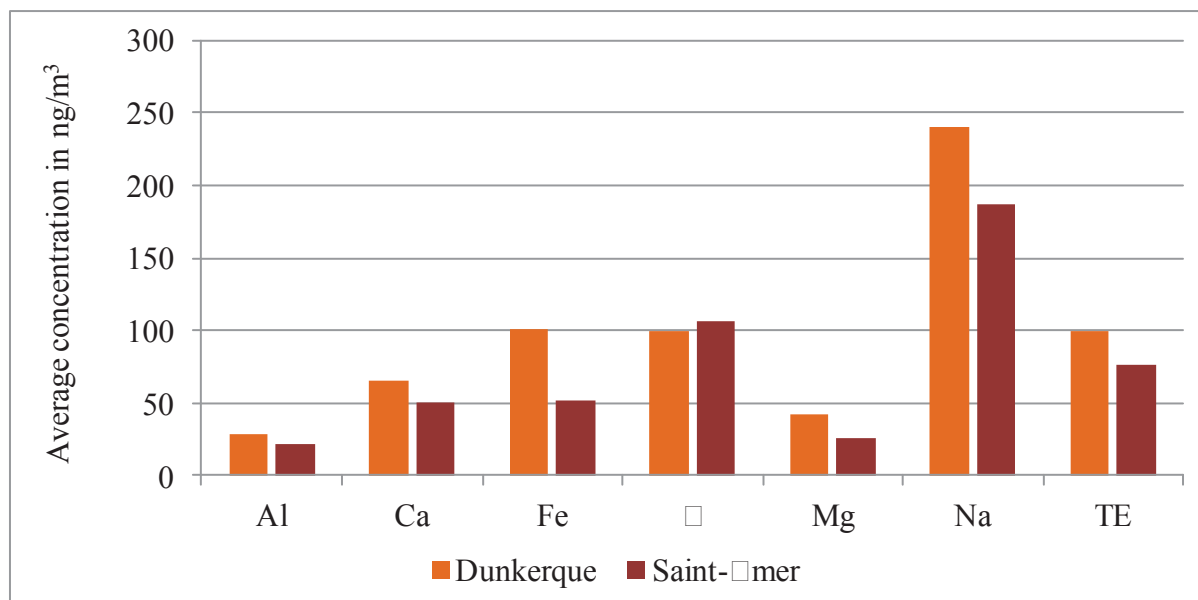


Figure 18 and average concentrations at Dunkerque and Saint-mer

Finally, for this spring campaign SI, ME, and TC concentrations comparison in Dunkerque and Saint-Quentin showed:

- Relatively higher values for major elements in Dunkerque.
- The highest concentration was observed in the case of NO_3^- , followed by TC, NO_4^- and SO_4^{2-} . The cumulative value of these species represented about 95% of the total $\text{PM}_{2.5}$ analyzed species.
- All ME except $\text{PM}_{2.5}$ are more concentrated in Dunkerque than in Saint-Quentin.

III.1.1.1. European concentrations comparison at a European scale

III.5.1.1. Location and characteristics of the comparison sites

The average concentrations are compared to other values found in similar studies accomplished at different sites in Europe (Figure 18). These sites were chosen depending on the pollution sources that affects them and the climate. All the selected studies focused on the $\text{PM}_{2.5}$ chemical composition in relation to different emission sources (direct and indirect traffic, natural (sea salt), industrial ...etc).



Figure 1 Comparison sites location on the European map (modified from Dalet, 2011)

Geographically, the sites are distributed between northern Europe (Finland, Sweden, Belgium, Netherlands and the United Kingdom), middle Europe (Switzerland and Hungary) and southern Europe (Spain, Italy and Greece).

Meteorological conditions play an important role in the chemical composition of fine PM (Seinfeld and Pandis, 2006). Therefore, within the chosen list of cities for comparison some are located in areas exhibiting similar climatic conditions when compared to our region like: West Midlands, Rotterdam and Ghent. Other sites represent relatively colder climate: Raahel, Vallila, Helsinki and Goteborg. Basel, Zurich and Budapest are inland sites, geographically positioned in the middle of Europe and can be subjected to intermediate climates between typical northern European and slightly warmer. To this category we add the Cantabria region that exhibits warmer climate fluctuations, but is located at a coastal site facing the Atlantic Ocean. Finally, the remaining sites: Madrid, Onda, Barcelona, Venice, Milan, Salento and Athens, are mostly subjected to warmer climates and are located in southern Europe.

In addition to the climate characteristics, we also explain the urban distinctiveness of the comparison sites as well as the major anthropogenic influences affecting them in Table 4. Some cities are located within regions that represent an urban density and population similar to those encountered in megacities (≥ 1 million inhabitants). Others are found less dense with a population ranging between a hundred thousand and one million inhabitants.

As for our sites: Dunkerque region (city and agglomeration) hosts about 223000 inhabitants, compared to 119000 inhabitants in Boulogne-sur-Mer and 64000 inhabitants in Saint-Émer.

Table 4. Characteristics of the comparison sites chosen from different European locations

Country	City	Site characteristics	References
Finland	Helsinki	Urban	(Pöli-Tuomi, et al., 2005)
	Tampere	Urban & Industrial (steelworks)	(Kivistö-Järvi, et al., 2003)
	Vaasa	Urban	(Koskanen, et al., 2001)
Sweden	Göteborg	Urban & Industrial	(Moloi, et al., 2002)
United Kingdom	West Midlands	Urban background	(Harrison & Yin, 2010)
Netherlands	Rotterdam	Urban	(Mooibroek, et al., 2011)
Belgium	Antwerp	Urban & Industrial (steelworks)	(Piana, et al., 2007)
Switzerland	Basel	Urban	(Ilacqua, et al., 2007)
	Zürich	Urban	(Bueglin, et al., 2005)
Hungary	Budapest	Urban	(Szigeti, et al., 2012)
Italy	Salento	Urban background (distant traffic)	(Ferrone, et al., 2011)
	Venice	Urban (& sea traffic) & light industry	(Stortini, et al., 2009)
	Milan	Urban (city center)	(Conati, et al., 2005)
Spain	Cantabria region	Urban & Industry	(Arruti, et al., 2011)
	Barcelona	Urban background & Industrial	(Piana, et al., 2007)
	Madrid	Urban	(Salvador, et al., 2012)
	Valencia	Urban background & Industrial	(Querol, et al., 2001)
Greece	Athens	Urban & Industrial	(Kateraki, et al., 2012)
	Athens	Urban	(Ilacqua, et al., 2007)

III.5.2. Comparison of ME, SI, and TC average concentrations

Table 5 illustrates arithmetic average concentrations of ME, SI and TC found in our study as well as those found at the comparison sites. The values found in our study ranged between low, comparable and high when compared to those found all around Europe. In this section, we grouped the compared chemical species by aerosol type. Hence Na, Cl⁻ and Mg will be grouped under “Marine major elements”. Also, “SIA major ions” will group: N₄⁺, N₃⁻ and S₄²⁻. Finally, the TC group will be represented by carbon and the last group will enclose the rest of the major elements: Al, Ca, Fe and Si.

Table III.10: Critical element concentrations in nm³ comparison between our region and Europe

City	Other ME metals				Marine major elements			SIA major ions			TC	References
	Al	Ca	Fe	□	Mg	Na	Cl ⁻	N□ ₃ ⁻	S□ ₄ ²⁻	N□ ₄ [□]		
Dunkerque winter	1□	□□	□3	13□	3□	□3□	□□□	□□□□	□□□	1□□□	□□□□	our study
Dunkerque summer	13	□□	□3	1□3	□□	□□□	□□□	□□□□	□□□□	1□□□	□□□□	□
Dunkerque spring	□□	□□	1□□	□□	□□	□□□	□□3	11□□□	□□□□	□3□□	□□□□	□
Frankfurt spring	□□	□□	□□	1□□	□□	1□□	□□□	□□□□	□□□□	□□□□	□□□□	□
Hallila (□M _{2,3})	59	71	96	85	25	170	43	1600	2500	1100	-	(Kakkanen, et al., 2001)
Rotterdam	36	83	206	130	51	251	400	3500	2600	1600	5700	(Mooibroek, et al., 2011)
Zurich	48	54	124	223	17	96	72	3500	3500	2100	6500	(Kueglin, et al., 2005)
Cantabria	-	600	30	100	100	800	800	800	1800	200	3100	(Arruti, et al., 2011)
West Midlands	544	82	102	152	170	2474	470	1600	2200	-	4300	(Garrison □□□□, 2010)
London	-	800	300	500	100	300	200	500	6200	1800	1200	(Querol, et al., 2001)
Naashe	38	116	473	268	26	185	-	-	-	-	-	(Kavitsarvi, et al., 2003)
Stockholm	-	41	77	120	-	-	-	-	-	-	-	(Moloi, et al., 2002)
Thessalonika (cold)	-	-	-	-	-	-	-	5000	3000	2600	6400	(Kiana, et al., 2007)
Thessalonika (warm)	-	-	-	-	-	-	-	1500	2200	1000	3000	□
Barcelona (cold period)	-	-	-	-	-	-	-	3800	3600	2300	7900	□
Barcelona (warm period)	-	-	-	-	-	-	-	300	4200	1200	4500	□
Athens	-	-	-	-	-	-	800	1330	5190	1300	6260	(Kateraki, et al., 2012)
Helsinki	163	174	752	118	-	-	-	-	-	-	-	(Kli-Tuomi, et al., 2005)
Basel	502	102	97	332	471	2437	-	-	-	-	-	(Ilacqua, et al., 2007)
Budapest	-	-	214	-	-	-	110	2500	2300	1270	9180	(Szigeti, et al., 2012)
Venice	634	-	98	229	-	1555	-	-	-	-	-	(Stortini, et al., 2009)
Madrid	-	-	-	-	-	-	-	1490	2400	1480	9800	(Salvador, et al., 2012)
Milan (cold)	-	-	-	-	-	-	600	20200	5800	5200	15000	(Conati, et al., 2005)
Milan (warm)	-	-	-	-	-	-	90	4600	4000	2200	6300	□
Athens	789	471	13	368	1045	5413	-	-	-	-	-	(Ilacqua, et al., 2007)
Salento	-	-	-	-	-	-	100	200	5590	2100	7100	(Ferrone, et al., 2011)

III.1.1. Marine macroelements

In this section, Na, Cl⁻ and Mg will be considered as sea salt elements. The average concentrations for Na and Cl⁻ found in our study were similar from one site to another, except for Mg which is found higher in Dunkerque when compared to Boulogne-sur-Mer and Saint-Omer.

The Na values are found comparable to geographically close sites like Laahe, Ballila and Rotterdam. Higher Na concentrations can be found in south European sites: Landa, Venice and Athens, but also in Cantabria region. This is probably due to the proximity of these sites to the sea and therefore they are subjected to higher wind circulation originating from the sea and loaded with marine particulates.

Within this type of comparison, we could not pass by the conclusions of a study that compiled sodium concentration data in 89 European sites to trace sea (Manders, et al., 2010). This work focused on PM₁₀ sea salts emitted in high concentrations from the sea, which highlights this latter as a major source of suspended particles. Hence, stretching along the facade of the North Sea, average concentration was about 5 µg/m³, whereas lower concentrations were found for inland European sites. Concentrations ranged between 2 and 5 µg/m³ in inland sites, almost 300 km away from the sea, and decreased furthermore when moving deeper inland.

Low Na concentration is found lower than our results, and can be explained by the location of the city in the middle of Europe and away from the coastline. West Midlands and Basel represented exceptionally higher Na levels compared to our sites even though the first site is geographically close, and the second is located further inland in Europe. West Midland is located within the island of the United Kingdom and can be hit by winds carrying sea salts from all directions. As for Basel, the high atmospheric salt content might be linked to the use of salt to defreeze road pavements in winter. This is probably the only logical explanation to this high salt content, since Basel is an inland site in middle Europe. During dry periods, crystal salt will be found in dust form on the ground. This salt is probably re-suspended into the atmosphere by traffic activities. The dates during which sampling occurred in that study (Ilacqua, et al., 2007) confirm our suggestion on the origins of the atmospheric salt, since sampling was conducted between winter 1997 and spring 1998.

On the other hand, Cl⁻ average concentrations are also found similar from one site to another in our study, but when compared to the other sites, it was found to be comparable to the averages of Athens and Cantabria region and higher than the rest. The low values found in

coastal sites around Europe can be explained by chloride depletion phenomenon that is frequently encountered after sea Cl^- reaction with acidic emissions from anthropogenic sources. Actually, freshly emitted sea salts carry a certain Cl^- load that is related to Na concentration ($\frac{\text{Cl}^-}{\text{Na}^+} \approx 1.789$ is the mass ratio Cl/Na in sea water). When the fresh sea salt aerosol passes over an atmosphere loaded with anthropogenic emissions (such as NO_x and SO_2) that transform into acidic species, a reaction between these species and sea salts will occur which leads to replacing Cl^- with sulfates or nitrates. This will eventually lead to a decrease in the amount of Cl^- in fresh sea aerosol which is also called “chloride depletion” described also in (Seinfeld & Pandis, 2006). The aerosols referred to as “sea salt” at the beginning will be known as “aged sea salt” after these chemical changes.

However, in our study we noticed that Cl^-/Na^+ ratios ranged between 2.3 and 2.7 from one site to another. This observation pushes us to consider other sources of Cl^- than the marine one, a point that was also raised in a previous work conducted in our laboratory (Bedoux, et al., 2006). Ratios of Cl^-/Na^+ in the particles were compared between different granulometric sizes of particles collected using a cascade impactor, to conclude that the ratio tend to be higher in smaller sized particles ($\leq 2.5 \mu\text{m}$). This conclusion was explained by considering additional sources of Cl^- other than marine. In fact, ratios rose up to 10 with winds blowing from the East sector, whereas the air mass originated from continental Europe. Cl^- ions can be generated by many anthropogenic activities in this case like combustion related emissions (biomass and incineration), or sintering in industrial emissions (Heis, et al., 2013). Furthermore, Bedoux in 2006 demonstrated that a part of Cl^- ions could be neutralized by ammonium ions (Bedoux, et al., 2006).

Finally, Mg average concentrations were doubled at Dunkerque when compared to the two remaining sites of our study. Mg values found in Ballila, Bahe and Burich are comparable to those found for Boulogne-sur-Mer and Saint-Omer, and low when compared to Dunkerque's values. The latter was found comparable to the averages found in Rotterdam, and low when compared to the rest of the comparison studies, most of which are located in southern Europe.

III.3.3.3 major ions

Secondary inorganic components appear to be predominant in $\text{PM}_{2.5}$ in the three studied sites. This observation is also verified on the European scale as well (Gutaud, et al., 2010).

III.5.2.2.1. Nitrates

Comparable nitrates average concentrations were found between Dunkerque and Boulogne-sur-Mer during the winter season, whereas during the spring campaign, Dunkerque's average was found much higher than Saint-Omer's. Furthermore, the levels encountered in our samples are higher than all the comparison sites except for Milan in the cold season, in which NO_3^- levels peaked to slightly cross the $20 \text{ } \mu\text{g}/\text{m}^3$ barrier.

III.5.2.2.2. Sulfates

Sulfates average concentrations are found comparable between our sites during the sampling campaigns. The average concentrations are also comparable to μallila , West Midlands, $\mu\text{otterdam}$, μhent , Budapest and Madrid. With the exception of μallila , the rest of these comparison cities are much more urbanized than our studied ones, including Dunkerque. However, sulfate levels in Cantabria region exhibited relatively lower levels than the ones found in our sites for both winter and spring periods. Finally, higher sulfate levels were found mostly in the studies in the Mediterranean zone, especially Spain, Italy and Greece.

III.5.2.2.3. Ammonium

The highest average concentration for NO_4^+ was found at Saint-Omer, which is an inland city, followed by Dunkerque and Boulogne-sur-Mer. The spring period showed higher concentrations than the winter one in our samples. Furthermore, the results are comparable to most of the comparison sites after omitting Saint-Omer high value during the spring period. The latter was only comparable to Milan high average concentration.

For the remainder of our sites, the values are found similar to the geographically close studies like $\mu\text{otterdam}$, μhent and μurich . Finally, lower values are noticed in northern Europe (μallila), but also in big cities towards the south such as Madrid, Budapest and Athens.

III.3.3. Total carbon

The winter period samples are characterized by the highest TC concentrations, with a maximum average reached at Dunkerque. This latter was found comparable to the values found in μurich , μhent (during the cold period) and Athens. For the rest of our sites, the values for TC are found comparable to $\mu\text{otterdam}$, West Midlands and Barcelona.

Higher averages are found in big cities like Barcelona, Budapest, Madrid, Salento and Milan. In the latter, a high peak of TC concentration is reached, in the warm period, which

makes more than the double of Dunkerque winter season high value. These cities exhibit higher traffic densities than the rest of the sites, including ours.

Finally, relatively low TC averages are encountered in Cantabria, Ónda and Óhent (warm period) when compared to our study results.

III.3.3.3.4. Other elements

The average concentrations for Al are found comparable to Óotterdam and Óaahe values, and lower than in the rest of the comparison sites. Peaks of Al can be noticed in Athens, West Midlands, Basel and Óenice in decreasing order. At these sites, Al levels can be associated to locally resuspended dust caused by high traffic density.

However, Ca levels are comparable to those found in Óallila, Óurich and Óoteborg. When in the same time, higher Ca values are found in the close Óotterdam study, West Midlands, Óaahe, Óelsinki and Basel. The Ca average concentration observed in Cantabria, Ónda and Athens were the highest between the studies used for comparison including our own results. The reason behind these levels was linked to crustal sources in Ónda, and to traffic resuspended road dust in Athens.

Furthermore, Fe levels are twice higher in Dunkerque when compared to the rest of our study sites during both winter and spring periods. But when compared to the other European sites, the high values encountered at Dunkerque are found comparable to those found in Óallila, Óurich, West Midlands, Óoteborg, Basel and Óenice. Much higher Fe concentrations were observed in northern Europe (Óotterdam, Óaahe, and Óelsinki) as well as in southern Europe (Ónda and Budapest). Traffic sources are found to probably cause the Fe elevation in Óotterdam, Óelsinki and in Budapest. Crustal enrichment was found to be behind the high Fe levels at Ónda, whereas steelworks were possibly behind the high Fe concentration at Óaahe.

Ó is found to fluctuate depending on the seasons. It is found higher in winter compared to spring. This correlates well with the fact that Ó is an indicator for biomass combustion, but also for other sources as well. Therefore, when compared to other sites, our values are found to be comparable to the values found for Óallila, Óotterdam, Cantabria, West Midlands, Óoteborg and Óelsinki. Higher values in Óurich and Basel were linked to biomass combustion. In the same time, high crustal enrichment was found responsible of Ó increase in Ónda and Óenice. As for Óaahe, high Ó levels were linked to the waste gas dust in the steel works sintering plant.

Finally, we can conclude that the elemental average concentrations measured in the atmosphere of the three sites in the NÓdC region are comparable to those measured in other

European sites. However, observed differences could be explained by the specific geographical position and/or the difference in population densities between the reference sites.

III. Diurnal evolution of ME, SI, and TC

In this section we will discuss the daily evolution of ME, SI, and TC concentrations in $M_{2.5}$ samples during both the winter and spring campaigns. Some elements and ionic species were separated in groups, for which the concentration is calculated by the sum of each element or ions concentration included within the group. The evolution of these groups will be compared and will include: sea salts, secondary inorganic aerosols (SIA), TC, and the rest of the ME group.

Sea salts concentrations in our sampled ME are evaluated by adding the concentrations of the analyzed typical sea elements and ions. To accomplish this goal, we calculated the sea salt concentration of ME elements using Na concentration as a reference with respect to sea water composition. Na is considered here as totally generated by sea spray, and therefore its presence is considered as a marker of sea originated aerosols. Following this principle, the sea salt (ss-) and non sea salt (Nss-) elemental concentrations, expressed in ng/m^3 , are calculated as follows:

From (Seinfeld and Pandis, 2006):

- $ss-Cl^- = 1.789 Na$ and $Nss-Cl^- = Cl^- - ss-Cl^-$
- $ss-Mg^{2+} = 0.1205 Na$ and $Nss-Mg = Mg - ss-Mg^{2+}$ (the maximum values of $ss-Mg^{2+}$ was forced to equalize total Mg instead of exceeding it).

From (Wang and Shooter, 2001):

- $ss-Ca^{2+} = 0.0385 Na$ and $Nss-Ca = Ca - ss-Ca^{2+}$
- $ss-NO_3^- = 0.037 Na$ and $Nss-NO_3^- = NO_3^- - ss-NO_3^-$
- $ss-SO_4^{2-} = 0.2516 Na$ and $Nss-SO_4^{2-} = SO_4^{2-} - ss-SO_4^{2-}$

Following this method, sea salt concentration for each sample is calculated by summing the sea salt components of each sample:

- $Sea\ salt = Na + ss-Cl^- + ss-Mg^{2+} + ss-Ca^{2+} + ss-NO_3^- + ss-SO_4^{2-}$

Furthermore, SIA form another interesting group which concentrations are calculated following this method:

- $SIA = N_4^- + N_3^- + Nss-SO_4^{2-}$

Finally, the rest of the elements including: Fe, Al, Nss-Ca, Nss- \square , Nss-Mg and TC are also included in this section for temporal evolution study. Fe and Al evolutions will be compared with the evolution of Nss-Ca and Nss-Mg respectively, because these elements usually points at a crustal source of \square M but also can point at industrial sources in the region. We lay this possibility as we acquired information in previously conducted studies about our regional air quality, especially in Dunkerque ((\square leis, 2010) and (\square edoux, et al., 2006)). Also, TC and Nss- \square variations will be studied together as they are considered as important tracers for combustion processes.

III.6.1. Winter campaign

III.6.1.1. Sea salts diurnal evolution

Table 6 compares the mean distributions of some selected species (Ca, Mg, \square , Cl^- , and $\text{S}\square_4^{2-}$) between sea salt and non sea salt fractions for both Dunkerque and Boulogne-sur-Mer during the winter campaign.

Table 6: Percentage of sea salt and non sea salt fractions in sea salt components in winter

Dunkerque				Boulogne-sur-Mer			
<i>Sea salt</i>	%	<i>Non sea salt</i>	%	<i>Sea salt</i>	%	<i>Non sea salt</i>	%
ss- Ca^{2+}	18.4	Nss-Ca	81.6	ss- Ca^{2+}	17.9	Nss-Ca	82.1
ss- Mg^{2+}	79.5	Nss-Mg	20.5	ss- Mg^{2+}	94.1	Nss-Mg	5.9
ss- \square	6.6	Nss- \square	93.4	ss- \square	6.1	Nss- \square	93.9
ss- Cl^-	73.4	Nss- Cl^-	26.6	ss- Cl^-	65.1	Nss- Cl^-	34.9
ss- $\text{S}\square_4^{2-}$	2.4	Nss- $\text{S}\square_4^{2-}$	97.6	ss- $\text{S}\square_4^{2-}$	2.1	Nss- $\text{S}\square_4^{2-}$	97.9

In Dunkerque for example, 79.5% from total Mg average concentration is ss- Mg^{2+} . Similarly, 73.4% of total Cl^- , 18.4% of Ca, 6.6% of \square , and 2.4% of $\text{S}\square_4^{2-}$ average concentrations was sea salt.

Boulogne-sur-Mer samples follow similar patterns for the percentage of contribution of each element total concentration. About 94.1% of Mg concentrations is found as sea salts, while 65.1, 17.9, 6.1, and 2.1% constitute ss- Cl^- , ss- Ca^{2+} , ss- \square , and ss- $\text{S}\square_4^{2-}$ respectively from their corresponding totals. These calculations confirm that Cl^- ions are not only related to a marine origin as suggested earlier (26.6% and 34.9% of Cl^- is in Nss- Cl^- form).

As for the diurnal evolution, we can notice a resemblance in the temporal evolution of calculated sea salt concentrations between the two sites (Figure 19), with a ground level constantly below 300 ng/m³ interrupted with peaks reaching 3500 ng/m³. This similarity

proves the presence of regional influence of sea spray in this coastal region. For example, some peaks of sea salt concentrations were observed in both sites and occurring simultaneously with sea sector winds (N-W winds in 12/12/2010 and N-E winds in 12/23-25/2010). However, sea salt peaks were not chronologically synchronized all the time between the two sites. Some peaks were observed in Dunkerque (11/22-26/2010 and 12/16-17/2010) and were not matched by others in Boulogne-sur-Mer. The latter exhibited similar peaks also in 12/14 and 12/15/2010. This shows that punctual differences are present between the two sites, which refer to the presence of local influences linked to the position of the site on the coast, as well as regional influences, found on a lower frequency. Therefore, we can conclude that sea salt concentrations during the winter campaign exhibited temporal variability instead of geographical.

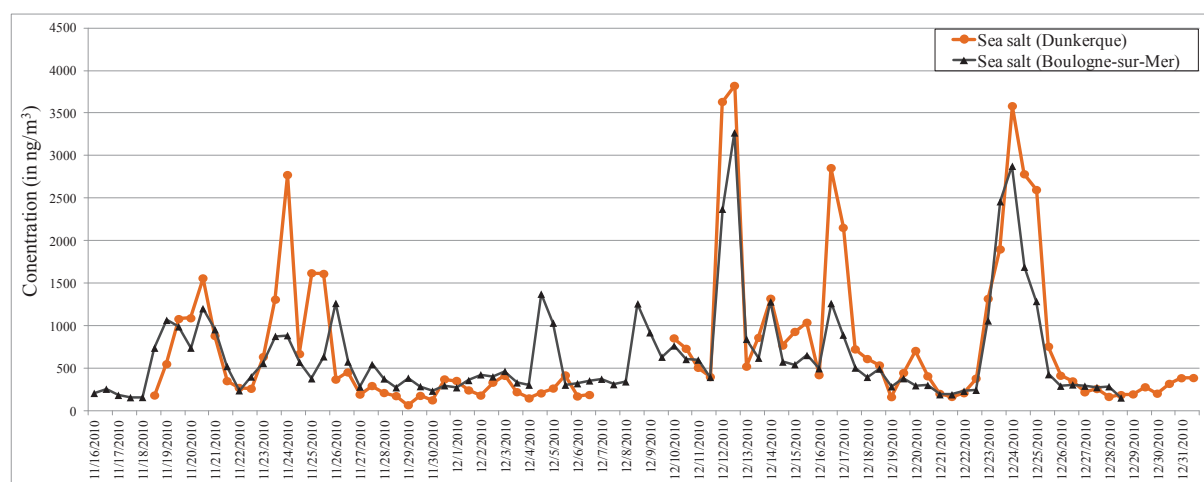


Figure 1 Diurnal evolution of sea salts concentrations in ng/m^3 in Dunkerque and Boulogne-sur-Mer during the winter campaign

III.1.1. Fe and Nss-Ca diurnal evolution

Total Fe and Nss-Ca diurnal evolution are illustrated in Figure 20. The evolution of Fe concentrations shows globally higher levels in Dunkerque, in addition to high peaks found frequently during the sampling period that are not matched at Boulogne-sur-Mer. However, Fe peaks identified at Boulogne-sur-Mer are limited to 5 samples that presented slightly higher Fe concentrations than the corresponding samples in Dunkerque. The difference in this trend between these two sites proves that local sources of emissions are affecting Fe levels instead of regional ones, with higher local contribution found in Dunkerque compared to Boulogne-sur-Mer.

Nss-Ca concentrations followed to a certain extent the style of Fe evolution, suggesting that local sources play a major role in Nss-Ca fluctuations. Moreover, the highest concentration peak value of Nss-Ca at Boulogne-sur-Mer is found to be close to the maximum peak reached at Dunkerque, which proves the extent of local pollution sources contribution in the two sites.

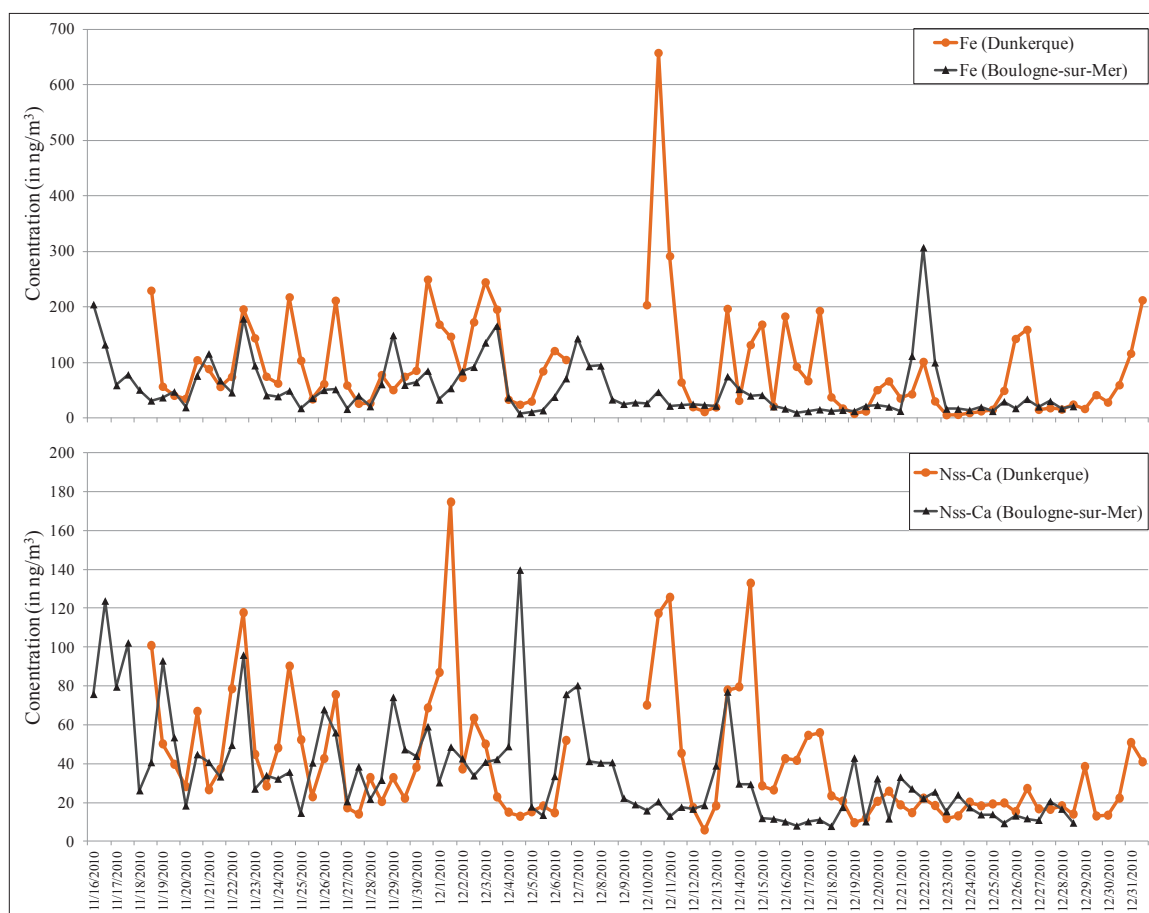


Figure 11: Diurnal evolution of Fe and Nss-Ca concentrations in Dunkerque and Boulogne-sur-Mer during the winter campaign

If we analyze Fe to Nss-Ca evolution at Dunkerque, we can notice that for almost every Fe peak there is a Nss-Ca increase. This link, which is missing at this frequency in the case of Boulogne-sur-Mer, points at a combined source of Fe and Nss-Ca in Dunkerque.

For Dunkerque's site, these observations can be partially related to steelmaking type of emissions. In fact, a previous study demonstrated that Fe and Ca were largely used for the production of iron. Emitted particulates from the different installations are therefore constituted from these elements (Leis, et al., 2013) and have an impact on the chemical composition of atmospheric PM. In our study, it is essential to determine if these Fe and Ca

peaks can be related to the steel-making industry. An answer to this question will be developed in chapter I and II.

III.1.3. Al and Nss-Mg diurnal evolution

Following the same logic used in the case of Fe and Nss-Ca, we compared Al and Nss-Mg concentrations evolution during our winter sampling period (Figure 21). The diurnal variation of Al concentrations in Dunkerque and Boulogne-sur-Mer is not similar, which suggests the influence of a local phenomenon. In general, Al is known to be generated by different sources of PM emissions, but many scientists classify this element as originating from soil dust. In this case, its presence in the atmosphere can be related to dust re-suspension. Furthermore, in urban environments, these dust emissions can be encountered mainly in the vicinity of transportation related traffic and/or in certain areas exhibiting particular wind turbulences. These phenomena can partially explain the temporal Al fluctuations at both sites.

However, the identification of higher Al concentrations peaks frequency in Dunkerque when compared to Boulogne-sur-Mer shows the participation of local Al emissions at the first site. The same observation can be noted for Fe and Ca, which high concentrations can be related to the emissions from the steelmaking industry in Dunkerque.

For Nss-Mg concentrations, we noticed that some values remains at the zero level, which proves that in these cases ss-Mg concentration was equal to the total Mg content. This also shows that Mg loads are resulting mainly from marine origins. In addition, independent peaks also appears in Dunkerque and Boulogne-sur-Mer, which suggest local sources of Mg enrichment, especially in the case of Dunkerque where Nss-Mg peaks are found higher and more frequent than in Boulogne-sur-Mer.

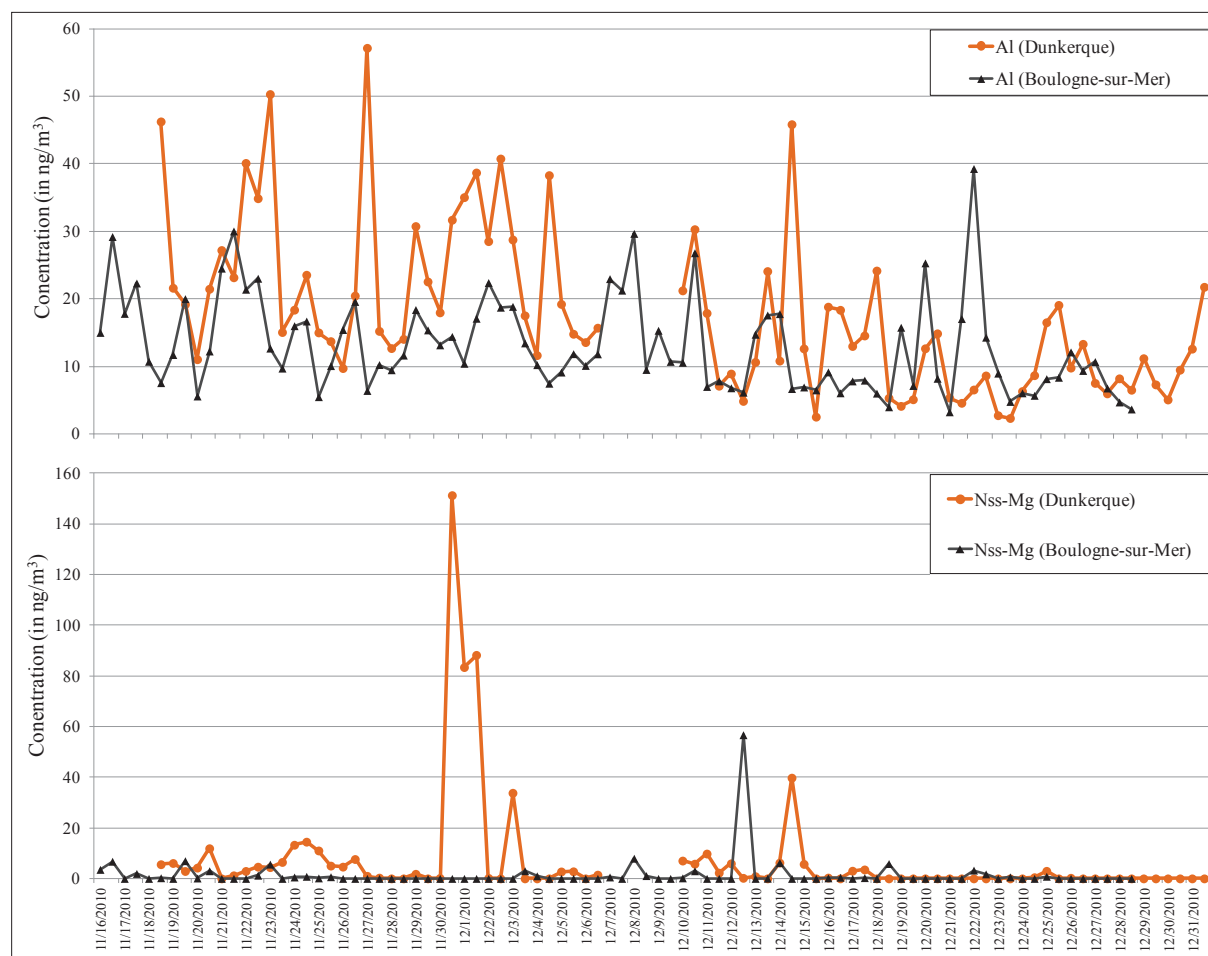


Figure 1 Diurnal evolution of Al and Nss-Mg concentrations in Dunkerque and Boulogne-sur-Mer during the inter campaign

III.1.1. Al and Nss-Mg diurnal evolution

In this section we will discuss the evolution of TC and Nss-Mg, which can both be tracers of combustion processes ((Sillanpaa, et al., 2006) (Pateraki, et al., 2012)), during the sampling period. Figure 22 illustrates these variations, and shows that TC patterns are similar to a certain extent between Dunkerque and Boulogne-sur-Mer. The maximum values reached at the two sites proves that the emission source impact is similar, which leads to the possibility of having a same source of TC emissions located at both sites.

On the other hand, and under a much smaller scale, diurnal Nss-Mg fluctuations followed a hilly pattern, close to TC. Similar high Nss-Mg values at both sites point toward a similarity between the types of local emission sources.

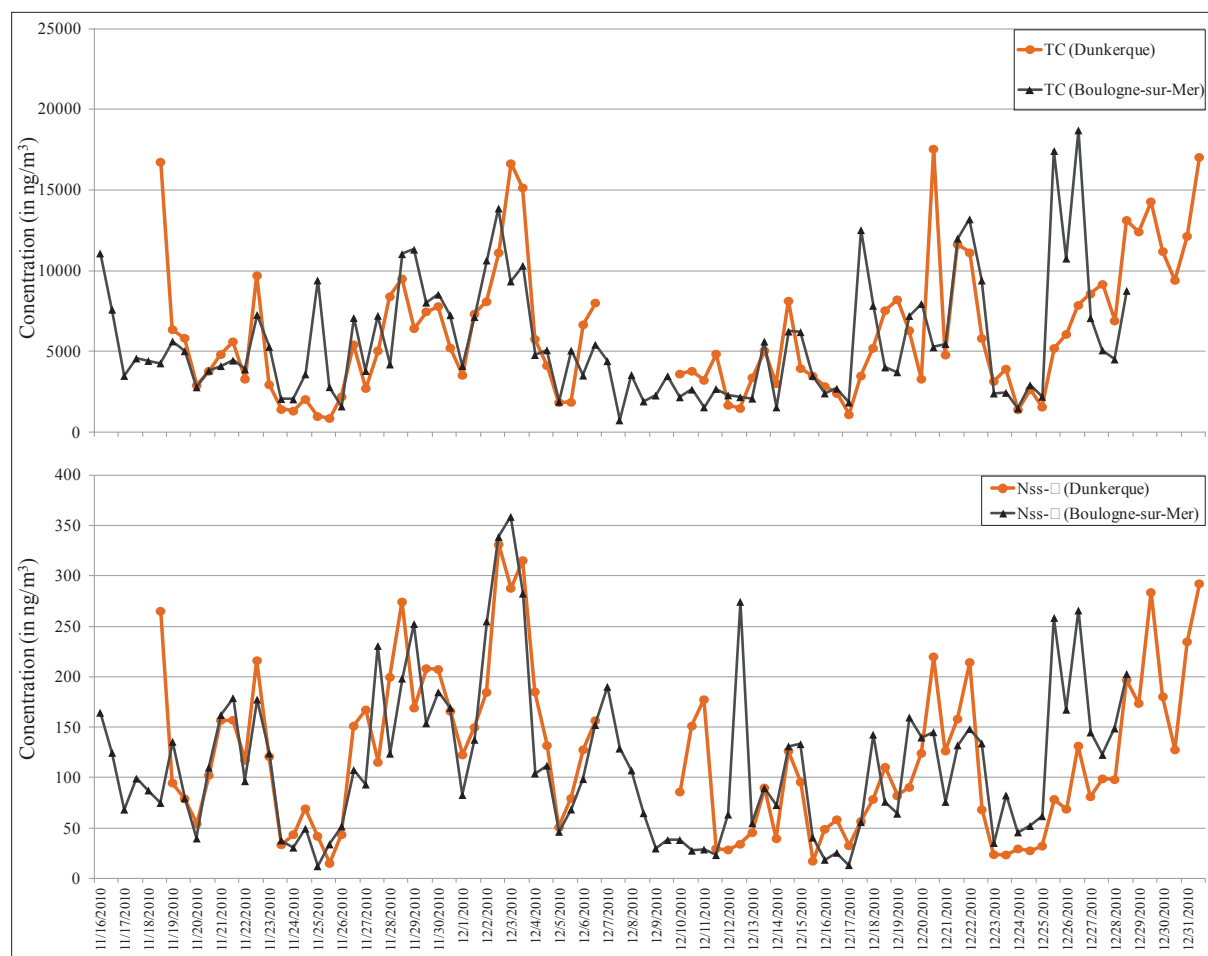


Figure 11: Diurnal evolution of TC and Nss concentrations in Dunkerque and Boulogne-sur-Mer during the inter campaign

By comparing TC and Nss concentrations evolution at each site, we can notice that it is homogeneous with some rare exceptions. This observation indicates that these species concentrations evolution represent mainly a regional tendency. Local specificity can be responsible for some differences rarely observed between the two sites (peaks occurring between 12/26 and 12/28/2010 at Boulogne-sur-Mer).

Finally, it is important to mention that high TC and \square concentrations were observed during a very cold period of the campaign stretching from 11/27/2010 to 12/4/2010. This phenomenon was also observed at the end of the sampling campaign but in less intense peaks, but during which low temperatures were coupled to snowing events. These high levels of TC and \square could be partially due to residential heating emissions that increased during these episodes.

III.1.1.1 diurnal evolution

SIA as well as NO_4^- , NO_3^- and SO_4^{2-} concentrations evolution during the winter campaign at the two sampling sites are illustrated in Figure 23. We can notice that SIA followed a globally similar pattern between the two sites, indicating the presence of regional background pollution of SIA. Local differences are restricted to few samples at both sites as well, which suggest the presence of local low contributions.

SIA is calculated by adding the concentrations found for NO_4^- , NO_3^- and SO_4^{2-} in the samples. These ions evolution, next to SIA in Figure 23, shows that NO_4^- and SO_4^{2-} are fluctuating under 5000 ng/m^3 level, with few exceptions for SO_4^{2-} punctual peaks that rose to almost 10000 ng/m^3 . However, NO_3^- peaks elevated to 20000 ng/m^3 and 25000 ng/m^3 in Dunkerque and Boulogne-sur-Mer respectively. The trends for these species show that between the ions, the major contributor of the SIA content is actually NO_3^- .

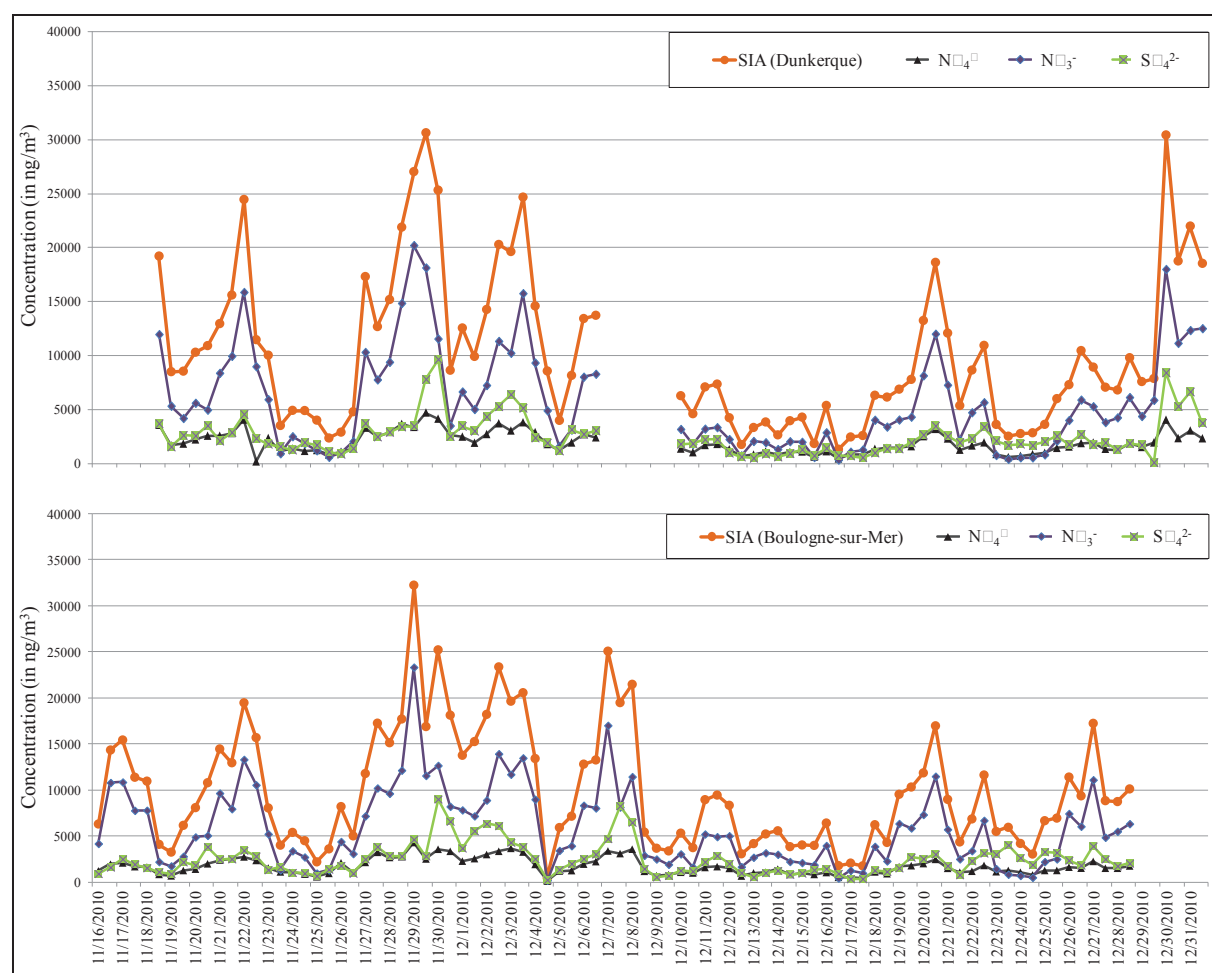


Figure 23 Diurnal evolution of NO_4^- , NO_3^- , SO_4^{2-} and SIA concentrations in Dunkerque and Boulogne-sur-Mer during the winter campaign

III.6.2.Spring campaign

III.6.2.1.Sea salts diurnal evolution

The percentages of sea salt and non sea salt contents for some ME and SI are found fluctuating between high and low values in the samples of the spring campaign (Table 7).

Table 7: Percentages of sea salt and non sea salt fractions in sea salt components in spring

Dunkerque spring				Saint-mer spring			
Sea salt	%	Non sea salt	%	Sea salt	%	Non sea salt	%
ss-Ca ²⁺	14.2	Nss-Ca	85.8	ss-Ca ²⁺	14.1	Nss-Ca	85.9
ss-Mg ²⁺	67.3	Nss-Mg	32.7	ss-Mg ²⁺	86.3	Nss-Mg	13.7
ss- ⁺	9.0	Nss- ⁺	91.0	ss- ⁺	6.5	Nss- ⁺	93.5
ss-Cl ⁻	75.2	Nss-Cl ⁻	24.8	ss-Cl ⁻	66.0	Nss-Cl ⁻	34.0
ss-S ₄ ²⁻	2.1	Nss-S ₄ ²⁻	97.9	ss-S ₄ ²⁻	1.7	Nss-S ₄ ²⁻	98.3

In Dunkerque ss-Cl⁻ constituted about 75.2% of total Cl⁻ average concentration. The rest of the values were 67.3, 14.2, 9, and 2.1% for ss-Mg²⁺, ss-Ca²⁺, ss-⁺, and ss-S₄²⁻ respectively. On the other hand, Saint-mer results showed different percentages, in the sense that Mg had the highest sea salt fraction with an 86.3% of its total average concentration in the form of ss-Mg²⁺. As for the rest of the chemical species, we found 66, 14.1, 6.5, and 1.7 % for ss-Cl⁻, ss-Ca²⁺, ss-⁺, and ss-S₄²⁻ respectively.

The diurnal evolution of the calculated sea salt concentrations was similar between the coastal (Dunkerque) and inland (Saint-mer) sites (Figure 24). This observation proves the presence of significant amounts of sea salts in Saint-mer despite the distance between the site and the marine facade. Individual peaks of sea salts can be identified at both sites, but at higher frequency in Dunkerque. In each case, an examination of the meteorological conditions showed that the increase in sea salts concentration is related to high wind activity ($\geq 7\text{m/s}$), mostly under the SW or N-NE sectors and sometimes accompanied with wind gusts.

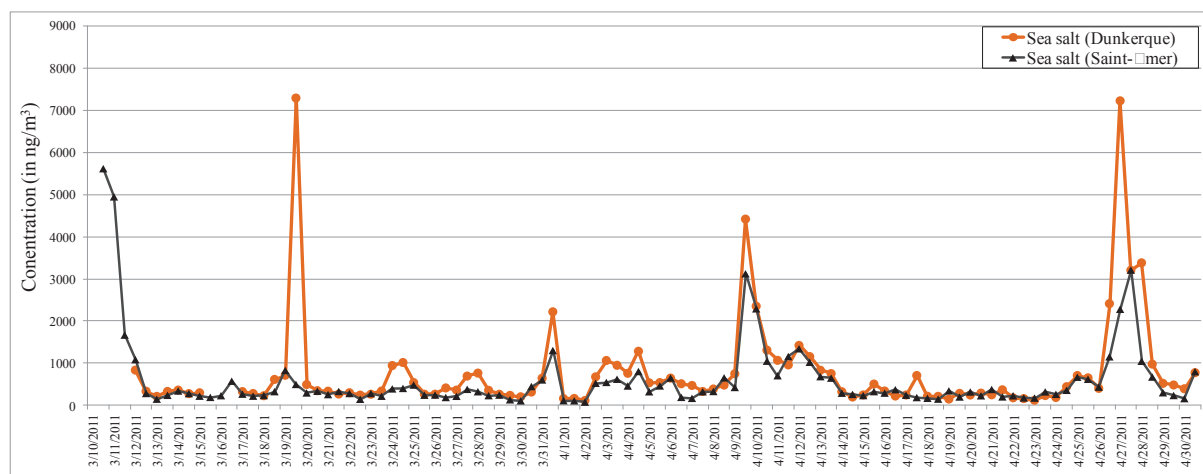


Figure 25 Diurnal evolution of sea salts concentrations in Dunkerque and Saint-Omer during the spring campaign

III.3.3. Fe and Nss-Ca diurnal evolution

The diurnal evolutions of Fe and Nss-Ca in Dunkerque and Saint-Omer are illustrated in Figure 25. Some Fe peaks are noticed exclusively at the coastal industrialized site, which points at a local source of Fe emissions. When compared to the winter variations, the results emphasize on the local sources of Fe instead of the global regional ones. Nss-Ca follows the path of Fe in the heterogeneity of the diurnal evolution between the two sites. Furthermore, the similarity between the two patterns creates a link between the source of Fe and Nss-Ca at Dunkerque. With a resemblance to the first campaign, the high levels of Fe and Ca can be explained by steelmaking activities.

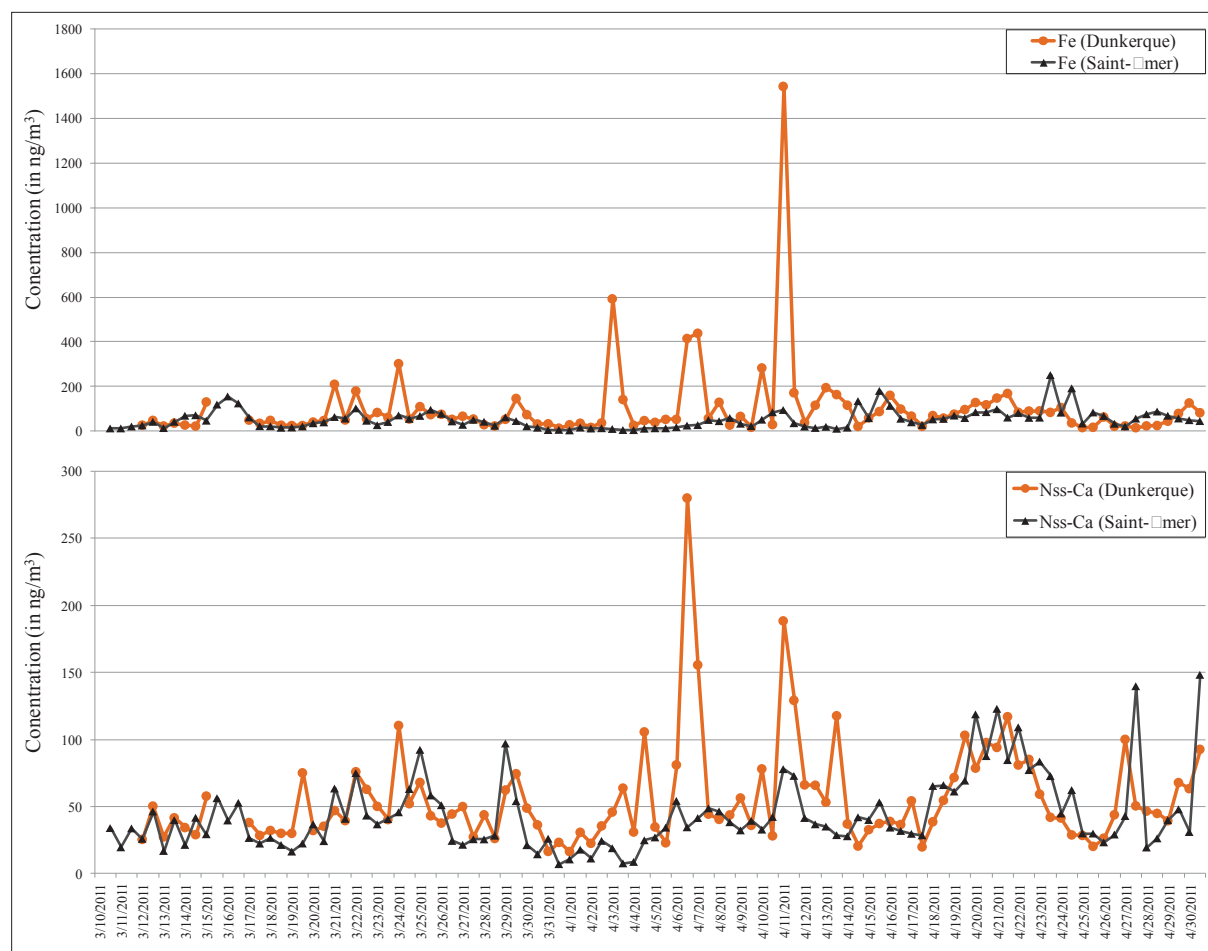


Figure 25 Diurnal evolution of Fe and Nss-Ca concentrations in Dunkerque and Saint-Émer during the spring campaign

III.1.3. Al and Nss-Mg diurnal evolution

The evolution of Al and Nss-Mg concentrations is studied following the same resolution used in section (III.6.1.3). The evolution of Al concentrations is different between Dunkerque and Saint-Émer (Figure 26). The tendencies are found to fluctuate independently between the two sites, proving that Al concentrations in the atmosphere of these areas are linked to local sources. Furthermore, higher peaks of Al can be identified at the Dunkerque sampling site when compared to the peaks found at Saint-Émer.

On the other hand, Nss-Mg concentrations were found extremely low to almost absent in the majority of the samples in both sites, suggesting that Mg have mainly marine origins. However, high peaks of Nss-Mg can be observed in many cases at Dunkerque, whereas it was found in only two successive samples at Saint-Émer. This means that local sources of Mg are more frequently present in Dunkerque.

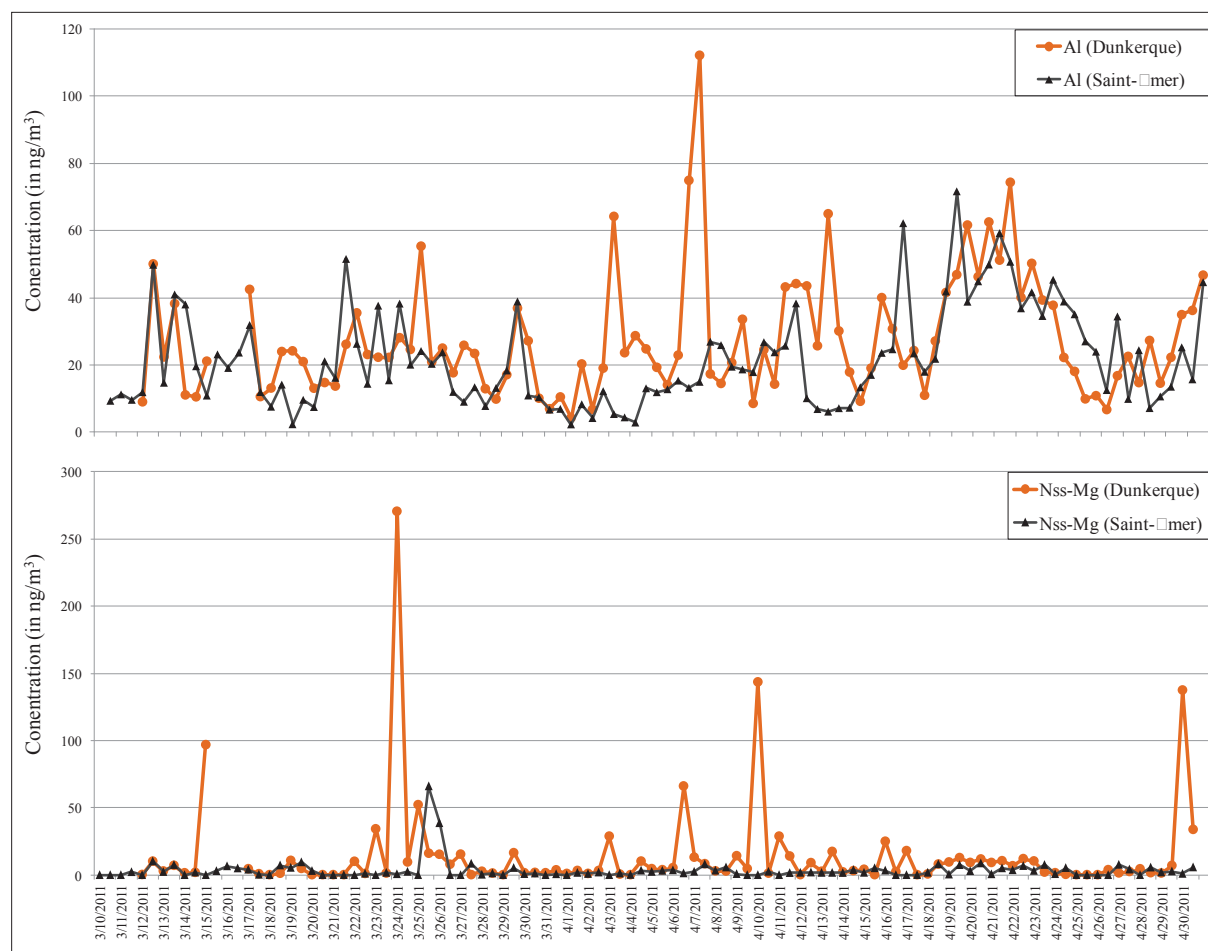


Figure 26 Diurnal evolution of Al and Nss-Mg concentrations in Dunkerque and Saint-Émer during the spring campaign

III.3.3.3 Al and Nss-Mg diurnal evolution

The diurnal evolution of these combustion processes tracers is displayed in Figure 27. The trend of TC shows slightly higher values for Saint-Émer in general when compared to Dunkerque. The global trend at the two sites is highly similar with only few disruptions pointing at local carbon emissions.

The same observation can be noticed in the case of Nss-Mg. High peaks found at Saint-Émer were matched on a smaller scale at Dunkerque. However, other Nss-Mg peaks were found in isolated cases at Dunkerque, which are probably generated by local sources at the site. Another high peak can be observed in both the coastal and inland site before the end of the sampling campaign, proving that at these dates a regional Nss-Mg pollution phenomenon occurred.

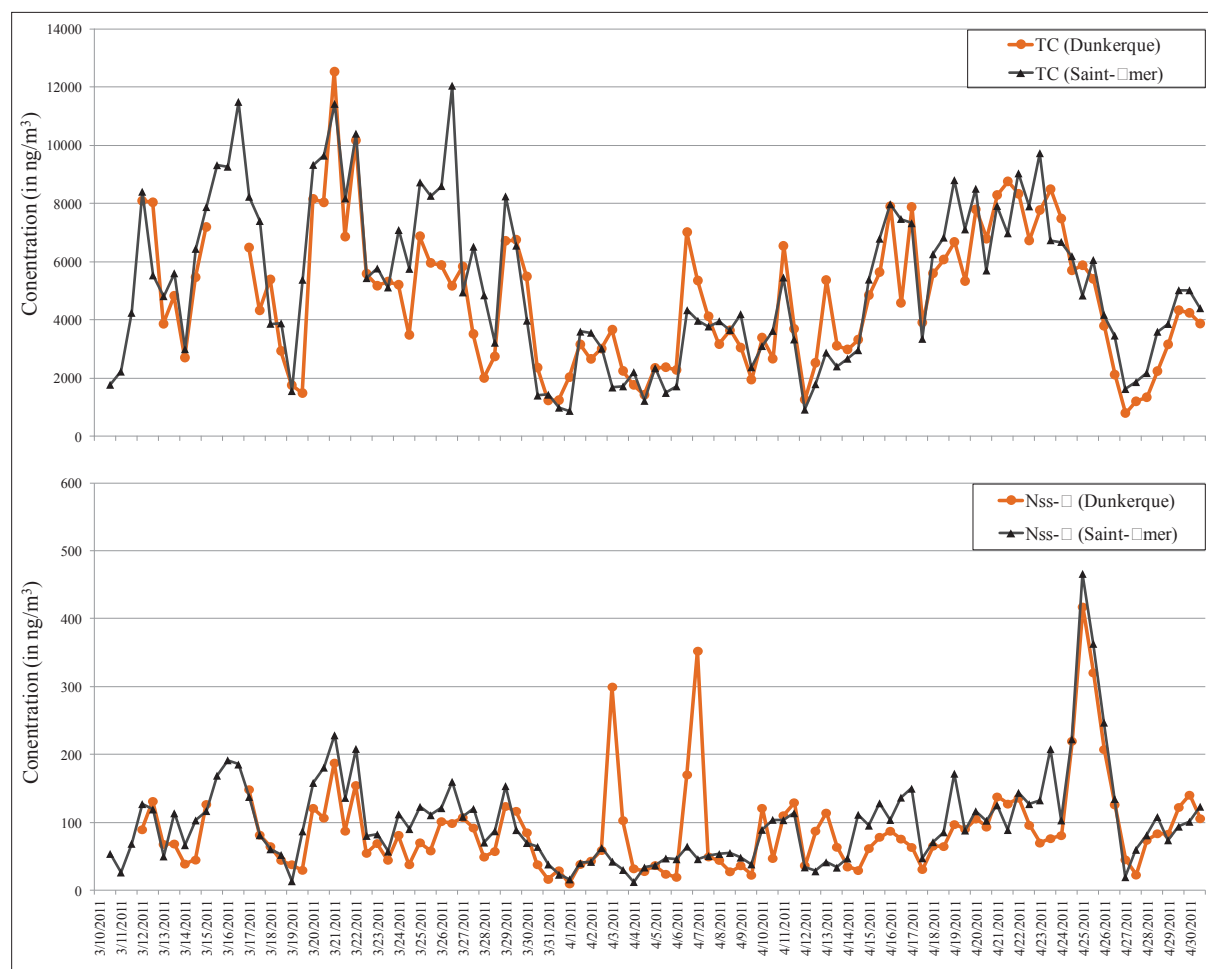


Figure 28 Diurnal evolution of TC and Nss-PM₁₀ concentrations in Dunkerque and Saint-Émer during the spring campaign

III.3.3.1 diurnal evolution

SIA diurnal evolution in Figure 28 shows a general homogeneous variation between Dunkerque and Saint-Émer. This proves the influence of regional emissions of this type of aerosols. Between the samples, Dunkerque peaks topped those of Saint-Émer in some cases, when in others the levels at Saint-Émer were found higher. Deeper investigations are needed in order to uncover the possible reasons behind these peaks.

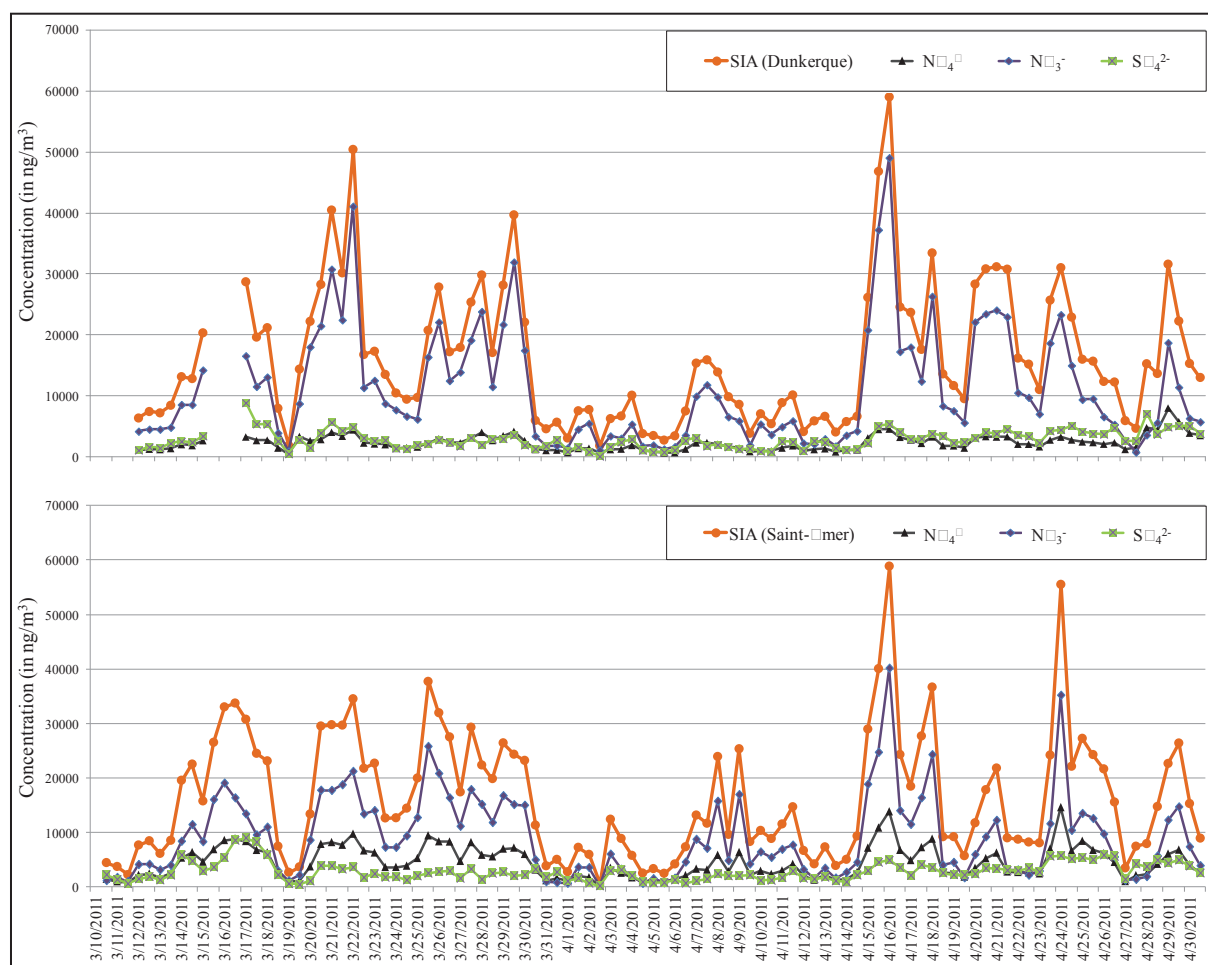


Figure 3.1. Diurnal evolution of NO_x concentrations in Dunkerque and Saint-Pol-sur-Mer during the spring campaign

III.3. Statistical analysis of above limit peaks of $\text{PM}_{2.5}$

III.7.1. Identification of above limit-value peaks of $\text{PM}_{2.5}$

To be able to identify above limit peaks of fine PM episodes that occurred during our winter and spring campaign, we turned to Atmo air monitoring network data for the daily evolution of $\text{PM}_{2.5}$ and PM_{10} . Atmo sites for the measurements of $\text{PM}_{2.5}$ and PM_{10} mass in Dunkerque are located in Malo-les-bains (East side) and Saint-Pol-sur-Mer (West side) respectively, whereas in Boulogne-sur-Mer and Saint-Pol-sur-Mer, Atmo installed only one automatic PM_{10} measuring station per site. Data on $\text{PM}_{2.5}$ and PM_{10} mass were acquired from Atmo web site (<http://www.atmo-npdc.fr>), which allowed drawing their daily evolution and hence identifying the daily peaks of PM levels at our sites. In the following segment we will discuss the method for selecting the dates during which episodes of PM pollution occurred, as well as explain the main chemical species contribution in the total analyzed $\text{PM}_{2.5}$.

concentration which is defined here as the sum of all analyzed chemical species concentration in each sample.

III.1.1. Winter campaign above limit peaks

The evolution of $\text{PM}_{2.5}$ and PM_{10} at Dunkerque and Boulogne-sur-Mer during the winter campaign period is illustrated in Figure 29.

A closer look at the trends shows that above limit peaks of $\text{PM}_{2.5}$ recorded by Atmo follow the same pattern of our total analyzed fine particles. Atmo- $\text{PM}_{2.5}$ values are found sometimes higher than those for PM_{10} in Dunkerque. This can be explained by the fact that the measurements were taken at two different sites: in Malo-les-Bains (East) and Saint-Omer-sur-Mer (West) respectively. Malo-les-Bains is probably more exposed to PM than Saint-Omer-sur-Mer. On the other hand, the evolution of both PM classes in Dunkerque is also found similar to the one measured at Boulogne-sur-Mer for PM_{10} . This shows a global regional trend that controls the daily variations of PM levels. Furthermore, in Boulogne-sur-Mer, a high similarity between the trends of Atmo- PM_{10} and our total analyzed $\text{PM}_{2.5}$ can be clearly seen in Figure 29. These correlations allow us to rely on these trends for the selection of above limit peaks of PM . However, we have noticed that total $\text{PM}_{2.5}$ was higher than total PM_{10} for certain dates. This is abnormal and could not be explained at this level, but we suspect that the cause of this difference is related to the fact that $\text{PM}_{2.5}$ and PM_{10} monitoring stations are located at two different sites.

The limit values for both PM classes, $50 \mu\text{g}/\text{m}^3$ for PM_{10} and $25 \mu\text{g}/\text{m}^3$ for $\text{PM}_{2.5}$, were exceeded many times in Dunkerque as well as in Boulogne (Figure 29). In parallel, similar variations occurred in other measuring stations in the region (www.atmo-npdc.fr). This proves that the load of PM is increasing regionally. Hence, we were able to identify high fine PM loaded samples individually at Dunkerque and Boulogne-sur-Mer, which are consisted of 44 samples (22 days): 21, 22, 27, 28 – 30 for November, in addition to 1 – 4, 6, 7, 19 – 22 and 26 – 31 during December 2010. We will be investigating the chemical composition of these selected samples later in this chapter.

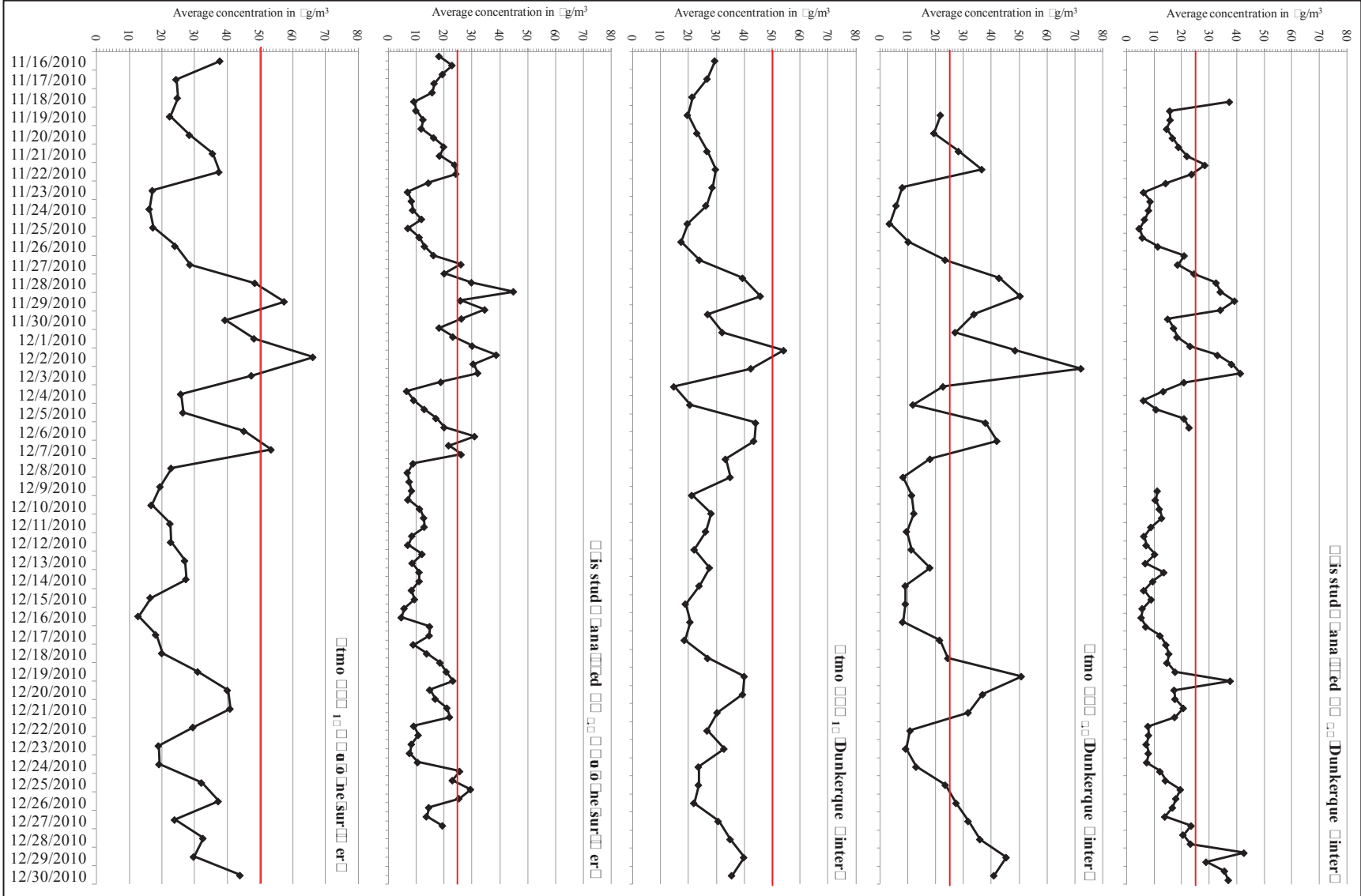


Figure 1: Evolution of the recorded data and the total analyzed species in Dunkerque and Dunkerque inter during the inter campaign. Red lines: limit values of $\mu\text{g}/\text{m}^3$ and $\mu\text{g}/\text{m}^3$.

III.1.1.1. Campaign above limit value peaks

The variations of $\text{PM}_{2.5}$ and PM_{10} at Dunkerque and Saint-Émer during this period are illustrated in Figure 30. A comparison between the trends acquired from Atmo surveillance network and our study result for Dunkerque shows that Atmo- $\text{PM}_{2.5}$, Atmo- PM_{10} and the total analyzed $\text{PM}_{2.5}$ values have similar trends, with almost synchronized increases exceeding the limit values for both classes of PM .

A similarity can be noticed in the case of Atmo- PM_{10} and our $\text{PM}_{2.5}$ collected in Saint-Émer. The two trends follow each other especially in high PM episodes, during which limit values were exceeded. These above limit peaks correspond to specific $\text{PM}_{2.5}$ samples taken from Saint-Émer. These samples were identified as in the case of Dunkerque to find that they match in Dunkerque and in Saint-Émer.

A total of 29 days (58 samples) is chosen for chemical species contribution analysis. During March the dates are: 12, 14, 15 – 17, 19 – 22 and 24 – 28. As for April we identified the following dates of $\text{PM}_{2.5}$ peaks: 7, 15 – 25 and 28 – 30. The detailed analysis of the chemical composition of these selected samples will be realized in the following section.

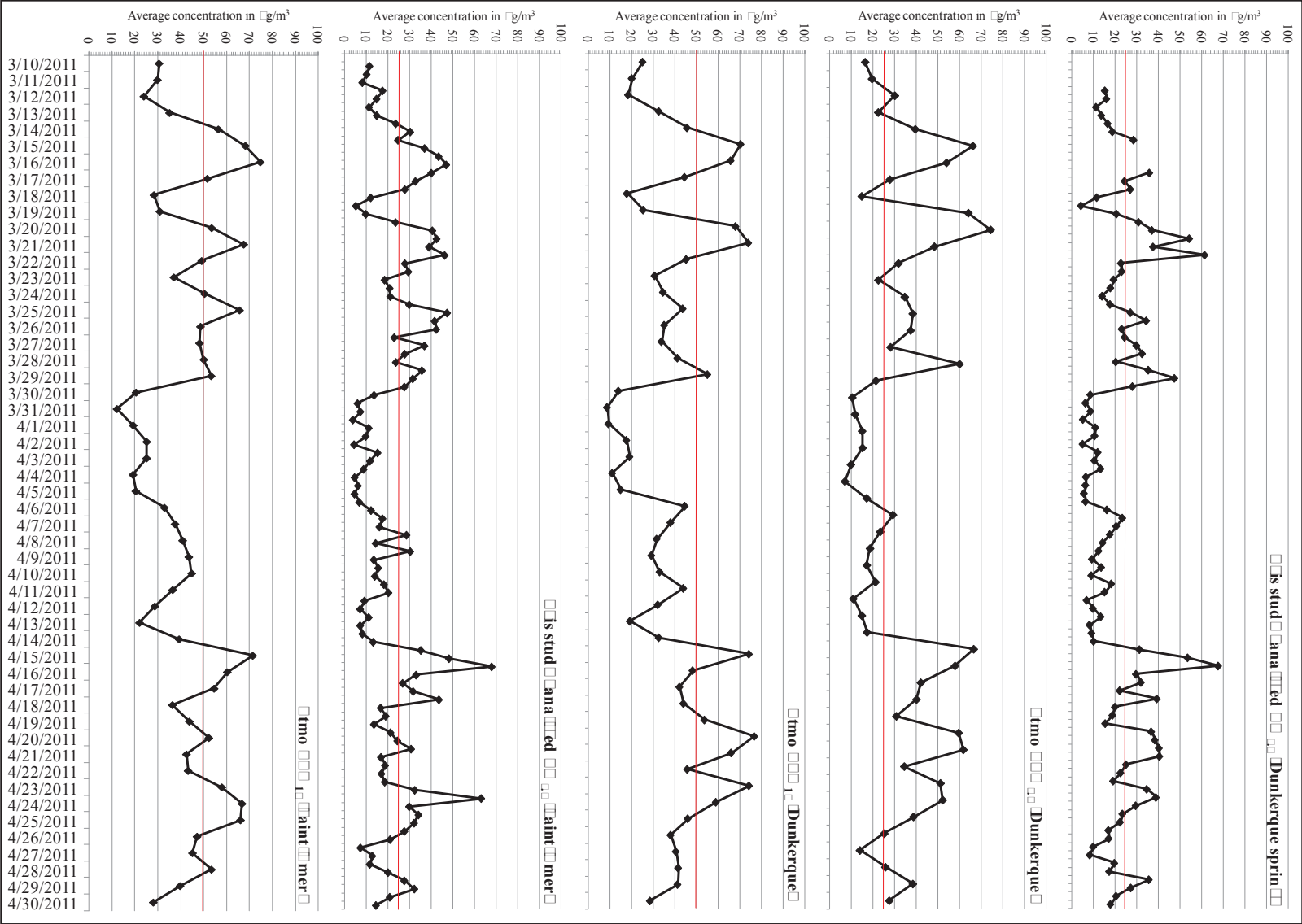


Figure 3: Evolution of the recorded data and the total anaerobic species in Dunkerque and during the spring campaign. The lines represent the initial and final concentrations.

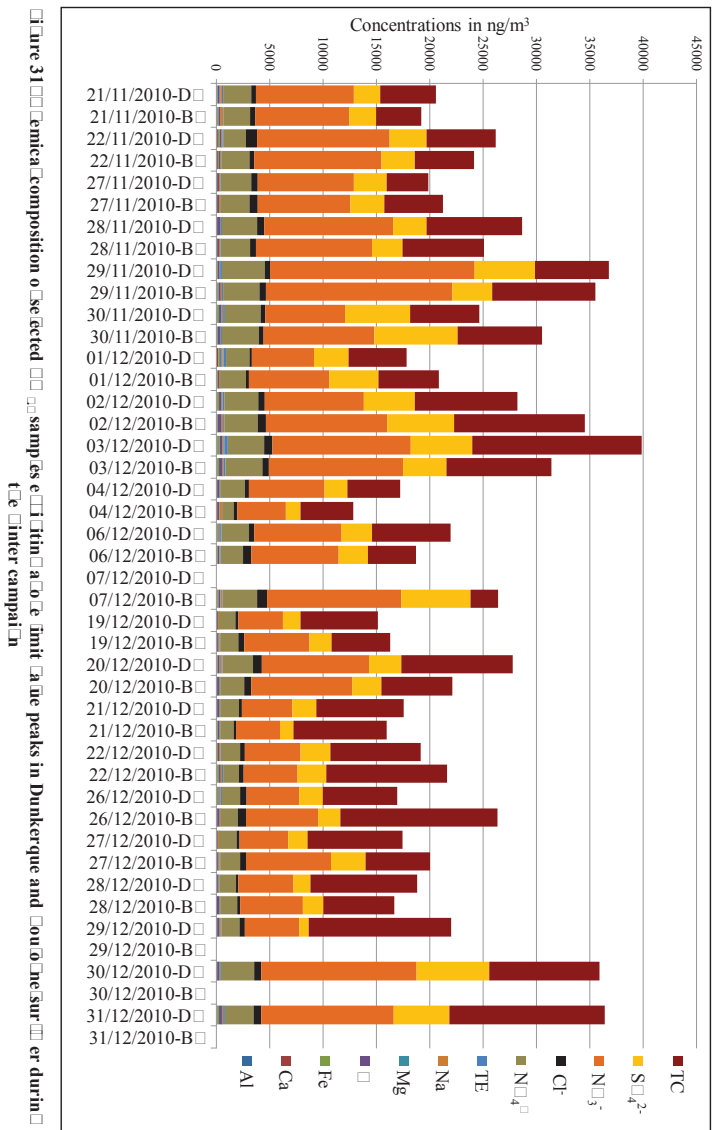
III.7.2.Detailed analysis of above limit peaks of $\Sigma M_{2.5}$

III.7.2.1. $\Sigma M_{2.5}$ inter campaign episodes

III.7.2.1.1. General observation

Figure 31 shows the chemical composition of the selected $\Sigma M_{2.5}$ samples from Dunkerque and Boulogne-sur-Mer, except for the day of 7/12/2010, during which we faced a technical problem and sampling was not realized. TC is found to fluctuate independently when compared to the elevation of the total analyzed $\Sigma M_{2.5}$ concentration in the corresponding sample. However, $S\text{O}_4^{2-}$, NO_3^- and NO_2^- seem to contribute the most in the total $\Sigma M_{2.5}$ concentration during the episodes. The rest of the analyzed species contribution is found to be negligible when compared to the above discussed ones.

The contribution in the total $\Sigma M_{2.5}$ for certain species at Boulogne-sur-Mer had a different aspect when compared to the respective case observed in Dunkerque (Figure 31). For example, TC is found linked to the increase in total analyzed $\Sigma M_{2.5}$ except during 11/29/2010 and 12/7/2010 in Dunkerque and Boulogne-sur-Mer respectively. NO_3^- and NO_2^- contribution to the load can be evidenced in almost all the peaks. Finally, $S\text{O}_4^{2-}$ was found increasing with the total analyzed $\Sigma M_{2.5}$. The rest of the analyzed metals followed the same pattern as the one observed in Dunkerque as their contribution was insignificant compared to the previously discussed ones. Finally, we note that we could not compare the contributions for the 29th, 30th and 31st samples because the sampling campaign in Boulogne-sur-Mer ended on the 28th.



III.7.2.1.2.Detailed interpretation of $PM_{2.5}$ above limit values for the winter campaign

Our objectives in this section are to examine under which conditions these above limit episodes are occurring, and establish a link between these episodes and wind directions and/or temperatures in the studied sites. In order to backup our analysis, we have regrouped in Figure 32 the diurnal evolutions of the recorded temperatures, $PM_{2.5}$ levels recorded by Atmo, TC, SIA and AI corresponding to each of the previously selected samples. In addition, Figure 33 regroups some air mass backward trajectories drew using $SCIT$ transport and dispersion model from the NOAA-Air Resources Laboratory (Draxler & Polph, 2012) online server, to illustrate some examples that can uncover some PM origins, especially during long range transport mechanisms.

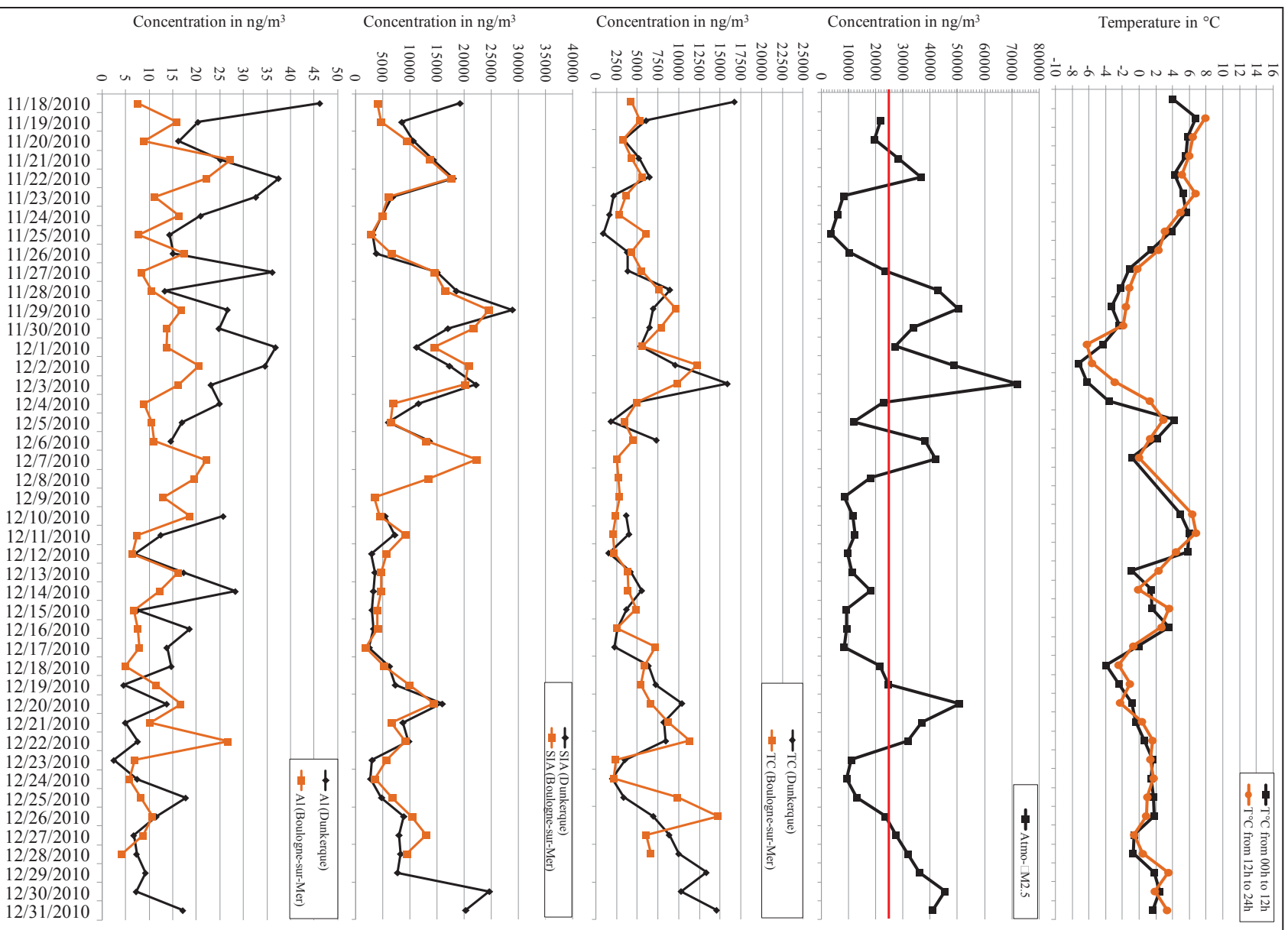


Figure 3: Diurnal evolution of temperature, SI, SI-A and TC concentrations in ng/m^3 in Boulogne-sur-Mer and Dunkerque.

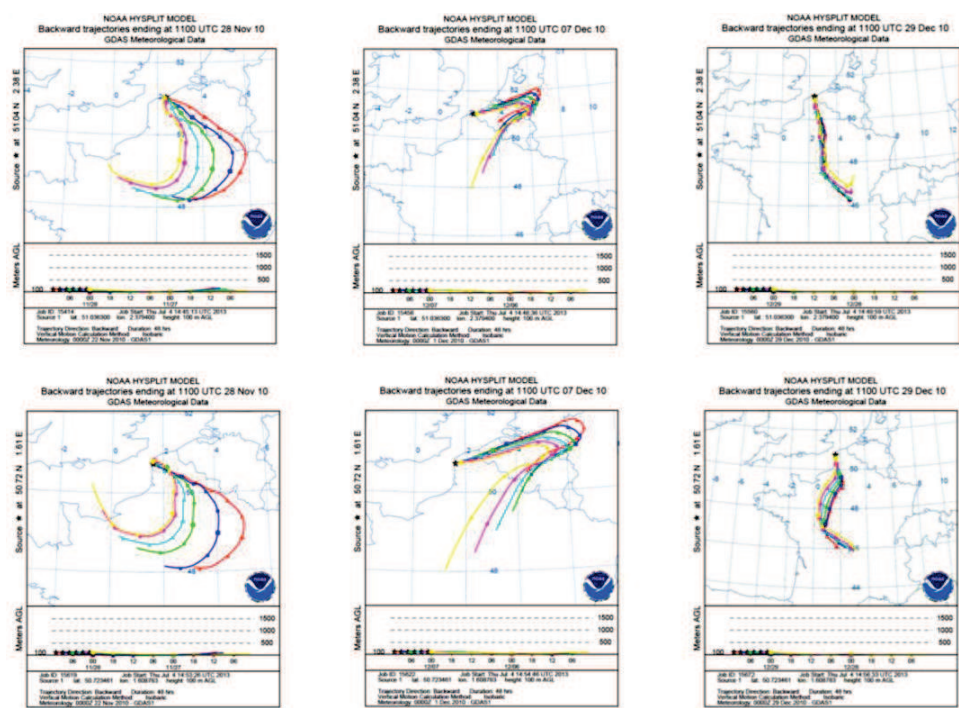


Figure 33: Backward trajectories are used to draw a map, for three selected samples of December 10, December 15 and 17 in Dunkerque (a) of the tree and (b) of the surface of the tree, Duration 1000s, Start 110000, Vertical motion isobaric, of the trajectory of the air parcel.

III.7.2.1.2.i.Episodes on the 21st and 22nd of November 2010

The episodes occurred in a dry climate period during which temperatures tend to drop, but always staying above 0°C. Wind directions analysis show that wind blowing initially from the S-SE sector since November 19th, changed directions to N-E during the time of the episode. The chemical composition of the collected particles in both Dunkerque and Boulogne-sur-Mer sites, it is mainly composed of secondary inorganic aerosols (SIA) which rose in those samples along with a smaller scale contribution of TC. The episode ends on November 23rd following a wind direction inversion towards the N-W sector accompanied by rainfall.

III.7.2.1.2.ii.Episodes from November 27th to December 4th 2010

The event takes place during an episode of dry climate, and starts when daylight and nightfall temperatures drops below 0°C, all the way to a minimum of -7°C encountered in the 2nd of December 2010. At the beginning of this episode, we can notice the inversion in wind direction: initially under NW direction, the air masses changed direction to pass over East of France before returning to the N-E region (Figure 33).

The region in that period kept being subjected to S-E winds, but $\text{PM}_{2.5}$ levels dropped significantly in the middle of this episode (November 30th, 2010). Associated to this phenomenon is some temporary wind reinforcement from the East sector (between 9 and 10 m/s).

In both Dunkerque and Boulogne-sur-Mer, the episodes could be explained by the concentrations in inorganic secondary aerosols and total carbon. However, it is important to mention that the evolution of these species is not the same: SIA concentrations increased more than TC at the beginning, followed by an increase in TC concentrations (reaching 15 $\mu\text{g}/\text{m}^3$ in December 2nd 2010) but remaining under SIA high loads. This observation is found occurring with the minimum recorded ambient temperature. Therefore, heating activities could be a source of TC emissions during this event and could also contribute to the above limits peaks. Furthermore, this suggestion can be backed up by the increase in potassium levels, which is considered as a tracer of biomass combustion.

The episode ends by the end of the 4th of December, marked by a large increase in temperature and rainfall occurrence.

III.7.2.1.2.iii.Episodes on the 6th and 7th of December 2010

This episode is shorter and less intense than the one observed between the 27th of November and the 4th of December 2010. Meteorological conditions during these two days exhibited average temperatures of 0°C, sometimes lightly negative, and an N-E sector winds. The backward trajectory shows slow inland air mass movement that is directed towards Belgium and Holland. Then it returns to our regions under the influence of NE winds. This behavior is found similar for our two sites (Dunkerque and Boulogne-sur-Mer).

The episode terminates at the beginning of high speed wind event, followed by a shift in wind direction to the N-W sector and an increase in the temperature.

III.7.2.1.2.iv.Episodes from December 19th till 21st

An increase in PM_{10} concentrations can be observed also synchronized with a decrease of temperatures to negative values for a couple of days. The difference with previous observations resides within wind directions that are under the S-E sector, which is a rare event in our studied region. Same as in the case of N-E winds, the N-Paris region is subjected to continental air masses, which probably crossed over European neighboring countries as well as other French regions.

The episode ends in the evening of December 21st, after an increase in wind speed (10 m/s) coupled to an increase in temperature.

III.7.2.1.2.v.Episodes from December 26th till 30th

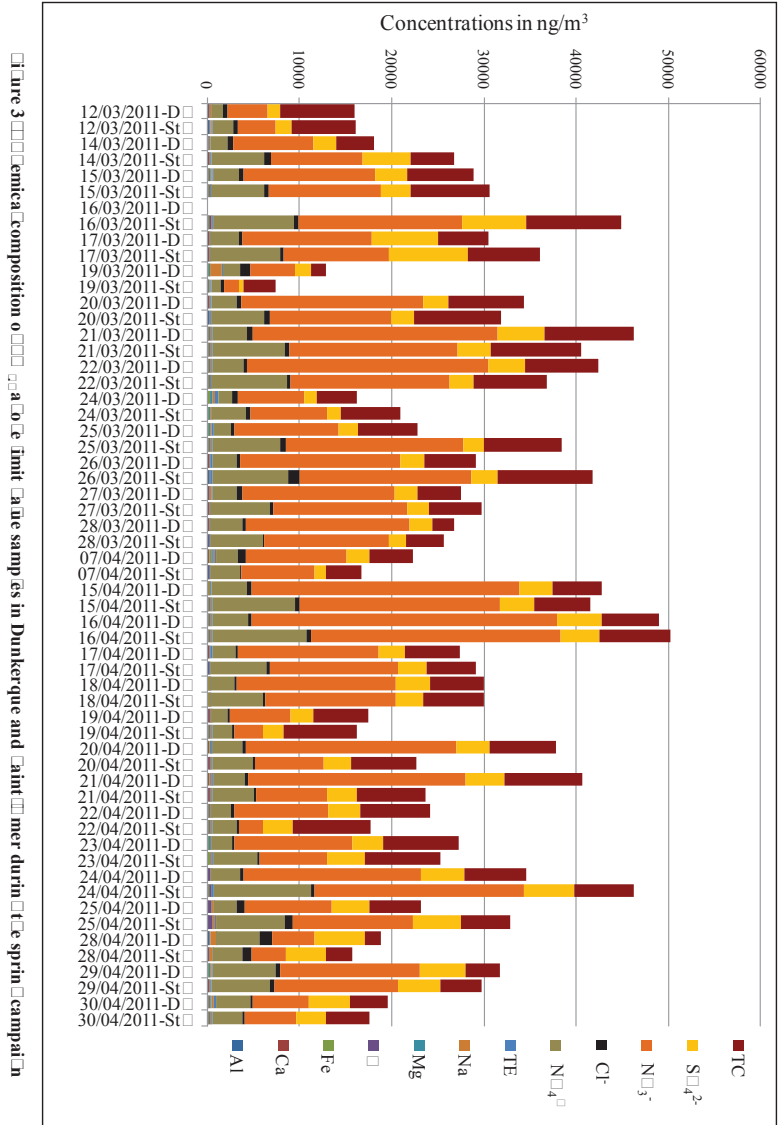
This episode is also observed under a cold dry weather conditions, whereas winds were originating from the S-E sector. In a similarity between this episode and the one of the 2nd of December, TC concentrations increased noticeably (December 26th and 27th), and can be attributed to the increase in domestic heating activities. We can also notice that the air mass is originating from the South of France and crosses the region of “Ile de France” before settling in ours.

From all the previous episodes analysis we can conclude that each one from the winter campaign was characterized by similar meteorological conditions. The exceedance of the limit value was encountered under dry weather, with cold winds blowing from N-E to S-E continental sectors. Another interpretation can be applied herein considering the Long Range Transport of particles also evidenced by air mass back trajectories.

The analysis of the chemical composition proves that these episodes can be explained by the increase in SIA and TC concentrations. SIA are well known to be associated with long

III.7.2.2.1. General observations

146



III.7.2.2.2.Detailed interpretation of above limit values for the winter campaign

Using the same strategy used for the winter campaign, we examined the meteorological conditions encountered during the spring episodes, which raised the level of $\text{PM}_{2.5}$ to reach high values between 60 and 70 $\mu\text{g}/\text{m}^3$. Figure 35 illustrates the diurnal evolution of the temperatures, Atmo- $\text{PM}_{2.5}$ levels, TC, SIA and AI in Dunkerque and Saint-Omer sites during the spring campaign. Six air mass backward trajectories are also given in Figure 36 that confirms the global meteorological situation occurring during some of the above limit samples.

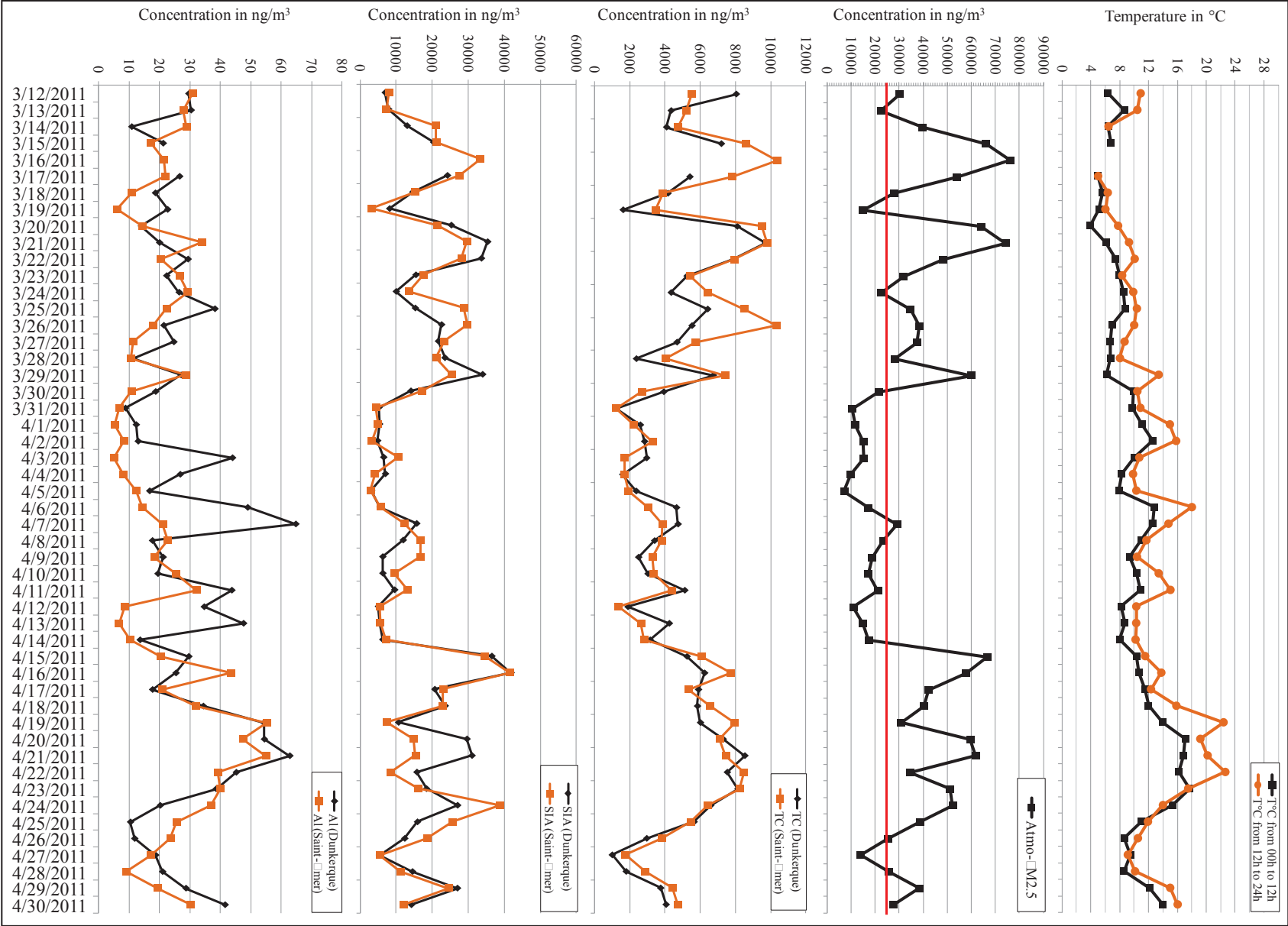


Figure 3: Diurnal evolution of temperature, A1, SIA, TC, and AIMO-M2.5 concentrations in ng/m³ in Dunkerque and Saint-met.

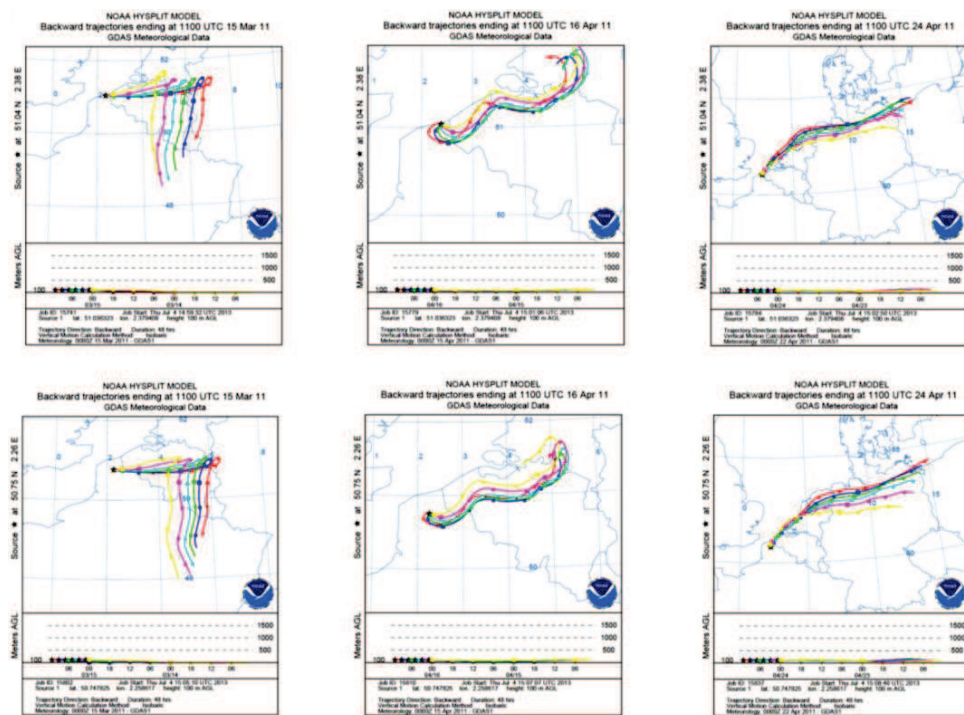


Figure 3 shows air mass backward trajectories derived using NOAA HYSPLIT model for three selected samples in 15, 16 and 24 April in Dunkerque coastal area and Saint-Omer meteorological station. Duration, direction, vertical motion, isobaric, and trajectory error bars, and trajectories

III.7.2.2.2.i.Episodes succession between 12 and 28 March 2011

The increase of fine $\text{PM}_{2.5}$ above limit value is found associated to a dry climate and low average daily temperatures which did not increase above 10°C. Succeeding high $\text{PM}_{2.5}$ concentrations (till March 22nd) were observed under N-E winds. The decrease of $\text{PM}_{2.5}$ levels detected in 18 March is synchronized to a sudden shift in wind direction towards the S-W sector. During the first episode of this period we can observe that air masses have crossed over the continent (East of France and Germany) resulting in an important increase in $\text{PM}_{2.5}$ records. Meanwhile, and as illustrated for 03/15/2010 in Figure 36, we had a comeback of the air mass with N-E wind flux towards the NordC region. However, on the 18th of March, a break was noticed during which a temporary shift of S-W winds had occurred.

The situation is found different between the 24th and the 28th of the same month, since wind activities were almost absent.

The episode terminates after a shift of wind directions to the S-W sector. The chemical composition of the samples during this episode shows that the elevations in $\text{PM}_{2.5}$ loads are due primarily to SIA and TC. The remaining major elements, especially Al, Fe and Ca concentrations do not increase remarkably during this period.

III.7.2.2.2.ii.Episode starting the 15th to 25th of April 2011

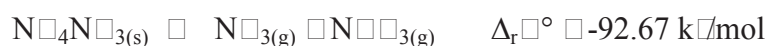
In this episode, the limit threshold was crossed when wind direction shifted to the N-E sector in 14 April. Backward trajectories show the arrival of air masses to our sites that had already crossed over Holland and Belgium before that (Figure 36).

The following days were marked by a gradual decrease in wind speed to get to stagnant conditions, especially at Saint-Omer. Furthermore, we observed that temperatures increased to reach summer values between 18 and 14 April. During these days, daylight average temperatures were around 20°C, which is an unusual episode since these temperatures are above the seasonal averages that are encountered in the region.

As for the concentration evolution, a particular phenomenon was observed and deserves a detailed explanation. In fact, diurnal fine $\text{PM}_{2.5}$ evolution shows three successive peaks: 15, 20 and 23 April. The chemical species evolution shows that SIA concentrations increase is well synchronized with the elevation of fine $\text{PM}_{2.5}$ loads, just like the previous cases. However, it seems that TC, Al, Ca and Fe presented similar evolutions characterized by a progressive augmentation. This increase got to a maximum during April 21st then the levels decreased in the following days. The aspect of the trends for Al, Ca and Fe points at an accumulation

phenomenon in the air, which is not totally surprising if we consider the stagnant meteorological conditions recorded during this period (dry weather, almost complete absence of wind and above normal seasonal average temperatures).

This accumulation could not explain the SIA evolution during this episode due to the degree of stability of SIA, and mostly ammonium compounds which are temperature dependant. The stability of suspended NH_4NO_3 particulates in a gas is governed by the direction of the chemical equilibrium (Seinfeld & Pandis, 2006):



In this reaction, $\Delta_r G^\circ$ corresponds to the Gibbs function (free enthalpy) of the reaction in standard conditions and under 25°C. If we consider the link between the equilibrium constant K and $\Delta_r G^\circ$, it is possible to demonstrate that K decreases by a factor of 1000 when temperature increases from 0°C to 25°C. This proves that ammonium nitrate is less stable under high temperatures, and thus tends to decompose into its primary gaseous species.

The SIA concentration increases dramatically to reach its maximum under N-E sector winds, when in the mean time temperatures remain under 20°C. However, despite the stable meteorological conditions, we observe a decrease in SIA accompanied by an increase of temperatures beyond 20°C. This decrease can be explained by ammonium nitrate decomposition as previously explained.

Our explanation can be backed up by the fact that SIA levels in Saint-Omer were lower than those of Dunkerque during April 21st and 22nd, even though average temperatures were higher in the first site than the second.

Equally, we observed at the end of the episode another temperature increase (in April 24th) followed by an important atmospheric cooling during the following days. This temperature gradient can also have an effect on SIA concentration evolution. In this case, we can consider that SIA precursors exist in the air, but the relatively high temperatures kept the precursors from transforming into particulate form, especially particulate ammonium nitrate. On the opposite, when temperatures started to drop gradually (in April 24th under N to N-E sector winds), the conditions for the transformation of precursors into particulate ammonium nitrate became favorable, thus the increase in its concentration was observed. In parallel, we observed an entrance of continental air mass which was located over northern Germany 48 hours earlier.

Lower levels of fine PM were again encountered as of April 25th 2011, with wind origin maintained from the N to N-NE sectors and speed between 6 to 9 m/s.

To resume the spring campaign PM_{2.5} above limit value increases, we noticed that there are two conditions linked to these episodes:

- N-E sector winds, corresponding to inland air masses, under which the increase in PM loads is related to higher SIA and TC concentrations.
- Extremely low wind activities leading to accumulation of fine particles in the atmosphere.
- High atmospheric temperatures decreased the contribution of ammonium nitrates in the PM concentrations.

III.3. Concentration evolution by wind sector

After the diurnal evolution which helped in determining regional versus local pollution sources in the sampled sites, another possible analysis is discussed hereafter. It analyzes the relationship between wind sectors and chemical species concentrations at the studied sites of each campaign. Therefore, wind roses are drawn for each ME, SI, and for TC as well, which determine concentration variations in relation to wind directions.

For each sample, we were able to associate an average wind direction and sector:

- The average wind direction represents the average of recorded wind directions in the 12 hours sampling period that corresponds to one sample.
- The defined wind sector is the sector (in degrees) in which the recorded wind directions fluctuated for the same 12 hours as above for each sample. For example, in the case of a sample for which the recorded wind directions ranged between 40° and 80° has a defined wind sector of 40°-80°.

In addition, certain samples were excluded from the calculations especially:

- The samples for which wind directions were extremely variable (sector range increased beyond 90°). For these samples we could define neither a wind sector nor direction.
- The samples for which no wind direction could be recorded (stagnant winds having 0 m/s speed).

Hence, the concentration roses were drawn based on the following principle:

- The wind rose was decomposed in sectors of 10° each, which define 36 possible wind directions: 0°, 10°, 20°... 340°, 350°.

- The wind sector of each analyzed species that ranges between D_x - D_y is divided into wind directions as follows: D_x , D_x+10 , D_x+20 ..., D_y , to each of which is associated the concentration of the analyzed species in the considered sample.
- After applying the same method to all the collected samples, we can then find for each wind direction the concentrations of the chemical species found when wind was blowing from that same direction but for the whole campaign.
- The geometric averages of these concentrations for each of the 36 wind directions will serve then to draw a “radar” chart type that represents the concentration rose.

The following example (Table 8) summarizes our used method for Al, considering 4 samples only:

- Sample 1: 20°-40° sector Al concentration: 100 ng/m³
- Sample 2: 0°-20° sector Al concentration: 40 ng/m³
- Sample 3: 20°-50° sector Al concentration: 70 ng/m³
- Sample 4: 50°-90° sector Al concentration: 30 ng/m³

Table 8: Example of concentration roses calculations

Wind Direction D	Sample 1 C	Sample 2 C	Sample 3 C	Sample 4 C	Average D in ng/m ³
0		40			40
10		40			40
20	100	40	70		70
30	100		70		85
40	100		70		85
50			70	30	50
60				30	30
70				30	30
80				30	30
90				30	30
...					
360					Mean (350°)

This method was applied to all the analyzed chemical species in our study, which allowed us to draw the concentration roses for all these species and for the two sampling campaigns. This also helped us to identify which wind directions were contributing in the increase of certain species.

Finally, after drawing the concentration roses we were able to notice that wind activities in Dunkerque (winter) and Boulogne-sur-Mer from the S to E sector were at very low frequencies, which forces us to consider this fact in the analysis of the roses especially for the SE quarter sector.

III.8.1. Winter campaign

III.8.1.1. a) For marine element origins

Na, Cl^- , and Mg are considered to have a predominant marine origin in this section. Concentration roses of our sites during the winter campaign show that Na, Cl^- and Mg are mainly observed under the N sector in Dunkerque, and under NE and SW sectors in Boulogne-sur-Mer (Figure 37). These wind directions originated from the sea put in evidence that these elements are indeed in sea salt form. Sea salts are expected to be linked to SW sector winds for both sites (Ledoux, 2003). In this winter campaign, we must recall that meteorological conditions shifted than the normal seasonal variations, and specifically with a much less SW sector winds.

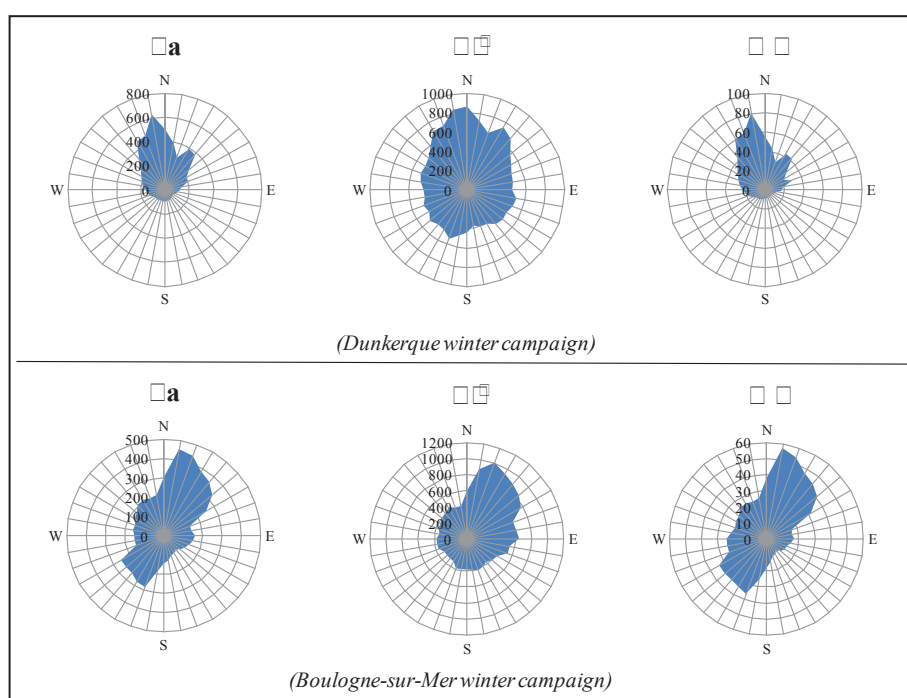


Figure 37 a) For marine elements concentration roses for Dunkerque and Boulogne-sur-Mer during the winter campaign

III.1.1.1 major ions origins

The highest concentration of the different SIA components are found associated to a major SE and SW wind directions in Dunkerque, and E direction in the case of Boulogne-sur-Mer (Figure 38). These directions represent the continental sector influence, as discussed in the previous part in which the E-SE wind directions were associated to inland air masses holding PM_{10} particles. On the opposite side, species like NO_3^- , SO_4^{2-} and NH_4^+ exhibited the lowest contributions when subjected to marine sector winds.

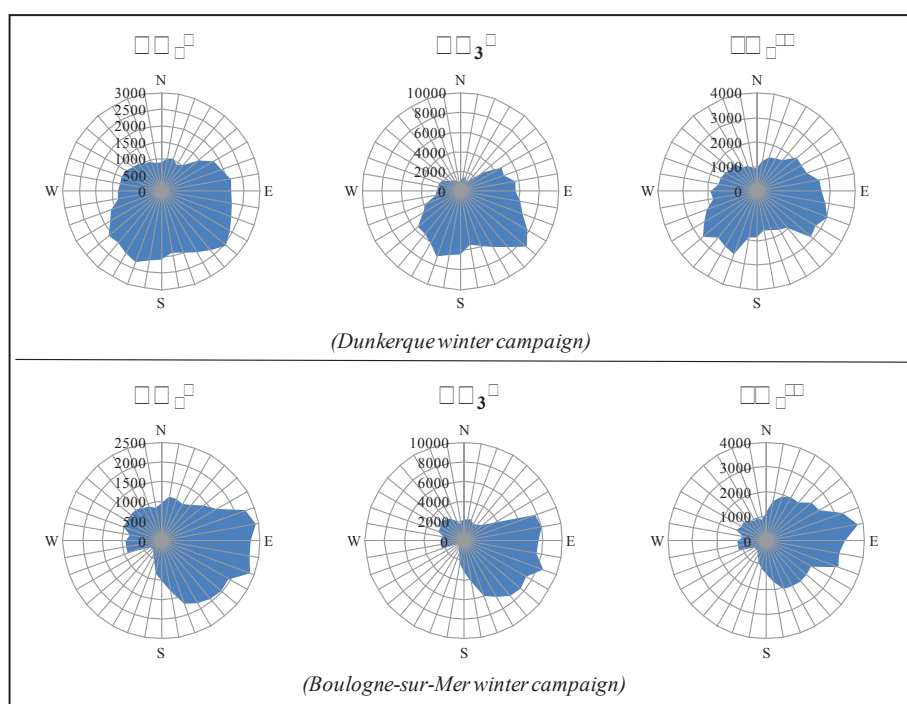


Figure 38 Major ions concentration roses for Dunkerque and Boulogne-sur-Mer during winter campaign

III.1.1.3. Combustion elements origins and

Total carbon and total potassium are considered as major tracer for combustion processes. At Dunkerque site, the origin of these elements is mainly under the E-SW sector showed by the concentration roses and points at the city area as well as other possible continental sources (Figure 39).

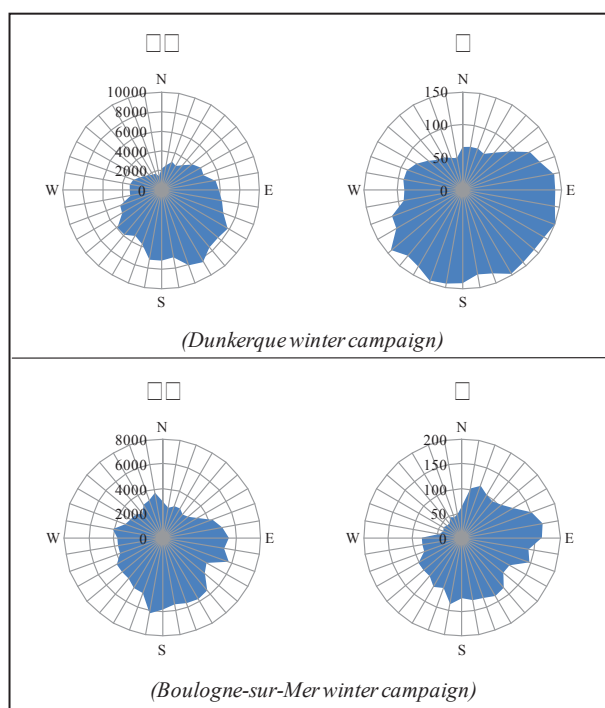


Figure 3 and **concentration roses for**
Dunkerque and Boulogne-sur-Mer during the winter
campaign

The origins of these elements in Boulogne-sur-Mer are found similar to Dunkerque, in the sense that the major wind direction under which an elevation in TC and Fe concentrations are recorded was urban and/or continental. However, we also noticed two sectors of TC concentrations coming with N-NW and W-NW winds, which is the westerly sector of Boulogne-sur-Mer.

III.1.1. Fe, Ca, and Al origins

The remaining ME elements concentration roses are illustrated in Figure 40. The roses show important differences between the sources sectors of elements but also between the sites. Fe, Ca and Al at Dunkerque are relatively linked and enriched when winds are blowing from the industrial sector, with particularly high Fe levels to which is added another source from the SW and E sectors possibly linked to urban sources. The latter also contributed in Ca and Al high concentrations. It is important to mention that the samples that demonstrate the industrial sector influence correspond to high Fe loads identified in Figure 20. We can also notice that high Al concentrations are originated from the SE and S-SW sectors, which correspond to continental influences without excluding the local urban ones nonetheless.

The sectors enriching in these elements are different at Boulogne-sur-Mer, where Ca origin was mainly coming from the SW urban and marine mixed sectors. This observation

should be considered with prudence as explained in section III.8. Fe, partial Ca, and Al were observed under E winds which can be generated from Boulogne-sur-Mer urban influences and/or Dunkerque's industrial site emissions.

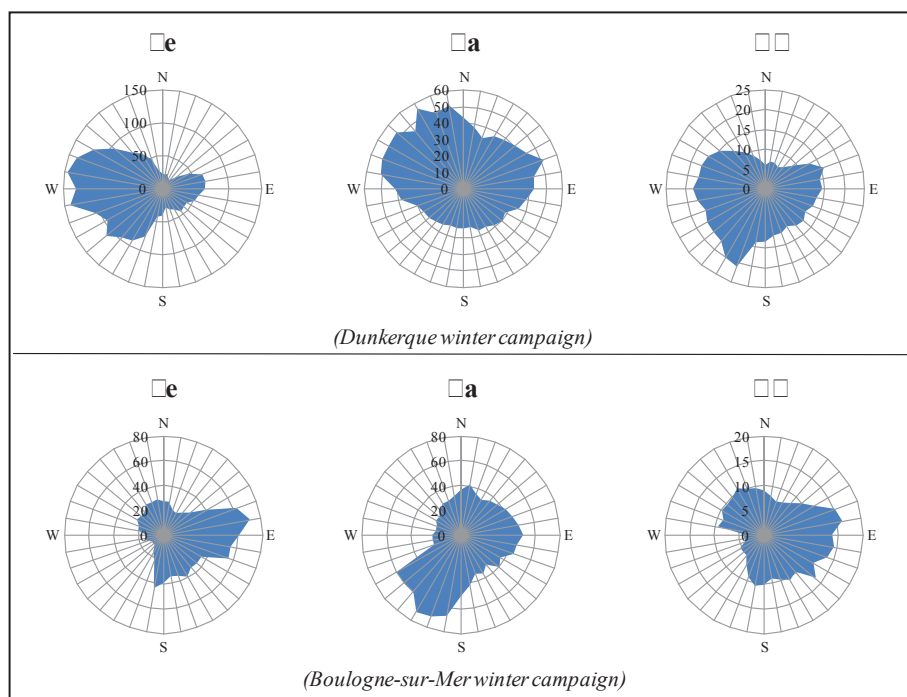


Figure 40: Fe, Al, and Ca concentration roses for Dunkerque and Boulogne-sur-Mer during the winter campaign

III.8.2.Spring campaign

III.8.2.1. Air for marine element origins

Major marine elements concentrations are originated from the nearby sea sector during this campaign, which can be observed in Figure 41.

Concentration roses show that Na, Cl⁻, and Mg are presented in high concentrations when winds blow from the W sector in Dunkerque. The latter is a source of dominant winds usually loaded with sea salts, which is mentioned in section III.8.1.4.

However, sea salt aerosols are also found in Saint-Omer atmosphere despite the inland geographic position of this site. Marine components are found to be coming from the large SW to N sector which encloses the coastline of the region including Boulogne and Dunkerque's sea fronts.

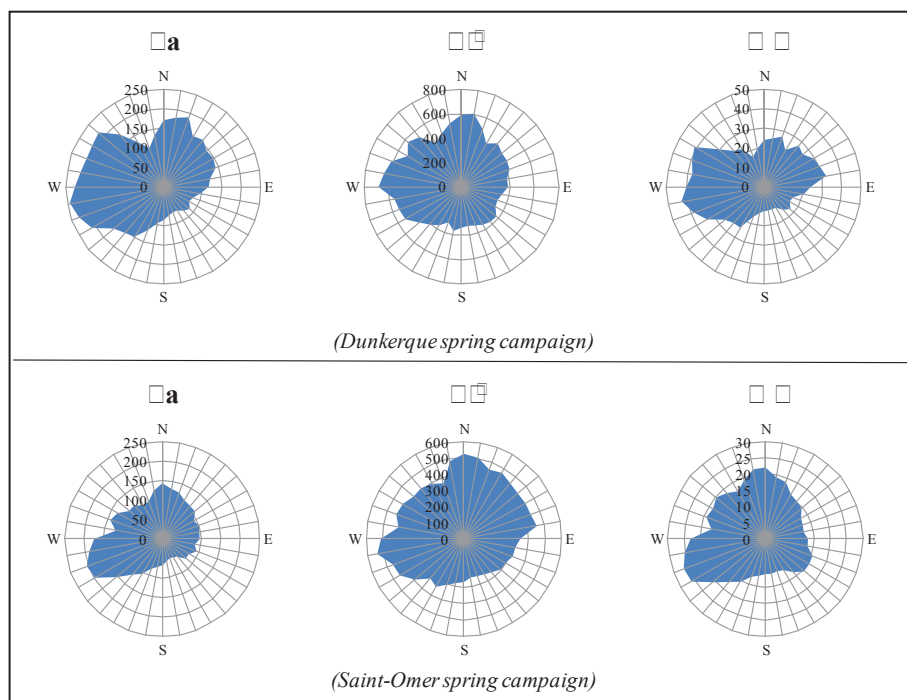


Figure 41 Sulfate elements concentration roses for Dunkerque and Saint-Omer during the spring campaign

III.3.3.1 Major ions origins

The concentration roses for SIA ions (Figure 42) demonstrate the participation of the SE sector in the levels of these ions in Dunkerque. In Saint-Omer, wind directions are able to carry highest concentrations which are originated from the eastern side.

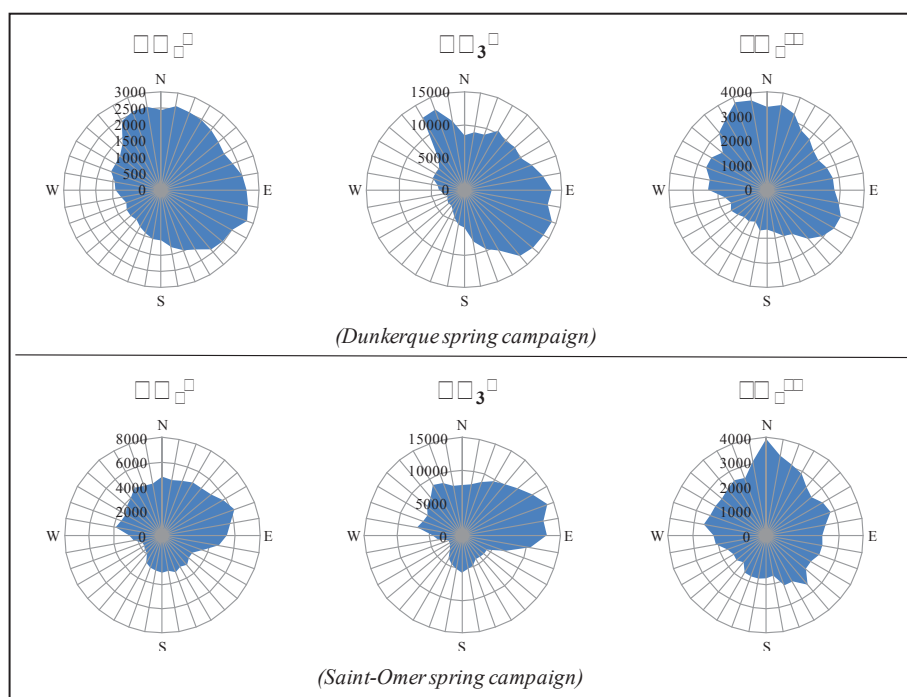


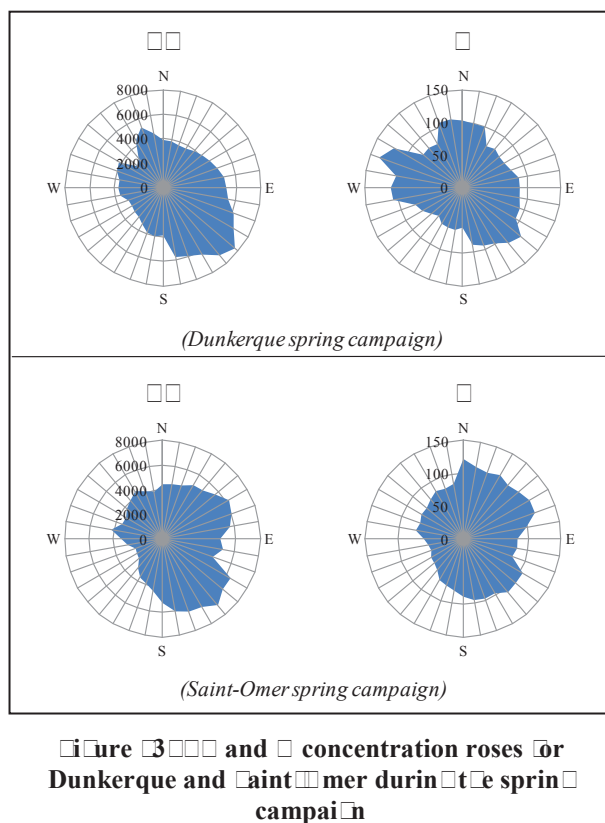
Figure 3.1: Species concentration roses for Dunkerque and Saint-Omer during the spring campaign

However, in Dunkerque, contributions to these ions can also be identified coming from the NW side that includes the ISW site as well as the seafront.

On the other hand, in addition to the urban sector participation in the loads of SIA in Saint-Omer, we can notice a high peak pointing at the N and a lower one from the SE direction, particularly in the case of SO_4^{2-} ions. The first one indicates a possible contribution from Dunkerque's industrial site whereas the second sets the possibility of a nearby glass factory participation in Saint-Omer.

III.3. Combustion elements origins and

Combustion tracers concentration roses show similar aspects between TC and SO_4^{2-} at both coastal and inland site (Figure 43). This observation is in accordance with a previously demonstrated link between these two chemical species.



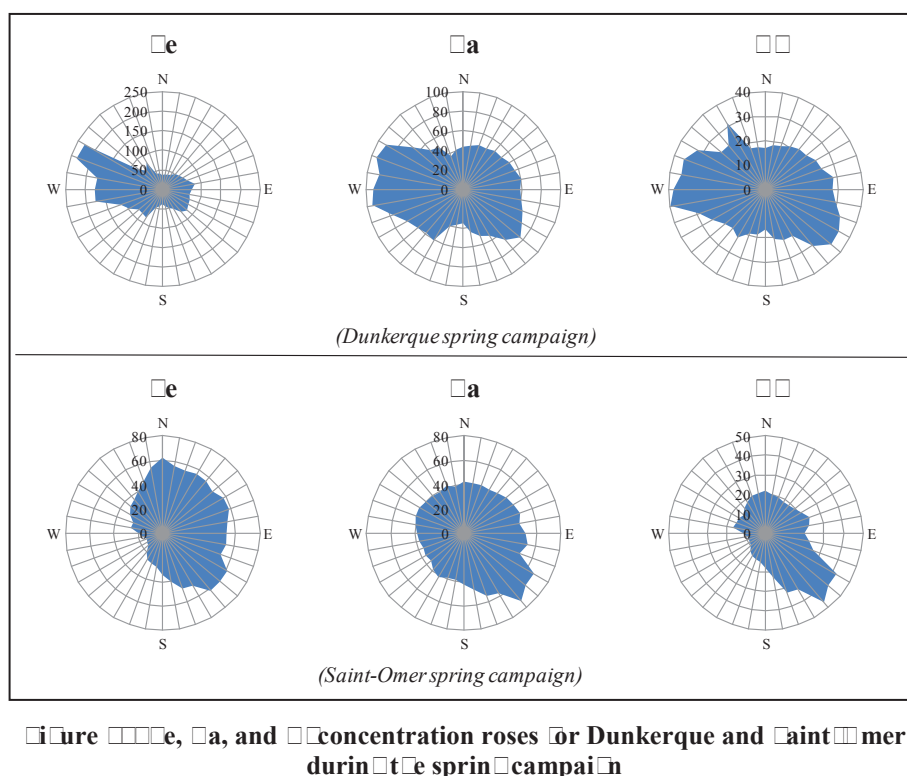
In Dunkerque however, TC and SO_2 maximum concentrations were linked to winds blowing from the SE sector, which points at an urban origin, but also from the NW sector that encloses the industrial site. In particular, high SO_2 concentrations are recorded when wind was blowing from the $270\text{--}290^\circ$ direction and could be linked to the ISW sintering unit emissions as it was found to be in a published work realized by D. Heles (Heles, et al., 2013). Whereas at Saint-Omer, the concentrations of TC and SO_2 were both linked to many wind directions, mainly SE, W-NW, and E-NE. However, some SO_2 increase can be noticed also coming with N winds.

III.6.1.2. Fe, Ca, and Al origins

The 260° to 290° wind sector is found to highly influence the concentrations of Fe, Ca, and Al in Dunkerque as it is demonstrated in Figure 44. This examination agrees with the Fe – Ca relation suggested in section III.6.1.2, and proves that the ISW activities may influence Fe, Ca and in a less extent Al atmospheric concentrations when wind blows from the western directions. Smaller concentrations of these elements are also found related to the both SE and SW urban sectors.

In addition to the urban sector moderate participation, Fe, Ca and Al also had a common enriching SE sector in Saint-Omer, from which the industrial influence of the nearby glass

factory might be the reason behind it. However, it should be noted that under SE winds effect, meteorological conditions favor the accumulation of atmospheric pollutants. Thus, air masses can be heavily loaded in elements which explain the high concentrations found under these conditions. Furthermore, Fe rose peaked from the N direction as well proving that the possibility of Dunkerque's industrial emissions can be identified as a source of this element enrichment.



III. Discussion of the results

A comparison of the concentrations found in this study for Dunkerque, Boulogne-sur-Mer and Saint-Omer was achieved internally between the sites, but also to other European studies in order to classify the N-dC region. We were able to find that for each element, the studied sites exhibited comparable, high, and low values depending on the characteristics of the local activities and geographical position. Furthermore, the diurnal evolution between some analyzed species, regrouped in marine elements, SIA ions, Fe and Ca, Al and Nss-Mg, TC and Σ , enabled the differentiation between regional and local sources of pollution. And finally, a detailed analysis of each species concentration in relation to wind direction was realized using concentration roses in order to point at the direction of the emissions sources.

The following sections will discuss in details the significance of this previous analysis, to be able to point at specific possibilities of regional and local atmospheric pollution sources.

Sampling during the winter campaign (11/18/2010-12/31/2010) took place in Dunkerque and Boulogne-sur-Mer simultaneously. The weather during that period was characterized with lower than usual temperatures and rainfall, but most importantly wind directions influenced the sampling site with different sources of fine $\text{PM}_{2.5}$. In Dunkerque, continental sector winds were the most abundant, followed by industrial and marine mixed sector, then finally by less frequent marine sector winds. However, Boulogne-sur-Mer was affected by only two major wind sectors: the continental inland winds and less frequent marine sector winds.

Total $\text{PM}_{2.5}$ element average concentrations show that Dunkerque had higher values for all ME elements, TC, and ions except for NO_3^- which results were comparable between the two sites.

The spring campaign was held between 03/10/2011 and 04/30/2011 in Dunkerque and Saint-Omer. Meteorological conditions were characterized with below seasonal averages values, with an exceptionally lasting anticyclone episode during which average diurnal temperature increased beyond 20°C . As for wind activities, the situation was closer to the normal seasonal observations with N-E sector winds in the dry period, or SW winds accompanied with less than seasonal average rainfall level during the sampling period.

In this campaign, the concentrations of TC, NO_3^- and SO_4^{2-} were found comparable between the two sampling sites. However, NO_4^- concentrations were found higher in Saint-Omer, whereas the average concentrations of Fe, Ca and Mg were higher in Dunkerque.

It is important to mention that during winter and spring campaigns, diurnal evolutions of species concentrations had similar tendencies at the three studied sites, very much linked to the encountered meteorological conditions. This illustrates that the local $\text{PM}_{2.5}$ concentration trends follows the fluctuations of a regional atmospheric baseline. To this we can add some local emissions impact observed in the differences in the concentrations of certain species between the sites.

Deeper investigations in the sea salt components lead us to find a minor difference between Dunkerque and Boulogne-sur-Mer, which are both regional coastal sites. On the European level, the results showed comparable values except when compared to some Mediterranean sites in which the sea salt fraction was highly concentrated. This difference can be explained by wind circulation pattern of the Mediterranean region. Concentration roses for sea salt elements proved the marine origins of these elements since they were found abundant

with wind directions coming from the marine sector. Unsynchronized peaks of sea salts were identified in Dunkerque and Boulogne-sur-Mer to demonstrate that local variations exist in this natural source of emissions, probably due to the position of the seafront.

Anthropogenic activities were identified by the analysis of Fe and Ca concentration averages and fluctuations. The inter-sites comparison shows that Fe was higher at Dunkerque than in Boulogne-sur-Mer, whereas Ca was found comparable between the two sites, but remaining in slightly higher concentrations in Dunkerque. This observation is common since industrial activities in Dunkerque might be responsible of Fe enrichment. Dunkerque is known to host one of the largest integrated steel works plant in Europe, as well as other industrial activities that can enrich the atmosphere with these elements. However, the comparison on the European level showed that the values found in our study can be compared to the ones found in the case of big cities, in which iron levels were found to be resulting from traffic, but it is still lower than the values found in other industrialized sites in Europe. Daily Fe concentration evolution shows that high levels of Fe identified as punctual peaks are observed regularly. During the peaks, Fe levels increase well beyond the average value then decrease to low levels afterwards. Meanwhile, Ca levels at Dunkerque are found linked to Fe levels, which is not the case at Boulogne-sur-Mer. Finally, concentration roses confirm the industrial origins of Fe and Ca at Dunkerque with slight participation from the marine and continental sectors. On the other hand, the origins in Boulogne-sur-Mer are found to be within the inland continental sector for Fe and Ca.

Aluminum concentration levels were found to be comparable between Dunkerque and Boulogne-sur-Mer, but lower than the European comparison sites. The diurnal evolution of Al shows that it is not linked to a regional tendency. Traffic can be a major source of Al enrichment through non-point source emissions (like dust re-suspension), but also can be emitted by industrial activities from point and non-point sources. Concentration roses of Al at the two coastal sites proves the participation of the traffic sources coming from the city center at the two sites, but also the industrial site influence at Dunkerque and the marine sector at Boulogne-sur-Mer.

TC and Σ concentrations were also compared to find that their levels at the three sites are comparable to most of the large north European cities and industrialized sites, but lower when compared to megacities like Budapest and Milan. In this case combustion processes, including traffic, participated in the loads of TC. Furthermore, the daily successive evolution of these two elements shows that TC is affected by local emissions at the sites, especially with the presence of unsynchronized peaks between the sites of each campaign. These sources can

range from traffic to residential at Boulogne-sur-Mer. The industrial source can be added to these sources in the case of Dunkerque. Concentration roses came to confirm that TC and PM_{10} sources at Dunkerque are mainly from the continental sector, meaning that the effect of the city is clear with some minor participation from the industrial, especially for PM_{10} , and marine sectors. The same observation can be noted in Boulogne-sur-Mer for both elements, but with an absence of industrial participation. Possible marine sources of TC and PM_{10} can be related to marine transportation activities that are high in the region.

NO_3^- , SO_4^{2-} and NH_4^+ concentrations of the SIA group were also analyzed and compared. SIA levels are found comparable between the three sites, and their diurnal evolution shows regional background pollution effect since the concentration levels and trends between the coastal sites are similar. However, NO_3^- concentrations are found to be higher than in European sites except for Milan, in which extremely high concentration levels are probably due to accumulation phenomenon. Furthermore, SO_4^{2-} concentrations were found comparable to megacities levels in central Europe as well as in northern European sites. This indicates that the studied sites are clearly affected by regional as well as local pollution sources. A similar observation can be found in the case of NH_4^+ , which is found higher than nearby sites but lower than some Mediterranean ones. NO_3^- is mostly emitted in traffic dense areas as direct pipe emissions in the form of gaseous NO_x that react in the atmosphere and convert to form ions in particles under low temperature environments. As for SO_4^{2-} ions, it results from the conversion of SO_2 generated mostly by industrial activities like: petrochemical, cement factories, steelmaking...etc. These conditions are fulfilled in the region, as well as in north Europe in general. More confirmation on the source of SIA can be laid down through the analysis of the concentration roses. These latter clearly show that the highest SIA concentrations are encountered under continental sector winds. This origin involves the urban activities as well as the long range transport phenomenon as main SIA sources.

$\text{PM}_{2.5}$ concentration levels above the 2015 limit value ($25 \mu\text{g}/\text{m}^3$) were recorded in air quality surveillance stations during the sampling campaigns. The analysis of the chemical composition of the collected $\text{PM}_{2.5}$ allowed the identification of some species with very high concentrations.

During the winter campaign, episodes during which $\text{PM}_{2.5}$ increased beyond the limit value were encountered under dry and cold weather, and also under N-E to S-E sectors winds which carried continental air masses. In parallel, we observed an increase in TC and SIA (specifically NO_3^- and NH_4^+) concentrations.

Spring campaign episodes can be explained by:

- Particles accumulation situation encountered during stagnant winds and dry weather.
- Winds blowing from the N-E under dry weather and cold temperatures leading to the increase in SIA concentrations.

The observation of high SIA concentrations under the N-E sector deserves a profound interpretation. In fact, the results obtained simultaneously in two sampling sites demonstrate that SIA have not been generated locally. It is well known that secondary inorganic components can be transported to long distances within continental air masses. In the case of ammonium nitrate for example, NH_x and NO_3 precursors can be emitted by combustion processes and agriculture respectively. Therefore, it is normal to find that precursors are emitted in large quantities in inland European sites.

NH_x emitted into the atmosphere evolve into HNO_3 as a result of photochemical reactions. NO_3 reacts faster than NH_x in the atmosphere to give NO_4^- ions by undergoing acid-base reactions. This transformation can be limited when acidic species concentrations like HNO_3 is low ((Seinfeld & Pandis, 2006) and (Kim, et al., 2011)).

Inside the NordC region under study, air masses arriving from the N-E sector could have possibly crossed over the eastern European countries, northern Germany, Holland and Belgium before hitting the NordC region as it was deduced from air mass back trajectories analysis. It is important to note that many studies have demonstrated that NO_3^- and NO_4^- concentrations in Holland and Belgium are between the highest in Europe (Kim, et al., 2011). This phenomenon can be explained by the fact that NH_x and SO_2 emissions are also the highest in northern Europe. They are not only emitted from heavy urbanized and industrialized areas, but also from marine transportation sources in the North-Sea and crossing the Strait of Dover, which is one of the most frequently used around the world: 700 to 800 ships/day (Infrastructure-Maritime, 2013). In addition, NO_3 emissions are important themselves in these northern European countries. In France, three sectors contribute in ammonia emissions into the atmosphere, between which, agricultural activities is responsible of about 97%, followed by road transport (2%) and industries (1%) (CITEA, 2007). Agricultural activities emissions are actually generated by the application of mineral fertilization of the soil. This latter depends also on soil pH, the level of fertilization and some additional variables such as soil temperature and wind speed (Amaoui-Aguel, 2012). These emissions can also result from animal farming. This situation is similarly found in neighbor

European countries like in Belgium and Holland, in which agricultural activities are important.

The abundance of NH_4^+ and NO_3^- in northern European is explained by the rapid transformation of emitted ammonia into ammonium nitrate.

Finally, we remind that average temperatures in northern Europe are lower than those recorded in the south. This climatic condition is to be considered regarding the stability of particulate ammonium nitrate, which is found in higher concentrations in the relatively colder climates of northern Europe as explained before in this chapter. On the opposite side, in high temperatures regions, ammonium nitrate is unstable. For example, nitrate ions in Mediterranean countries are more likely to be found associated to Ca^{2+} , giving that $\text{Ca}(\text{NO}_3)_2$ is less temperature dependent (Arruti, et al., 2011).

III.1 Conclusion

Two sampling campaigns, realized simultaneously in Dunkerque and Boulogne-sur-Mer and Dunkerque and Saint-Omer respectively, allowed us to understand the evolution of $\text{PM}_{2.5}$ concentrations as well as to analyze the fine PM situation in the studied region. The winter campaign (11/18/2010 – 12/31/2010) was realized in Dunkerque and Boulogne-sur-Mer, followed by the spring campaign (03/10/2011 – 04/30/2011) in Dunkerque and Saint-Omer.

We were able to show that $\text{PM}_{2.5}$ concentrations evolved by following similar tendencies from one site to another, which proves the fluctuations of an atmospheric baseline level on the regional scale. These phenomena can be explained by ionic species (NO_3^- , SO_4^{2-} and NH_4^+) and total carbon (TC) concentrations variations. The cumulative contribution of these species constitutes about 93% of $\text{PM}_{2.5}$ total concentration in winter, and about 95% of the total in spring. The diurnal trends of these species were also found very variable and heavily linked to meteorological conditions.

During the two sampling campaigns, the $\text{PM}_{2.5}$ averages in Dunkerque were $24.8 \mu\text{g}/\text{m}^3$ in winter and $33.1 \mu\text{g}/\text{m}^3$ in spring. Daily above limit ($25 \mu\text{g}/\text{m}^3$) values were recorded many times (22 out of 44 days during winter, and 29 out of 49 days in spring). These high concentrations were observed under stable anticyclone conditions and with E winds, which favors the influx of continental air masses. In addition, significant and relatively higher TC concentrations were detected during winter episodes, and are found linked to the increased use of heating. On the other hand, a stable above limit increase in fine PM during spring was accentuated by stable meteorological conditions and almost a total absence of wind activities,

leading to an eventual accumulation. Finally, the diurnal study of Fe, Ca, Nss- \square , Mg and Al concentration variations from one site to the other enabled us to reveal local contributions in Dunkerque, which are probably linked to industrial activities as evidenced by the Fe concentration roses and in less extent with Ca and \square , all of which pointed at the ISW wind direction.

III.11. Works cited

- Arruti, A., Fernandez-Almo, I., Irabien, A. (2011). Regional evaluation of particulate matter composition in an Atlantic coastal area (Cantabria region, northern Spain): Spatial variations in different urban and rural environments. *Atmospheric research*, 101, 280-293.
- CITEPA. (2007). *Emissions dans l'air en France métropol: substances relatives à l'acidification, l'eutrophisation et à la pollution photochimique*. www.citepa.org.
- Dalet, D. (2012, September 13). *d-maps.com cartes gratuites*. Retrieved from d-maps.com: <http://d-maps.com>
- Draxler, R. R., Rolph, P. D. (2012). *Hybrid Single-Particle Lagrangian Integrated Trajectory*. (National Oceanic and Atmospheric Administration) Retrieved December 15, 2012, from <http://ready.arl.noaa.gov/SSPIT.php>
- Elamaoui-Aguel, M. (2012). *Les émissions d'ammoniac par les activités agricoles: impacts sur la qualité de l'air*. Paris: Université Paris II.
- Garrison, G., Yin, Y. (2010). Chemical speciation of PM_{2.5} particles at urban background and rural sites in the US atmosphere. *Journal of Environmental Monitoring*, 12, 1404-1414.
- Heis, D. (2010). *Evaluation de la contribution d'émissions sidérurgiques à la teneur en particules en suspension dans l'atmosphère à une échelle locale*. Thèse de l'Université du Littoral Côte d'Opale.
- Heis, D., Fernandez-Almo, I., Ledoux, F., Foury, A., Courcot, G., Desmonts, T., Courcot, D. (2013). Chemical profile identification of fugitive and confined particle emissions from an integrated iron and steelmaking plant. *Journal of Hazardous Materials*, 250–251, 246–255.
- Hueglin, C., Gehrig, G., Baltensperger, G., Gysel, M., Monn, C., Geronmont, G. (2005). Chemical characterisation of PM_{2.5}, PM₁₀ and coarse particles at urban, near-city and rural sites in Switzerland. *Atmospheric Environment*, 39, 637-651.
- Ilacqua, G., Manninen, G., Saarel, G., Tatsouyanni, G., Hnzli, N., Antunen, M. (2007). Source apportionment of population representative samples of PM_{2.5} in three European cities using structural equation modelling. *Science of the Total Environment*, 384, 77-92.
- Jim, G., Sartelet, G., Seigneur, C. (2011). Formation of secondary aerosols over Europe: comparison of two gas-phase chemical mechanisms. *Atmospheric Chemistry and Physics*, 11, 583-598.
- Ledoux, F. (2003). *Les aerosols particulaires atmospheriques sur le Dunkerquois: caracterisations chimiques, physiques, spectroscopiques et evaluation de leur toxicité*. Thèse de l'Université du Littoral Côte d'Opale.
- Ledoux, F., Courcot, G., Courcot, D., Aboukais, A., Huskaric, E. (2006). A summer and winter apportionment of particulate matter at urban and rural areas in northern France. *Atmospheric Research*, 82, 633–642.
- Monati, G., Iugliano, M., Butelli, G., Gomele, G., Tardivo, G. (2005). Major chemical components of PM_{2.5} in Milan (Italy). *Atmospheric Environment*, 39, 1925-1934.
- Manders, A., Schaap, M., Querol, G., Albert, M., Mercauteren, G., Hhlbusch, T., Hoogerbrugge, G. (2010). Sea salt concentrations across the European continent. *Atmospheric Environment*, 44, 2434-2442.
- Moloi, G., Chimidza, S., Selin Lindgren, E., Iksna, A., Standzenieks, G. (2002). Black carbon, mass and elemental measurements of airborne particles in the village of Serowe, Botswana. *Atmospheric Environment*, 36, 2447-2457.

- Mooibroek, D., Schaap, M., Weijsers, E., Ooogerbrugge, J. (2011). Source apportionment and spatial variability of PM_{2.5} using measurements at five sites in the Netherlands. *Atmospheric Environment*, 45, 4180-4191.
- Abaidullah, M., Bram, S., Perma, J. J., De Vuyck, J. (2012). A review on particle emissions from small scale biomass combustion. *International Journal of Renewable Energy Research*, 21, 147-159.
- Raviskar, J., Timonen, J., Wiikinkoski, T., Ruuskanen, A., Keinänen, J., Ruuskanen, J. (2003). Source contributions to PM_{2.5} particles in the urban air of a town situated close to a steel works. *Atmospheric Environment*, 37, 1013-1022.
- Rakkanen, T. A., Roukkola, J., Korhonen, C. J., Aurela, M., Makela, T., Villamo, J. E., . . . Maenhaut, W. (2001). Sources and chemical composition of atmospheric fine and coarse particles in the Helsinki area. *Atmospheric Environment*, 35, 5381-5391.
- Teraki, S., Assimakopoulos, J., Bougiatioti, A., Kouvarakis, J., Mihalopoulos, N., Asilakos, C. (2012). Carbonaceous and ionic compositional patterns of fine particles over an urban Mediterranean area. *Science of the Total Environment*, 424, 251-263.
- Terrone, M., Iazzalunga, A., Rato, M., Carofalo, I. (2011). Composition of fine and coarse particles in a coastal site of the central Mediterranean: Carbonaceous species contributions. *Atmospheric Environment*, 45, 7470-7477.
- Préfecture-Maritime. (2013). *Préfecture Maritime de la Manche et de la Mer du Nord*. Retrieved April 10, 2013, from <http://www.premar-manche.gouv.fr/services/zone/action/e-docs/00/00/20/76/documentmaritime.php>
- Taud, J., van Dingenen, J., Alastuey, A., Bauer, J., Birmili, W., Cyrys, J., . . . (2010). A European aerosol phenomenology - 3: Physical and chemical characteristics of particulate matter from 60 rural, urban and kerbside sites across Europe. *Atmospheric Environment*, 44, 1308-1320.
- Uerol, J., Alastuey, A., Rodriguez, S., Iana, F., Mantilla, E., Ruiz, C. J. (2001). Monitoring of PM₁₀ and PM_{2.5} around primary particulate anthropogenic emission sources. *Atmospheric Environment*, 35, 845-858.
- Salvador, J., Artalejo, B., Iana, M., Alastuey, A., Uerol, J. (2012). Evaluation of the changes in the Madrid metropolitan area influencing air quality: Analysis of 1999-2008 temporal trend of particulate matter. *Atmospheric Environment*, 57, 175-185.
- Seinfeld, J. N., Pandis, S. N. (2006). *Atmospheric chemistry and physics: from air pollution to climate change*. United States of America: John Wiley & Sons, Inc.
- Sillanpaa, M., Villamo, J., Saarikoski, S., Frey, A., Keinänen, A., Makkonen, J., . . . Salonen, J. J. (2006). Chemical composition and mass closure of particulate matter at six urban sites in Europe. *Atmospheric Environment*, 40, S212-S223.
- Stortini, A., Freda, A., Cesari, D., Cairns, W., Contini, D., Barbante, C. (2009). An evaluation of the PM_{2.5} trace elemental composition in the Venice lagoon area and an analysis of the possible sources. *Atmospheric Environment*, 43, 6296-6304.
- Szigeti, T., Mihucz, J. J., Vári, M., Baysal, A., Atilgan, S., Akman, S., Aray, J. (2012). Chemical characterisation of PM_{2.5} fractions of urban aerosol collected in Budapest and Istanbul. *Microchem.J.* doi:10.1016/j.microc.2012.05.029
- Iana, M., Maenhaut, W., Chi, J., Uerol, J., Alastuey, A. (2007). Comparative chemical mass closure of fine and coarse aerosols at two sites in south and west Europe: Implications for EU air pollution policies. *Atmospheric Environment*, 41, 315-326.
- Wang, J., Shooter, D. (2001). Water soluble ions of atmospheric aerosols in three New Zealand cities: seasonal changes and sources. *Atmospheric Environment*, 35, 6031-6040.
- WHO. (2006). *Air quality guidelines - Global update 2005*. World Health Organization.

- Li-Tuomi, T., Aarnio, A., Hiröla, A., Makela, T., Villamo, A., Antunen, M. (2005). Emissions of fine particles, NO_x, and CO from on-road vehicles in Finland. *Atmospheric Environment*, 39, 6696-6706.

C□A□TE□ I□:

Concentrations trends, statistical analysis
and source identification of Trace
Elements (TE)

TABLE OF CONTENTS

I.1. Introduction	1
I.2. Elemental concentrations and contriutions	1
I.2.1. Winter campaign (November – December 2010).....	175
I.2.2. Spring campaign (March – April 2011).....	178
I.3. Elemental concentrations comparison on the European scale.....	1
I.3.1. Location and characteristics of the comparison sites	180
I.3.2. Comparison of TE average concentrations.....	181
I.3.2.1. Alkali and Alkaline-earth metals	184
I.3.2.2. d-block elements	184
I.3.2.3. Other metals, metalloid and non-metals	185
I.4. Industrial Impact analysis	1
I.5. Enrichment factor analysis.....	1
I.5.1. Winter campaign.....	189
I.5.2. Spring campaign	190
I.6. Roadside correlations study.....	1
I.6.1. Oil combustion TE.....	194
I.6.2. Traffic non exhaust TE	195
I.6.3. Other TE	196
I.7. Concentration evolution in the industrial sector.....	1
I.7.1. Winter campaign concentration roses.....	197
I.7.1.1. Dunkerque winter concentration roses	197
I.7.1.2. Boulogne-sur-Mer winter concentration roses	199
I.7.2. Spring campaign concentration roses	202
I.7.2.1. Dunkerque spring concentration roses.....	202
I.7.2.2. Saint-Omer spring concentration roses.....	204
I.7.3. Correlations and slopes under industrial influences	207
I.7.3.1. The case of Dunkerque	208
I.7.3.2. The case of Saint-Omer's site.....	211
I.8. Conclusion.....	1
I.9. Works cited	1

LIST OF FIGURES

Figure 1: Winter TE average concentrations in Dunkerque and Boulogne-sur-Mer.....	177
Figure 2: Spring TE average concentrations in Dunkerque and Saint-omer.....	179
Figure 3: Comparison sites location on the European map (modified from (Dalet, 2012)).....	180
Figure 4: Winter campaign EF values for TE elements using Ba as reference in Dunkerque and Boulogne-sur-Mer.....	190
Figure 5: Spring campaign EF values for TE elements using Ba as reference in Dunkerque and Saint-omer.....	191
Figure 6: TE concentration roses for Dunkerque during the winter campaign.....	198
Figure 7: TE concentration roses for Boulogne-sur-Mer during the winter campaign.....	200
Figure 8: TE concentration roses for Dunkerque during the spring campaign.....	203
Figure 9: TE concentration roses for Saint-omer during the spring campaign.....	205
Figure 10: Air mass backward trajectories of selected samples showing the N-NE sector influence of Dunkerque in Saint-omer.....	214

LIST OF TABLES

Table 1: TE average concentrations (ng/m ³) and contributions (in %) in PM _{2.5} collected in Dunkerque and Boulogne-sur-Mer during the winter campaign.....	176
Table 2: TE average concentrations (ng/m ³) and contributions (in %) in PM _{2.5} collected in Dunkerque and Saint-omer during the spring campaign.....	178
Table 3: Characteristics of the comparison sites chosen from different European locations.....	181
Table 4: Arithmetic average concentrations (ng/m ³) comparison between our region and Europe.....	182
Table 5: Results of the Industrial Impact calculation in Dunkerque during the winter campaign.....	187
Table 6: Summary of highly correlated TE elements coefficients and slope values for Dunkerque and Boulogne-sur-Mer winter campaign.....	192
Table 7: Summary of highly correlated TE elements coefficients and slope values for Dunkerque and Saint-omer spring campaign.....	193
Table 8: Main anthropogenic influences, corresponding wind sector and TE elements in Dunkerque during winter.....	199
Table 9: Main anthropogenic influences, corresponding wind sector and TE elements in Boulogne-sur-Mer during winter.....	201
Table 10: Main anthropogenic influences, corresponding wind sector and TE elements in Dunkerque during spring.....	204
Table 11: Main anthropogenic influences, corresponding wind sector and TE elements in Saint-omer during spring.....	206
Table 12: Average elemental concentrations, minimum and maximum values (ng/m ³) in Dunkerque's samples under W-NNW industrial sector influence (n=20).....	209
Table 13: Average elemental concentrations, minimum and maximum values (ng/m ³) in Dunkerque's samples under NE-E industrial sector influence (n=12).....	209
Table 14: Selection of elemental ratios under industrial sources influence in Dunkerque compared to total average ratios found with all sectors included.....	210
Table 15: Average elemental concentrations, minimum and maximum values (ng/m ³) in Saint-omer under ESE-SSE industrial sector influence (n=5).....	211
Table 16: Average elemental concentrations, minimum and maximum values (ng/m ³) in Saint-omer under the N-NE industrial sector influence (n=8).....	212
Table 17: Selection of elemental ratios under industrial influences in Saint-omer compared to total average ratios found with all sectors included.....	213

LIST OF EQUATIONS

Equation 1.....	187
Equation 2.....	189

I□.1.Introduction

After the detailed explanation of ME, SI and TC fluctuations and sources identification that was achieved in Chapter III, we continue the interpretation of the findings that followed the chemical analysis of the □M_{2.5} samples by boarding the subēct of the trace elements group (TE). This group includes the following elements: Ag, As, Ba, Bi, Cd, Co, Cr, Cu, Mn, Nb, Ni, □, □b, □b, Sb, Sc, Sn, Sr, Te, Ti, Tl, □ and □n. Therefore, this chapter will include a first section which deals with the comparison between the TE average concentrations measured at the three sampling sites. We will also discuss the difference between our findings and those found in other sites around Europe in order to uncover the position of the three selected regional sites. Afterwards, the “Industrial Impact” will be discussed to reveal which elements were mostly influenced by the industrial activities. This last step will then be completed by an Enrichment Factor analysis for both campaigns, which will also help to determine the anthropogenic influence compared to the natural crustal source of metals. □owever, a statistical analysis will be applied to find which metals are mostly correlated to each other. This will form a first step in uncovering the origins of these trace metals. A concentration rose analysis will be added to this last section to confirm the origins of metals in relation to wind sectors. The chapter will then be concluded by an analysis of elemental ratios and the identification of signature elements that point at TE specific sources □M_{2.5} in the studied sites.

I□.□. □ēmenta□a□era□e concentrations and contri□utions

I□.2.1.Winter campaign (November – December 2010)

The average concentrations and contributions to the total analyzed TE of each TE element are illustrated in Table 1. Total TE concentration in Dunkerque is 1.6 fold higher than the one found for Boulogne-sur-Mer (86.21 versus 50.34 ng/m³).

Furthermore, □n, □b, □ and Mn average concentrations in Dunkerque ranged between 7 and 39 ng/m³ and accounted for about 81.5% of the total analyzed TE concentration, followed by 9.7% formed by □, Cr, Sn, Sb, Ti, As and Ba. These last group elements showed average concentrations fluctuating between 0.9 and 1.7 ng/m³. Ni and Cu average concentrations (3.23 ng/m³ and 2.74 ng/m³ respectively) participated in 7% of the total. Finally, the rest of the TE group contributed in 1.8% only and showed average concentrations ranging between 0.02 and 0.45 ng/m³.

Table 1: Average concentrations in μm^3 and contributions in % in samples collected in Dunkerque and Boulogne-sur-Mer during the winter campaign

Element	Dunkerque		Boulogne-sur-Mer		Total
	Mean	SD	Mean	SD	
Ag	0.05	± 0.06	0.06	± 0.03	0.06
As	0.91	± 0.68	1.06	± 0.48	0.91
Ba	0.90	± 0.68	1.04	± 0.49	1.77
Bi	0.14	± 0.17	0.16	± 0.09	0.25
Cd	0.30	± 0.63	0.35	± 0.14	0.36
Co	0.09	± 0.06	0.10	± 0.06	0.18
Cr	1.43	± 3.11	1.65	± 0.39	0.92
Cu	2.74	± 3.77	3.18	± 1.22	3.30
Mn	7.19	± 12.66	8.34	± 12.54	9.60
Nb	0.02	± 0.04	0.03	± 0.15	0.06
Ni	3.23	± 4.93	3.74	± 0.78	3.22
P	10.54	± 11.63	12.22	± 5.33	13.31
Pb	13.90	± 15.59	16.13	± 5.96	19.09
Pb	0.45	± 0.42	0.52	± 0.24	0.70
Sb	1.07	± 1.74	1.24	± 0.73	2.33
Sc	0.03	± 0.05	0.03	± 0.07	0.08
Sn	1.37	± 1.36	1.59	± 0.71	2.05
Sr	0.36	± 0.22	0.42	± 0.21	0.64
Te	0.03	± 0.03	0.03	± 0.02	0.03
Ti	1.00	± 1.63	1.16	± 1.52	2.54
Tl	0.06	± 0.06	0.07	± 0.05	0.09
V	1.71	± 1.20	1.98	± 0.83	2.37
Zn	38.70	± 46.48	44.89	± 14.94	36.14
Total	86.21		100	50.34	100

*Dunkerque winter campaign concentrations for Tl could not be obtained between the first sample until 12/13/2010 (44 samples), due to technical reasons.

On the other hand, Boulogne-sur-Mer trace elements contribution in total analyzed TE concentration shows that Zn, Pb, P and Mn which average concentrations ranged between 4 and 19 ng/m^3 , account for 78% of total TE. On the other hand, Cu, Ni, Ti, V, Sb, Sn and Ba (average concentrations between 0.9 and 1.7 ng/m^3) contributed in 18% of total analyzed TE concentration. Furthermore, 4% was the quota of the remaining trace elements which included average concentrations ranging between 0.02 and 0.46 ng/m^3 .

Finally, we noticed in Boulogne-sur-Mer and Dunkerque that the average concentrations of Pb, Mn, Ni, As and Cd did not increase beyond WHO, USEPA and the European directive limit and target values during this campaign. In fact, the obtained average

concentrations were all found below the annual mean limit values of 20, 10, 20, 6 and 1 ng/m³ respectively.

In addition to the contribution of each element in total TE concentration, we also discuss hereafter the difference in the concentrations between Dunkerque and Boulogne-sur-Mer for each of the TE metals (Figure 1).

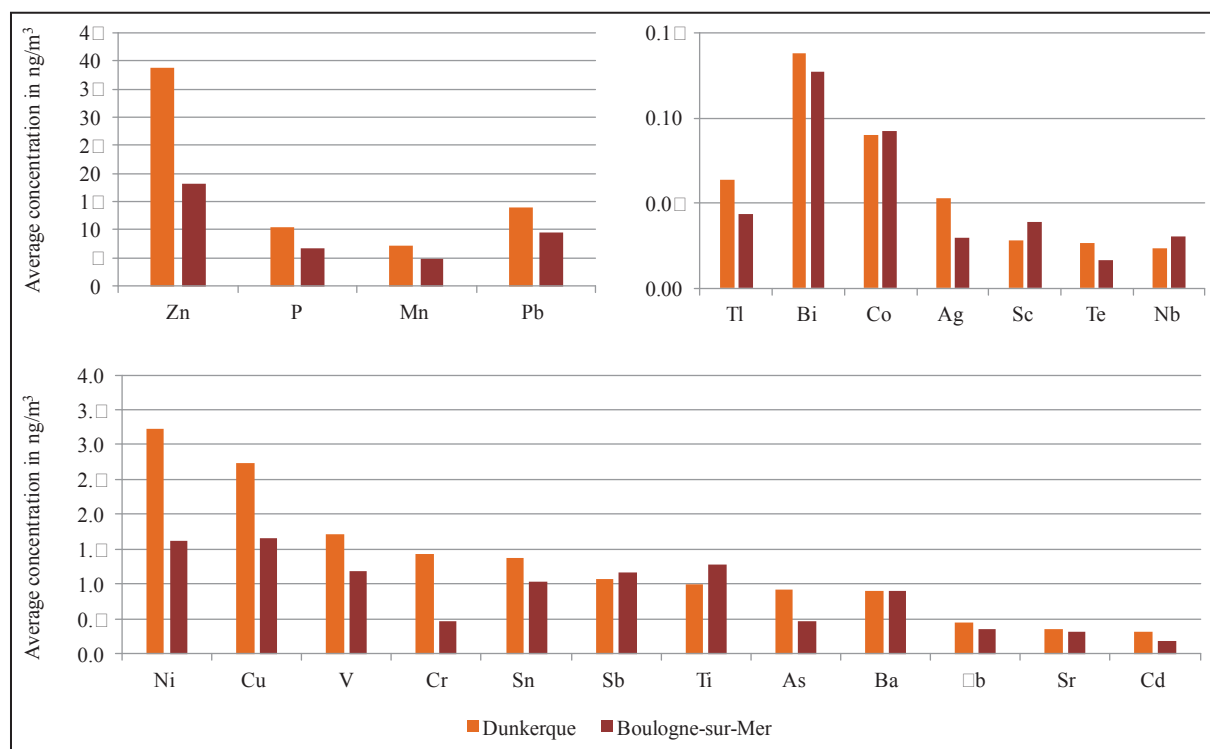


Figure 1: Winter TE average concentrations in Dunkerque and Boulogne-sur-Mer

In this section, the elements are divided between the ones found higher, moderately higher and comparable average concentrations at one site when compared to the other. Hence we find that Zn, P, Pb, Mn, Ni, Cu, V, Cr and As concentrations are much higher in Dunkerque compared to Boulogne-sur-Mer. Furthermore, Hg, Cd, Ag and Sn average concentrations are found moderately higher in Dunkerque, while Co, Ba, Sr, Sc, Bi, Nb, Te and Tl average concentrations are found comparable between the two sites. Finally, the remaining elements represented by Ti and Sb were found more concentrated on average in Boulogne-sur-Mer than in Dunkerque. Additional interpretation on the origins of these elements will be given later in this chapter as well as in chapter V.

IV.2.2.Spring campaign (March – April 2011)

A summary of the average concentrations and contributions of TE calculated for our spring campaign fine PM samples can be found in Table 2. We are able to distinguish that total average TE concentration in Dunkerque is about 1.3 fold higher than the average in Saint-Omer (99.9 $\mu\text{g}/\text{m}^3$ versus 74.9 $\mu\text{g}/\text{m}^3$). Total Te concentration values are also higher than the winter campaign ones. However, in a similar fashion as the winter campaign, the average concentrations of Pb, Mn, Ni, As and Cd regulated TE did not cross the WHO, USEPA and the European directive limit and target values during this campaign.

Table 2: TE average concentrations ($\mu\text{g}/\text{m}^3$) and contributions (%) in fine PM₁₀ collected in Dunkerque and Saint-Omer during the spring campaign

TE	Dunkerque		Saint-Omer		%
	Mean	SD	Mean	SD	
Ag	0.04	± 0.06	0.04	0.06 ± 0.08	0.08
As	0.77	± 1.02	0.77	1.36 ± 1.28	1.79
Ba	0.77	± 0.40	0.77	0.67 ± 0.38	0.88
Bi	0.11	± 0.10	0.11	0.19 ± 0.14	0.24
Cd	0.34	± 0.84	0.34	0.41 ± 0.53	0.67
Co	0.19	± 0.15	0.19	0.18 ± 0.14	0.24
Cr	1.23	± 2.27	1.23	0.74 ± 0.53	0.97
Cu	2.26	± 1.89	2.26	3.11 ± 4.79	4.10
Mn	8.11	± 14.56	8.12	4.19 ± 4.94	11.2
Nb	0.01	± 0.02	0.01	0.014 ± 0.03	0.02
Ni	4.63	± 3.68	4.63	2.91 ± 2.18	3.83
P	16.43	± 28.11	16.44	9.61 ± 13.58	12.64
Pb	9.77	± 8.19	9.78	16.71 ± 12.59	22.00
Snb	0.42	± 0.55	0.42	0.67 ± 0.67	0.88
Sb	0.79	± 0.64	0.79	2.61 ± 2.48	3.44
Sc	0.01	± 0.03	0.01	0.04 ± 0.04	0.04
Sn	1.01	± 0.77	1.01	3.10 ± 6.01	4.08
Sr	0.37	± 0.28	0.37	0.29 ± 0.20	0.38
Te	0.03	± 0.04	0.03	0.04 ± 0.07	0.04
Ti	2.22	± 2.25	2.22	3.73 ± 4.37	4.91
Tl	0.09	± 0.22	0.09	0.094 ± 0.13	0.13
V	6.34	± 5.06	6.34	3.98 ± 3.44	8.24
Zn	43.99	± 88.45	44.01	21.14 ± 16.40	27.84
Total	99.94		100	74.94	100

Furthermore, Dunkerque's spring results show that Zn, P, Pb and Mn contribute in about 78.4% of total TE, followed by V, Cu, Ni and Ti (1–4%), then Cr, Sn, Sb, Ba and As (4.6%), and the remaining elements constitutes 1.6% only, which is more or less the same distribution as observed in winter.

On the other hand, 68% of total average TE concentration in Saint-Omer is constituted from Zn, Pb, P and Mn, whereas Cu, Ni, Ti, V, Sb, Sn and Ba represent 26%. Finally, the rest of the elements contribution summed a remaining 6% of the total TE average.

The comparison between the TE levels found in Dunkerque and those found in Saint-Omer reveals a different scenario than the one observed for Dunkerque and Boulogne-sur-Mer during the winter campaign. More TE elements are found concentrated in the inland site than the coastal industrialized site (Figure 2).

Dunkerque average concentrations exceeded Saint-Omer's for Zn, P, Mn, V, Ni, Cr and Sr. Comparable levels were found for Co, Ag, Nb, Te and Tl at the two sites. Meanwhile, elemental concentration of As, Cu, Pb, Sb, Sn, Ti, Pb, Cd and Bi are found moderately higher in Saint-Omer. Finally, this latter is found to have higher concentration levels for the remaining TE elements.

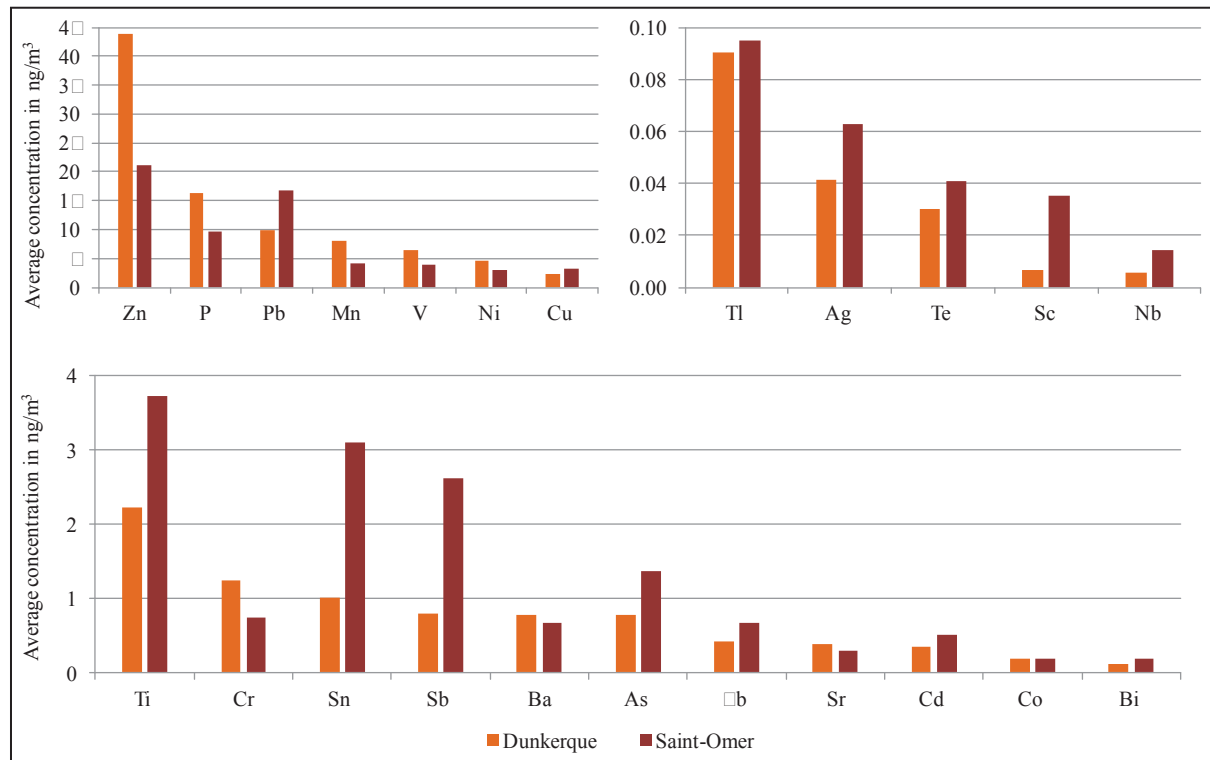


Figure 2: Spring TE average concentrations in Dunkerque and Saint-Omer

3.3.3. Average TE concentrations comparison on the European scale

IV.3.1. Location and characteristics of the comparison sites

In this section, the data used for comparison will be extracted from similar studies conducted around Europe (Figure 3). Geographically, the sites are distributed between northern Europe (Finland, Netherlands and the United Kingdom), middle Europe (Switzerland and Hungary) and southern Europe (Spain, Italy, and Greece).



Figure 3. Comparison sites location on the European scale modified from Dalet et al.

These studies include common $PM_{2.5}$ trace elements measurements. The characteristics of some selected sampling sites were detailed in chapter III, when many others were not. Therefore, we will illustrate the details about each study used hereafter with a small summary about the major influences encountered at these locations (Table 3).

The characteristics of the comparison sites range from typical urban sites to urban influenced by industries. As for the latter, it fluctuates between heavy and light industries that can be found combined in some sites.

Table 4: Characteristics of the comparison sites chosen for different European locations

Country	Site	Site characteristics	References
Finland	Jääskelä	Urban Steelworks	(Oravisto et al., 2003)
	Vallila	Urban	(Pakkanen, et al., 2001)
	Helsinki (22-24 October, 2003)	Urban	(Kuitu-Tuomi, et al., 2004)
	Helsinki (Fall, 1996 – Winter, 1997)	Urban	(Ilacqua, et al., 2007)
Spain	Onda	Urban Ceramic industry	(Querol, et al., 2001)
	Tarragona	Urban Petrochemical	(Moreno, et al., 2006)
	Barcelona	Urban	
	Huelva	Urban Heavy industry	
	Llodio	Urban Heavy industry	
	Cantabria region	Urban Industry	(Arruti, et al., 2011)
Switzerland	Zurich - Dübendorf	Urban	(Hueglin, et al., 2004)
	Basel (Spring, 1998 – Spring 1999)	Urban	
	Basel (Winter, 1997 – Spring, 1998)	Urban	(Ilacqua, et al., 2007)
Netherlands	Rotterdam	Urban	(Mooibroek, et al., 2011)
Hungary	Budapest	Urban	(Szigeti, et al., 2012)
Italy	Venice	Urban Light industry	(Stortini, et al., 2009)
Greece	Athens	Urban	(Ilacqua, et al., 2007)
United Kingdom	West Midlands	Urban background	(Harrison et al., 2010)

IV.3.2. Comparison of TE average concentrations

The approach that we will use in this section will be purely descriptive in order to rank TE elements concentrations of the NPdC region between other European sites that are influenced by similar types of emissions as our sites. These emissions can differ especially in the scales of the contribution from anthropogenic sectors from one site to the other.

The interpretation of the TE average concentrations summarized in Table 4 will take in consideration three groups depending on their characteristics in the periodic table of elements:

- Alkali and Alkaline-earth metals: Na, K, Sr and Ba.
- d-block elements: Ag, Cd, Co, Cr, Cu, Mn, Nb, Ni, Sc, Ti, V and Zn.
- Other metals, metalloid and non-metals: Sn, Sb, Tl, Pb, Bi, P, As and Te.

Table 4: Critical average concentrations in mg/kg for comparison between our region and Europe

Country	City	Ag	As	Ba	Bi	Cd	Co	Cr	Cu	Mn	Nb	Ni	P	References
Our Study	Dunkerque winter	0.004	0.001	0.001	0.001	0.001	0.001	1.00	0.001	0.001	0.001	0.001	1.00	Our Study
	Boulogne-sur-Mer winter	0.004	0.001	0.001	0.001	0.001	0.001	1.00	1.00	0.001	0.001	1.00	0.001	
	Dunkerque spring	0.004	0.001	0.001	0.001	0.001	0.001	1.00	0.001	0.001	0.001	1.00	1.00	
	Saint-Omer spring	0.004	1.00	0.001	0.001	0.001	0.001	0.001	1.00	0.001	0.001	0.001	0.001	
Finland	Naase	0.03	0.001	0.001	0.1	0.2	0.2	4.1	3.32	32	-	0.3	-	(Oravisto et al., 2003)
	Vallila	0.01	0.8	2.2	0	0.1	0.1	-	3.1	3.3	-	2	-	(Pakkanen, et al., 2001)
	Helsinki (22-24 October, 2003)	-	-	-	-	-	-	-	31	9	-	1	19	(Kali-Tuomi, et al., 2000)
	Helsinki (Fall, 1996 – Winter, 1997)	-	2.3	-	-	-	-	-	-	-	-	1.3	30	(Ilacqua, et al., 2007)
Spain	Onda	-	10	3	-	0.001	0.2	1.00	9	0.001	0.1	3	22	(Cuerpo, et al., 2001)
	Tarragona	0.001	-	3.2	-	0.2	-	2.2	31.7	2.8	-	3.00	-	(Moreno, et al., 2006)
	Barcelona	1.1	-	9.3	-	0.6	-	2.9	31.7	9.6	-	0.2	-	
	Huelva	4.2	-	2.00	-	0.8	-	0.9	32.9	3.2	-	3	-	
	Llodio	1.00	-	7.2	-	1	-	16	29.1	39	-	20.8	-	
	Cantabria region	-	0.3	-	-	0.1	-	2.4	1.9	18	-	0.7	-	(Arruti, et al., 2011)
Switzerland	Zurich - Baslerne	-	0.001	-	-	0.3	-	-	6.1	3.00	-	3.1	-	(Hueglin, et al., 2000)
	Basel (Spring, 1998 – Spring 1999)	-	0.4	-	-	0.001	-	-	6	3.1	-	1.7	-	
	Basel (Winter, 1997 – Spring, 1998)	-	0.6	-	-	-	-	-	-	-	-	2.1	72	(Ilacqua, et al., 2007)
Netherlands	Rotterdam	-	0.6	11	-	0.3	0.3	3.7	10.9	0.3	-	4.4	87.1	(Mooibroek, et al., 2011)
Hungary	Budapest	-	-	-	0.1	0.3	0.1	1.4	9.1	0.4	-	0.72	-	(Szigeti, et al., 2012)
Italy	Venice	1.02	3.6	-	-	3.00	0.3	-	-	0.2	-	12.2	-	(Stortini, et al., 2009)
Greece	Athens	-	23	-	-	-	-	-	-	-	-	4.8	116	(Ilacqua, et al., 2007)
United Kingdom	West Midlands	-	-	-	-	-	-	-	21.9	0.6	-	0.9	-	(Harrison & Yin, 2010)

Table 4 (continued)

Country	City	Pb	Co	Sb	Sc	Sn	Sr	Te	Ti	Tl	V	Zn	References
Our Study	Düsseldorf	1.00	0.00	1.00	0.00	1.00	0.00	0.00	1.00	0.00	1.00	0.00	Our Study
	Belgium	0.01	0.00	1.00	0.00	1.00	0.00	0.00	1.00	0.00	1.00	1.00	
	Düsseldorf	0.00	0.00	0.00	0.01	1.00	0.00	0.00	0.00	0.00	0.00	0.00	
	East Düsseldorf	1.00	0.00	0.01	0.00	0.01	0.00	0.00	0.00	0.01	0.00	0.00	
Finland	Lahti	7.96	2.37	0.17	-	-	0.33	-	0.49	0.09	3.63	29.3	(Oravisto et al., 2003)
	Vallila	0.8	0.24	0.77	-	-	0.46	-	0.83	0.02	-	14	(Pakkanen, et al., 2001)
	Helsinki (22-24 October, 2003)	7	-	-	-	-	-	-	1.0	-	2	33	(Pii-Tuomi, et al., 2000)
	Helsinki (Fall, 1996 – Winter, 1997)	4.9	-	-	-	-	-	-	3.2	-	4.9	10.6	(Ilacqua, et al., 2007)
Spain	Onda	330	2	1	-	1	2	-	28	-	-	186	(Quero, et al., 2001)
	Tarragona	17.0	-	2.6	-	0.9	1.2	-	6.1	-	0.3	19.3	(Moreno, et al., 2006)
	Barcelona	40.3	-	4.3	-	3.7	1.9	-	26.3	-	9.0	0.00	
	Huelva	26.9	-	1	-	1.9	1	-	21.8	-	3.6	42.6	
	Llodio	76.0	-	1.2	-	37	0.9	-	8.6	-	7	239	
	Cantabria region	3.0	-	-	-	-	-	-	1.3	-	0.8	-	(Arruti, et al., 2011)
Switzerland	Zurich - Baslerne	21	0.0	0.07	-	-	-	-	-	0.04	1.1	-	(Hueglin, et al., 2000)
	Basel (Spring, 1998 – Spring 1999)	19	0.08	0.41	-	-	-	-	-	0.03	1.2	-	
	Basel (Winter, 1997 – Spring, 1998)	21	-	-	-	-	-	-	6.0	-	3.0	39	(Ilacqua, et al., 2007)
Netherlands	Rotterdam	2.9	-	1.6	1.9	3	1.6	-	1.9	-	6.0	94.6	(Mooibroek, et al., 2011)
Hungary	Budapest	11	0.44	2	-	1.0	-	0.01	-	0.02	0.0	28	(Szigeti, et al., 2012)
Italy	Venice	18.08	-	-	-	-	-	-	186.1	-	14.06	84.0	(Stortini, et al., 2009)
Greece	Athens	1.0	-	-	-	-	-	-	10.8	-	14	46	(Ilacqua, et al., 2007)
United Kingdom	West Midlands	18.1	-	-	-	-	-	-	8.3	-	-	4.0	(Harrison et al., 2010)

1.1.1 Alkali and Alkaline-earth metals

This group includes some metals that are usually considered in a moderate frequency in PM_{2.5} studies. Between our sites, Dunkerque displayed comparable concentration values for Ba in winter and spring when compared to Boulogne-sur-Mer and Saint-Omer respectively. As for the rest of the European studies, our values are found slightly higher than the nearby site of Laahe, but much lower than the rest of the studies. On the other hand, Pb average concentration was found to be the highest in Saint-Omer, followed by Dunkerque winter concentration. When compared to other studies, these values are comparable to mid European sites (Zurich and Basel), but much lower than other industrialized sites (Onda and Laahe).

In general, these two elements (Ba and Pb) can be found in crustal dust (Wedepohl, 1995). Higher levels from one site to another can be explained by important dust re-suspension, and/or important industrial activities which include raw ore manipulations. Actually, this situation can be observed in Dunkerque, as well as in Laahe and Onda.

Finally, Sr average concentrations in Dunkerque is higher than in the other sites for the two campaigns, and is comparable to some values between the nearby sites studies (Laahe and Vallila). However, this metal is found in relatively higher concentrations in the remaining comparison sites.

1.1.2 Cd-Co-Cr-Ni-Mn-Pb-Zn

This group includes a list of metals that is extensively analyzed in similar studies around the European continent. Our first observation regarding this group revolves around the elements that have legislated concentration limit values in the atmosphere (Cd, Mn and Ni). Average concentrations are found lower in our study than the limits discussed in Chapter I (section I.4.3.) and we also notice that there is no case of limit values rupture recorded in the European sites either.

When compared to these studies, Ag concentrations are found to be generally higher than the values found in nearby sites and much lower than the rest of the comparison sites in Spain and Italy. Co concentration levels are comparable between our sites in each campaign, but when compared to most studies, the values are found lower. On the other hand, Cr average concentrations are found higher in Dunkerque than the remaining sites in our study. These averages are also higher than Huelva's, comparable to Onda and Budapest results, and finally lower than the rest of the comparison sites.

Furthermore, highest Cd average found in Saint-Omer was found to be comparable to Basel, Onda and Barcelona levels. However, the average was lower than in Huelva and

lodio, but much lower than the urbanized Venice area. In parallel, Cu averages followed Cr variations between our sampling sites, but were found higher than Cantabria's value (except for Boulogne-sur-Mer average), comparable to some north European sites, and finally much lower than the rest of the comparison sites. On the other hand, Mn levels in Dunkerque show higher and comparable averages when compared to most studies. However, lodia, lodio and Cantabria's Mn averages exceeded in many folds the values of our industrialized site. This is in accordance with the industrial characteristics of these sites.

Dunkerque's Ni averages are also found higher than the remaining sites of our campaigns, but also higher than most of the comparison sites in Europe as well. Few exceptions can be noticed for sites like lodio and Venice in which Ni concentration peaked well above our region values. In an opposite direction, Ti average concentrations in Saint-Omer is found to be the highest between the three studied sites, which can be resulting from crustal matter sources in that area. Nonetheless, this high Ti concentration value is found to be much lower than those found in Europe with very few exceptions. Furthermore, V average at Dunkerque during spring is found to be the highest between our campaigns, it is also the highest when compared to most European studies, with the exceptions of the following heavy urbanized sites: Rotterdam, Barcelona, Venice and Athens, and the industrial site of lodio in Spain. As for high Zn average concentration in Dunkerque, it is found higher than half of the comparison studies results, including some urban-industrial sites, but also very much lower than other heavy urbanized and industrialized sites.

Finally, Nb and Sc averages for comparison were down to one study for each metal. Both elements are found very much lower than the ones found in the two comparison studies.

4.4.4.4. Toxic metals: metalloids and non-metals

Within this group of elements, our first concern focuses on the elements that have legislated concentration limit values in the atmosphere (As and Pb). Average concentrations found in our study are lower than the limits discussed in Chapter I (section I.4.3.). We can also notice that Onda's industrial site as well as the urban site of Athens presented As concentration levels beyond the limit of 6 ng/m^3 .

On the other hand, Bi and Te average concentrations are found higher in our sampling sites than in the other comparison ones. P concentrations show higher values for Dunkerque in both winter and spring campaigns, but also lower than in other sites in Europe.

Furthermore, the highest Sn average concentration can be observed in Saint-Omer, when the other values of our campaigns are found to be almost comparable between each

other. But when compared to other sites, Saint-Omer value was higher and comparable in almost all the sites except for Llodio's value which was very much higher than our study's. Additionally, Tl average concentration showed a peak value in Dunkerque during the winter season, followed by Saint-Omer's average that was comparable to Dunkerque's spring one. However, our values tend to be higher than the ones observed on the European level.

Moreover, As highest average concentration is uncovered in Saint-Omer inland site. It is found higher than most north European sites (except in Helsinki and Basel "1997-1998") and lower than the rest of the comparison sites which includes heavily industrialized and urbanized cities. On the other hand, Saint-Omer has also the highest Pb concentration between our sites. This concentration is higher and comparable to the values found in other European cities that exhibit major urban influences, but also is much lower than the concentrations of Pb in industrial sites (Onda and Llodio) as well as in heavy urbanized ones (Barcelona and Athens). Finally, Sb concentration levels followed to a certain extent the trend of Pb for our sites from which Saint-Omer held the highest average for this element. This average was still higher than most of the European comparison sites, including highly urbanized cities values (Budapest), but was also comparable and low when weighed against the heavy industrialized site of Tarragona and the heavy urbanized site of Barcelona respectively.

□ □ □ □ Industrial □ □ Impact analysis

The Industrial Impact calculation method was used by (Puchbaum, et al., 2004) and reproduced by (Arruti, et al., 2011) to quantify the impact of a certain anthropogenic sector on the total load of chemical species in atmospheric PM. Originally this method was used to evaluate the urban impact on the chemical composition of atmospheric aerosols using two sets of chemical concentration data □ reference site data (background) and impacted site data.

The source of impact we are searching for in this section is industrial, therefore we will be calculating this impact in Dunkerque (urban-industrial) using Boulogne-sur-Mer as a reference site (urban background). Both sites are influenced by many common sources (urban, marine and secondary inorganic aerosols) with the exception of the industrial sector that is present only in Dunkerque. The choice of taking into account Boulogne-sur-Mer site as reference can be verified to a certain extent by the averages found for TE at that site (Table 1). The calculations will allow us to estimate the percentage of the industrial activities

contribution in Dunkerque's TE load. Therefore, we will consider the winter campaign during which simultaneous sampling was accomplished between Dunkerque and Boulogne-sur-Mer.

However, this method could not be applied for the spring campaign since the choice of a reference site was impossible due to the presence of industrial facilities at both sites and the detection of high concentrations in many trace elements. In addition, the possible influence of Dunkerque industrial site emissions at Saint-Omer cannot be discarded as mentioned in the upcoming section IV. and section IV.7.2.2.

The estimation procedure was extracted from (Arruti, et al., 2011) but the symbols were modified from the original source in order to define our impact and reference in Equation 1 illustrated below.

$$I.I.(%) = (I.L. - U.L.) \times \frac{100}{I.L.} \quad \text{Equation 1}$$

In the equation we define

- I.I. as the industrial impact (in %)
- I.L. as the industrial level (the concentration at the industrial site in ng/m³)
- U.L. as the urban level (the concentration at the urban reference site in ng/m³)

Thus the average concentrations found in Dunkerque are used as I.L., whereas those measured in Boulogne-sur-Mer are used as U.L. The calculations lead to uncover the contribution of the industrial activity in Dunkerque summarized in Table . It must be noted that I.I. values for elements which are present in very low atmospheric concentrations should be carefully considered. Indeed, negative values are observed within the table for Co, Nb, Sb, Sc and Ti. In the same manner, the I.I. values obtained for Ag, Te and Tl are probably affected by a large uncertainty. In this case, the observed differences from one site to the other are not significant. These values can be resulting from possible non urban and non-industrial contributions at the reference site during the sampling period.

Table 1: Results of the industrial impact calculation in Dunkerque during the winter campaign

<i>Elements</i>	<i>Ag</i>	<i>As</i>	<i>Ba</i>	<i>Bi</i>	<i>Cd</i>	<i>Co</i>	<i>Cr</i>	<i>Cu</i>	<i>Mn</i>	<i>Nb</i>	<i>Ni</i>	<i>P</i>
I.I. (%)	44	0	0	8	40	-3	67	39	33	-27	0	36
<i>Elements</i>	<i>Pb</i>	<i>Rb</i>	<i>Sb</i>	<i>Sc</i>	<i>Sn</i>	<i>Sr</i>	<i>Te</i>	<i>Ti</i>	<i>Tl</i>	<i>V</i>	<i>Zn</i>	
I.I. (%)	31	22	-10	-37	20	10	39	-28	27	30	0	

The rest of the results indicate that high industrial impact can be observed for As, Cd, Cr, Cu, Ni, P and Zn compared to relatively less but still significant impact for Mn, Pb, □b, Sn and V.

Using the same approach, it is important to mention that I.I. were calculated for major elements such as Al, Ca and Fe which was evaluated to 26%, 12% and 43% respectively. It is known that these elements in addition to other trace elements such as Pb, Mn and Cd can be generated by the industrial activities linked to the metallurgic factory in Dunkerque. However, it is important to uncover if the particularly high Zn industrial impact value is limited to one or many industrial sources.

Further investigations will complete this analysis in the upcoming section that includes an enrichment factor followed by correlations and concentration rose analysis, in order to introduce an additional trustworthy method to determinate the most important sources of emissions.

□□ □□ **Enrichment Factor analysis**

In the previous section, we evaluated the impact of the industry on the loads of TE in PM_{2.5} at the urban-industrial site of Dunkerque. However, another evaluation criterion can be added as an additional step in the estimation of anthropogenic activities. This parameter is the enrichment factor which allows us to determine which element is more concentrated at one site when compared to a natural crustal source. It is widely used in the literature ((Torfs □ Van □rieken, 1997) □ (Chester, et al., 1999) and (Saliba, et al., 2007)), because it enables the differentiation between a natural source of emissions (soil crust in our case) for a certain element and the additional sources for the same element (without differentiating between these latter).

Between the studies that use enrichment factor method, we can notice that different elements can be used as reference, between which □ Ti, Al, Fe, Si, Sr and Ba are commonly used. The principal selection criterion is embodied in the fact that the reference element should not be emitted in considerable quantities by any nearby anthropogenic source in the studied region. By following this method, we discarded Ti, Al and Fe, which are emitted by industrial sources in Dunkerque. On the other hand, silicon was not analyzed in this study, which leaves us two choices □ Sr and Ba. The first can be present partially in marine aerosols, which is not the case for Ba.

Hence, the enrichment factor for each of the TE list was calculated using Ba upper crust and aerosol content as references. This element is present in high concentrations (668 ppm) in the upper crust (Wedepohl, 1995), and is not significantly emitted from any known nearby anthropogenic sources which makes it the best choice for a reference element in our case. Te enrichment could not be calculated in our study because of a lack in information about its crustal concentration.

The concentrations for the remaining TE elements in the upper crust were retrieved from (Wedepohl, 1995) and used in the following equation

$$EF = \frac{[X]_{\text{aerosol}}/[REF]_{\text{aerosol}}}{[X]_{\text{crustal}}/[REF]_{\text{crustal}}} \quad \text{Equation 1}$$

With

- $[X]_{\text{aerosol}}$ as the average concentration of the element in our samples (in ng/m³)
- $[X]_{\text{crustal}}$ as the average concentration of the element in the upper crust (in ppm)
- $[REF]_{\text{aerosol}}$ as the reference element concentration in our samples (in ng/m³)
- $[REF]_{\text{crustal}}$ as the reference element concentration in the upper crust (in ppm).

Ba was used as reference element in our study.

Significant enrichment for any given element can be considered starting from an EF value that increases beyond 10. Finally, the results of the calculations are illustrated and discussed hereafter for each campaign separately.

IV.1. Winter campaign

Figure 4 illustrates the EF results for the winter campaign which shows that enrichment is not significant for Co, Mn, Nb, Sc, Nb, Sr and Ti in both Dunkerque and Boulogne-sur-Mer. In this latter, Cr (EF≈10) and P (EF<10) were also not enriched in comparison to Dunkerque's values. On the other hand, Bi and Sb were found to be highly enriched with EF values similar between our two sites. For the rest of the elements, EF values vary depending on the site. In Dunkerque, they are always higher than those found for Boulogne-sur-Mer, especially for Ag, As, Cd, Cr, Cu, Ni, P, Pb and Zn which indicates the presence of an anthropogenic contribution in Dunkerque.

Finally, these observations can be compared to the industrial impact calculations discussed earlier (section IV.4) to find that both calculations lead to similar results.

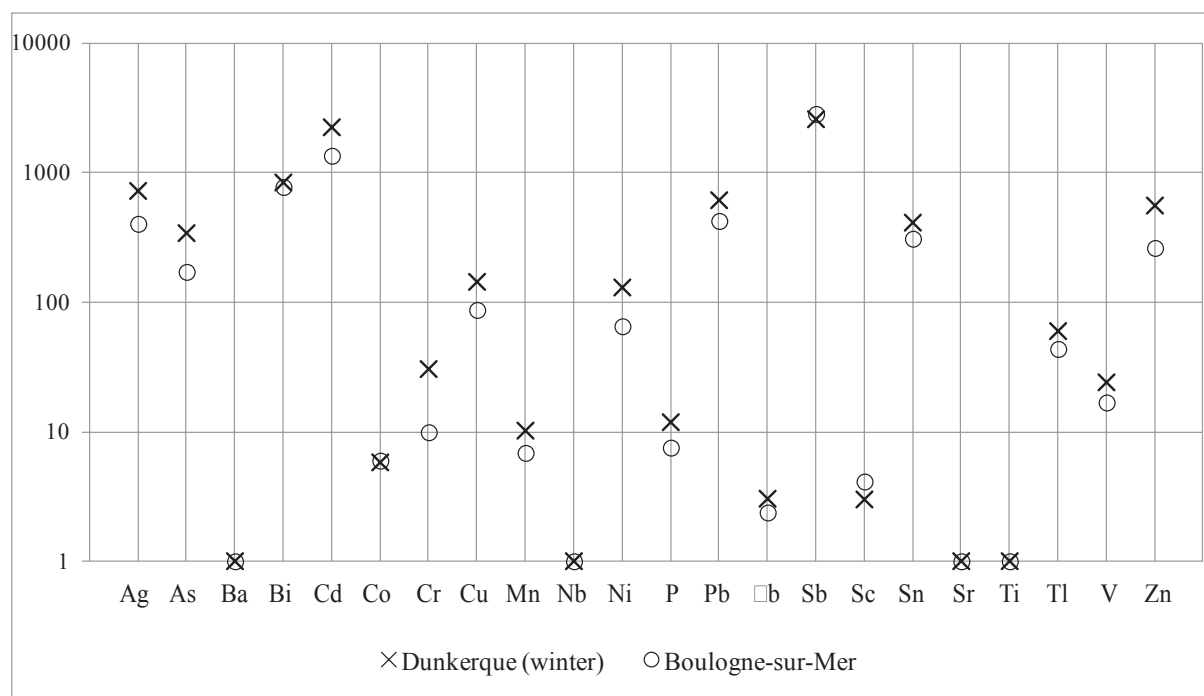


Figure 4: Winter campaign EF values for TE elements using Ba as reference in Dunkerque and Boulogne-sur-Mer

IV.2. Spring campaign

The spring campaign EF values for TE elements are illustrated in Figure 5. The results show that enrichment is not significant for Mn, Nb, Sb, Sc, Sr and Ti at both sites of this campaign except for Mn which is slightly enriched in Dunkerque. At this latter, Cr, Ni, P, V and Zn are found slightly enriched compared to Saint-Omer. On the other hand, Co and Tl can be identified as equally enriched elements between the two sites, whereas Ag, As, Bi, Cd, Cu and Pb enrichment factors are slightly higher at the inland site of Saint-Omer. At this latter, EF values peaked when compared to Dunkerque's for Sb and Sn.

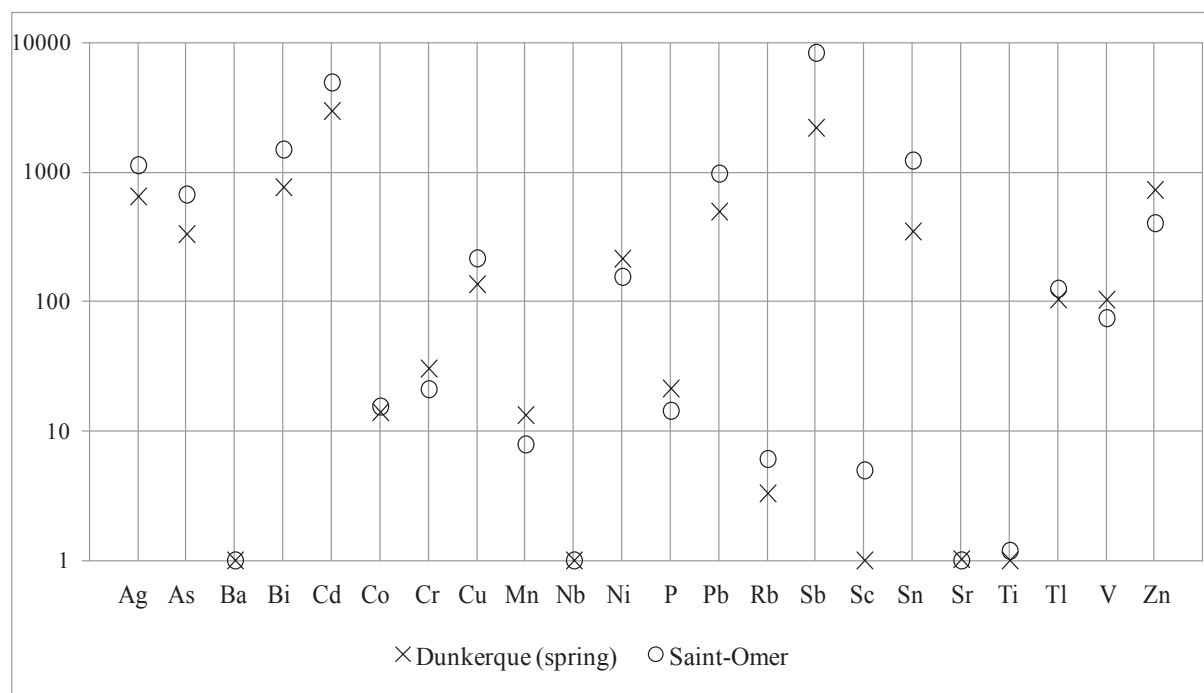


Figure 4-1 Spring campaign EF values for TE elements using Ba as reference in Dunkerque and Saint-Omer

By comparing the three sites, we can notice that EF values are systematically higher for Cr, Mn, Ni, P, V and Zn to which Al, Ca and Fe can be added in Dunkerque during both winter and spring season. We also found high EF in Saint-Omer for many elements—Sn, Sb, Pb, Cd and As which needs profound interpretations. The investigations needed should specifically focus on the presence of an additional local emission source at Saint-Omer that can explain these results, especially glass making industry. In parallel, it is also necessary to verify if the industrial emissions from Dunkerque affect PM_{2.5} composition in Saint-Omer or not.

4.3.3.3. Local TE correlations study

In this section we will board the relationship between each of the TE concentrations in all the samples. This comparison will allow us to define which elements are correlated, as well as the possible origins of these elements by comparing their mean ratios to ones found in the literature for specific sources. Therefore, correlation coefficients (r^2) and slopes ($y = ax$) tables and scatter plot matrices (SPOM) were built using Microsoft Excel 2007 and SPSTAT 10 respectively. The data sets used in this step include all species concentrations of all samples for a given sampling site regardless of the emission source or wind sector.

For SPMM calculations were divided into two steps. First one was accomplished using all data in order to identify possible extreme values found in some samples then compared to others as a single sampling simulating its identification and in order to avoid any biased correlations corresponding samples were discarded from the correlation study. SPMM and R^2 presentation are summarized in APPENDIX and references.

The calculated correlation coefficients values so far and elements are found in all correlated to each other when $R^2 \geq 0.60$ otherwise elements are found moderately correlated in an average coefficient value R^2 is presented in the results. Elements are called or not correlated at all.

The correlation coefficients and the corresponding slope values obtained using the linear regression analysis are illustrated in Table.

Table 6: Summary of highly correlated TE elements coefficients and slope values for Dunkerque and Boulogne-sur-Mer winter campaign

TE ratios	Dunkerque winter		Boulogne-sur-Mer	
	R^2	Slope	R^2	Slope
V-Ni	0.78			
Bi-Pb	0.77			
Ag-As	0.73			
Cd-Pb	0.73			
Cu-Pb	0.72			
As-Cd	0.72			
As-Bi	0.69			
Ag-Rb	0.68			
Pb-Rb	0.67			
Ag-Ba	0.66			
As-Rb	0.66			
Mn-Ni	0.65			
Co-Nb	0.65			
As-Pb	0.65			
Co-Ni	0.64			
Cd-Rb	0.64			
Mn-V	0.63			
Ag-Cd	0.61			
Cu-Sb	0.60			

The listing of elements as chosen to represent decreasing order of correlation coefficient values for Dunkerque's samples. Values in bold represent high correlations ($R^2 \geq 0.60$) whereas lighter shades values correspond to the light correlations found in Boulogne-sur-Mer. The range between an average and a correlation.

The results show that there are poor correlated species and higher correlations coefficients in Dunkerque than in Boulogne-sur-Mer. The results belonging to the first site showed a total of good correlations with values ranging from 0.4 to 0.9. In Boulogne-sur-Mer, the results show so-called weak and poor correlations. The values for R^2 are less than 0.5 for a number of combinations giving a weak and reasonable correlation as linked to the fact that the correlation slope results show a close value is observed in the same cases of Ag-As-Cd-Pb-Pb-Rb and As-Pb.

The correlation results obtained using the spring data were summarized in Table 7. In R^2 , the correlation values are observed but not all corresponding to the same combinations. Several high coefficients are found for Ni-V, Co-As, Bi-Cd and Rb correlations. The values in bold for both sites columns in addition to the combinations are identical slopes for As-Bi. It is observed a higher slope in Saint-mer. This general observation points a possibility of a similar source of emissions. It is not a possibility of a higher influence to a specific source as on-site transfered. It indicates to the source.

Table 7: Summary of highly correlated TE elements coefficients and slope values for Dunkerque and Saint-mer spring campaign

TE ratios	Dunkerque spring		Saint-mer	
	R^2	Slope	R^2	Slope
V-Ni	0.98	0.0000	0.97	0.0000
Co-Ni	0.95	0.0000	0.86	0.0000
Co-V	0.93	0.0000	0.82	0.0000
As-Pb	0.71	0.0000	0.0000	0.0000
As-Bi	0.65	0.0000	0.61	0.0000
Cr-Cu	0.65	0.0000	0.0000	0.0000
Pb-Rb	0.63	0.0000	0.0000	0.0000
As-Zn	0.61	0.0000	0.0000	0.0000
Ag-Bi	0.61	0.0000	0.0000	0.0000
Cd-Rb	0.60	0.0000	0.65	0.0000
Ag-Rb	0.0000	0.0000	0.70	0.0000
Ag-Tl	0.0000	0.0000	0.62	0.0000
Cu-Sn	0.0000	0.0000	0.63	0.0000
Cr-Zn	0.0000	0.0000	0.64	0.0000
Rb-Tl	0.0000	0.0000	0.68	0.0000

In addition to the good correlations, Dunkerque's results include a weak and reasonable correlation. The correlations belong to Ag-Rb, Ag-Tl and Cu-Sn on one hand and Cr-Zn and Rb-Tl on the other. The results are all observed around the correlation in

Saini et al. So far, correlations are close or even identical slope values between the two sites like Ag/Rb and Cr/Zn respectively. This last observation occurring in our inland site along with the remaining correlation cases identified at the beginning require a round analysis in order to obtain some explanations about the possible origins of these elements should be noted that the origin of correlated T is identified as enriched elements or as elements inhibiting high industrial emissions.

The upcoming sub section will develop the analysis of the results illustrated in the tables above. Special attention will be given to the profiles of certain anthropogenic emissions of both urban and industrial nature.

V and oil combustion T

In the literature, Ni and V are extensively discussed with emphasis on “oil combustion” as a major source of emissions. These emissions can be identified in petrochemical industrial emissions. In V/Ni ratios ranging between the two global scenarios of the Scientific and Technical Commission and the oil combustion can also be used in residential heating emissions contain V/Ni ratio around the petrochemical in oil and Co can also be considered in these elements in correlations. The oil combustion in petrochemical industries is a role in addition to oil combustion sites emissions has been considered to a scientific action. In Ni and V/Vig ratio range between the two V/Ni is found in the same order of magnitude in emissions source of sites. Nigam and for a reactor cell under site emissions influence. Mathematical

The overall results in the univariate demonstrated good Ni/V and Co/Ni coefficients during winter and spring. In addition, a Co/V correlation. These good correlations are also observed in Saini et al. These slopes are very similar to those in the univariate leading us to consider a possible regional background source of emissions. This suggestion can be backed up by the fact that all samples in the urban and scientific selection are considered in establishing these correlations. In all sites, the calculated slopes corresponding to concentration ratios slope values are very close to the petrochemical ratios identified in the literature. For the univariate V/Ni winter slope is found closer to the residential combustion signature source. All these observations can be explained by the presence of a petrochemical industrial influence at the sites in addition to significant residential heating emissions influence. The average ratios lie in the case of univariate during winter.

Sainr string samples only. This observation discusses the possibility of isolating a first road emissions signature in our study. In all road campaigns, car can also enrich PM in some of these elements as well as a crucial characteristic like Al, Mg, Ca and Ti.

V in T

Both in the case of T, As, Ag, Bi, Cd, Cu, Pb and Rb, the correlation coefficients are also observed in the following periods. Sainr correlation coefficients values also showed in the following results in the form of good correlations for the same previous discussed list of elements for Pb. In addition, Boulogne-sur-Mer showed some characteristic features of the same elements for As, Ag, Cd, Cu, Pb and Rb. The combinations of significant differences in the order of magnitude of the correlation coefficients in Boulogne-sur-Mer are not significant. This observation joins the ones found in the previous sections for the combinations of elements that require further investigations in order to elucidate all the possible details concerning their origins.

The significant correlations found in the case of the unrefined can be linked to the following emissions and specifically to iron or sintring activities. In addition, the process is based on iron and dusts, sources of PM emissions characterized by high concentrations of Pb, Cd, As, Ag and Rb. This was confirmed by a direct chemical analysis of a reference sample that showed that the industrial processes observations are also in accordance with the chemical characteristics identified in source samples. This is also the case for lead and in PM collected directly under the influence of industrial installations. The main conclusion is that

7. Concentration evolution by wind sector

After the identification of the correlations and slopes, comparison to literature procedures is required to observe the elements and wind sectors contributing in the loads of the T. This step is achieved through the analysis of calculated global average concentration roses that were obtained for each site in both campaigns. Following the same calculations detailed in Caenor section, the unrefined roses were found for some of these elements in the samples and should be analyzed carefully due to their exceptionally sharp features. These are Bi and Ti in the unrefined during winter, Ag and Ti in Boulogne-sur-Mer, Ag and Tl in the unrefined during spring, Ag and Nb in Sainr during

The correlation factor relating the seasonal loading to the seasonal scale of the roses is the average of the seasonal trends and the local concentrations under the wind directions for the directions identified in the roses.

Global roses show that in PM a portion of the roses is related to a mixture of wind sectors and sources in our study. To be able to explain the loading of the seasonal trends in the roses will consider the seasonal trends linked to the wind sector origins: urban, rural, marine or industrial. The roses can originate from a number of sources depending on the wind direction and the function. The roses can also represent a mixture of sources. The roses for the different approaches will not be conclusive since the previously identified seasonal correlation combinations will also be taken into consideration.

V in the campaign concentration roses

7.1.1. Dunkerque winter concentration roses

Figure illustrates the results of the calculations for T₀ during the campaign in Dunkerque. This is characterized by the mixture of anthropogenic activities as well as the presence of natural sources: marine and rural. The roses in PM show industrial sector in Dunkerque. The roses consist of a mixture of a number of industrial sources including a number of sources of emissions: iron or steel, iron casting, glass, blast furnaces, steel mills, oil refineries, metallurgy, etc.) In addition, the roses for the winter campaign are related to the electric steel plant located in the Dunkerque area and the urban emission sources are grouped under the urban sector stretching from the city passing through the S and ending at the direction. This sector includes the residential and rare traffic emissions. In addition to the residential emissions sources, in all cases, the roses show anthropogenic activities and natural sources represented by the marine sector, NNE and/or soil dust suspension through fan activities.

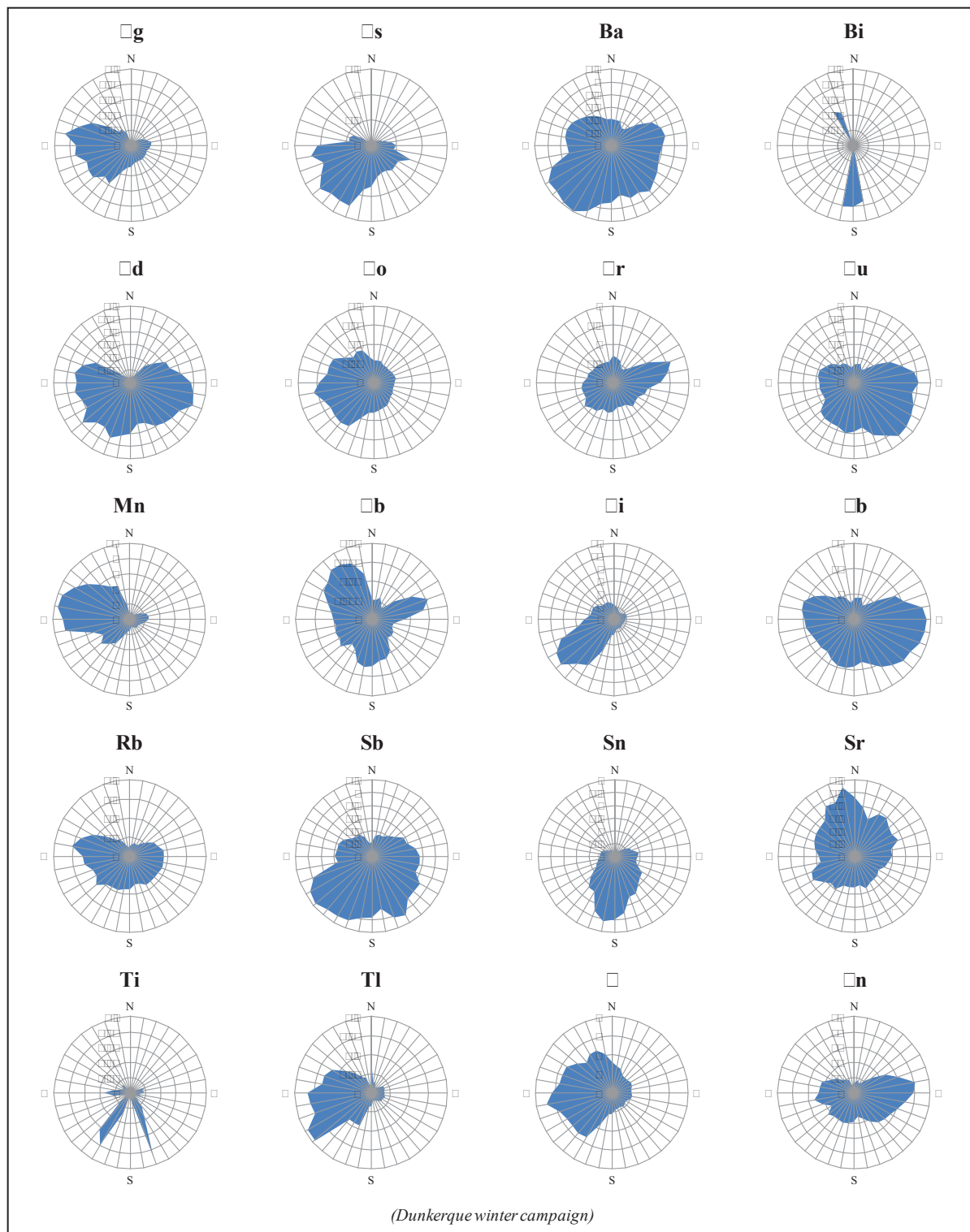


Figure 6: TE concentration roses for Dunkerque during the winter campaign

Unsurprisingly TE concentration roses show that a few elements can be carried by winds blowing from a few directions and thus are found generated by a few sources of emissions. However, it is still reasonable to divide them into a few groups depending on the wind sector that induces the highest concentrations (Table 1).

The first group including Ag, As, Ba, Bi, Cd, Co, Cr, Cu, Nb, Ni, Pb, Rb, Sb, Sn, Tl and V exhibits its highest concentrations under the largest of the sectors. This sector encloses urban emissions and continental emissions neighboring regions and countries. The sector also shared a large list of elements emissions in the integrated sources situated in urban area Ag, As, Cd, Co, Cu, Mn, Pb, Rb, Tl, V and Zn. Also cannot exclude a possible influence in the levels of Mn and Pb coming from a nearby iron refinery located in the sector. It is

high concentrations are observed under the N wind sector for the third group. It encloses Ba, Cd, Cr, Cu, Nb, Pb and Zn. The possible influences of an electric steel plant located in the industrial area to the east of the sampling point is considered as a possibility that can explain the average concentration rose.

Table 8: Main anthropogenic influences corresponding wind sector and TE elements in Dunkerque during winter

Sources of emissions	ind sector	corresponding elements
Urban	SW	Bi, Sn, Nb, Sb, Ba, Cd, Co, Cu, Pb, Sb
Urban and integrated sources	ENE	Ag, As, Cd, Cu, Mn, Pb, Rb, Tl, V, Co, Sr, Zn
Urban and electric steel plant	NNE	Cd, Cr, Pb, Zn, Nb, Cu, Ba
Fossil fuel combustion	SSW, SSE	V, Ni

7.1.2. Boulogne-sur-Mer winter concentration roses

The variation of the atmospheric concentrations depending on wind directions in Boulogne-sur-Mer is illustrated in figure

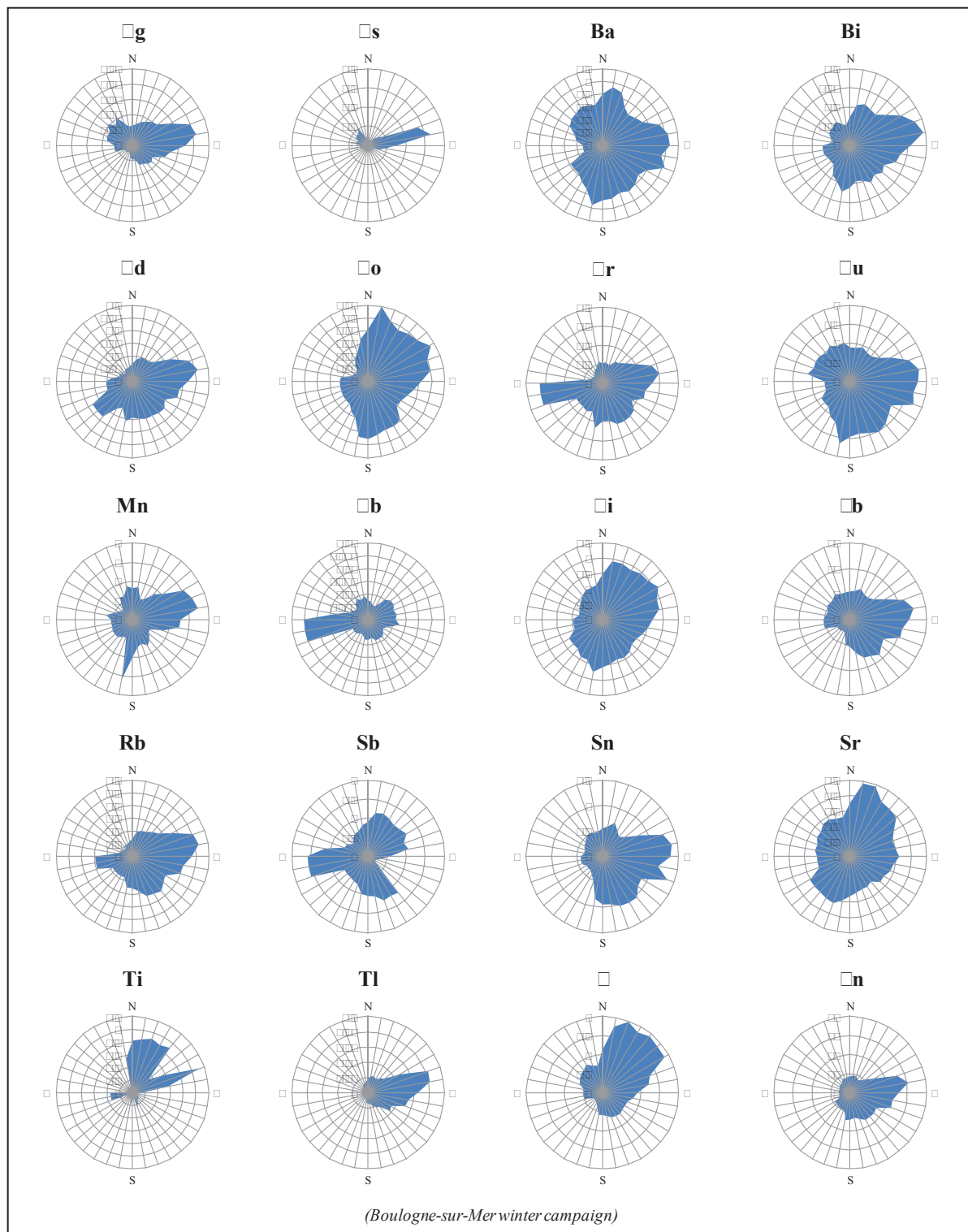


Figure 7: TE concentration roses for Boulogne-sur-Mer during the winter campaign

Boulogne-sur-Mer does not have any local industrial sources of emissions. The influence of nearby industries cannot be excluded. This site can be affected by sea salt emissions from the sea coming from the large SS, N, S, and urban emissions. The emissions contribute to the N as well as the S to S sectors, as urban emissions.

wind influence can generate both N and S directions in all industrial influences can arrive at a regional scale. In the Boulogne-sur-Mer's atmosphere from two principal directions, the first is the N direction, which corresponds to a marine-urban-industrial site of Dunkirk and the second is the S direction, which corresponds to Sainthomme. This is an urban-industrial influence. Therefore, the analysis of the roses should consider these directions in the future.

The concentration roses illustrated in Figure 10 show a large sector stretching from the S to the N and passing by the E. This is responsible for all the analysed TE and TE concentrations. Ag, As, Ba, Bi, Cd, Co, Cr, Cu, Mn, Ni, Pb, Rb, Sb, Sn, V and Zn. These sectors enclose all the emissions originating from the urban sector of Boulogne-sur-Mer. But they also include particles which come from other distant sources. As this is the case, we should recall that the winds are generally blowing slowly and found associated with dry weather conditions. These latter induce pollutant accumulation and could explain the TE concentrations are recorded for these wind directions. The concentration roses for Co, Ni and V allow us to find a possible contribution from a fossil fuel combustion of emissions. In parallel, the roses of Ag, Bi, Cd, Mn, Pb, Rb, Tl and Zn are characterized by a N sector orientation, which is a regional contribution under this wind sector. This is the case for an industrial site located in Dunkirk. Boulogne-sur-Mer's coastal relatively distant site, under certain wind directions, the most significant concentrations of TE are generally found low. This site is under the marine sector influence. A concentration roses analysis subsequently can be found illustrated further in Table 10 and includes the possible origins and observations leading to the classification of TE elements by groups of industrial or specific sources.

Table 9: Main anthropogenic influences—corresponding wind sector and TE elements in Boulogne-sur-Mer during winter

Sources of emissions	Wind sector	Corresponding elements
Urban	SSE	Bi, Ba, Sn, Cu
Anthropogenic continental	NNE	Ag, As, Cd, Cr, Cu, Pb, Rb, Tl, V, Ni, Co, Sr, Mn, Zn
Fossil oil combustion	N	V, Ni, Co

In addition, the participation from the harbours in Boulogne-sur-Mer is clearly present and has contributed partially in a possible concentration of the following elements: Cd, Cr, Nb, Rb and Sb. This can be related to activities like ship cargo unloading and/or maintenance.

V Spring campaign concentration roses

7.2.1. Dunkerque spring concentration roses

The concentration roses calculated using TSP concentrations for Dunkerque's spring campaign are illustrated in figure 7.2.1. During this spring campaign, Dunkerque's wind sectors displayed an important role in the identification of specific source categories for TSP. The urban and industrial sources and this industrial coastal sites possess a similar approach of roses analysis as they are adopted before. Therefore, the recorded data are divided into groups depending on their origins.

The urban and sailing sites can be influenced by urban sources of PM emissions and are previously detailed in this chapter section V.

Table 10: Main anthropogenic influences corresponding wind sector and TE elements in Dunkerque during spring

Sources of emissions	ind sector	corresponding elements
industrial sources	N	Ag, As, Cd, Cr, Cu, Mn, Pb, Rb, Tl, V, Ni, Co, Nb, Ti, Bi
oil combustion	All	Co, Ni, V, Nb
urban electric steel plant	N	Cr, Zn, Cu

This analysis of the source of the industrial emissions shows that the main sources contributing to the high concentrations of the industrial elements are the S₀ sector (which includes the urban influence) and oil combustion (grouped with the corresponding elements Ni, V and Co) in addition to a partial load of Nb. The electric steel plant in the industrial zone contributes along with the urban activities in the loads of Cr, Cu, Pb, Sn and Zn. In all, the Sr rose represents an isolated case in which the influence is generating almost equally to all the above mentioned sectors.

7.2.2. Saint-mer spring concentration roses

Saint-mer spring concentration roses displayed in figure 15 shows a correlation of the wind sectors contribution in the loads of TE concentrations. This similarity is characterized by its inland geographic position. The same is true for the coastal environment encountered in the cases of Dunkerque and Boulogne-sur-Mer. The possibility of an natural contributions is particularly for the soil dusts which can be resuspended by the urban activities in the city.

In the other hand, the influence of the industrial activities should not be neglected. This similarity is the result of a narrow glass making sector (S₀ side of the sailing site) which represents a significant industrial influence in the PM loads. In the area of the second industrial influence concerns the area of industries located in the industrial zone can participate in the winds blowing from the NNE sector.

The concentration roses in figure 16 show that the main wind sectors are responsible of the high concentrations. The S₀ sector corresponds to glass making sector (N to S₀ (varies from 110°) related to Dunkerque's distant industrial emissions, and finally the SW to the S₀ sector. The urban influence can be added to this list as it is encountered to all around the sailing site.

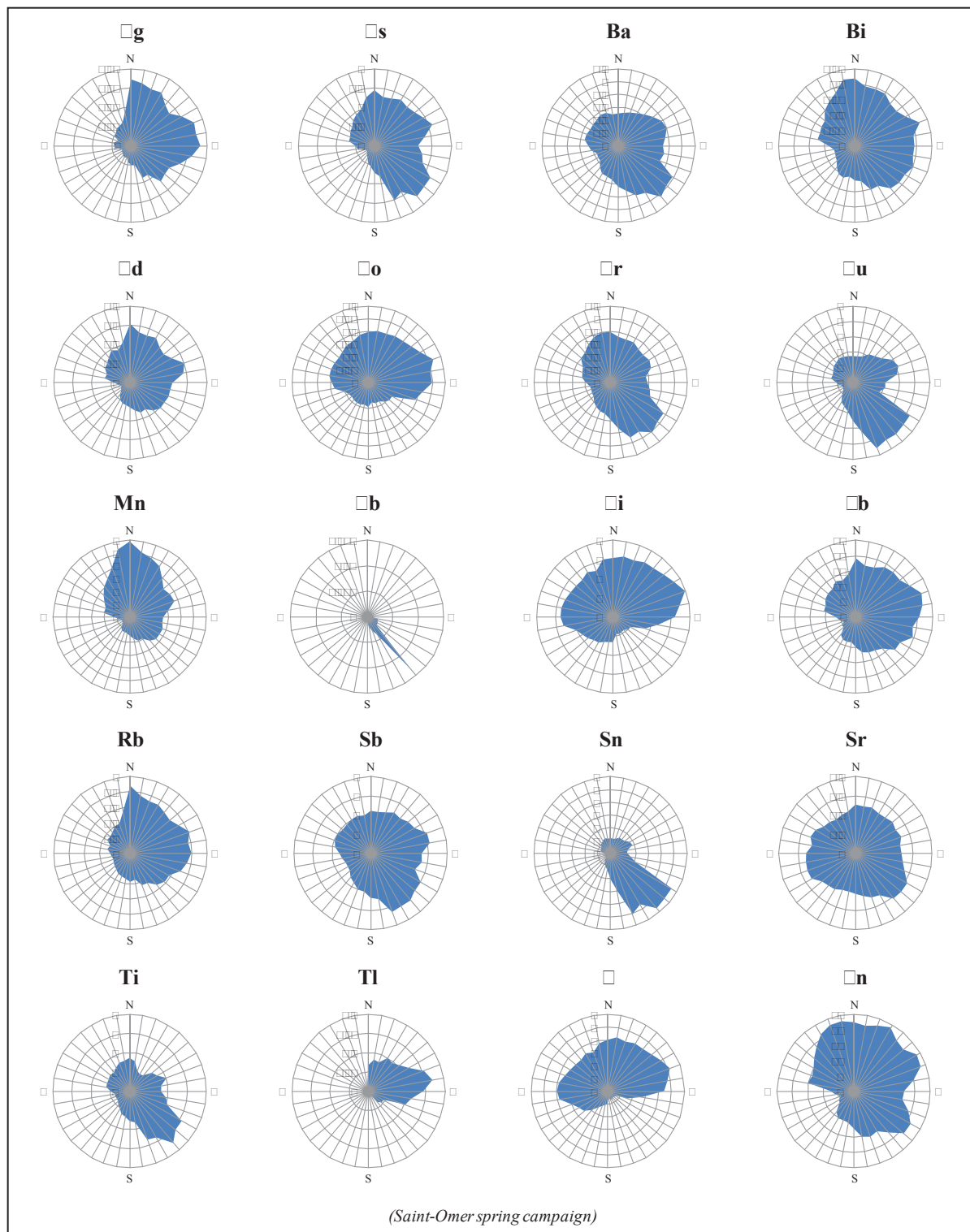


Figure 9: TE concentration roses for Saint-Omer during the spring campaign

In order and Table 1 shows the factor scores contributed in the concentration values of a large list of elements for the T group. To identify the sampling sites of Saint-Omer to the glass factory enabled us to determine a large list of elements enriched for the factor As-Ba-Cr-Cu-Pb-Sb-Sn-Sr-Ti and Zn. The urban

contribution was also refined by using the scores to identify a specific urban influence larger than the ones observed in the training data sets.

Table 11: Main anthropogenic influences corresponding wind sector and TE elements in Saint-Omer during spring

Sources of emissions	Wind sector	Corresponding elements
Urban	All	Cd, Cr, Zn, Cu, Ni, Pb, Sb, Sr, V, Zn
Urban and industries	NW	Ag, As, Cd, Cr, Mn, Pb, Rb, Tl, V, Ni, Co, Sr
Urban and glass-making	SE	As, Bi, Ba, Sn, Cu, Cr, Nb, Sb, Sr, Ti
Coal oil combustion	SE and	Ni, V, Co

In all the results of this analysis showed that the different sources contribute in the emissions of similar elements combinations. The elemental ratio stoichiometric analysis allowed us to determine the different mix of sources that are able to identify the specific sector contributing the most in certain metals concentrations. For example, Cu and Sb are the most generating from the traffic activities in the urban sector. Coal oil combustion is another good example of a concern Ni, V and Co that could be identified by the emissions to the marine translocation sector that is important in the Straits of Dover and the North Sea.

Our first correlation concentration roses allowed us to consider a large possibility of each sites emissions influences on each other. Dunkerque's steel industry (Ag, As, Cd, Cu, Mn, Pb, Rb and Zn) and coal oil combustion (Ni, V and Co) could be contributing in the load of certain elements in Saint-Omer. The other industrial sector is in some cases found to be linked to other sectors marine or urban for example.

In order to analyse specific industrial influences within a given site and also to know the site to another will be in a list of elements that is found far and under the industrial influences in the upcoming. Furthermore in addition to this first selection will be using the concentrations found in certain selected samples only. These samples will be chosen based on the average wind direction. That means only a few industrial sources specific influences are under study.

V Correlations and slopes under industrial influences

In order to distinguish the effects of industrial influences on the observed a scientific selection of PM₁₀ samples collected under finds blowing from industrial emission sources directions was achieved for each site. The industrial effects will be studied carefully in an attempt to determine a scientific ratio between the elements that could be considered as a fraction of successive emissions.

The choice to limit our discussion in this section to a list of elements showing a significant increase in concentration under combined industrial influences, i.e. without an distinction between the sites Zn, Cr, Mn, Ni, Cu, As, Rb, Ag, Cd, Sn, Sb, Tl and Pb for a given site all the elements are not necessarily industrial factors, it is precisely the reason for this that will be able to propose a scientific elemental ratio for a given emission source. In the following complicated cases where several sources are present, a combination of ratios could be suggested to determine the source or sources.

The selection of PM₁₀ samples under industrial influences was achieved using the following method:

a) For unrefractory samples selection included the sectors:

- The samples under – – – – – ind sector under the integrated smelters influence. Between the samples the selected ones contributing and concentrations above 100 ng/m³
- The – – – – – ind sector under Ascorbal electric steel plant influence. For each the selected ones showing Zn concentrations above 100 ng/m³

b) For Saintré samples the sectors:

- The samples under – – – – – ind sector unrefractory smelters influence and contributing and concentrations above 100 ng/m³
- The samples under – – – – – ind sector (Saintré glass making factor) and showing Sn concentrations higher than 100 ng/m³

The samples in unrefractory and Saintré are selected using wind directions recorded during the sampling campaign. For additional confirmation on the industrial smelters influence at Saintré was achieved by drawing air mass back trajectories using the Air Resources Laboratory (ARL) of SPOT trajectory in turn based model (Traj) of Rolando in the case of Boulogne-sur-Mer since the study of the samples collected under the N of the sector revealed a possible industrial emissions influence at the

significant air mass back trajectories did not confirm this hypothesis as finally discarded.

7.3.1. The case of Dunkerque

Table 11 and Table 12 gather statistical data (average concentration, minimum and maximum value about selected PM₁₀ samples collected under NN, integrated sectors and NN electric steel plant influences in urban area) under different sectors influence on average concentrations are clearly given than the total average of the whole campaign in urban area (Table 13) specially for Mn, Ni, As, Rb, Ag, Cd, Tl, Pb and Zn. Furthermore, the observed different concentration fluctuations in the selected samples in different cases are illustrated in Table 14. Sectors sintring slag and fugitive emissions in order to explain the differences in the correlation and the main integrated steelworks complex is a “multi-sources” site, with a large stock of iron ore coming from iron ore sintring blast furnaces and slag from the T₀ installations. In the articles the physico-chemical characteristics are different from source to another. In addition, it has been demonstrated in the previous studies that the T₀ installations have different impacts in the air quality contributions in the local context. In the local level in the city of urban area, considering the knowledge on the chemical composition of the PM₁₀ in the air quality installations, it is possible to suggest the influence of sintring slag and fugitive emissions on the steel plant in the first cases. The noticed relationship between concentrations in the air and the Rb, Ag, Tl and Pb. These observations are in accordance with the physico-chemical characteristics of PM₁₀ sources related to industrial and analyzed in the laboratory. Furthermore, the characteristics are also mentioned in other studies. The main reason for this is that the T₀ installations and the steel plant are also different. As for the fugitive emissions, the noticed average concentrations levels are related to the collected by the local levels of Zn, Mn, Cr, Ni, Cu, As and Pb. In comparing the observations to the PM sources characteristics as well as to the literature (Mac²⁺ and the other) and the statistical analysis, it is found that this is a significant influence.

Under the influence of the electric steel plant, the NN sector concentrations of Zn, Pb, Cr and Cu are found to be particularly high than the total average concentration of the whole campaign in urban area. All sectors combined in a less or more way can also be given for Mn, As and Sn (Table 15). These results

samples to be corroborated considering the nature of the annual emissions declared by the industrial PRTR and are usually corroborated by the literature. Sampling is also

Table 12: Average elemental concentrations, minimum and maximum values (ngm³) in Dunkerque's samples under E-E industrial sector influence in 2012

Element	Average	Minimum	Maximum	Sinter stack	Fugitive emissions
Ca	100000	100000	100000	100000	100000
Fe	100000	100000	100000	100000	100000
Zn	10000	10000	100000	10000	100000
Cr	1000	10000	10000	10000	1000
Mn	10000	10000	100000	100000	10000
Ni	100	10000	100000	100000	100000
Cu	10000	10000	10000	10000	10000
As	10000	10000	10000	10000	10000
Rb	10000	10000	10000	10000	10000
Ag	10000	10000	10000	10000	10000
Cd	10000	10000	10000	10000	10000
Sn	10000	1000	10000	10000	10000
Sb	10000	10000	10000	10000	10000
Tl	10000	10000	10000	10000	1000
Pb	10000	10000	100000	10000	100000

These samples are selected between the first 20 samples under the sector, and constitute a signature of the two different industrial sources

Table 13: Average elemental concentrations, minimum and maximum values (ngm³) in Dunkerque's samples under E-E industrial sector influence in 2012

Element	Average	Minimum	Maximum	Total average Dk2	Total average Dk1
Ca	100000	100000	100000	1000	10000
Fe	100000	10000	100000	10000	1000
Zn	100000	100000	100000	100000	10000
Cr	10000	10000	100000	10000	10000
Mn	10000	10000	100000	10000	10000
Ni	10000	10000	100000	10000	10000
Cu	1000	10000	10000	10000	10000
As	10000	10000	10000	10000	10000
Rb	10000	10000	10000	10000	10000
Ag	10000	10000	10000	10000	10000
Cd	1000	10000	10000	10000	1000
Sn	10000	10000	10000	10000	10000
Sb	10000	10000	10000	10000	10000
Tl	10000	10000	10000	10000	10000
Pb	10000	10000	100000	10000	10000

The observations in this case of unconstrained natural concentrations are indeed based on identified industrial activities in order to distinguish emissions sources and suggest specific elemental ratios (Table 14) in order to recognize source specific ratios compared to natural ratios values calculated under the influence of industrial sector. The ratios obtained through the independent calculations using all samples

- *ISW and Electric steel plant specific ratios:* The ratio of Zn and Zn/Mn ratios allow a clear separation between integrated steelworks “ISW” (Zn and Electric steel plant “ESP” Zn and emissions facing respectively. The same conclusion can be also used for Cr/Cd and for Sn and for Pb/Cd and for Sn and for Sn ratios respectively.
- *Steelmaking source specific ratios:* The ratios suggest that to separate between the two sources of emissions is significant for an and allow to identify in the bottom sources fugitive versus coin source as for the action of PM elemental composition.

The comparison between the different influences allows us to select the following ratios for sintering stack facing Rb/Cr and Cu/Cr and Pb/Cd and As/Ag and in parallel ratios of Zn/Mn and As/Ag and Cu/Cd can be suggested to recognize the influence of different emissions from the following industries

Table 14: Selection of elemental ratios under industrial sources influence in Dunkerque compared to total average ratios found with all sectors included.

Ratios	IS	IS sintering stack	IS fugitive	Electric steel plant	Total average Dunkerque
Zn	10000	10000	10000	10000	10000
Zn/Mn	1000	1000	1000	10000	1000
Rb/Cr	10000	10000	10000	10000	10000
Pb/Cr	10000	10000	1000	1000	1000
Cr/Cd	10000	10000	10000	10000	10000
Cu/Cr	10000	10000	10000	10000	10000
Cu/Cd	10000	10000	100000	100000	10000
Pb/Cd	10000	10000	10000	10000	100000
Sn/Cr	10000	10000	10000	10000	10000
Sn/Sb	10000	10000	10000	10000	10000
As/Ag	10000	10000	100000	100000	100000

7.3.2. The case of Saint-Omer's site

Table 14 and Table 15 regroup statistical data regarding concentration minimum and maximum values on selected PM₁₀ samples site over collected under SSES glass-making influence and NNE direction Dunkerque's industrial activities influence industrial sectors in Saint-Omer over under glass-making influence calculated average concentrations for Zn-Cr-Cu-As-Ag-Cd-Sn-Sb and Pb are higher than compared to total average concentrations calculated for whole Colca region in Saint-Omer

Table 15: Average elemental concentrations minimum and maximum values ng m^{-3} in Saint-Omer under ESE-SSE industrial sector influence in 5

Elements	Average	Minimum	Maximum	Total average Saint-Omer
Fe	10000	10000	10000	10000
P	100000	10000	100000	1000
Ni	1000	10000	1000	10000
Cr	1000	1000	1000	1000
Mn	1000	1000	1000	1000
Pb	1000	1000	1000	1000
Cu	10000	1000	10000	1000
As	1000	1000	100	1000
Rb	1000	1000	100	1000
Ag	1000	1000	100	1000
Cd	100	1000	1000	1000
Sn	10000	100	10000	100
Sb	1000	1000	1000	1000
Tl	1000	1000	1000	100
Pb	10000	10000	100	10000

Transactions of so-called elements are declared by the industrial PRTR in addition different sources on transactions of glass-making industry mentioned and emission possibilities for this activity in fact a first round of emissions can be linked to the iron used to make or can be loaded by a few elements that are included in the composition of glass but also other added elements used to adjust the composition and/or used for design purposes like refining additives and colorants Raw materials that other and so products have to undergo additional control near ranges before finalization So-called products require a second round of balancing that eventually leads to additional emissions

Table 16: Average elemental concentrations, minimum and maximum values ng m^{-3} in Saint-mer under the E industrial sector influence in 8

Elements	Average	Minimum	Maximum
Fe	100000	100000	100000
P	100000	100000	100000
N	10000	10000	10000
R	10000	10000	10000
Mn	10000	10000	10000
i	10000	10000	10000
u	10000	10000	10000
s	10000	10000	10000
Rb	10000	10000	10000
g	10000	10000	10000
d	10000	10000	10000
Sn	10000	10000	10000
Sb	10000	10000	10000
Tl	10000	10000	10000
b	10000	10000	10000

In order and as reported in concentration roses of Saint-mer in sub-cell to influence of this industrial figure of specific factor for glass-making activities are Sn-Cr-As and Cu-and this influence principal specific ratios Table b in elements are Sn-Cr, Sn-Sb, Cu-Cd and As-Ag. The obtained values for these ratios are clearly different from those obtained by independent calculations using all samples.

Table 17: Selection of elemental ratios under industrial influences in Saint-Omer compared to total average ratios found with all sectors included.

Ratios	Glassmaking	Non-Ferrous sector	Total average Saint-Omer
Zn/Cr	0.0004	0.0004	0.0004
Zn/Mn	0.0004	0.0004	0.0004
Rb/Cr	0.0004	0.0004	0.0004
Pb/Cr	0.0004	0.0004	0.0004
Cr/Cd	0.0004	0.0004	0.0004
Cu/Cr	0.0004	0.0004	0.0004
Cu/Cd	0.0004	0.0004	0.0004
Pb/Cd	0.0004	0.0004	0.0004
Sn/Cr	0.0004	0.0004	0.0004
Sn/Sb	0.0004	0.0004	0.0004
As/Ag	0.0004	0.0004	0.0004

Finally, it is important to search for a possible impact of Dunkerque's emission on the elemental atmospheric concentrations measured in Saint-Omer and under the NN influence in the direction of the air currents. This is observed for the elements Zn/Ag/As/Cd/Mn/Pb/Rb and Tl (Figure and Table).

To begin with, in the industrial and local wind directions at Saint-Omer can be found a large regional level of the air mass backward trajectories are calculated for some selected samples representing relative high concentration levels of elements usually emitted by Dunkerque's industrial activities (Figure). This latter process in an cases the air mass passes over Dunkerque's agglomeration before settling in Saint-Omer or in other cases the mass may have occurred in the air mass circulation in the region and returns inland towards our sampling site.

In a second phase and in order to grasp additional information on the origin of the elements considered elemental ratios values were calculated under the NN influence at Saint-Omer in the specific ratios obtained in the vicinity of Dunkerque's industrial sources (Table and Table). The comparison showed that the calculated elemental ratios at Saint-Omer under the NN influence are close to the values of Pb/Cd, Cu/Cr, and As/Ag. These ratios are linked to a range of values obtained under smelting sector. These results and to some extent the activities in the urban area can indicate an atmospheric load of PM₁₀ in Saint-Omer's atmosphere, specifically under NN influence. Moreover, the calculated ratios do not reflect any specific smelting activities influence. These latter

cannot be concluded since Zn and Zn/Mn concentrations are identified in rare samples. This observation could not be understood since there are not enough samples to draw a reasonable conclusion.

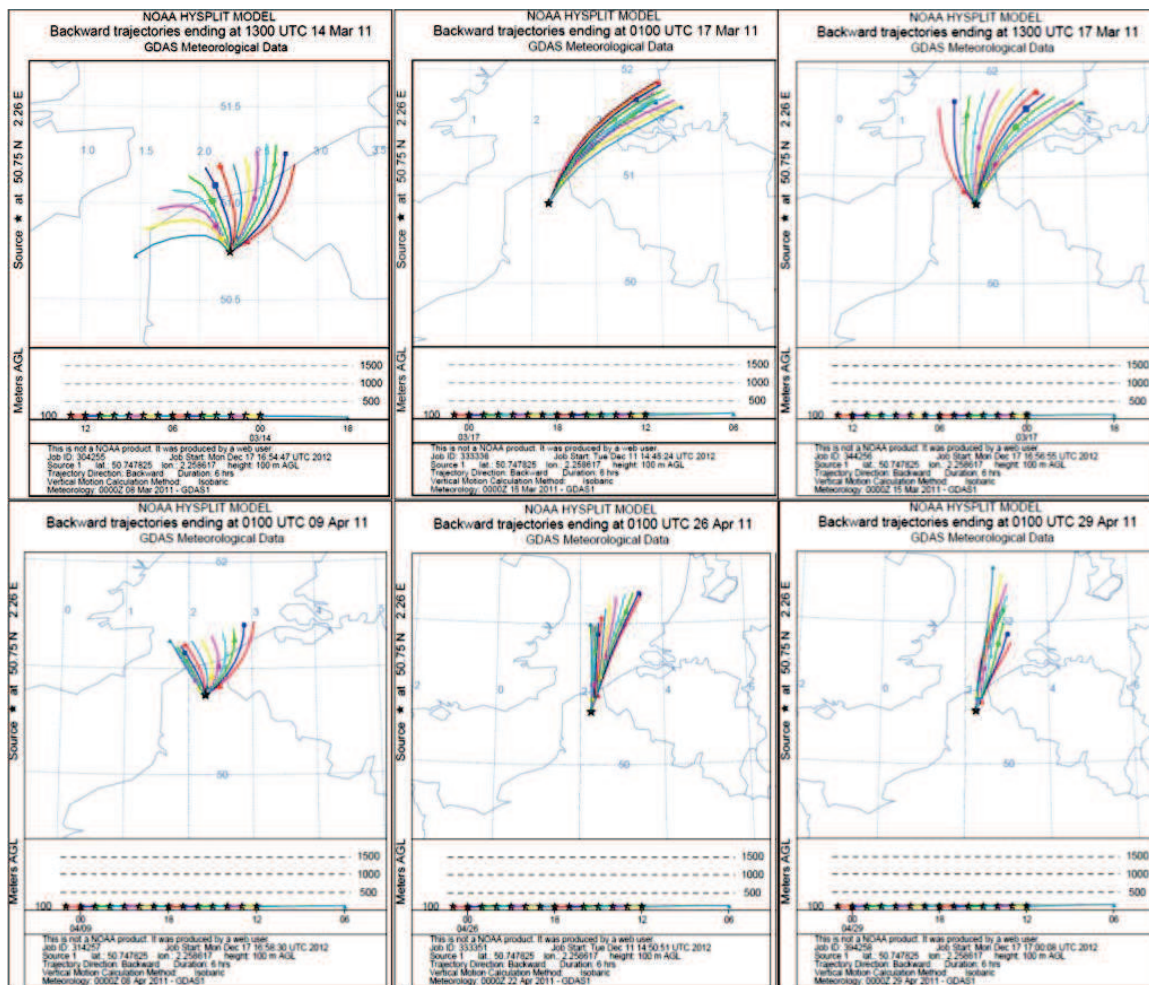


Figure 10: Air mass backward trajectories of selected samples showing the W-E sector influence of Dunkerque in Saint-Omer

9. Works cited

- Adachi Tainosho et al.: Characterisation of aerosol particles emitted in
Iridus *Environment International*, 30 (2004) 697–708
- Arruti A., Fernandez-Ibanez Rabiñán A.: Regional evaluation of particulate
matter composition in an Atlantic coastal area (Cantabria region), northern Spain.
Spatial variations in different urban and rural environments. *Atmospheric research*,
101 (2004) 103–118
- Cassirer R., Niño M.: Presence of trace metal cations in organic drif-
twood: seasonal collection at Caparra, a coastal site in southern
Mediterranean. *Marine Chemistry*, 68 (2000) 1–12
- Dalgaard S.: [d-maps.com cartes gratuites](#). Retrieved from [dalsco.com](#)
- Gallardo M., Booy M., Siems J.: Review of air pollution studies
distributions and meteorological characteristics of airborne particles in
large integrated sites. *Aerosol Science and Technology*, 42 (2005) 103–118
- Gongarrón Manno Varrica: Possible effects of traffic-related emissions
Environ Monit Assess, 154 (2004) 1–12
- Hartmann R.: Role of Hybrid Single-Particle Lagrangian Integrated
Trajectory National Oceanic and Atmospheric Administration. Retrieved from
[http://radar.noaa.gov/SPT.html](#)
- PRTR: [SbR The European Pollutant Release and Transfer Register](#).
Retrieved from PRTR: [http://ec.europa.eu/TSP/Pollutants/Releases.asp](#)
- Johansson V.: Indgren S.: Seasonal variation in the concentration of
airborne concentrations and deposition fluxes of acid and trace species at
various stations in southern Scandinavia. *Atmospheric Environment*, 30 (1996)
103–118
- Harrison R.: Intercontinental transport of PM₁₀: Particles at urban background
and rural sites in ambient atmosphere. *Journal of Environmental Monitoring*, 12 (2010)
1–12
- Förhans T., Bergback B.: Aggregated Air Quality Measurements for
linings and structures: studies of Swedish Steel and Iron. *Environ.*
Sci. Technol., 41 (2007) 1–12
- Lisowski: *Evaluation de la contribution d'émissions sidérurgiques à la teneur en
particules en suspension dans l'atmosphère à une échelle locale.* Université
du Littoral Côte d'Azur P.T.S.
- Lisowski et al.: Douvroux: An Air Courcouronnes Tour Courcouronnes
Chemical identification of fugitive and confined particle emissions
from an integrated iron and steel plant. *Journal of Hazardous Materials*, 250–
251 (2004) 1–12
- Buglino C.: Rigor Balansberg S.: Monn Vonon: Chemical characterisation of PM₁₀ and coarse particles at urban, peri-urban
and rural sites in Switzerland. *Atmospheric Environment*, 39 (2005) 1–12
- Lacua V.: Annin N.: Saarland: a southern German state. An urban monitoring
Source attribution of population respiratory health status of PM₁₀ in
Germany cities using structural equation modelling. *Science of the Total Environment*,
384 (2005) 1–12

- aison Characterization des particules Atm et identification de leurs sources dans une atmosphere urbaine sous influence industrielle. ni rsi d ill P T sis
- Can C Paa ro P Application o osi i a ri ac ori a ion in sourc a or ion n o ar icula ol luan s in ong ong Atmospheric Environment , 33
- Mac r S Carac ri a ion o airborne and bul ar icula ro iron and s anu ac uring acili s Environmental Sciences and Technology, 38
- Ma i Al ssandro A ucar lli Na a S Pra i P Valli V cc i R Carac ri a ion o ar icula a r sourc s in an urban n iron n Science of the total Environment, 401
- Mooibro Sc aa M i rs oog rbrugg R Sourc a or ion n and s a ial ariabili o PM using asur n s a i si s in N rlands Atmospheric Environment, 45
- Mor no T u rol Alas u A Viana M Sal cador P Sanc d la Ca a A ibbons Varia ions in a os ric PM rac al con n in S anis o ns llus ra ing c cical co cl i o inorganic urban a rosol coc ail Atmospheric Environment, 40
- Niga A c o u l sul ur con n and con rol ec nolog on PM ission ro s i s au iliar n gin Proc ding in rna ion al a rosol con r n c
- ra is ar i Ti on n i i n os i T Ruus an n A n an n Ruus an n Source contribu ions o PM ar icl s in urban air o a o n si ua d clos o a s ill or s Atmospheric Environment, 37
- Pa an n T A ou ola or on n C Aur la M Ma la T illa o R Ma n au Source s and c cical co osi ion o a os ric in and coars ar icl s in l sin i ar a Atmospheric Environment, 35
- Pu bau o is B alina M Bau r Sala A S o r S auc A dual si s u d o PM and PM a rosol c is r in larg r r gion o Vienna Austria Atmospheric Environment, 38
- u rol Alas u A d la Rosa Sanc d la Ca a A Plana Rui C R Source a or ion n anal sis o a os ric ar icula s in an indus rialis d urban si in sou s rn S ain Atmospheric Environment, 36
- u rol Alas u A Rodrigu S Plana Man illa Rui C R Moni oring o PM and PM around ri ar ar icula an ro ogenic ission sourc s Atmospheric Environment, 35
- Ra a o c cical c arac ri a ion o PM i d b glass ac ori s in Murano V nic al Chemosphere, 71
- Saliba N A ou ou d ian Rou i M c o local and long rang rans or issions on l n al co osi ion o PM and PM in B i ru Atmospheric Environment, 41
- Sa u M Noac Ros Zinc s cia ion in s ill lan a os ric issions a ul i c nical a roac Journal of Geochemistry, 88
- S or i ni A r da A C sari Cairns Con i ni Barban C An alua ion o PM rac l n al co osi ion in V nic agoon ar a and an anal sis o possibl sourc s Atmospheric Environment, 43
- S i llic i r i R Source c arac ri sa ion o C nral uro an a os ric a rosol using ul i a r sa isical o ds Nuclear Instruments and Methods in Physics Research B, 109/110

CAPTCH V

Identification of sources of risks and
contributions using a NMRC or
modeling

TABL E C O N T E N T S

1.1.	Introduction	223
1.2.	Early development and use of receptor modeling.....	224
1.3.	Comparison between receptor models.....	225
1.4.	Matrix factorization methods	227
	V..... Basics of Matrix factorization	
	V..... Positive Matrix factorization (PM)	
	V..... Non-negative matrix factorization (NMF)	
	V..... Fitted NMF	
1.5.	Application of weighted MF for source apportionment.....	230
	V..... Preparation of input data	
	V..... Matrix of species concentrations	
	V..... Matrix of measurements uncertainties (matrix Σ)	
	V..... Matrix of initialisation	
	V..... Matrix of “equality” constraints	
	V..... Matrix of “inequality” constraints	
1.6.	Weighted MF operating conditions.....	236
1.7.	Verification of calculations reliability.....	238
	V..... NMF calculated versus observed data for Boulogne-sur-Mer	
	V..... NMF calculated versus observed data for Dunkirk	
	V..... NMF calculated versus observed data for Saint-Etienne	
1.8.	MF calculated sources profiles matrix.....	245
	V..... Common calculated profiles	
	V..... Seasonal	
	V..... Crucial	
	V..... Secondary organic Aerosols (SOA)	
	V..... Combustion	
	V..... Traffic non-exhaust	
	V..... Additional calculated profiles in Dunkirk	
	V..... Additional calculated profiles in Saint-Etienne	
1.9.	Sources contributions matrix.....	250
	V..... Average contributions	
	V..... Inter-campaign average source contributions	
	V..... Spring campaign average contributions	
	V..... Diurnal contribution trends	
	V..... Inter-campaign diurnal source contributions	
	V..... Spring campaign diurnal source contributions	
	V..... Average source contributions to chemical species	
	V..... Inter-campaign average source contribution to species total loads	
	V..... Spring campaign average source contributions to species total loads	
1.10.	Conclusion.....	267
1.11.	For ks cited.....	269

$$\boxed{}\boxed{}\text{ST} \quad \boxed{}\boxed{}\boxed{}\boxed{}\boxed{}\text{R}\boxed{}\text{S}$$

Figure 1: Classification based on *a-priori* knowledge requires no methods used to derive in source's affiliation, using recursive models trained from Viana's algorithmic structure produced in the Scourmal algorithm.

Figure 3: A section from a matrix Σ of uncertainties expressed in %

Figure 1: Illustration of a section of the initial data set.

Figure 1: Qualitative constraints arising from location of social constraints in the rolls

Figure 1: Qualitative constraints second arising from values of second constrained lines in so

source ro il s

Figure 1. Qualitative constraints arising from ordering of abundance of species

Figure 1. Comparison between total NM calculated and total observed PM_{2.5} species concentrations.

ing in Boulogne-sur-Mer during in the campaign

Figure 1. Comparison between NM calculations and measured and observed species concentrations.

ing in Boulogne-sur-Mer during in the campaign

Figure S10 Comparison between calculated and observed PM_{2.5} species concentrations

ing in unru during bo in r and s ring ca aigns

Figure 1. Comparison between NM calculations and observed analysis results.

concentrations ng mL^{-1} in $\mu\text{g mL}^{-1}$ during both winter and spring campaigns

Figure S10. Comparison between calculated and observed PM_{2.5} species concentrations.

ing in Sainr during spring campaign

Figure 1 Comparison between NM calculations and analysis and observed analysis results

concentrations in Saint Pierre during spring campaign

Figure 1. Comparison of NM and roils identified in the r-sampling sites.

Figure 1. Industrial NM₁₀ roils identified in unroof during both winter and spring campaigns

[illegible]

Figure 1. Industrial NMROil's identified in Sainr during spring campaign

Figure A.4: Aggregate contributions of sources in ${}^{222}\text{Rn}$ load in Boulogne-sur-Mer during winter 2018.

Figure A.4: Contributions of sources in PM_{10} load in $\mu\text{g}/\text{m}^3$ during winter

Figure A.4: A rag contributions of sources in PM_{10} load in $\text{un}^{\text{r}}\text{u}$ during spring

Figure 4. Average contributions of sources in PM₁₀ load in Saint-Etienne during spring.

Figure 1. Journal finds of source contributions in Boulogne-sur-Mer during winter sampling and

on **c** b r

Figure 1. Journal trends of source's contributions in "un/ru" during "in/r" missing data binned

c and **a**r**c**aus**b**s**a**ling **r**obl**s**

Figure 1. Journal funds o source s contribu tions in un ru during spring Marc and

Missing data are caused by sampling problems and errors in responses

discard d du o un ainabl ig conc n ra ions

Figure 1. Journal trends of source contributions in Saint John during spring campaign 2000.

Missing sample 1 is on April 11 and both on 11 and 12 are outliers discarded due to

unalignable ^{210}Pb and ^{210}Po concentrations respectively

Figure NM source's renag contributions to total load of each analysis in

[illegible]

Figure NM source's relative contributions to total load of each analgesic in

[illegible]

Figure 11: NM source's re-nag contributions to total load of each analysed scis in 2014

[illegible]

Figure NM source's renag contributions to total load of each analysis in

saints are not saints during spring

ST TABS

Table Natural and anthropogenic emissions source profiles and their characterising species

Table Characteristics of data sets used for NM calculations

ST ATNS

Equation	
Equation	
Equation	
Equation	
Equation	

1. Introduction

The authors are in various centres and V. Boulognès, M. and Saincteur are subjected to different natural and anthropogenic influences. These influences have a direct consequence on the chemical composition of PM_{10} as evidenced by a wide range of previous studies. This chapter includes the final section aims at the identification of the sources that are contributing in the PM_{10} chemical composition and the quantification of their respective contributions.

Boulognès, M. and Saincteur are located on the coast and inland of the NPdC region and are subjected to different sources that can be responsible for the PM_{10} emissions. Both sources are identified in all the studies in the inland of Saincteur in addition to the dust generated from soil erosion and other natural sources of PM_{10} . Urban activities are also found to be responsible for the PM_{10} and is responsible for the main part of the atmospheric activities in addition to the natural and anthropogenic sources mentioned earlier. Industrial activities are responsible in Boulognès and Saincteur. Air quality is an integrated system as well as an electric system and industrial located on the eastern border of Boulognès in the vicinity can be identified in some PM_{10} samples of the inland site of Saincteur. Contribution of Arques' glass-making factor in the PM_{10} release is identified as well as the influence of the railway line located in Boulognès.

Following the chemical analysis of the inorganic fraction and total carbon and after the detailed interpretation of the chemical results in order to determine the possible origins of the collected PM_{10} data, a further analysis and a statistical treatment of our chemical data through modelling of the chemical data to find a better factorisation of the data in order to identify and quantify the contributions of each emission source in the total collected PM_{10} .

This section of the study was accomplished by the combined efforts of the "Unité de Chimie Environnementale et Interactions sur le Vivant" (CIV) for chemical aspects and the "Laboratoire d'Informatique, Signal et Image de la Côte d'Opale" (LSIC) for computing aspects, which are two research units within the "Université du Littoral Côte d'Opale". The factorisation model will be used in this chapter as developed by Perrillès and Perrillès (2005) and is based on a rigid non-

negative correlation method NM under constraints of fair and fair and fair

Matrix factorization methods are widely used in the fields of signal processing and analysis but also for the manipulation of environmental data. B... methods... Principal Component Analysis (PCA) results a group of variables in a small number of synthetic variables called principal components. PCA is a... negative factors... is... difficult

Position factorization algorithms such as Position Matrix factorization (PM) are successfully used in an environmental study on... using... commercial version of... PM... PM... loaded by... and... Environmental Protection Agency (EPA) [a go... asd... rod... s... l...](#) is in... collated... required in order to... calculations... is... studies... is... larger... is... used as... data... or... reliable... results... using PM... to... an increase in... in... usually leads to an increase in... of... consumption... addition... version does not allow an control on... initialization and ending criteria. Thus... remaining essential... used in... PM is... inclusion of... uncertainty in... calculations... stability... solution

Many reasons... us... NM as an alternative to PM... in... of NM... depending on... choice of... initialization criterion... is an algorithm... used by... a... for signal analysis and its Matlab codes are easily accessible. Typical NM models do not consider uncertainty or... assurance... Therefore... to... our own version of NM... in... uncertainty in... calculation process

2. Early development and use of receptor modeling

The use of multivariate receptor modeling started in the 60's with I. H. Billford. Billford... M... as... followed by... creation of... chemical... balance... known as chemical mass balance "CMB"... that was realized in the 70's... inc... Ni... Mill... and... and... Modeling improvements kept on being searched and applied during this period until the early 80's, during... a... on... modeling... to... us... algorithms... M... and... Receptor Models... on... in... os

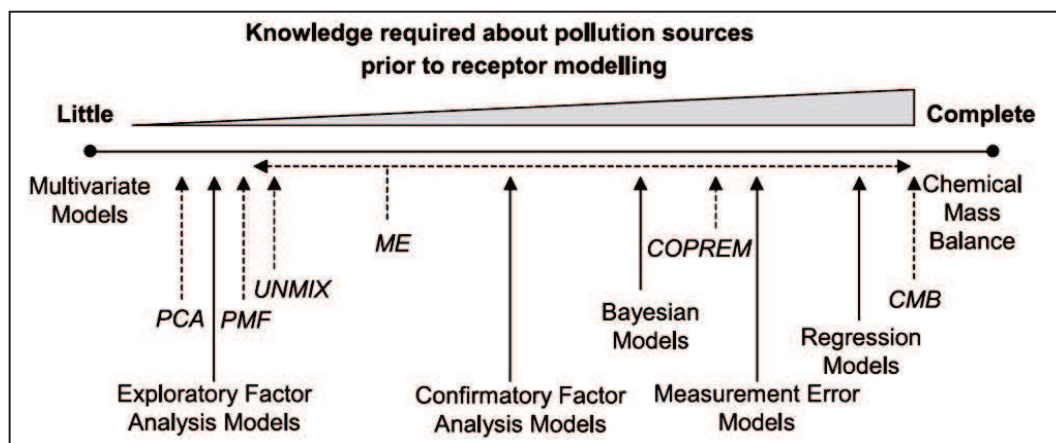


Figure 1: Classification based on *a-priori* knowledge requirements of methods used to determine sources apportionment using receptor models extracted from Iana et al. 2008 which reproduced it from Schauer et al. 2006

An important section of the review deals with a comparison of different source apportionment methods. Many considerations are required when comparing between different European studies, which are not only linked to the geographical differences but also to the different modelisation and application of different receptor models using the same data set. The different results in details, scientific content and difficulties in finding to obtain coinciding results will be using different models with the same data set. This observation was also noticed when using constrained models and hence the recommendations cannot be used towards finding robust source apportionment methods to be evaluated and standardised methods.

In addition, the review can provide a crucial list of important recommendations to fill the gaps in the current used models. Based on the recommendations, the following

- The use of uncertainty
- The use of natural sources contributions
- The identification of biomass combustion sources
- The separation between regional "secondary sulphate" and "secondary nitrate" profiles
- The use of hybrid models

The model development costs are a significant factor in the use of a rigid non-negative least squares factorisation model. The costs are also considered by the scientific community in addition to the *a-priori* data is also considered in the model calculation and can also be used for model validation. Thus, it will be necessary to a certain number of recommendations on the use of modelling in source apportionment.

studies. A detailed explanation on the principles of variational methods can be found in the paper.

4. Matrix factorization methods

Venn Basics of Matrix Factorization

As previously mentioned, variational factorization is used in many research domains and is used in environmental sciences. In fact, it is not only used as a model, but it is also used as a linear combination of a variational and different sources.

For a given observation variational concentration of chemical species in our case, taking a similar to “ $n \times m$ ” where “ n ” is the number of samples and “ m ” is the number of analyzed chemical species. Matrix factorization follows this equation:

$$X = (G \times F) + E \quad \text{Equation 1}$$

In this equation, we consider that:

- X is the variational observation matrix of size “ $n \times m$ ” where “ n ” and “ m ” as the number of samples and analyzed chemical species respectively. It is expressed in the case of atmospheric environmental studies in ng/m³. We consider an element x_{ij} for the variational concentration of chemical species “ j ” of sample “ i ”.
- G is the contribution variational “ $n \times p$ ” where “ n ” as the number of samples and “ p ” as the number of sources. It is applied in environmental studies. A given element “ g_{ik} ” is measured in ng/m³ and represents the mass contributions of source “ k ” in sample “ i ”.
- F is the profiles variational constituted for “ $p \times m$ ” where “ p ” as the number of sources and “ m ” as the number of studied chemical species. A given element “ f_{kj} ” is expressed in ng/g and represents the mass of a chemical species “ j ” in the total mass of chemical species in source “ k ”.
- E is the error variational of “ $n \times m$ ” dimension and is expressed similarly to the variational observation matrix. In this variational, a random selection of a variable “ e_{ij} ” represents the error of reconstruction resulting from the factorization of chemical species “ j ” in sample “ i ”.

In general, the number of sources “ p ” is much lower than the number of samples “ n ” and analyzed species “ m ”. The choice of the number of sources depends essentially on *a-priori* information on the studied system.

Vertical Matrix Factorization (PM)

The first and most common current available factorization method is the Vertical Matrix Factorization (PM) initially created by Paatero & Tapper (1994) and follows the calculation principle described in Equation 1. The objective of the model is to minimize the quadratic error “ e_{ij} ” resulting from data reconstruction. Equation 1 can also be written in this form:

$$x_{ij} = \sum_{k=1}^p g_{ik} f_{kj} + e_{ij} \quad \text{Equation 2}$$

However, in environmental sciences, the data can be tremendously difficult to induce a liaison between the species measured and an uncertain factor. In addition to a random add error Σ of uncertainties in the given value “ σ_{ij} ” is associated to the observation matrix, and represents the error on species “ j ” associated value in sample “ i ”.

Therefore the model searches for the minimal error “ e_{ij} ” and includes measurement uncertainties “ σ_{ij} ” under the constraints of having ($g_{ik} \geq 0$) and ($f_{kj} \geq 0$). Thus, the minimization criterion is given by:

$$\{G, F\} = \arg \min_{G, F} \sum_{i=1}^n \sum_{j=1}^m \left(\frac{e_{ij}}{\sigma_{ij}} \right)^2 \quad \text{Equation 3}$$

Following this last calculation method, the modeling approach confronts many problems, between which we cite the sensibility of the model to the initialization that deeply affects the results. The initial Paatero approach (Paatero & Tapper, 1994) was based on optimizing through calculations the results by alternately searching for matrix G and F. The first version was based on the research of matrix G with a constant matrix F and vice versa.

Another method enhanced the calculation procedure by adding a third step which refine G and F directly by transforming negative values to “0”.

In 1994, an updated version of positive factorization (PMF v.2) was introduced, which was used extensively in many scientific domains. However, inconveniences remained in this last version, especially when matrix dimensions increased an important number of local minima appears (Paatero & Tapper, 1994) and (Paatero, 1994).

4.4. Non-negative matrix factorization (NMF)

Similar to the principles of positive factorization, the NMF use the approached factorization of $X = GF$ under positivity constraints and minimizing the following criteria under the constraints of having ($g_{ik} \geq 0$) and ($f_{kj} \geq 0$):

$$\{G, F\} = \arg \min_{G, F} \sum_{i=1}^n \sum_{j=1}^m (x_{ij} - (GF)_{ij})^2 \quad \text{Equation 4.1}$$

We can notice the similarity between this algorithm and the one used in the case of PMF (Equation 4.1). The difference between the two resides in the positivity constraint applied on each element of matrices G and F (meaning that sources cannot have negative concentrations or negative source contribution) as well as the lack of measurements uncertainties consideration in the NMF. This latter appears to be an important setback in the receptor modeling of chemical data. On the other hand, the Non-negative Matrix Factorization has many advantages when compared to PMF: NMF is lighter than PMF in terms of calculation time and accessible MATLAB scripts, which can easily be modified. Finally, the goal was to develop a model calculation and implement it, therefore we naturally turned to the NMF method.

4.4.4. Weighted NMF

By default, the NMF algorithm does not consider any differed variance data in the calculations. Therefore, constructing a new version of the NMF that considers individual variances on the data input was essential and forms an important extension to the model. This upgrade is realized in the “weighted NMF” based algorithm which enables the consideration of individual measurement uncertainties in the calculations (Kleis, 2014) (Delmaire, et al.,

Q-Q-F and (Delmaire, et al., 2014b)). The uncertainties are inserted in the model in a matrix form, and the calculation equation turns to the following form:

$$\{G, F\} = \arg \min_{G, F} \sum_{i=1}^n \sum_{j=1}^m \left(\frac{x_{ij} - (GF)_{ij}}{\sigma_{ij}} \right)^2 \quad \text{Equation 4}$$

Furthermore, the weighted Q-Q-F algorithm has been modified in order to take into account the *a-priori* knowledge on the source chemical composition by applying constraints. The first type is the “equality” constraint which defines the presence or absence of an element in the source profile, and eventually forces its concentration to a specific value. On the other hand, the second type called “inequality” constraint classifies an element order of abundance between the sources (for example $x_{\text{source1}} \leq x_{\text{source2}}$). Additional information about our weighted Q-Q-F model is given in (Leis, 2014) and (Delmaire, et al., 2014b). The following section includes detailed explanations on the entry data needed to perform a successful weighted Q-Q-F calculation.

4.2. Data preparation for Q-Q-F calculation

4.2.1. Preparation of input data

In order to perform a calculation of matrix G and F following the previously explained method, many data matrices are required:

4.2.1.1. Matrix of species concentrations

The columns of this matrix correspond to each analyzed chemical component concentration values (in ng m^{-3}) in the samples. On the other hand, a line represents the concentration values of all analyzed species for a given sample. Figure 4 illustrates an example of a matrix of species concentrations.

	Ca	Co	Cr	Cu	Zn	...
1.1	49	11.9	4	9.4	99	...
19.1	4	4	91.49	4	99	...
11.4	41.1	4.4	4	44.4	94	...
1.4	4	14.4	1	9.9	4	...
		4	1	1		...
1	41.44	1	1	14.4	1	...
4	1.4	4.1	1	1		...
⋮	⋮	⋮	⋮	⋮	⋮	

Figure 3 section from a matrix Σ of uncertainties in Σ

In some samples, some elements concentrations were not acquired due to technical reasons or because their values were below the detection limit ($\mu\text{g/L}$). If the reading is below $\mu\text{g/L}$, the value in the matrix is replaced by $\mu\text{g/L}$. On the other hand, if the concentration data is missing due to technical reasons, the missing data is then replaced with the mean concentration of the species in that campaign ((Polissar, et al., 1994), (Jim, et al., 2004) and (Liu, et al., 2000)).

Matrix of measurements uncertainties (matrix Σ)

Similar and identical in size as matrix Σ , this matrix includes the values of relative measurements uncertainties ($\%$) related to the analysis and sampling process. We should note that for below $\mu\text{g/L}$ concentration values in matrix Σ , the uncertainty was raised to 100% . On the other hand, for matrix Σ missing values, the uncertainty is raised to 400% ((Polissar, et al., 1994), (Jim, et al., 2004) and (Liu, et al., 2000)).

	Ca	Co	Cr	Cu	Zn	...
1	1	14	1	14	1	...
14	14	14	1	14	1	...
1	1	14	1	100%	1	...
1	1	1	1	100%	1	...
14	1	100%	14	100%	14	...
1	1	14	14	1	14	...
14	14	14	14	1	1	...
⋮	⋮	⋮	⋮	⋮	⋮	

Figure 3 section from a matrix Σ of uncertainties in Σ

3.1.3.1 Initialization of F_{init}

The matrix of initialization (F_{init}) serves as a starting point to launch the calculations. The initialization represents a crucial point when using factorization methods (Frangou, et al., 2011). F_{init} matrix values should be carefully defined in order to avoid reaching any local minimum and to ensure the best quality in the obtained results. This matrix contains chemical profiles of each source of emissions (Figure 4). Hence, a line represents the chemical composition of particles emitted by a given source. The number of sources is defined by the users, as well as their chemical composition which includes the same list of analyzed species as the ones in matrix \mathbf{X} and $\mathbf{\Sigma}$. The values of each species within a profile are defined based on bibliographical analysis of previously conducted studies on the same type of emission source. The values in each profile are finally normalized to 1000.

F_{init}	PM	PM _a	PM _{2.5}	PM ₁₀	PM _{10-2.5}	PM _a	...	PM	PM ₁₀
Profile 1	19.9	14.4	1000	19.9	14.4	14.4	...	1000	1000
Profile 2	1.1	9.1	1000	1.1	4.4	4.4	...	1000	1000
Profile 3	1.1	14.91	1000	1.1	4.4	4.9	...	1000	1000
Profile 4	9.9	4.9	1000	4.1	9.9	9.9	...	1000	1000
Profile 5	9.9	4.1	1000	9.9	9.9	9.9	...	19.4	1000
⋮	⋮	⋮	⋮	⋮	⋮	⋮	⋮	⋮	⋮

Figure 4: Initialization of the F_{init} matrix

The data used to fill the F_{init} matrix were selected based on numerous studies conducted using modeling or PMF methods for source apportionment analysis. Table 1 illustrates all identified sources in this study as well as the major constituents on which sources profiles are based. Between these latter, only two profiles are found to be related to natural emissions (sea salt and crustal), whereas the remaining are all emitted or chemically modified by anthropogenic emissions.

Table 1: PM₁₀F chemical composition and identification of sources and their contribution to PM₁₀F

Source	Emission type	Chemical composition	Reference
Sea salt	Natural	Cl ⁻ , Na ⁺ , SO ₄ ²⁻ , Mg ²⁺ and Ca ²⁺	(Allius, et al., 2004) (Du, et al., 2004) (Ooibroe, et al., 2011) (Oreno, et al., 2011)
aged sea salt	Anthropogenic	SO ₄ ²⁻ , Na ⁺ , SO ₄ ²⁻ , Cl ⁻ , Mg ²⁺ , Tl, Ca and Cr	(Du, et al., 2004) (Mato, et al., 2009)
Crustal	Natural	Al, Ca, Fe, Tl, Mg, SO ₄ ²⁻ , Ti, Si, Cl ⁻ , Na ⁺ and Ca	(Allius, et al., 2004) (Du, et al., 2004) (Ooibroe, et al., 2011) (Oreno, et al., 2011)
Secondary sulfates	Anthropogenic	SO ₄ ²⁻ , SO ₄ ²⁻ , Tl, Si, Ca, Fe, Pb, Mn and Ti	(Du, et al., 2004) (Mato, et al., 2009) (Ooibroe, et al., 2011)
Secondary nitrates	Anthropogenic	SO ₄ ²⁻ , Tl, SO ₄ ²⁻ , Ca, Fe, Mn and Cu	(Du, et al., 2004) (Mato, et al., 2009) (Ooibroe, et al., 2011)
Traffic non-exhaust	Anthropogenic	Cu, Pb, Fe, Mn, Al, Ca, Cr, Si, Pb, Ti, Si, Cd, Mn, Mn and Cr	(Schauer, et al., 2004) (Mato, et al., 2009) (Ooibroe, et al., 2011)
Combustion 1	Anthropogenic	Tl, SO ₄ ²⁻ , Mn, SO ₄ ²⁻ , Fe, Ca, Al, Si, Pb, SO ₄ ²⁻ , Cd, Cu, Cu, Mn, Si, Pb and Mn	(Allius, et al., 2004) (Schauer, et al., 2004) (Du, et al., 2004) (Mato, et al., 2009) (Ooibroe, et al., 2011)
Combustion 2	Anthropogenic	Tl, Si, Al, SO ₄ ²⁻ , SO ₄ ²⁻ , Ca, SO ₄ ²⁻ , Fe, Al, Mg, Ca, Cu and Mn	(Allius, et al., 2004) (Du, et al., 2004)
Industrial fugitive	Anthropogenic	Fe, Ca, Mn, Al, Mg, Mn, Pb, Si, Mg, Si, Ca, Cr, Al, SO ₄ ²⁻ , Si and Si	(Leis, 2011) (Leis, et al., 2011)
Industrial sintering stack	Anthropogenic	Al, Si, Fe, Tl, SO ₄ ²⁻ , Ca, Ca, Pb, Al, SO ₄ ²⁻ , Mg, Mg, Si, Cd, Pb, Mn and Cu	(Leis, 2011) (Leis, et al., 2011)
Electric steel plant	Anthropogenic	Mn, Fe, Mg, Ca, Mn, Pb, Cr, Cu, Al, Si, Cd, Si, Pb and Mn	Based on the composition of some samples selected under the corresponding industrial sector
Glassmaking	Anthropogenic	Al, Ca, Mn, Cu, Si, Fe, Ti, Pb, Cr and Ca	Based on the composition of some samples selected under the corresponding industrial sector

Between the profiles of Table 1 we define the following profiles:

- Traffic non-exhaust: including road resuspended crustal dust mixed with emissions from brake linings and tyre wear abrasion.

- Combustion 1: including fossil fuel combustion (coal, diesel, gasoil, and oil). In this profile we also regroup tailpipe emissions from transportation, which encloses road traffic, heavy industrial and marine transportation.
- Combustion 2 representing the combustion of biomass materials such as wood logs, grass and green wood pellets.
- 4.4.4 Fugitive: is the integrated steel works non point sources emission in 4.4.4 F.
- 4.4.4 Sintering stack is the main point source emission of the integrated steel works plant in 4.4.4 F.

4.4.4.1 at 4.4.4 F “Quality” constraint

The first constraints used by 4.4.4 F are the equality constraints, which consist of two matrices. The first one (Figure 4.4.4.1) signals the presence (cell value = 1) or absence (cell value = 0) of the constraint. In this last case, even if the second matrix contains a certain value, the model will not consider it.

	4.4.4 F	4.4.4 F	4.4.4 F	4.4.4 F	4.4.4 F	4.4.4 F	...
Profile 1	1	1	1	0	0	0	...
Profile 2	1	1	1	1	1	1	...
Profile 3	0	0	0	0	0	0	...
Profile 4	1	1	1	1	1	1	...
Profile 5	0	0	0	0	1	1	...
⋮	⋮	⋮	⋮	⋮	⋮	⋮	⋮

Figure 4.4.4.1: Equality constraint matrix at 4.4.4 F
 4.4.4 F in 4.4.4 F: definition of 4.4.4 F constraint in 4.4.4 F
 4.4.4 F

In the other hand, when cell value = 1, the second matrix defines the value of the constraint for a selected chemical species within the profile. This defined value is considered at each step of the calculation and constraint the model to find this value in the final 4.4.4 F matrix result. The values that can be inserted in the matrix should range between 0 and 100%, knowing that the final result is automatically normalized to 100%, but will always respect the constrained values.

	Cl	Ca	Fe	S	g	a	g	...
Profil 1	1	1			1			...
Profil 2	1	1	1		1			...
Profil 3		4	4				1	...
Profil 4		1		1				...
Profil 5		1		1				...
Profil F	4	4						...
Profil G						1	4	...
Profil 6		1		1			1	...
Profil 7		1		1				...
Profil 8				4			1	...
Profil 9	1			1			1	...
⋮	⋮	⋮	⋮	⋮	⋮	⋮	⋮	

Figure 4.1: Inequality constraints on the contribution of each source profile to the total analyzed P_{PM10} value.

These inequality constraints are favored when compared to the “equality” ones because of their flexibility and lightness on the calculations. In fact, these constraints do not force the QMRF model to calculate under stringent conditions; instead, it pushes only towards the respect of an order of abundance of species between different source profiles.

4.1.2. Identification of sources profiles and contributions

The use of the weighted QMRF allows us to acquire chemical profiles as well as their contributions to P_{PM10} composition. The profiles allow us to identify the emission sources of P_{PM10}, whereas the second represents an estimation of the identified sources impacts on the total analyzed P_{PM10} value.

We have demonstrated at the beginning of this chapter that P_{PM10} collected at the three selected sites exhibits similar but also different influences. Thus the QMRF calculations using each site dataset should identify similar as well as different source profiles between these sites. However, similar profiles between the sites could be attributed to similar local sources such as local traffic, but they could also be linked to common regional sources. Additional specific local sources can be added if found by the model. This profile buildup is actually defined in the literature as the *Unschow* method (Unschow, et al., 1991). This latter considers that the atmospheric P_{PM10} concentrations are resulting from the addition of many contributions: regional background + urban background + local traffic + local industries +...etc. The regional background contribution is considered to be originating from large scale

emissions, to which is added the local traffic. This last source can also be considered as an urban background stage, but at the local sampling region level.

However, in order to evidence a regional versus local scale contributions, the use of PM₁₀ chemical data obtained simultaneously in two different sites is an essential step. It is made possible through our sampling strategy described in Chapter 3, thus we will achieve this phase by comparing source profiles identified in two sites for the same period. The results of the PM₁₀F modeling will be examined to uncover these profiles buildup, in case they existed. Furthermore, the model will allow us to quantify the impact of each of the identified sources, which will eventually lead to uncovering the contribution of regional and local influences.

The strategy used while performing PM₁₀F calculations is based on increasing the number of sources until the identification of an additional source profile is not possible. In parallel, constraints were considered in the form of a matrix that was initially built relying on *a-priori* knowledge on the sources profiles. The “equality” constraints were used in very few cases in order to exclude some species from certain profiles (in this case their values were forced to “0” in the final output). On the other hand, the “inequality” constraints were mainly used to guide the model to refine the final results.

The operational strategy was based on three calculation procedures, considering three datasets respectively, each of which corresponds to one sampling site and is independent from the season. Furthermore, considering our *a-priori* knowledge on the local sources influencing the site, the preliminary PM₁₀F calculations showed that the best results can be obtained when considering 11 and 1 source profiles for Doulogne-sur-Mer, Dunkerque and Saint-Mer respectively. Table 4 summarizes the characteristics of the data sets used to run the PM₁₀F.

Table 4: Characteristics of the data sets used to run the PM₁₀F calculation

Site	Season	Number of profiles	Number of samples	Number of species
Doulogne-sur-Mer	inter	11	11	11
Dunkerque	inter-spring	11 (109)	11	11
Saint-Mer	spring	9	9	9

The 11 source profiles were identified using Doulogne-sur-Mer data in the beginning of this search. Then followed a second step in which we used Dunkerque’s data, which allowed us to increase the number of profiles to 11. The third step allowed us to determine the 11

source profiles found for paint_{mer} by re-launching the \mathbf{Q}^2 F with \mathbf{Q} sources as starting point (identified at the first step), and then finally adding \mathbf{Q} new source profiles.

Finally, under these conditions, the developed weighted \mathbf{Q}^2 F calculations gave interesting results, which will be discussed extensively hereafter.

4.3.3.3 Validation of the calculation reliability

Before discussing the results of the weighted \mathbf{Q}^2 F, we verified that the calculations are not biased by comparing the modeled data to the observed data. In order to accomplish this task, we recalculated the concentrations of each chemical species, while considering the contributions (matrix \mathbf{Q} and the profiles (matrix \mathbf{P} of sources. In fact, the matrix multiplication of \mathbf{Q} and \mathbf{P} allows us to calculate the modeled concentrations of each analyzed species based on the \mathbf{Q}^2 F calculations: these ones are named “calculated” concentrations. On the other hand, matrix \mathbf{P} represents the observed concentrations obtained by direct chemical analysis of the samples. The verification of calculations reliability can be realized on two scales:

- Global: by summing, for each sample, all the calculated concentrations for each species, we are able to acquire the total calculated concentration of analyzed species in the P_{tot} samples. The same procedure can be done using the observed data, and thus we obtain the total observed concentrations in P_{tot} . Then by comparing the “total calculated concentrations” to the “total observed concentrations”, it becomes possible to evaluate the reliability on a global level. When plotted, if “total calculated” versus “total observed” shows a linear relationship with a slope equals to 1, that means that the total P_{tot} mass has been correctly modeled, globally speaking.
- Specific: this phase is realized by comparing, for each species, the “calculated concentrations with the “observed” ones. In general, a slope equals 1 means no data reconstruction problems occurring. Whereas if the slope is superior to 1, the calculated concentrations are overestimated, and inversely, when the slope is below 1, the calculated concentrations are then underestimated. This specific species by species check can point at specific problems in data reconstruction.

Finally, it is always recommended to consider the reconstruction of each species by itself, because when following the global checking method, an overestimated species

concentration can compensate an underestimated one to give a final appearance of good correlations, when in reality they are not.

4.1. PMF calculated versus observed data for Boulogne-sur-mer

The comparison between total PMF calculated and total observed species concentrations in PM₁₀ for Boulogne-sur-mer winter campaign is illustrated in Figure 4.

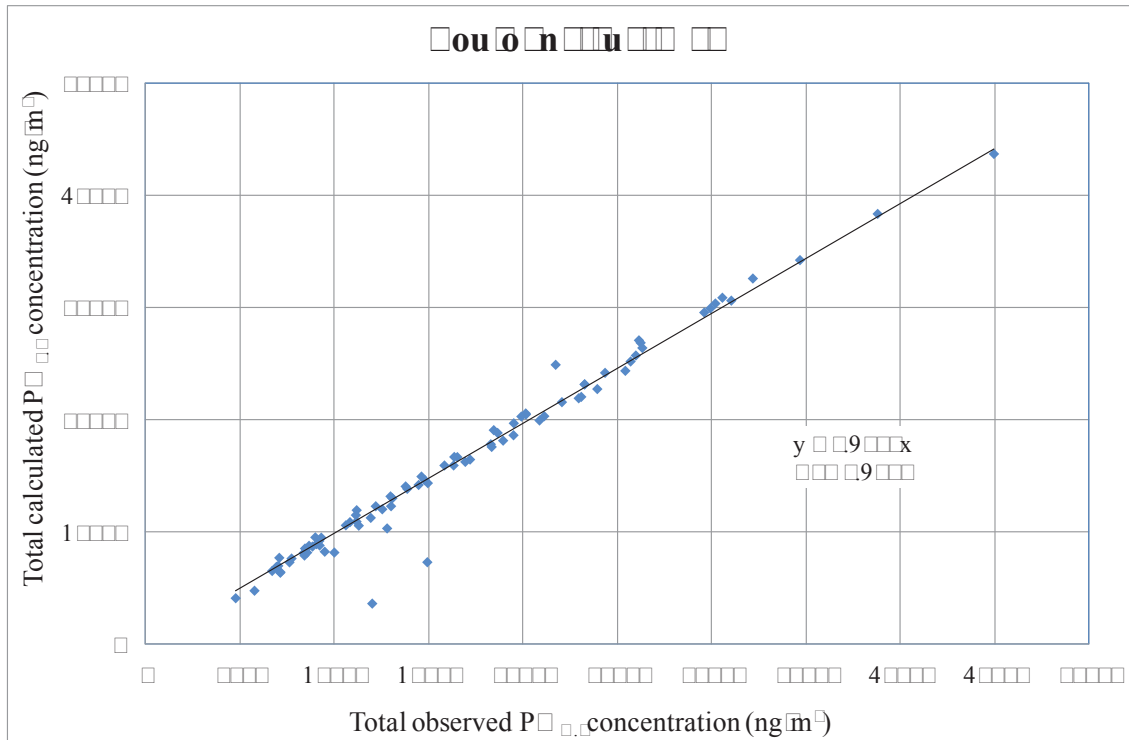
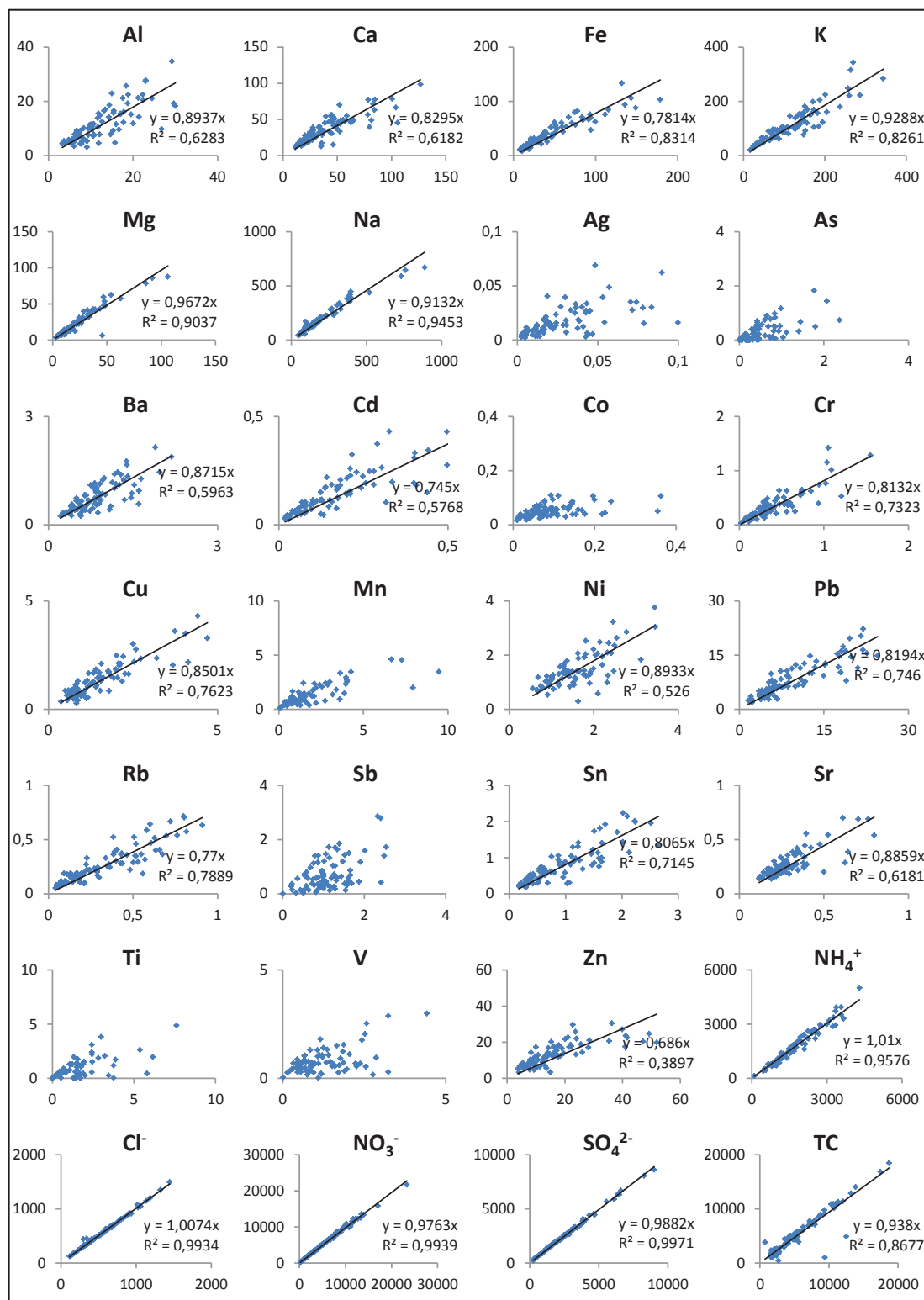


Figure 4: Comparison between total PMF calculated and total observed species concentrations in PM₁₀ for Boulogne-sur-mer winter campaign

The results shows that the total calculated concentrations are very well correlated ($R^2 = 0.99$) with the total observed concentrations. The slope value is 0.99, which means that the global reconstruction error for total species concentration is below 1%. On the other hand, the specific comparison gave similar results for major ions, TSP, and some of the most concentrated metals like: Fe, Pb and Cu (Figure 9). Highly concentrated species are well reconstructed, which partially explains the closeness of our total calculated and observed species concentrations.



The remaining analyzed species calculated concentrations were found well correlated to the observed ones, with the exception of Ag, As, Co, Sb, Sn and Ti. One must pay attention that in general, if some species are not well reconstructed, this means that the contribution value is

not correct or that the species is not correctly represented in the source profiles. Therefore, the identification of the source profiles should not be based on the presence of such species.

Slopes values did not exceed 1.0 (value for PMF_4), proving that the model we used does not overestimate the species concentrations and consequently the total PM_{10} concentrations.

4.4.4 PMF calculated versus observed data for Lunerue

The total calculated concentrations in Lunerue in both winter and spring correlated very well ($R^2 = 0.99$) with the corresponding total observed concentrations (Figure 10). The slope value (1.000) proves that the total species concentration in PM_{10} is also very well estimated.

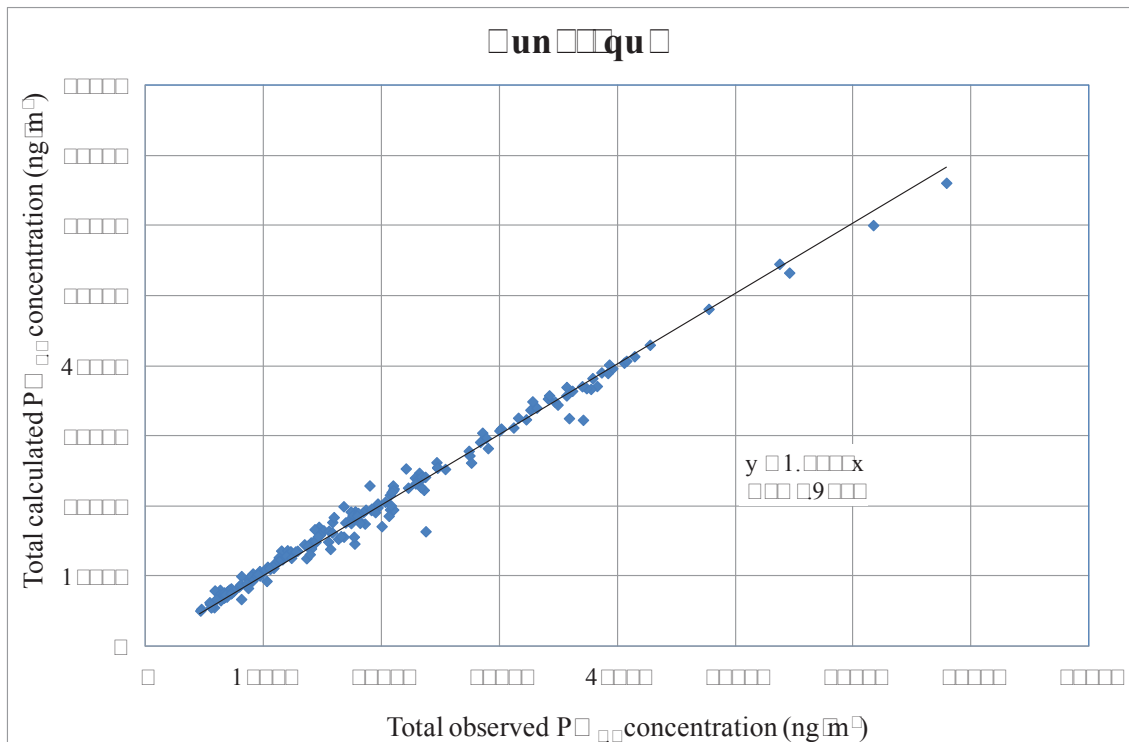


Figure 10: Comparison of total observed and calculated and total observed and calculated concentrations in Lunerue in winter and spring.

Furthermore, anions concentrations are well reconstructed (Figure 11). Correlations of NO_3^- and SO_4^{2-} are not as good as those obtained in the case of Boulogne-sur-mer, but remained very acceptable nonetheless. The remaining species are found well correlated when comparing calculated to observed concentrations, except for g , s , d , o , n and Ti .

Nevertheless, in the case of s , n , and d , some tendencies seem to exist only for the lowest concentrations, whereas at high concentrations these tendencies disappear.

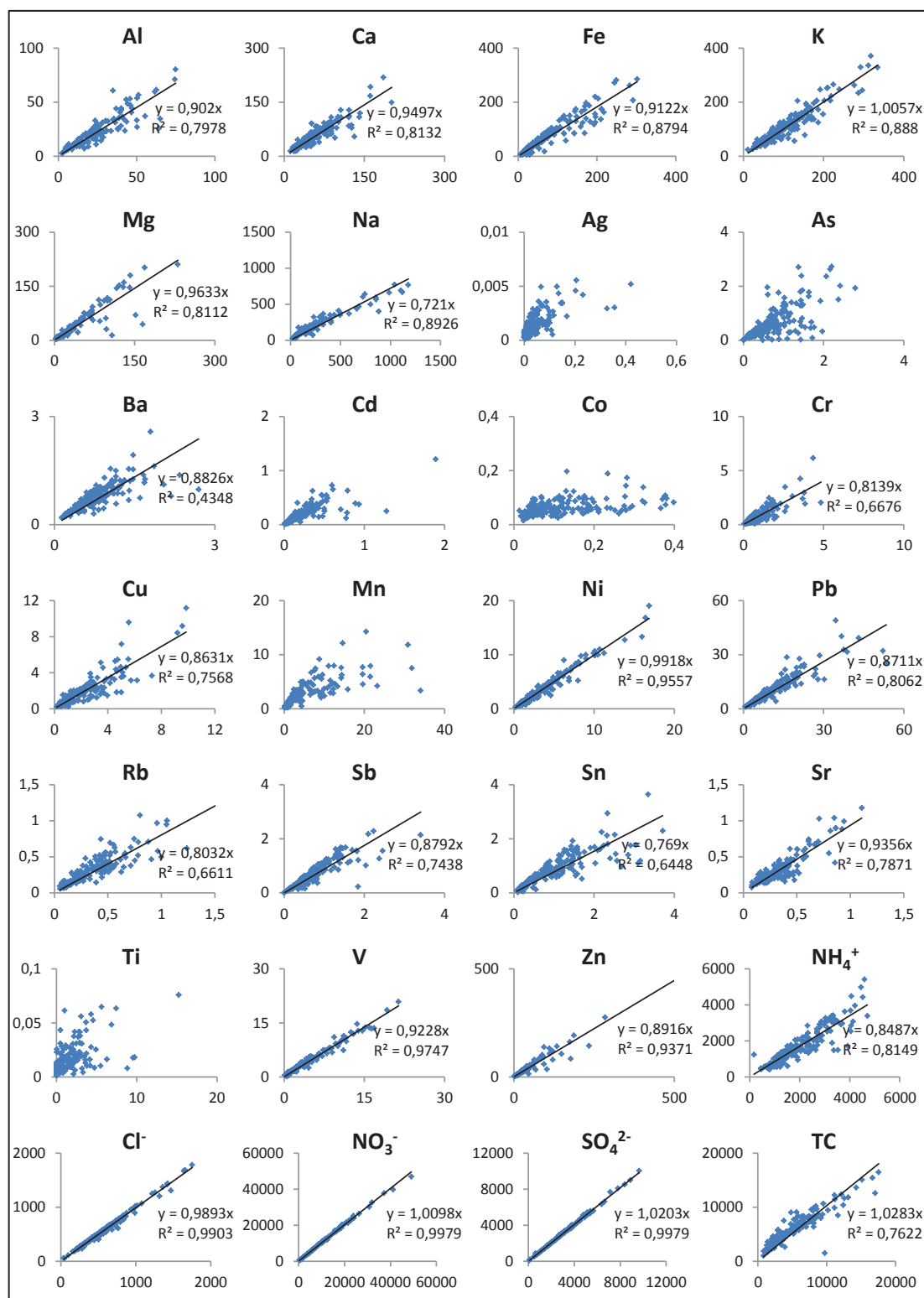


Figure 4.10: Scatter plots of chemical elements versus total carbon (TC) showing the relationship between the elements and TC. The regression equations and R^2 values are provided for each element.

4.4.4.4 PMF calculated versus observed data for Saint-Ermer

In a similar procedure, the total calculated concentrations in Saint-Ermer were found very well correlated ($r^2 = 1.00$) to the total observed concentrations as illustrated in Figure 14. The slope between the two correlated data equals 0.99, which proves that the total calculated species concentration in PMF is perfectly modeled.

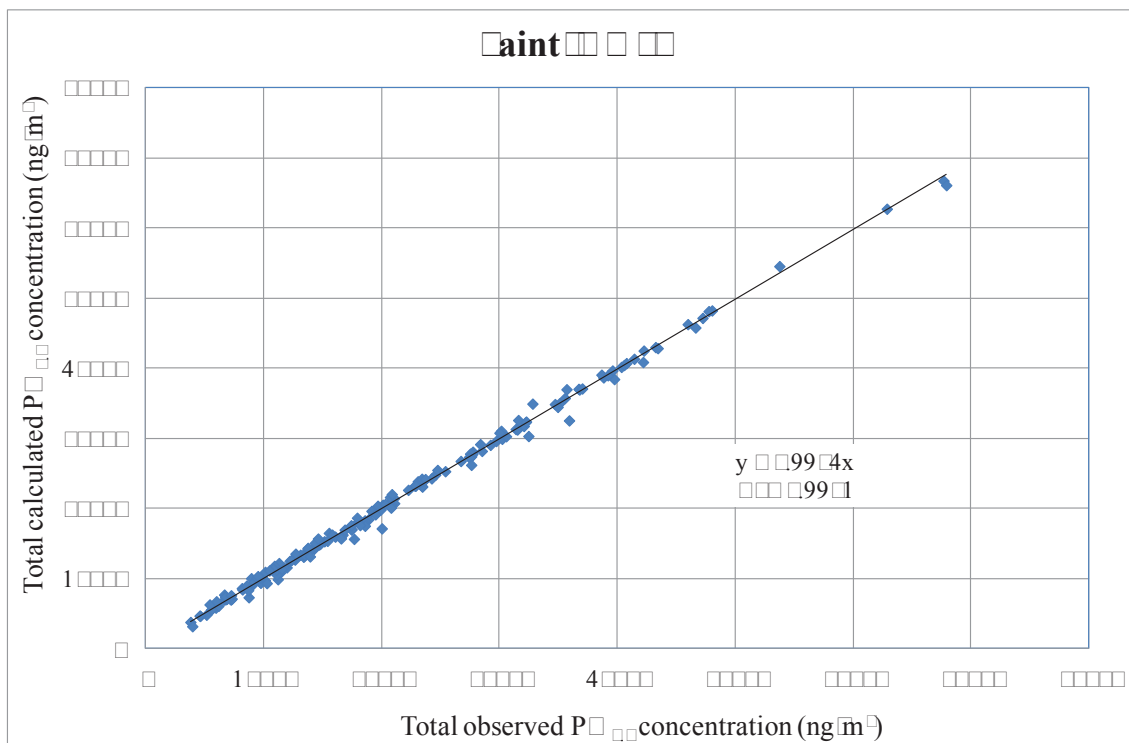


Figure 14: Comparison of the total PMF calculated and total observed concentrations in PMF in Saint-Ermer using PMF.

On the other hand, as observed in the case of Boulogne-sur-Mer, ions and T_{sp} calculated and observed data were well correlated, with a slope value close to 1 (Figure 15). Other metals are also found well correlated except for Ag, As, Co, Cu and Ti, which are found less correlated with the corresponding observed concentrations.

Between these elements, Cd and Cu shows good reconstruction tendencies at low concentrations, whereas in the case of As and Ti, some values are reconstructed well for some samples, and in the same time not reconstructed at all for others. This indicates a lack of As and Ti in some source profiles, which prevents the correct modeling of As and Ti concentrations in some PMF samples.

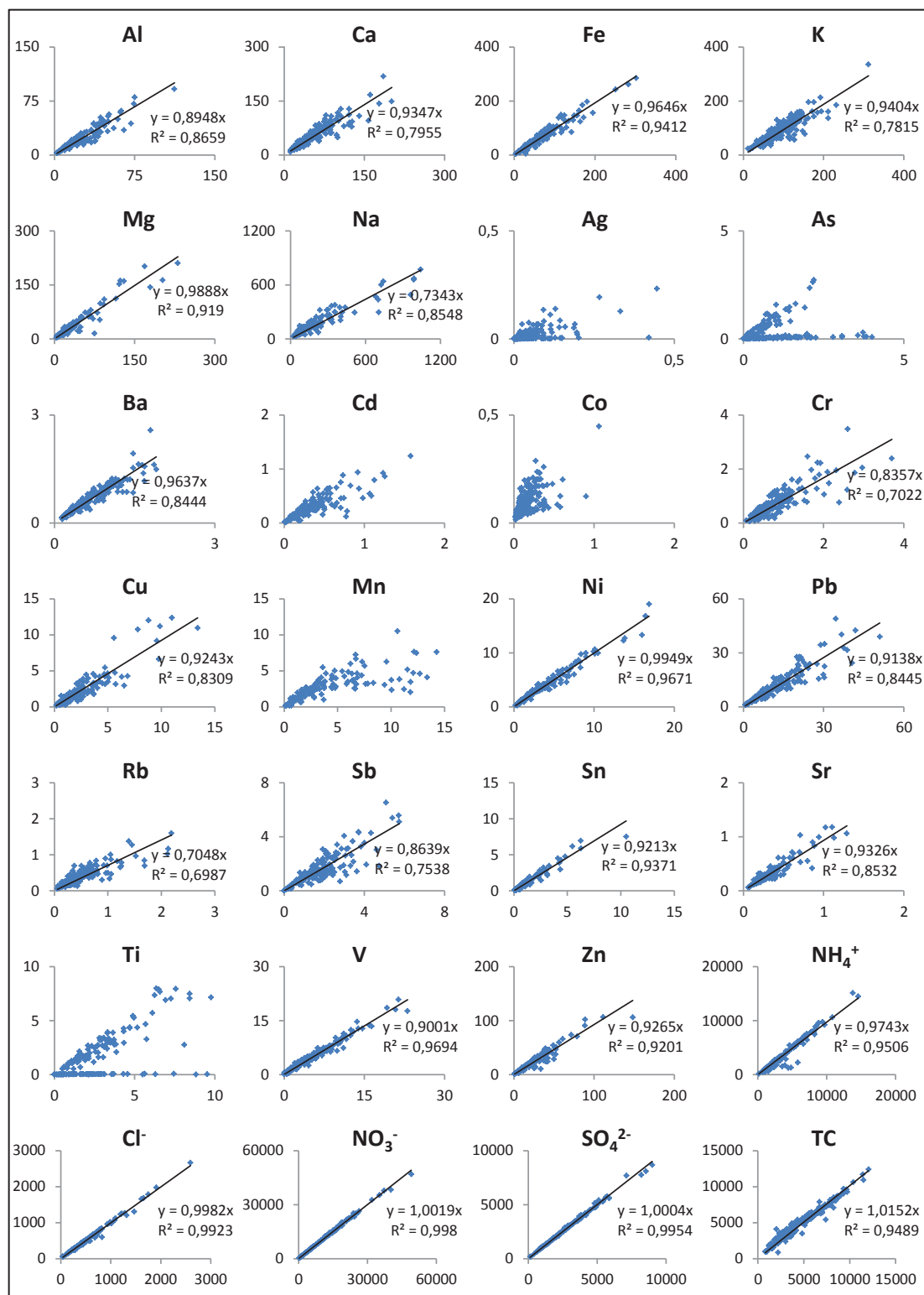


Figure 3: Scatter plots showing the relationship between various chemical elements and compounds. The plots are arranged in a 7x4 grid. Each plot includes a linear regression line and its equation ($y = mx$) and R^2 value.

4.1.3. Identification of sources profiles and contributions using PCA-F

4.1.3.1. Common calculated profiles

After running the PCA-F under the conditions described in section 4.1, we were able to identify eight profiles shared between Boulogne-sur-mer, Dunkerque and Saint-omer. The profiles are illustrated in Figure 14.

4.1.3.1.1. Sea-Salts

The “Sea-Salts” profile did not show many differences between the three sites. The presence of high loads of Na and Cl, as well as some major metals (Ca, Mg and Si) and sulfate ions constituted a signature of this profile. On the other hand, the “Aged Sea-Salts” profile shows more elemental loads than the “Sea-Salts”, especially trace elements like Ni, Pb, Cr and Cu. However, some differences in some ions levels can be found between the sites. For example, additional sulfate can be found in the profile of Dunkerque, meanwhile more nitrates are found in the profile of Saint-omer whereas more ammonium are found in the profile of Boulogne-sur-mer.

4.1.3.1.2. Crustal

The “Crustal” profile showed similarities in the major elements loads and some differences on a minor scale for trace elements and some ionic species. Major elements like Al, Ca, Fe, Si, and Mg are found the highest, a normal observation since these elements, which is in accordance with the profiles found in the literature (Table 1). Another important observation concerns Na levels, which are found almost equal between the sites and is the highest for all three in this “crustal” profile when compared to the remaining common profiles. Cr and Ti also characterize crustal sources; however, the absence of Ti in the profile of Boulogne-sur-mer was unexpected. The reason behind this result might be very possibly linked to the poor correlations of this element with others at this site (see Appendix 1).

4.1.3.1.3. Secondary sulfates and nitrates

Generally, this profile includes “Secondary Sulfates” and “Secondary Nitrates” which are mainly constituted with sulfates and nitrates respectively, associated to ammonium. In this study, this last hypothesis is found respected in the identified profiles. In addition, these latter contained Cu, Pb, Zn and NO_4^- which are found in moderate to high amounts.

Differences between the sites are found at first in the “Secondary Sulfates” profiles, in which Saint-omer exhibited relatively non negligible TSS and NO_3^- levels. In the same profile,

unburned exhibited higher $\delta^{13}C$ levels compared to the remaining sites. Correspondingly, the “Secondary nitrates” is also displaying similarities and differences between the three sites. Similar levels are found for SO_4^{2-} , NO_3^- , Pb, Cu and Zn, whereas Cl⁻, NO_4^{2-} and TSS were only present in unburned and Saint-Omer’s profiles.

4.1.2.2. Combustion profile

This type of profile is found characterized by high TSS concentration, and regroups two types of combustion: “Combustion 1” and “Combustion 2”. Both profiles show high amounts of TSS, SO_4^{2-} and NO_3^- , but also non negligible concentrations of trace elements like Pb, Cu and Zn.

On the other hand, the comparison showed also some differences between the profiles. For example, Ni and Cr were present in “Combustion 1” showing the impact of oil combustion in this profile ((Callius, et al., 2004), (Mato, et al., 2009) and (Ooibroe, et al., 2011)). On the opposite, Zn levels are found much higher in the second combustion profile, which is a signature of biomass combustion ((Illanpa, et al., 2004) and (Patera, et al., 2010)).

In addition to the differences between the combustion profiles, other distinctions can be noted within each profile but between the three sites. For example, Na, Ni, Cr, Zn and Cl⁻ in “Combustion 1” are higher in unburned and Saint-Omer than in Boulogne-sur-Mer. Moreover, differences in “Combustion 2” profile are highlighted in the case of NH_4^+ and NO_4^{2-} . The first is found higher in unburned and Saint-Omer, whereas the second was present only in Saint-Omer’s profile.

4.1.2.3. Major and non-major cations

This profile is a typical major and trace element containing profile, without any ionic or carbon species contributions (see Table 1). Our results illustrated in Figure 14 shows that this characteristic is respected in our $\delta^{13}C$ model. Between the three sites, the common features of this profile is found expressed by the levels of Cl⁻, Fe, Zn, Cd, Cu, Ni, Pb, Cr and Mn. The differences were limited to the remaining elements, especially Na (absent in unburned), Zn (high values in unburned) and Cr (low levels in Boulogne-sur-Mer).

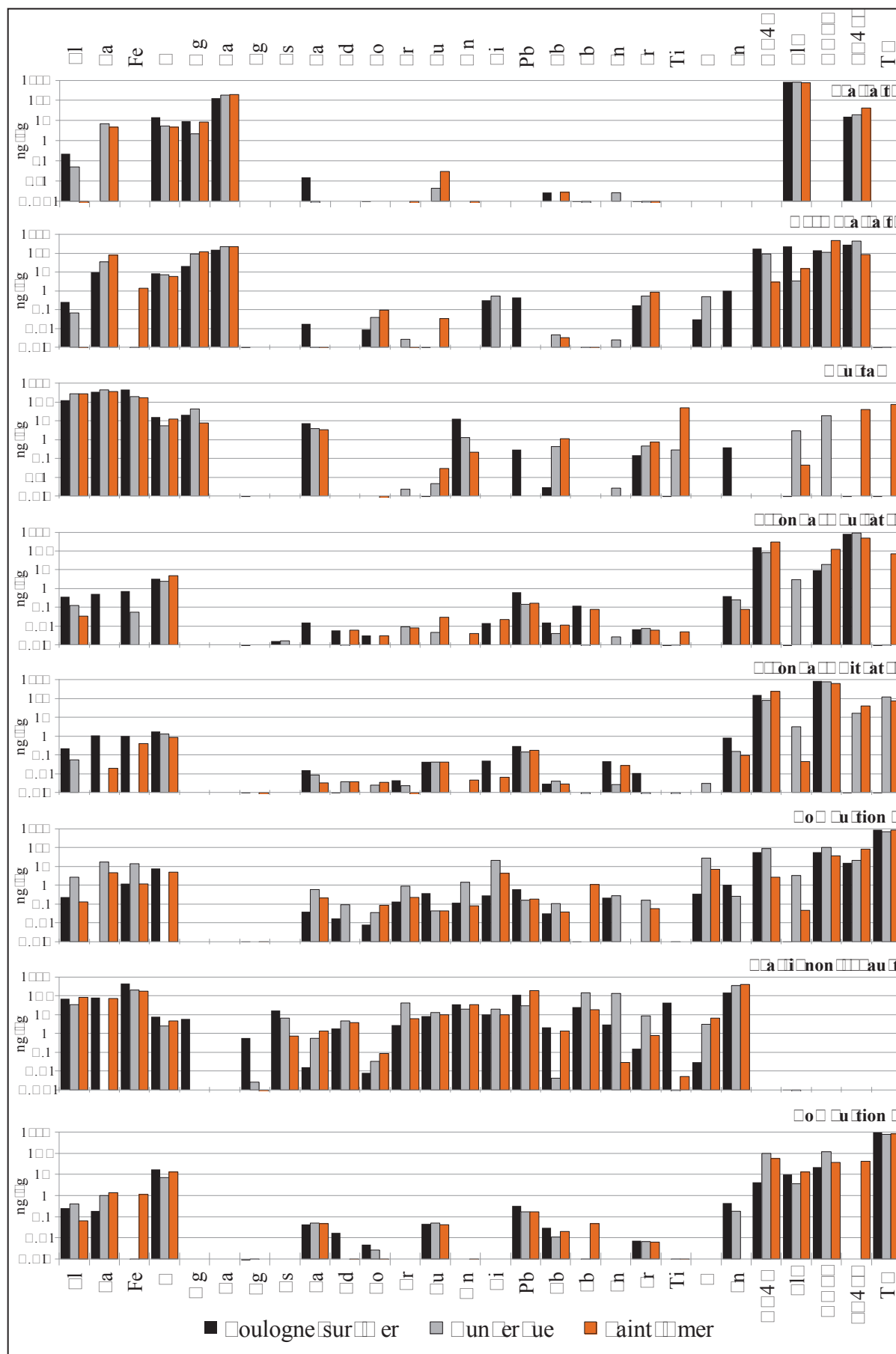


Figure 4.1: Evolution of the concentration of various elements in the sediment samples from the three locations.

4.4.4 Additional calculated profiles in Dunkerque

Three supplementary profiles were identified in Dunkerque, to increase the total number of identified profiles in this site to 11 in total. These local specific profiles are identified as the integrated steelworks main emissions (the fugitive and the sintering stack) and the nearby electric steel plant emissions.

The first two conserved almost the same chemical characteristics of sources samples. High levels of Fe, Ca, Al, Mn, Na, Pb and Zn were respected as well as the presence of nitrates and sulfates in the fugitive emissions. On the other hand, we found that the absence of Mg in the two profiles constitutes an unexpected result as its presence was anticipated (Oleis, et al., 2014). Furthermore, the sintering stack emissions profile respected to a certain extent the chemical composition of these emissions with the presence of Fe, Ca, Pb, Cd, Sb, Al and SO_4 (Oleis, et al., 2014), but with some differences as well: Na, Mg, Na and Tl are absent in the calculated sintering stack profile. These results remain however in accordance with another study in which the application of PCA-F revealed the same elements that characterized the sintering activities at the same site (Olleman, et al., 2014).

These differences between our knowledge on the sources composition and the calculated ones remain moderate since the species exhibiting these variations do not constitute the basis of these profiles determination.

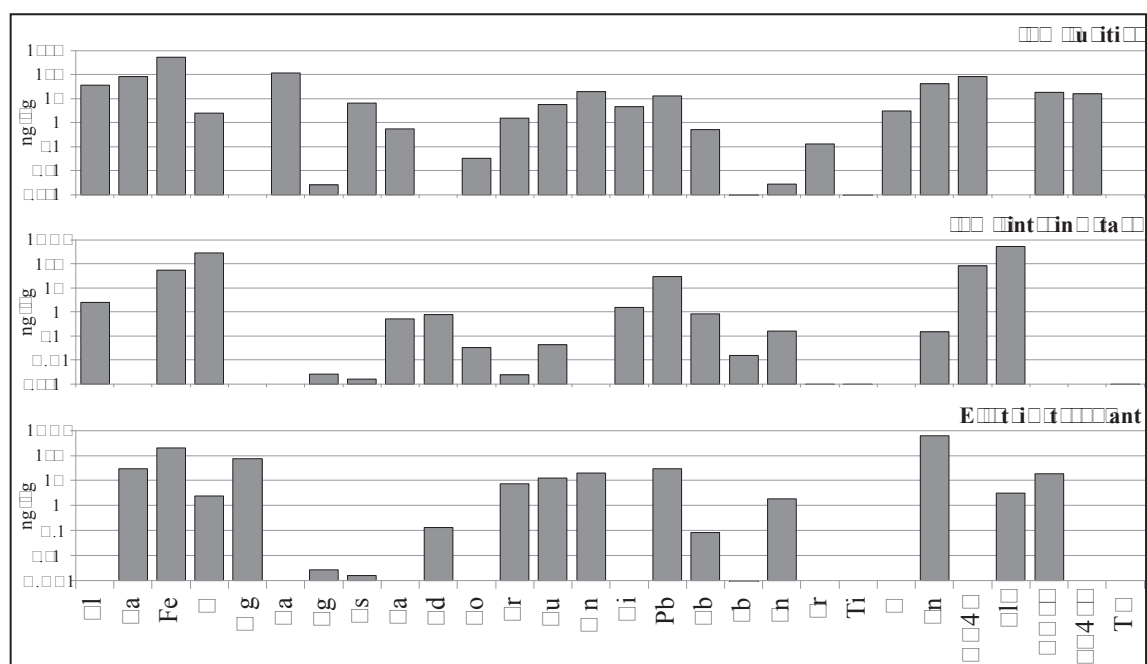


Figure 4.4.4: Concentration (ng/g) of elements for the three profiles identified in Dunkerque: Fugitive emissions, Sintering stack, and Electric steel plant.

Finally, the electric steel plant calculated profile respected to a high extent the chemical composition, as we show it, for this type of emissions: Mn, Fe, Mg, Al, Si, Pb, Cr and Cu are all found high to fairly concentrated in the calculated profile, which is in accordance with our knowledge on this profile (see Table 14 in Chapter 3). One difference can be noted in this case which is the absence of Cl in the calculated profile. However, the final result remains satisfactory.

4.3.3 Additional calculated profiles in Saint-Omer

Similar to the calculated profiles of Dunkerque, Saint-Omer's data modeling gave two additional calculated profiles, which raised the total number of identified profiles for this site to 14 sources profiles in total.

The first profile resembles to the emissions from the steel works industrial site of Dunkerque. A deeper look on this profile composition shows that it cannot be classified neither as fugitive or sintering stack profile. In fact, it represents a mixture of both: high Al, Fe, Mg, Si and SO_4 emphasize the fugitive face, whereas Pb, Cd, Sb, Cl, Cr and SO_4 represent the sintering stack side of the profile.



The second profile exhibits chemical features resembling to glassmaking type of emissions. The profile is characterized by high Al, Cu, Pb, Sb, Mn and Si, all of which can be emitted by a glassmaking activity. This latter is present in the region of Dunkerque, in the form of a large glass factory located to the north sector of the city. This calculated profile is found to be in accordance with the concentration roses calculated for T₁ of Saint-Omer campaign and

previously discussed in Chapter 3 (Table 13), as well as with the values found in similar studies ((Antonovan, et al., 2011) and (Pampazzo, et al., 2011)).

4.3.2. Combustion contribution at the sites

The PMF calculations can also determine the contributions of each identified source profile in the samples. The result of these contributions is given in matrix 4, which will be discussed hereafter. For this next step, we combined the contributions of the two combustion profiles in one representing the combustion contribution in general.

In fact, major elements in both profiles are similar, which makes the distinction between the two sources very difficult as discussed by Frangou (Frangou, et al., 2011). While running the PMF calculations, we noticed in many occasions a decrease in Combustion 2 contributions matched by an increase in Combustion 1. However, the sum of both contributions did not significantly vary. Finally, having these results in hand, the choice fell on the consideration of a single global contribution for combustion sources.

In the case of Lunerue, sources contributions for each PM₁₀ sample have been determined using one PMF calculation using the winter and spring samples species concentrations data combined. Thus, we were able to extract the contributions data corresponding to each season, and analyze the results separately.

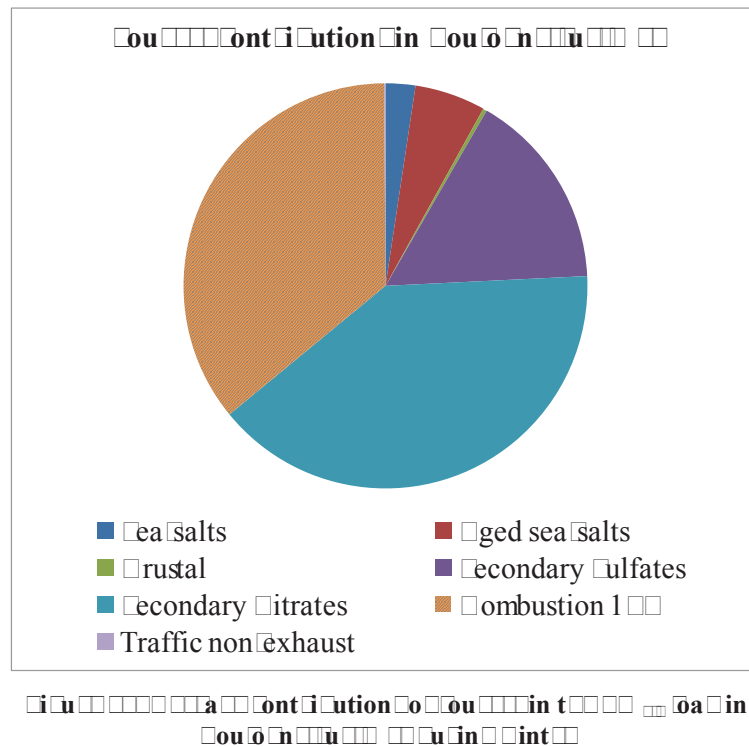
4.3.1. Average contributions

4.3.1.1. Average contribution at the sites

During this campaign, the results obtained from the PMF calculations showed the presence of 12 and 11 sources profiles in Boulogne-sur-mer and Lunerue respectively. The PMF based model also calculated these source profiles contributions in the PM₁₀ samples, which allowed us in return to calculate the average contribution of each source to the PM₁₀ load during the winter campaign, and consequently discuss the evolution of these contributions between the sites.

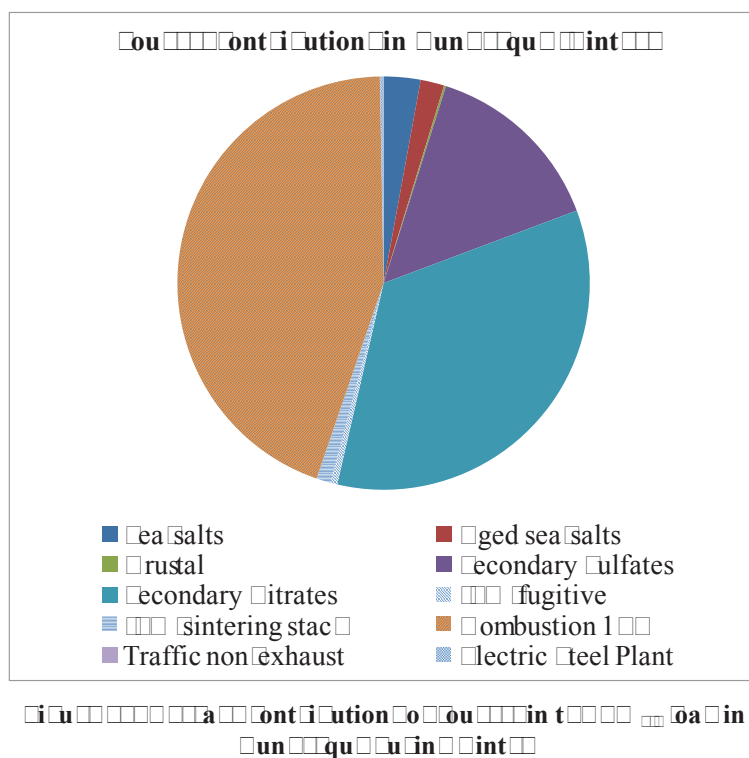
The average contribution calculated for Boulogne-sur-mer (see Figure 13) shows that secondary nitrates and combustion profiles participated in 9.1% and 11.9% of the PM₁₀ load in that site during winter. The secondary sulfates profile came third (11.9%). It must be noted that these three sources contributed in about 91.1% of the total PM₁₀ atmospheric load. On the other hand, the marine source contributed in 1% divided between aged and freshly emitted

particles (0.3% and 0.4% respectively). The remaining sources contributions including crustal and traffic non-exhaust were barely quantified (0.0%).



On the other hand, Dunkerque's source profile study showed 3 industrial sources that are added to the first 4 common ones also identified in Boulogne-sur-mer. Dunkerque's winter contributions displayed a slightly different scenario (Figure 10). Combustion emissions contributed the most at this site during winter (44.4%), followed by secondary nitrates (44.4%), secondary sulfates (14.4%), sea salts and aged sea salts (0.9% and 1.9% respectively). Finally, the integrated steelworks average contribution was about 1.0%, including fugitive (0.3%) and sintering stack (1.1%) sources, whereas the remaining 0.3% was resulting from crustal, traffic non-exhaust and electric steelplant average contributions combined. For this last source, the contribution is 0.0%.

The analysis of these results shows that in Dunkerque, the main sources contributions are estimated to be 90% in total compared to 90% in Boulogne-sur-mer. In fact, these values are found very close to each other, which prove that the 4 sources responsible of these contributions constitute the major part of PM_{10} measured at the two sites: secondary sulfates, secondary nitrates and combustion sources.

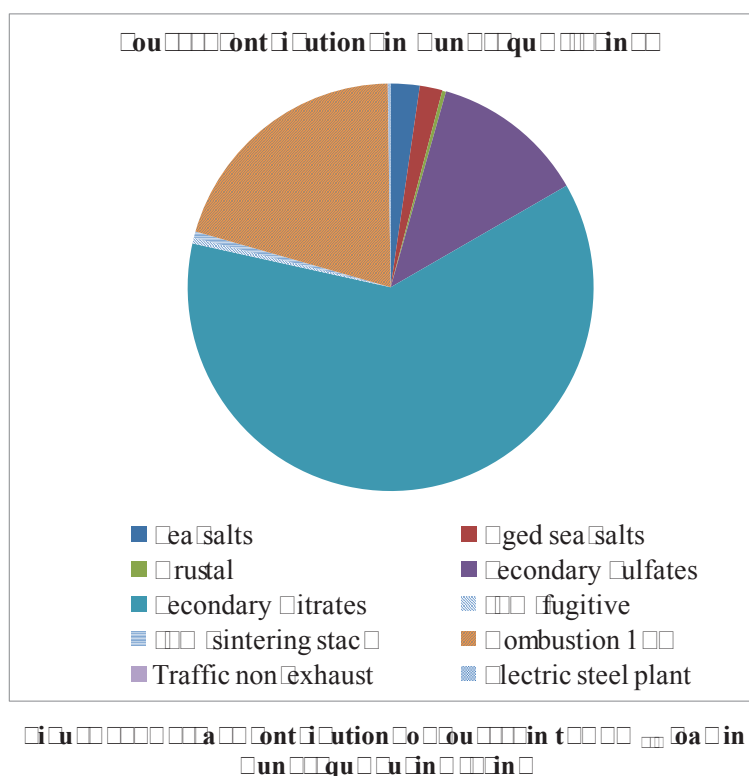


Dunkirk is more populated than Boulogne-sur-mer, and combustion sources contribution is ranked 1st (44%) between the rest (Figure 10), whereas it is ranked 2nd (10.9%) in Boulogne-sur-mer after secondary nitrates (Figure 10). The reason behind this difference could be linked to the presence of heating related combustion emissions during winter, which can also be correlated to very low temperatures recorded during that period. A comparison between these observations and the respective ones of the spring season should confirm this hypothesis.

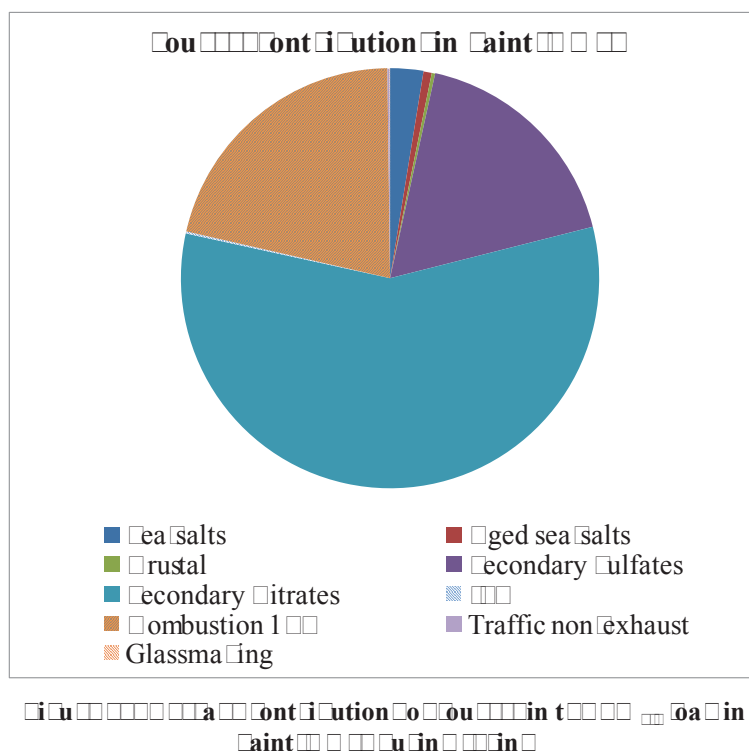
Nitrates and sulfates secondary aerosol sources are another major contributor to the PM₁₀ load. The secondary inorganic aerosol, which encloses both profiles, can be considered as the first contributor at both sites since its contribution is about 44%. These results are in accordance with the diurnal evolution study of SO₂ and TSP concentrations held in Chapter 3. Marine sources contributions are evidenced at both sites, which is not surprising due to their coastal location. Rustal and traffic non-exhaust sources gave marginal contributions to the PM₁₀ load. Finally, the industrial activities located in Dunkirk had an impact estimated to 1.9% during winter. This relatively low value must be carefully considered since the industrial emissions could have a specific effect on some elemental concentrations due to the nature of the industrial activities.

4.4.4.2. Identification of sources profiles and contributions

The spring campaign average contributions in Lunerue (Figure 19) show a major contribution from the secondary nitrates profile (41.0%). The combustion profile participated in 14.0%, followed by secondary sulfates (14.0%) and the marine particles (4.1%). The remaining 1.0% contributions are found divided between crustal, traffic non-exhaust and industrial profiles (1.0%). For this latter, the fugitive contribution appears to be 1% (1% for each of the 2 sources) and the electric steel plant contribution is equal to 0.1%.



A slightly different scenario can be observed for the contributions in Saint-mer site. Secondary nitrates held the first position with 44% average contribution in the total fine PM load, followed by combustion (14.0%), then secondary sulfates (14.0%). Marine contributions were also present in this inland site, and estimated to 4.1% (1% for sea salts and 0.1% for aged sea salts). The remaining profiles contributions were estimated to 1.0%, in which the distant fugitive and the glassmaking sources contributed in 0.1% and 0.0% respectively.



In spring, PM₁₀ sources contribution at Aintamer and Un'erue shows evident similarities. To begin with, the high impact of secondary nitrates in PM₁₀ load is found to be between 40% and 50% of the total PM₁₀. These contributions were followed by the combustion source ones which were about 25% in both sites. When compared to the winter season, the combustion sources contributions in Un'erue decreases from 40% (winter) to 25% (spring). This difference could be linked to the decrease in the use of heating combustion in the spring season during which high temperatures were recorded. Hence, the hypothesis proposed in the previous section is confirmed. Conversely, secondary nitrates held the third place with 15% and 10% contributions in PM₁₀ concentrations depending on the site.

Secondary inorganic aerosols appear mainly in the form of nitrates in spring, when its distribution between nitrates and sulfates profiles is much less defined in winter. However, the high 40% contributions found in spring can be highly related to the accumulation phenomenon that often occurred during the spring campaign.

The marine sources were identified in both sites having similar contributions: 4.1% for the coastal site versus 1.1% for the inland one. The proximity of the source of emissions to the sampling site explains that difference, just like in the case of the 40% influence which contributions were found to be 15% in Un'erue and 10% in Aintamer.

Finally, two additional remarks can be noted concerning the used strategy that gave the contribution results:

- The results obtained for Dunkerque in winter are comparable to those for Boulogne-sur-mer, and similarly for the spring results between Dunkerque and Saint-mer. However, the results for Boulogne-sur-mer are found very different when compared to those found for Saint-mer. In addition, the fact that the calculations were performed using Dunkerque's winter and spring data, and only winter or spring data for the remaining sites, proves the good performance of the weighted $\square\square\square$ F model in defining the source profiles and their relative contributions.
- The amount of data used to perform the calculations was different in each time, but globally included: 11, 11 and 9 samples for Boulogne-sur-mer, Dunkerque and Saint-mer respectively, as well as 11 species concentrations and 11 to 11 sources profiles. It is well known that the quality of calculations results is directly linked to the amount of used data as well as to the number of variables and sources. The weighted $\square\square\square$ F model was able to provide coherent results between the sites of each campaign, even when running under the different above mentioned conditions. This proves the good performance of the model.

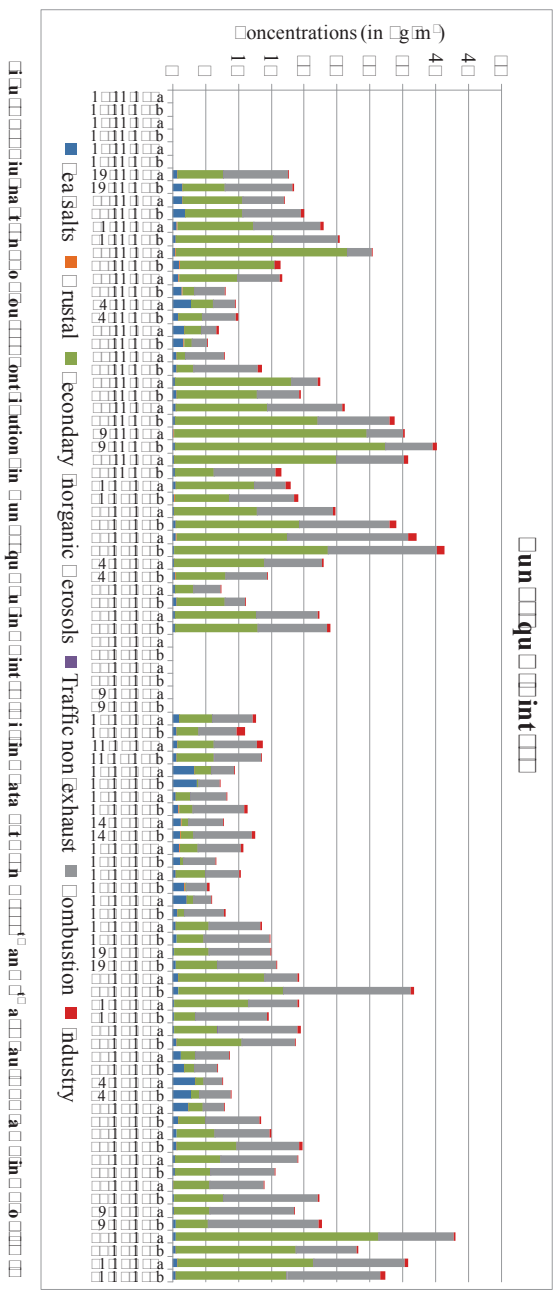
4.9.4 Diurnal contribution trends

In order to facilitate the interpretation as well as the visibility of the charts, in this section, "Sea salts" and "Roged sea salts" will be regrouped in a global "sea salts" source, "Secondary nitrates" and "Secondary sulfates" in "SIA" source, "Combustion 1" and "Combustion 2" in "Combustion" source, and finally "Fugitive" with "Sintering stack" and "Electric steel plant" in "Industry" source.

4.9.4.1 Dunkerque and Boulogne-sur-mer diurnal contribution

Figure 41 and Figure 42 illustrates the sample by sample winter contributions trends in Boulogne-sur-mer and Dunkerque respectively.

Chapter 4: Identification of sources profiles and contributions using $\square\square\square$ F



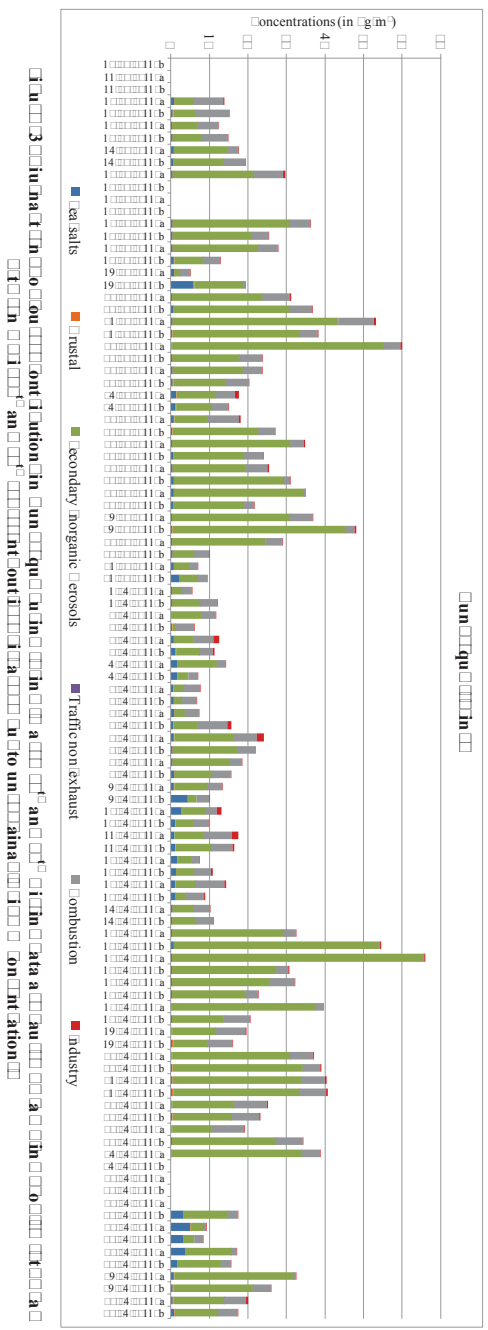
In Boulogne-sur-mer, crustal and traffic non-exhaust contributions barely existed, whereas sea-salts contributions are found low but noticeable most of the sampling period with some exceptions, during which the contribution increased to 10 g m⁻³. These exceptions are found mainly when the total concentration is low, which is in agreement with the situation under a marine air flux. Moreover, the contribution value of the marine source is very similar between the two sites, with high and low values found synchronized.

This seems to indicate that the marine source does not contribute on the local scale, but mostly on a regional one. On the other hand the mostly regional PM₁₀ and mostly local combustion source profiles are found contributing in the majority of PM₁₀ atmospheric concentrations, especially during pollution episodes. It should also be noted that in some cases of above PM₁₀ limit values measurements, the PM₁₀ source can be found exclusively involved in the increase in PM₁₀ concentrations.

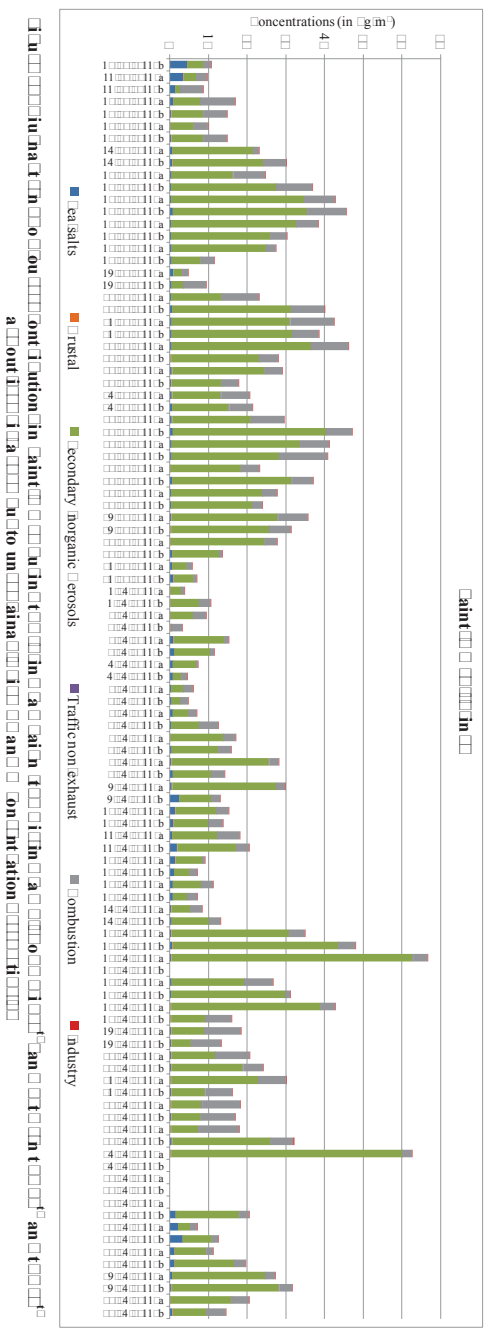
The contributions in Dunkerque's case followed to a high extent the trends of Boulogne-sur-mer, in the sense where sea-salts and crustal evolved on a low level, and PM₁₀ and combustion represented the majority of the contributions. One difference between the two sites is the presence of industrial contributions in Dunkerque, which contributions appear episodically and remained low. The industrial source is not directly involved in the increase in the PM₁₀ load to above limit values.

PM₁₀ and PM_{2.5} in Dunkerque and Boulogne-sur-mer contribution

In Dunkerque and Boulogne-sur-mer, during the spring campaign, “sea-salts”, “crustal”, “traffic non-exhaust” and “industrial” contributions followed a similar hilly shaped evolution (Figure 4.1 and Figure 4.4). High and low concentration periods are found synchronized, but some minor differences existed between the sites in each concentration period. PM₁₀ trends showed very high daily contributions in the total PM₁₀ loads, whereas combustion contributions decreased when compared to the previous observations of the winter period as shown in section 3.9.1. The 10 g m⁻³ limit value is broken very often just by taking the PM₁₀ source by itself.



☐ chapter ☐ : identification of sources profiles and contributions using ☐ ☐ ☐ F



333

On the other hand, the diurnal evolution of “sea-salts” source indicates that it contributes episodically to the PM₁₀ concentration. As during the winter campaign, this evolution is synchronized between the two sites, despite the fact that Saint-Mer is 10 km away from the coastline. The sea-salts source seems to contribute at a regional level as in the case of PM₁₀ source. The combustion profiles diurnal evolution does not show any large variations between the samples. In the spring season, the combustion source can be considered as essentially related to traffic. This latter can be considered as a local source having a constant emission factor. On the other hand, the daily variations could be explained by the fluctuations of the meteorology (rainfall and wind) which favors, depending on the circumstances, the accumulation or dispersion of traffic exhaust emissions. Furthermore, crustal, traffic non-exhaust and industry exhibited very low daily contributions except during some days taken in summer.

Finally, this diurnal trend study agrees with the stage divisions mentioned in Lenschow method (Lenschow, et al., 2001) about the presence of the regional background (sea-salts, crustal and PM₁₀ in our study), topped by an urban background (traffic non-exhaust and mainly combustion), and then on a higher level by local sources (industries). We can also conclude that the regional and urban background profiles contribute the most in the total PM₁₀ concentrations found in this study.

4.9. Average source contributions to the chemical species

In this section we will discuss the origins of each analyzed species between the identified source profiles. By considering the mean contribution and the composition of each source, we were able to determine which source contributes most in the load of a given species. In other words, we were able to identify the main origins of a given species during this period. On the other hand, we should remind that certain elements had bad reconstructions. It is possible that these elements are not perfectly positioned in the identified source profiles. Therefore, the contributions of different sources in the load of these specific elements should be carefully analyzed, and the origins distribution in this case has a higher uncertainty.

4.9.3. Average source contributions to the chemical species

Figure 4-1 illustrates these contributions for Boulogne-Sur-Mer during the winter campaign.

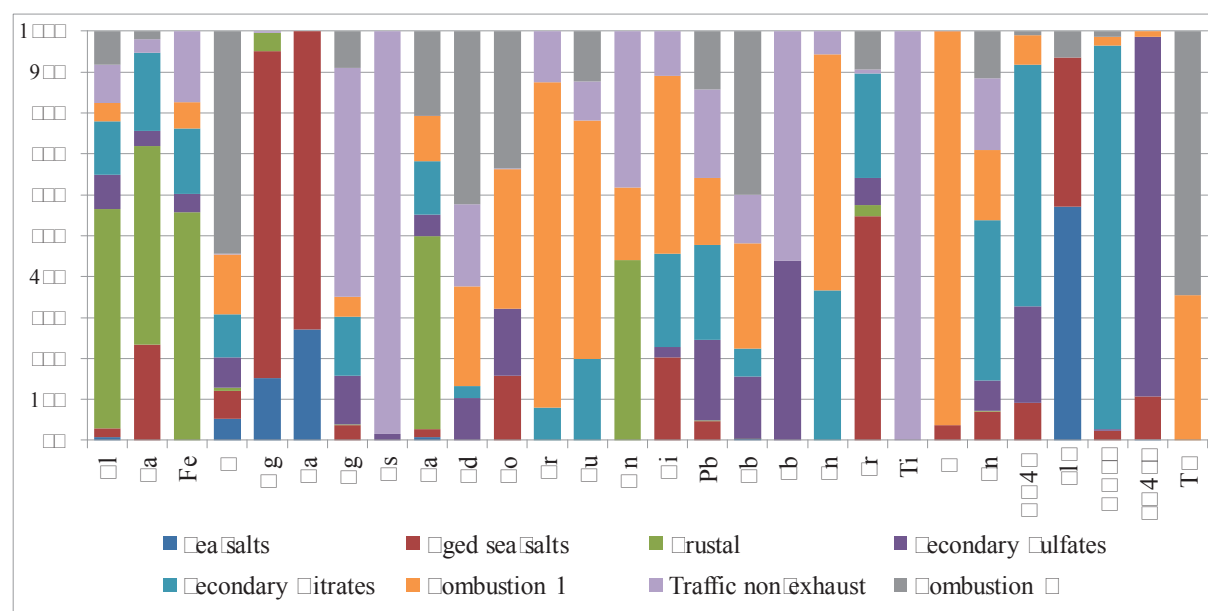


Figure 4.1: Contribution of sources to the total mass of chemical species. The contribution of each source is shown as a percentage of the total mass of the chemical species.

We will start our analysis by looking at the chemical species affected by a small number of sources, like in the case of Ti and Cl which are found resulting from the two combustion profiles. In addition, V is found to be generated by the “Combustion 1” profile which also contributed in an important part of Cd , Pb , Cr , Cu , Ni and Mn . Sulfates and nitrates are also found originated mainly from secondary sulfates and nitrates respectively. These two last profiles are found responsible of the majority of SO_4^{2-} also. On the other hand, “traffic non-exhaust” profile is found to contribute in most of Ti , S , g and b . Furthermore, Ca , g and Cl are found divided between “sea salts” and “aged sea salts”, with more contributions in the first two elements from this last profile. The “crustal” profile contributed mainly in Cl , Ca , Fe , Na and Mn . However, Pb , b and Mn loads are found generated by almost all profiles except those related to natural emissions (sea salts, aged sea salts and crustal). Finally, the aged sea salts and secondary nitrates profiles contributed in the majority of Cr loads.

These results representations are important as an additional examination of the model distribution of the analyzed chemical species between the sources. Ti repartition for example shows that Ti concentrations are explained by only one source. However, in section 4.1, bad correlations were evidenced between Ti reconstructed and observed values, hence we conclude that the model did not find sufficient source combination possibilities in the case of Ti concentrations.

In conclusion, the contributions in each species total load showed some different scenarios (Figure 4.10), and the elements are found well distributed between the sources. The “sea salts” profile contributed in most of Na and Cl. On the other hand, “Aged sea salts” profile is found to contribute importantly in Ca but also in Mg, Fe and Cr loads and mainly in total Mg. The “Crustal” profile participated in important percentages of Al, Ca, Ba and Ti loads. Meanwhile, “Secondary sulfates” profile is found contributing in almost all SO₄ loads and partial SO₄. Furthermore, “Secondary nitrates” profile contributions was partially enriching the Fe and SO₄ loads, but highly contributing in the NO₃ level.

In addition, the first combustion profile (Combustion 1) is found to enrich mainly C and Si, when in the same time the second combustion profile (Combustion 2) is contributing in a large amount of S, Mg, Ca, Fe, SO₄ and T. Nevertheless, trace elements such as Cr, Pb and Sn are found enriched by the contributions of the “traffic non-exhaust” profile.

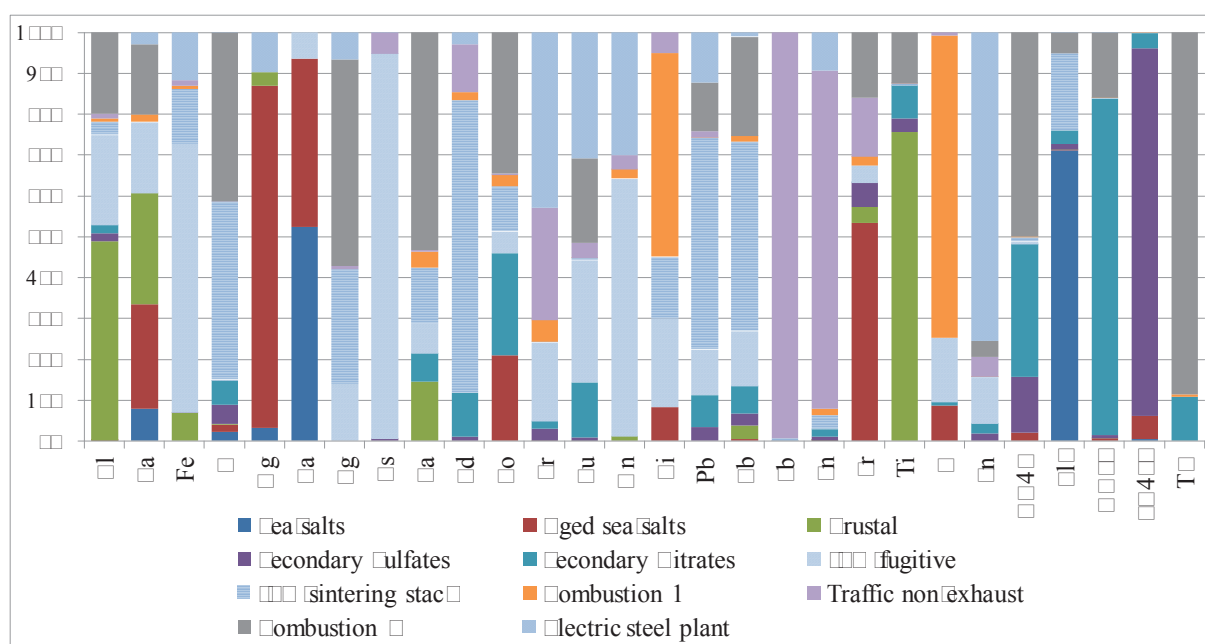


Figure 4.10: Contribution of sources to the total load of elements in the final industrial profile.

Finally, the industrial influences are found to enrich most of the elements. For example, the fugitive profile is contributing in the major loads of Fe, S and N, as well as partial percentages of Al, Ca, Mg, Cr, Cu, Si, Pb, Sb, B and Ni. The input of the sintering stack is found to be more segregated between S, Mg, Fe, Pb, Sb and Cl loads. Thus, the final industrial profile of the “Electric steel plant” contributes the most in Zn, Cr, Cu and Ni loads. These results are not incompatible with the low contribution found for “industries”

source in the analysis of PM₁₀. In fact, industrial sources contribute at a low level to the total PM₁₀ concentrations, but at a high level to specific metals concentrations that are directly linked to industrial activities.

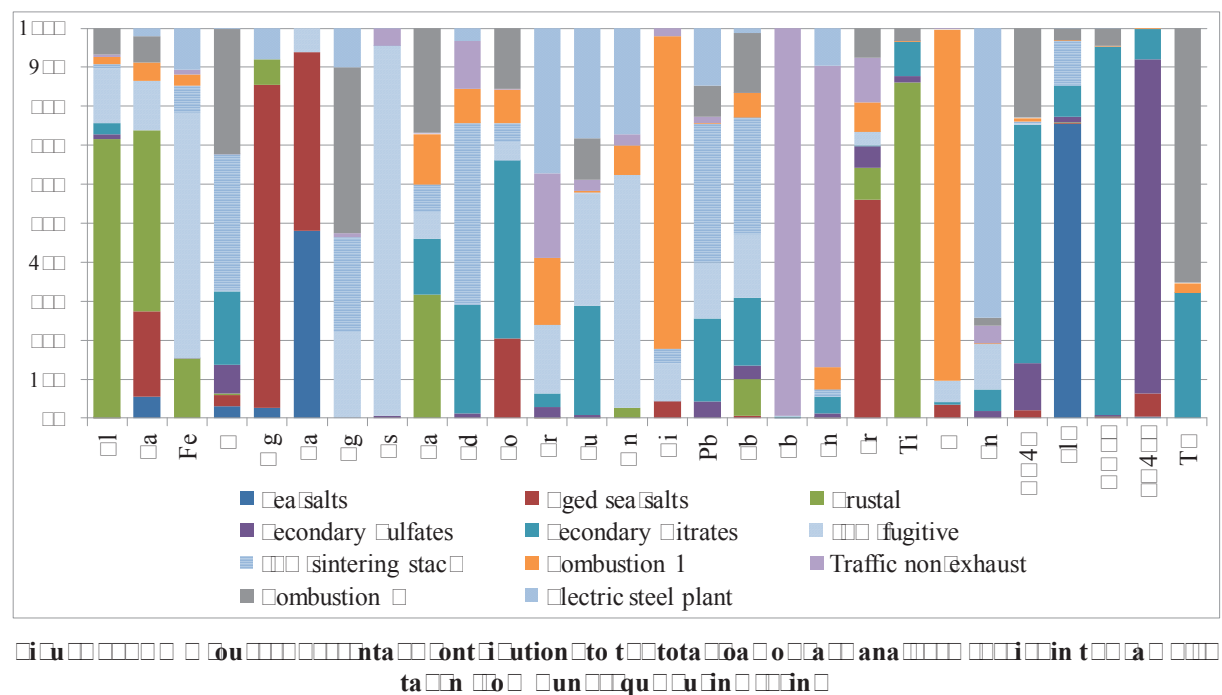
3.3.3. Identification of source profiles and contribution to total PM₁₀

Using the spring campaign data, the PMF calculated sources contributions to the species show that in winter (Figure 3.1), the “Sea salts” profile participated essentially in the loads of Na and Cl. On the other hand, Ca, Mg, Al, Si and Fe are found affected by the contributions of the “Aged sea salts” profile. The “Crustal” profile contributed in most of Al and Ti, and partially in Ca and Si loads. Nevertheless, trace elements such as Cr, Pb and Mn are found enriched by the contributions of the “traffic non-exhaust” profile.

On the other hand, the “Secondary sulfates” contribution is found limited to almost all SO₄²⁻ concentrations and to a small fraction of the SO₄²⁻ loads. Whereas the “Secondary nitrates” largely contributed in NO₃⁻ and SO₄²⁻, and moderately in TSP, Pb, Cu, Fe and Cd. Furthermore, the “Combustion 1” profile contributed essentially in most of V and Ni contents, in the time when “Combustion 2” was enriching TC, K, Mg, Ca and SO₄²⁻.

The industrial profiles followed almost exact contribution patterns as in the case of the winter campaign for winter. A small difference can be noted for the contributions of SO₄²⁻ fugitive in SO₄²⁻ loads and of SO₄²⁻ sintering stack in SO₄²⁻ loads, which was slightly lower than the winter respective contributions.

Finally, the source profiles used to calculate these source contributions in spring were the same as the ones used in winter. Thus, the difference between the main origin of each element (Figure 3.1 and Figure 3.2) is only due to the different contribution values. The contribution of a local industrial source could vary when local meteorological conditions, such as wind directions, also vary. Consequently, the difference between winter and spring campaigns in winter can be explained by the different meteorological conditions recorded during the two seasons.



The case of Saint-Omer's contributions (Figure 11), a difference can be noticed in the distributions. Sea salts contributed in Na, Mg and most of Cl⁻, when in the same time the "Aged sea salts" profile was contributing in most of Mg loads, followed by Sr then Na and Ca. The "Crustal" profile was as usual participating in large percentages of Al, Ti and Fe loads, followed by moderate contributions in the case of Fe, Na and Mn. The "Secondary sulfates" profile contributed in the loads of SO₄²⁻, CO₃²⁻ and some of Ca and Mn loads. In addition, "Secondary nitrates" contributed in most of NO₃⁻ and CO₃²⁻ levels, as well as moderate contributions noted for TSS, CO₃²⁻, Mn, Cu, Pb, Zn, Cd and Cr. Furthermore, trace elements such as As, Cd, Cr, Cu, Pb, Zn and Mn are found enriched by the contributions of the "traffic non-exhaust" profile, which marked a different behavior when compared to the usual contributions found for the other sites.

The “Combustion 1” profile is found responsible for most of V and Ni loads, and part of Co and Sb concentrations at this site. Meanwhile, the “Combustion 2” profile shows a major contribution in Tl and Pb loads followed by a less intense participation in the loads of Ba and Cu.

Finally, the industry in Lunenburg () participated mainly in the load of Mg, followed by more moderate contributions in the concentrations of Fe, S, Cd, Cr, Ni and Pb in Saint-Omer. However, the “Glassmaking” influence was exhibited largely in the case of Zn, pursued by less severe contributions in Cu, Cr and Pb loads. The previous list of elements appears to be source specific, which explains the high contributions found when searching for

their origin. In fact, the total contributions of NH_4^+ and Glassma in PM_{10} concentrations at Saint-Emer were estimated to 1% and 1% respectively.

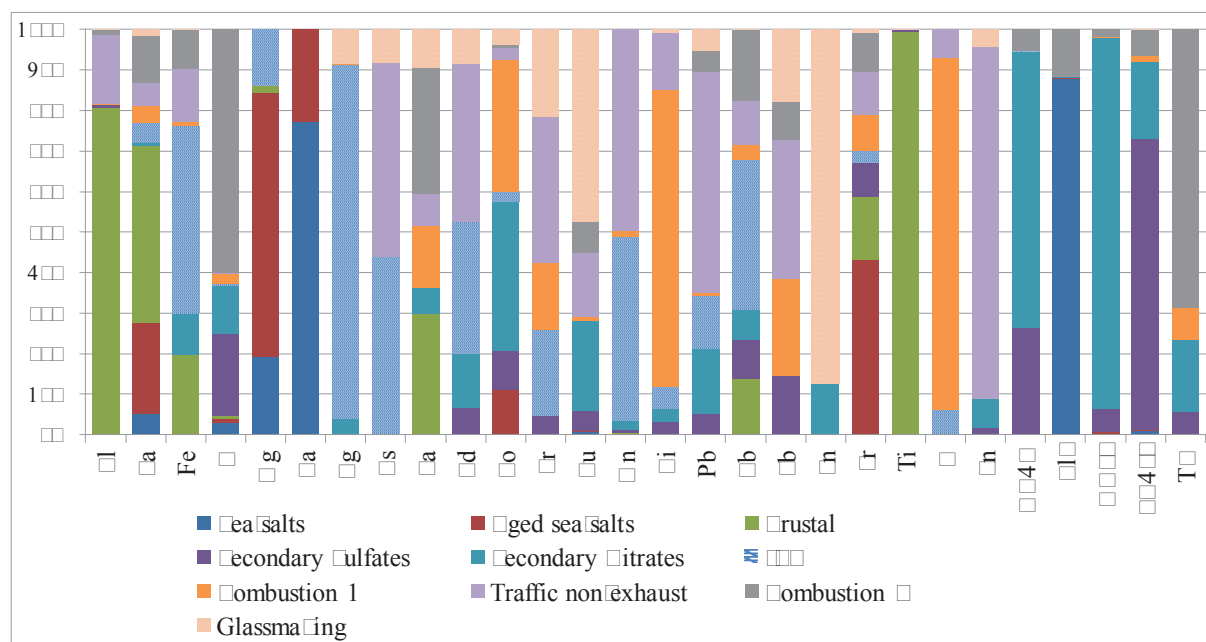


Figure 4.1: Contribution of sources to the total PM_{10} concentration at Saint-Emer. The contribution of sources is expressed in %.

4.1.1. Introduction

The use of the weighted α - α -F model considering our chemical data evidenced 14 source profiles divided between natural and anthropogenic: sea-salts, aged sea-salts, secondary sulfates, secondary nitrates, crustal, traffic non-exhaust, combustion 1 (close to fossil fuel combustion), combustion 2 (close to biomass combustion), and finally, four additional industrial profiles, starting with α - α -F fugitive, followed by α - α -F sintering stack, electric steel plant and glassmaking.

Between 4 and 11 sources that contribute to the load of atmospheric PM_{10} were identified in different sites. The first 4 non industrial sources were identified at Boulogne-sur-Mer. In Dunkerque, 4 steelmaking sources are added to the first 4 identified profiles. Finally in Saint-Omer, 2 industrial sources: local glassmaking and Dunkerque's steel works were detected in addition to the first 4 non-industrial sources.

The study of the contributions of these different sources showed seasonal variations. Hence, the winter campaign was characterized by a high contribution in PM_{10} loads from combustion sources (44.1% in Dunkerque and 44.9% in Boulogne-sur-Mer). The contribution of this source decreases to about 10%, in Saint-Omer and Dunkerque, during the spring campaign, which is a possible consequence of the decrease in the need for heating. Secondary inorganic aerosols constituted the essential mass of measured PM_{10} , which in addition to combustion sources form 90% (Boulogne-sur-Mer) and 90% (Saint-Omer) of the measured PM_{10} concentration.

The diurnal evolution study of the different sources identified at the sites that were sampled simultaneously (Boulogne-sur-Mer, Dunkerque and Saint-Omer, Dunkerque) showed a synchronized evolution of α - α -F and marine salts contributions. Furthermore, we have demonstrated that the levels of contributions of these two sources were not linked to local sources, instead it was found to be associated to a regional background origin, which fluctuates in time. The variation of this non local background level is found responsible of the variation of PM_{10} concentrations. The PM_{10} concentrations beyond the limit values appear directly linked to the increase of this regional background level. Consequently, the actions taken in order to decrease the levels of PM_{10} should stretch to cover a larger scale since local emission sources are slightly contributing to PM_{10} loads (an exception should be considered concerning local heating during winter).

The industrial sources are found to directly contribute in fewer amounts of PM_{10} measured mass: 1 to 10% in Dunkerque and about 10% in Saint-Omer. However, these

sources can sensibly change the sampled PM₁₀ composition, and notably the concentrations of certain elements such as Fe, Mn, Ni, Pb, Cd, Zn, Cr, S, Mg, Cu and B in urban area as well as in winter. In fact, we have observed that industrial origins are mainly behind these elements loads. Nevertheless, we must not forget the indirect role that these industrial sources play on the concentration levels of PM₁₀ in the region, especially through SO_x and NO_x emissions, which are precursors of secondary inorganic aerosols formation.

References

- Alleman, M., Camaison, M., Perdrix, M., Obache, M., & Gallo, M. (2010). PM₁₀ metal concentrations and source identification using positive matrix factorization and wind sectoring in a French industrial zone. *Atmospheric Research*, 96, 1000–1010.
- Amato, F., Pandolfi, M., Scrig, M., Querol, M., Alastuey, M., Pey, M., . . . Poppe, P. (2009). Quantifying road dust resuspension in urban environment by multilinear engine: comparison with PMF. *Atmospheric Environment*, 43, 1000–1010.
- Billford, M., & Seiler, G. (1990). A factor analysis model of large scale pollution. *Atmospheric Environment*, 1, 1400–1410.
- Delmaire, G., Roussel, G., Leis, M., & Ourcot, M. (2010b). Factorization matricielle non négative sous contraintes. Application à l'identification des sources industrielles. *Workshop Conférence Internationale Francophone d'Automatique IFAC*.
- Delmaire, G., Roussel, G., Leis, M., & Dedoux, F. (2010a). Une version pondérée de la Factorization matricielle non négative pour l'identification de sources de particules atmosphériques. Application au littoral de la mer du Nord. *Journal Européen des Systèmes Automatisés*, 44/4-5, 400–410.
- Frangou, M., Ouros, M., Oussiopoulos, M., & Elis, M. (2011). Review of the current evaluation methodologies used for source apportionment applications in EU countries. European Environmental Agency. <http://fairmode.eu.eea.europa.eu>
- Friedlander, M. (1990). Chemical element balances and identification of air pollution sources. *Environmental Science and Technology*, 7, 1000–1010.
- Leis, M. (2010). Evaluation de la contribution d'émissions sidérurgiques à la teneur en particules en suspension dans l'atmosphère à une échelle locale. *Thèse de Doctorat Université du Littoral Côte d'Opale PhD Thesis*.
- Leis, M., Fernandez-Almo, M., Dedoux, F., Foury, M., Ourcot, M., Desmonts, T., & Ourcot, M. (2010). Chemical profile identification of fugitive and confined particle emissions from an integrated iron and steelmaking plant. *Journal of Hazardous Materials*, 250–251, 400–410.
- Lim, M., Poppe, P., & Edgerton, M. (2004). Improving source identification of Atlanta aerosol using temperature resolved carbon fractions in positive matrix factorization. *Atmospheric Environment*, 38, 4900–4910.
- Menschow, P., Abraham, M., Outzner, M., Outz, M., Preu, M., & Eichenbacher, M. (2001). Some ideas about the sources of PM₁₀. *Atmospheric Environment*, 35(1), 1000–1010.
- Mu, M., Wang, M., Russell, M., & Edgerton, M. (2000). Atmospheric aerosol over two urban-rural pairs in the southeastern United States: chemical composition and possible sources. *Atmospheric Environment*, 39, 4400–4410.
- Antovan, M., Ado, M., Ampazzo, G., & Isin, F. (2000). Correlations among inorganic elements in particulate matter (PM₁₀) in urban area of Venezia Mestre. *Annali di Chimica*, 93, 414–420.
- Miller, M., Friedlander, M., & Iddy, G. (1990). Chemical element balance for the Pasadena aerosol. *Journal of Colloid Interface Science*, 39(1), 1000–1010.
- Moore, M., Schaap, M., Eijers, M., & Oogerbrugge, M. (2011). Source apportionment and spatial variability of PM₁₀ using measurements at five sites in the Netherlands. *Atmospheric Environment*, 45, 4100–4110.
- Oreno, T., Aranasios, M., Amato, F., Cucarelli, F., Aava, M., Galzoi, G., . . . Gibbons, M. (2011). Daily and hourly sourcing of metallic and mineral dust in urban air

- contaminated by traffic and coal-burning emissions. *Atmospheric Environment*, 68, 1144.
- Paatero, P. (1993). Least squares formulation of robust non-negative factor analysis. *Chemometrics and Intelligent Laboratory Systems*, 37, 1-11.
- Paatero, P., & Tapper, U. (1994). Positive matrix factorization: a non-negative factor model with optimal utilization of error estimates of data values. *Environmetrics*, 5, 111-126.
- Patera, I., Kassimopoulos, N., Ougiatoti, N., Kouvara, G., Ihalopoulos, N., & Asilakos, N. (2011). Carbonaceous and ionic compositional patterns of fine particles over an urban Mediterranean area. *Science of the Total Environment*, 424, 111-126.
- Polissar, N., Hopke, P., Paatero, P., Alm, N., & Isler, N. (1993). Atmospheric aerosol over Las Vegas: elemental composition and sources. *Journal of Geophysical Research*, 103, 19419-19434.
- Pampazzo, G., Asiol, N., Isin, F., Ampado, N., & Pavoni, N. (2000). Geochemical characterization of PM₁₀ emitted by glass factories in Turano, Venice (Italy). *Chemosphere*, 71(11), 1111-1120.
- Chauver, N., Cough, G., Hafer, N., Christensen, N., Rndt, N., Reinter, N., & Par, N. (2000). Characterization of metals emitted from motor vehicles. Health Effects Institute.
- Illanpa, N., Illamo, N., Aariak, N., Frey, N., Pennanen, N., Aakonen, N., . . . Alonen, N. N. (2000). Chemical composition and mass closure of particulate matter at six urban sites in Europe. *Atmospheric Environment*, 40, 1111-1120.
- Allius, N., Anssen, N., einrich, N., oe, G., uusanen, N., yrys, N., . . . Pennanen, N. (2000). Sources and elemental composition of ambient PM₁₀ in three European cities. *Science of the Total Environment*, 337, 141-150.
- iana, N., uhlbusch, T., uerol, N., lastuey, N., arrison, N., opke, P., . . . itzenberger, N. (2000). Source apportionment of particulate matter in Europe: a review of methods and results. *Aerosol Science*, 39, 1149.
- inchester, N., & ifong, G. (1991). Water pollution in Lake Michigan by trace elements from pollution aerosol fallout. *Water, Air and Soil Pollution*, 1, 114.
- u, N., f, arson, T. N., u, N., y, illiamson, N., estberg, N. N., & iu, N. N. (2000). Source apportionment of PM₁₀ and selected hazardous air pollutants in Seattle. *Science of the Total Environment*, 386, 411-420.

General conclusion

The main objectives of this study were to compare the levels and the chemical composition of atmospheric PM_{10} in cities located in the vicinity of the littoral of the Nord-Pas-de-Calais region, and to identify the different sources that are impacting the load of these atmospheric particulates.

In order to achieve these objectives, this work was divided into three successive sections:

- 1) The achievement of two PM_{10} sampling campaigns in Dunkerque, Boulogne-sur-mer and Aintamer. In details, the sampling procedure was accomplished following two sampling campaigns plan (winter and spring), applied simultaneously at two sites and in a 1-hour sample method:
 - winter campaign: held between November 1th and December 1st of 2011 in Dunkerque and Boulogne-sur-mer
 - spring campaign: held between March 1th and April 1th of 2011 in Dunkerque and Aintamer.
- 2) A profound chemical characterization of the samples was achieved, with a scope aiming at the determination of ionic species, major elements, trace elements and total carbon concentrations. The diurnal and geographical variations were analyzed while considering meteorological data and air masses origins. A detailed examination of element concentrations allowed to evidence elemental ratios that can be adopted as tracers of certain emission sources.
- 3) Particle sources identification was achieved by the use of a receptor model that is based on a non-negative matrix factorization method. This section aimed at the identification of emission source profiles as well as the quantification of their relative contributions in the samples.

Concentration levels and chemical composition of $PM_{2.5}$

During the two sampling periods, the average concentrations of PM_{10} were $4.4 \mu g m^{-3}$ in winter and $1.1 \mu g m^{-3}$ in spring, based on the Nord-Pas-de-Calais official air quality monitoring network recordings.

When comparing these data to the chemical composition of the collected particles, we found that major species concentrations (SO_4^{2-} , NO_3^- , NO_2^- and Total Carbon) exhibited similar diurnal variations from one site to the other in each period. The difference in the concentrations of these species from one site to the other is relatively low, which has been

attributed to the variability of a regional background level, and found heavily related to meteorological conditions.

Concentrations above $100 \mu\text{g m}^{-3}$ were recorded in many occasions in winter as well as in spring. These high concentrations were encountered mainly under stable anticyclone conditions and east sector winds, which boost the arrival of air masses of continental origins. In addition, significant high carbon concentrations were measured during cold episodes and were attributed to the important use of heating systems. Inversely, during the spring period, high concentrations episode was maintained by stable meteorological conditions and stagnant winds. These high concentrations can hence be related to accumulation phenomenon as well as the increase in PM_{10} formation which is a consequence of precursor release (NO_x and SO_2).

The influence of industrial emissions on the chemical composition of $\text{PM}_{2.5}$

Significant concentration differences were observed in the case of metallic and some trace elements. In particular, the comparison between Lunerue and Moulignon-sur data uncovered the industrial emissions impact at Lunerue, especially when comparing the levels of Fe, Al, Ca, Mn, Ni, Cd, Cr, Cu, Si, S and Na. This observation was confirmed by an elemental enrichment factor study (EF). Using this approach, the comparison between Lunerue and Saint-mer had not only confirmed the impact of industrial emissions in Lunerue, but also revealed significant enrichments for Mn, Pb, Cd and Na at both sites.

Furthermore, by examining the elemental concentration roses, it was possible to point at certain sectors under which metallic and other trace elements concentrations were found relatively high. This examination allowed the identification of industrial activities that could be responsible for these high concentrations. In addition, a selection of certain samples in which these influences are identified allowed us to calculate elemental ratios that can be considered as characteristic of the sources:

- the emissions from the integrated steelworks and electric steel plant industries in Lunerue are found characterized by specific elemental ratios of Mn/Fe , Ni/N , Cr/Cd and Pb/Cd , which allow the distinction between these sources
- the emissions from the glassmaking industry in Saint-mer can be identified by specific ratios of Ni/Cr , Ni/Pb , Cu/Cd and S/Cg .

Finally, by following the observations of the concentration roses, air mass back trajectories and the examination of elemental ratios, we proved that the integrated steelworks

emissions located in $\square_{un}\square_{er}\square_{ue}$ influence the metallic concentrations of $P\square\square\square$ air masses in $\square_{aint}\square_{mer}$.

Identification and evaluation of sources contributions using a source-receptor model

The acquired chemical composition data of $P\square\square\square$ was used as input data in a source-receptor model. The used software was developed by our partners of the $\square\square\square\square$ ($\square\square\square\square$). Essentially, it revolves around a weighted version of a non-negative matrix factorization method ($\square\square F$), which considers individual measurement uncertainties, in the sense where the model relies more on the concentrations affected by low uncertainties. In addition, this model allows the consideration of *a-priori* knowledge on the sources, which is included in the calculations in the form of constraints.

Based on the sources that were identified using our $P\square\square\square$ chemical composition data (chapter $\square\square$ and \square), we were able to introduce constraints in the model calculations, which was essentially in the form of an order of abundance given to the elements between the different source profiles.

The model output analysis allowed us to determine common source profiles shared between the three sampling sites:

- marine aerosols: composed from fresh sea-salts and aged sea-salts
- secondary inorganic aerosols: divided into secondary sulfates and secondary nitrates
- crustal source
- combustion sources: composed of two profiles in which total carbon is dominant
- traffic non-exhaust profile.

Additional profiles were also identified following the use of $\square_{un}\square_{er}\square_{ue}$ and $\square_{aint}\square_{mer}$ data, which reflects the impacts of the industrial emissions located in these sites. Three industrial source profiles were identified in $\square_{un}\square_{er}\square_{ue}$, two of which were attributed to the integrated steelmaking activities (one profile representing the point emissions in the sintering unit and another representing the fugitive emissions), and the third one was found to represent an electric steel making plant emissions. In $\square_{aint}\square_{mer}$, two additional profiles were obtained: a first one that corresponds to a glassmaking industry emissions, whereas the second represents the emissions from the integrated steelworks located in $\square_{un}\square_{er}\square_{ue}$.

These industrial sources are found to have small contributions to the particle average concentrations. Nevertheless, we maintain the fact that some of these sources emit particles charged with metallic and trace elements, some of which have low legislated limit values (Cd and S). Hence, it has been demonstrated that the origin of Fe , Ni , Cu , Pb , Cd , Ni , Cr , S , Co , Mn and B is mainly industrial, located in Lunenburg and Saint-James .

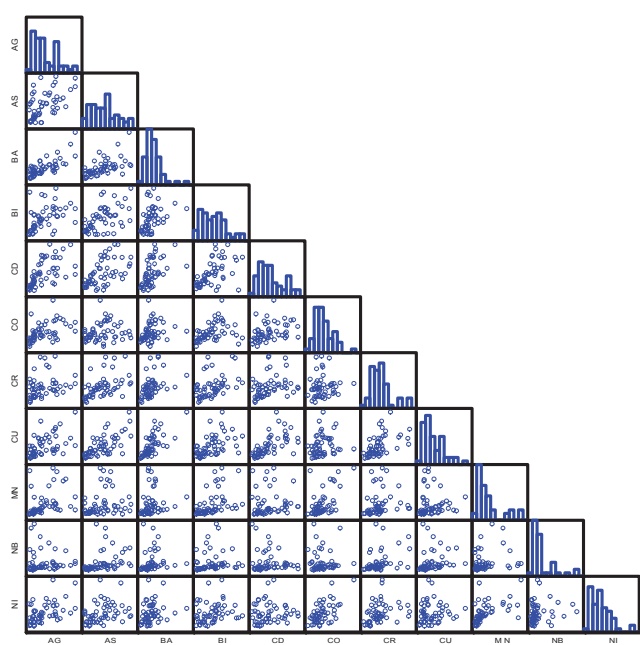
The secondary inorganic aerosols represent the highest contributions, specifically for secondary nitrates, in a similar fashion to the carbon rich particles emitted by combustion sources. The comparison between winter and spring campaign contributions showed accentuated seasonal variations. The highest impact of combustion sources during winter can be mainly explained by the use of heating processes. In spring, it is the secondary inorganic aerosols that exhibited the highest contributions, which can explain the high concentration levels of PM_{10} during this period (around $150 \mu\text{g m}^{-3}$).

By comparing the contribution results between the two studied sites, during the same period, we found that the contribution variations of PM_{10} and marine aerosols are similar. The contribution trends of these sources are found linked to regional scale phenomenon instead of a local one. This emphasizes the importance of considering large scale pollution reduction measures, on the national and international level, as recommended by the European Union. In addition, we insist on the fact that these measures should also consider the reduction in the emissions of gaseous pollutants: CO , CO_x and NO_x , which are precursors of fine particles formation.

□ppendices

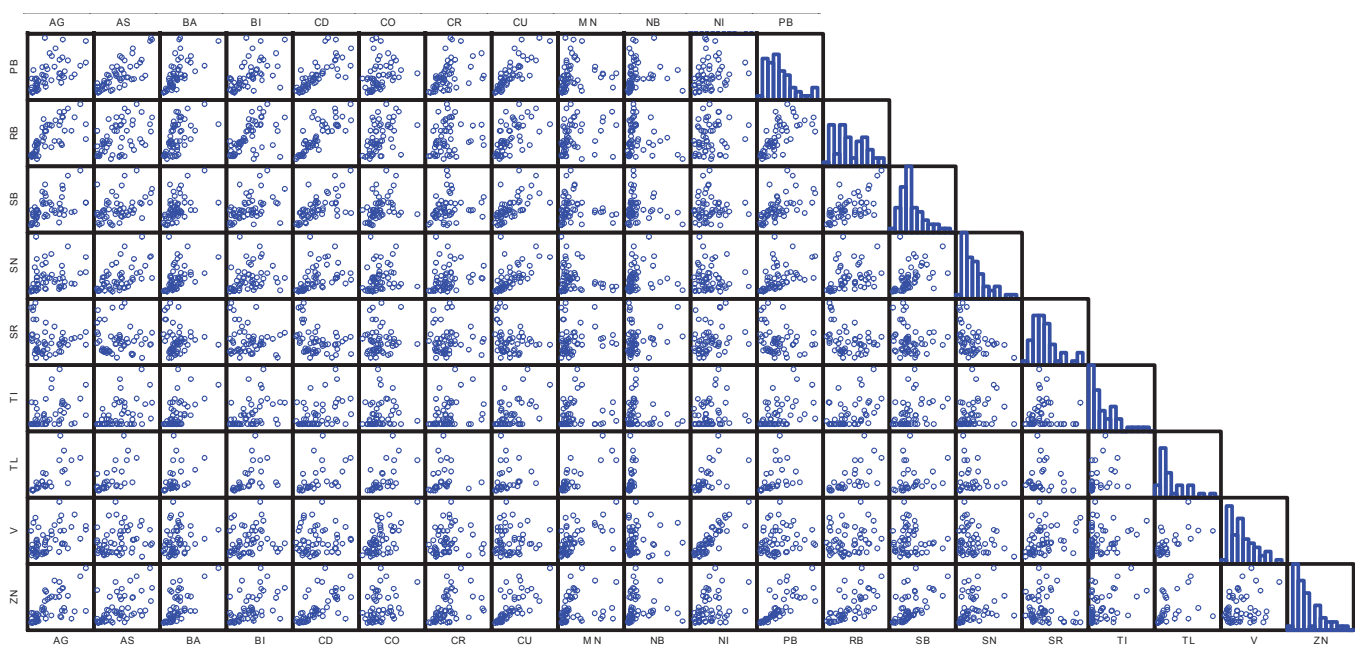
PP Scatter Plot matrix (P) of TE correlations

Dunkerque winter TE matrix correlations graphs (part 1)¹

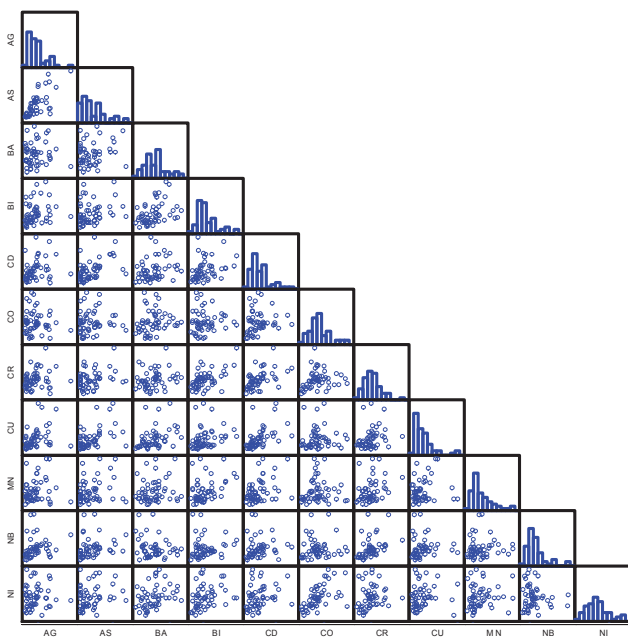


¹ The diagonal histograms represent the “Density histograms” which shows the number of samples (Y axis) versus their value range (X axis)

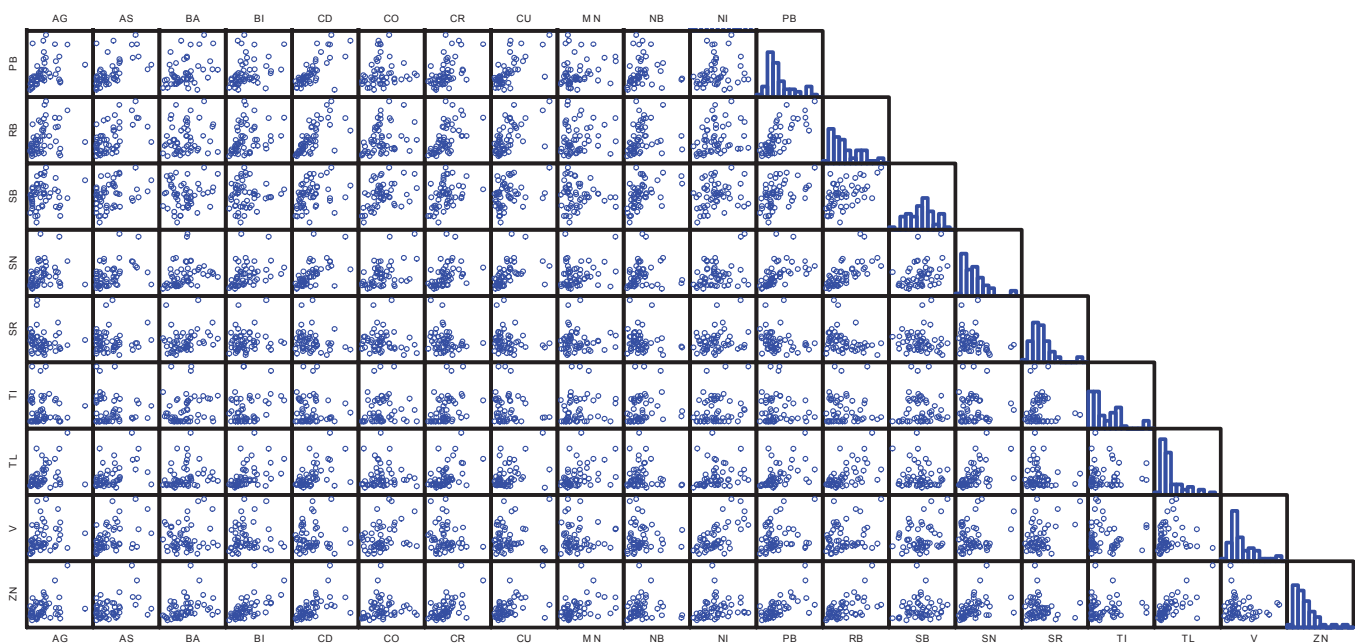
Dunkerque winter TE matrix correlations graphs (part 2)



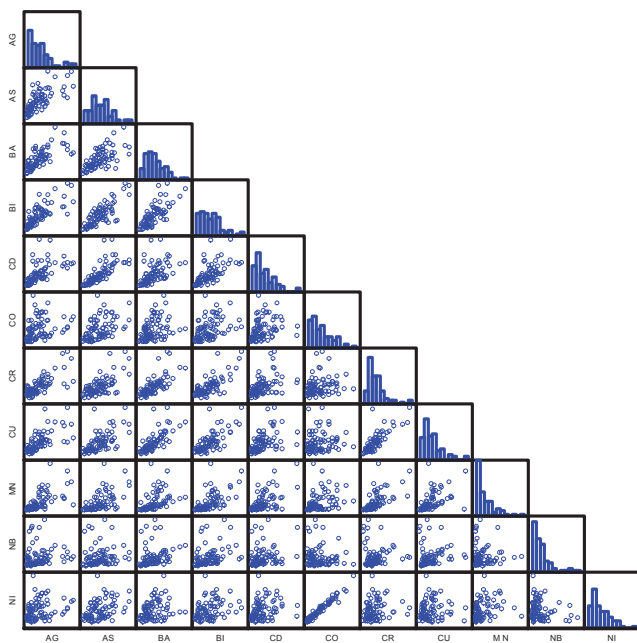
Boulogne-sur-Mer winter TE matrix correlations graphs (part 1)



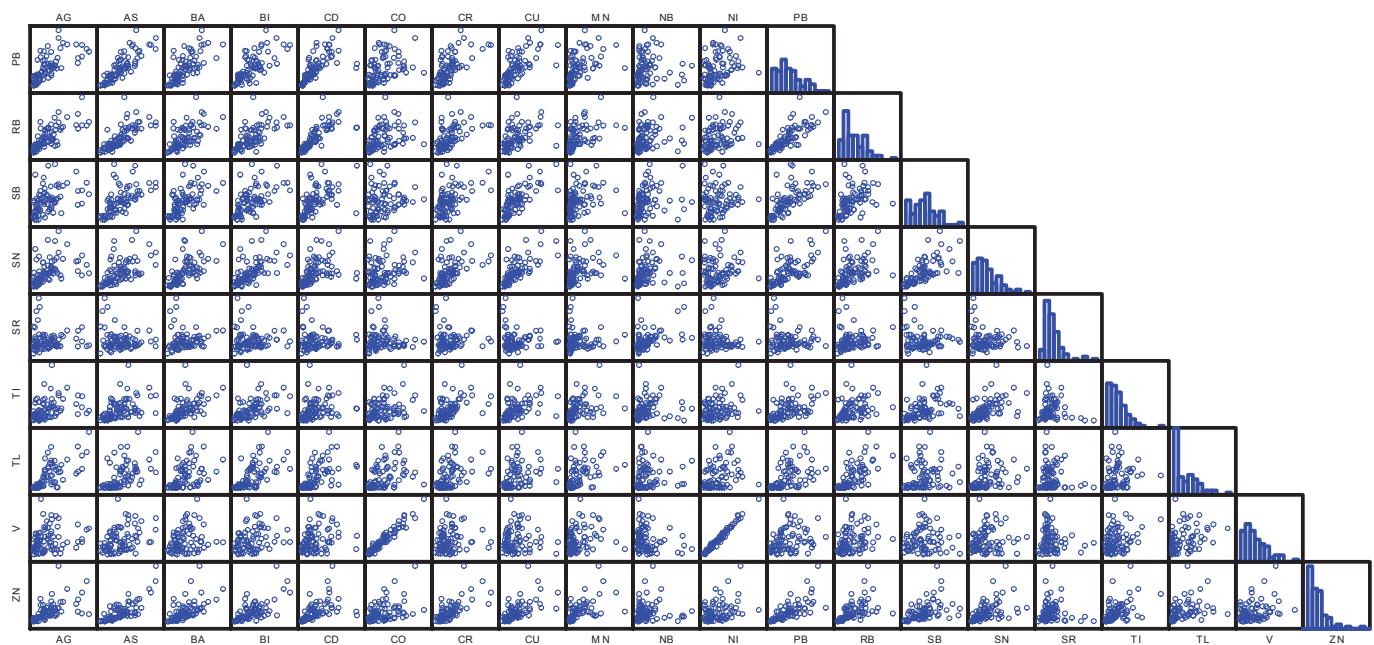
Boulogne-sur-Mer winter TE matrix correlations graphs (part 2)



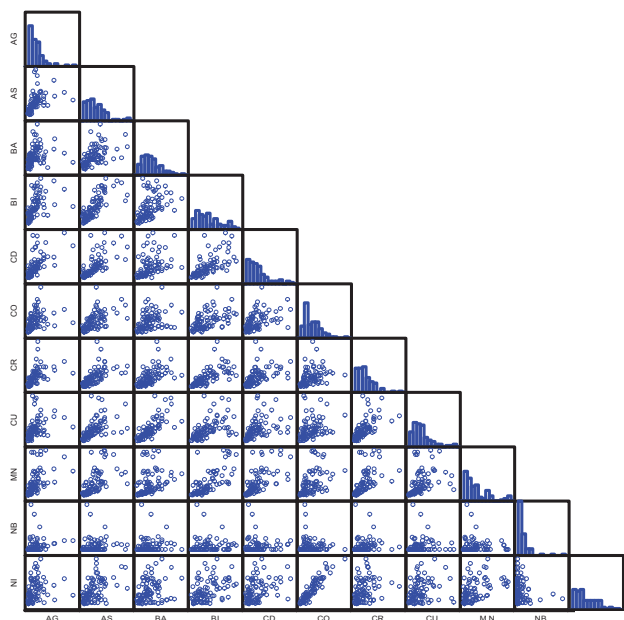
Dunkerque spring TE matrix correlations graphs (part 1)



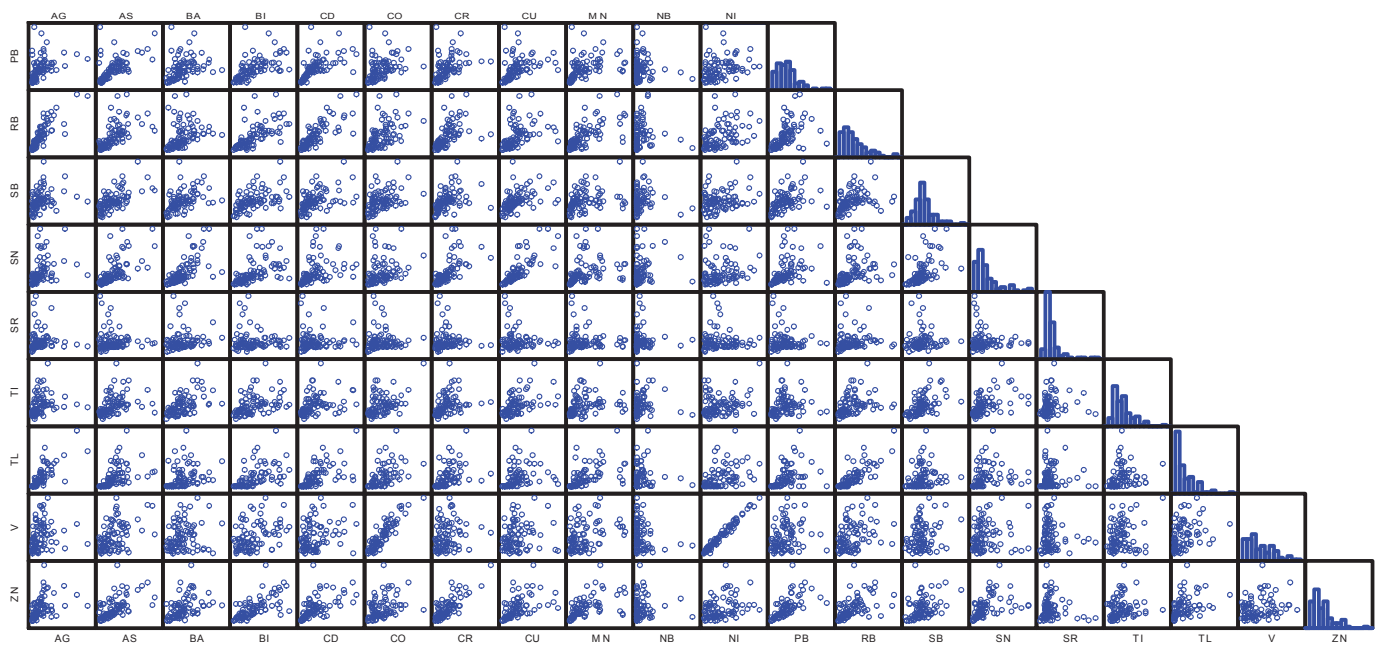
Dunkerque spring TE matrix correlations graphs (part 2)



Saint-Omer spring TE matrix correlations graphs (part 1)



Saint-Omer spring TE matrix correlations graphs (part 2)



PP matrix of TE correlation coefficients

Dunkerque winter TE correlation coefficient matrix²

	g	s	a	i	d	o	r	u	n	b	i	Pb	b	b	n	r	Ti	Tl		n
g	1																			
s		1																		
a			1																	
i				1																
d					1															
o						1														
r							1													
u								1												
n									1											
b										1										
i											1									
Pb												1								
b													1							
b														1						
n															1					
r																1				
Ti																	1			
Tl																		1		
																			1	
n																				1

²The coefficient represented in this matrix is equal to the square of Pearson correlation coefficient

Boulogne-sur-Mer winter TE correlation coefficient matrix

	g	s	a	i	d	o	r	u	n	b	i	Pb	b	b	n	r	Ti	Tl		n
g	1																			
s	0.40	1																		
a	0.41	0.41	1																	
i		0.40	0.19	1																
d		0.40	0.01	0.11	1															
o		0.01	0.01	0.00	0.00	1														
r	0.091	0.004	0.004	0.000	0.001	0.011	1													
u	0.190	0.400	0.140	0.000	0.090	0.000	0.000	1												
n	0.000	0.019	0.001	0.140	0.140	0.010	0.100	0.009	1											
b	0.000	0.004	0.009	0.000	0.009	0.041	0.109	0.044	0.000	1										
i	0.000	0.400	0.119	0.000	0.004	0.040	0.000	0.000	0.000	0.000	1									
Pb	0.100	0.001	0.100	0.104	0.090	0.000	0.009	0.400	0.044	0.000	0.000	1								
b	0.104	0.000	0.009	0.000	0.409	0.000	0.004	0.004	0.019	0.004	0.001	0.040	1							
b	0.000	0.110	0.094	0.009	0.094	0.100	0.1499	0.000	0.000	0.000	0.040	0.000	0.009	1						
n	0.044	0.104	0.001	0.100	0.040	0.000	0.100	0.000	0.009	0.009	0.094	0.000	0.400	0.109	1					
r	0.009	0.000	0.000	0.011	0.000	0.000	0.000	0.000	0.000	0.000	0.040	0.040	0.104	0.001	0.009	1				
Ti	0.000	0.004	0.004	0.000	0.009	0.000	0.109	0.004	0.004	0.000	0.000	0.000	0.000	0.001	0.000	0.000	1			
Tl	0.100	0.000	0.009	0.009	0.001	0.004	0.104	0.104	0.100	0.004	0.009	0.000	0.000	0.000	0.009	0.000	0.000	1		
	0.000	0.100	0.000	0.009	0.000	0.004	0.009	0.009	0.000	0.000	0.000	0.040	0.040	0.099	0.000	0.000	0.000	0.000	1	
n	0.100	0.100	0.109	0.000	0.000	0.0091	0.000	0.004	0.140	0.000	0.000	0.440	0.000	0.000	0.104	0.000	0.000	0.000	0.004	1

Dunkerque spring TE correlation coefficient matrix

	g	s	a	i	d	o	r	u	n	b	i	Pb	b	b	n	r	Ti	Tl		n
g	1																			
s		1																		
a			1																	
i				1																
d					1															
o						1														
r							1													
u								1												
n									1											
b										1										
i											1									
Pb												1								
b													1							
b														1						
n															1					
r																1				
Ti																	1			
Tl																		1		
																			1	
n																				1

Saint-Omer spring TE correlation coefficient matrix

	g	s	a	i	d	o	r	u	n	b	i	Pb	b	b	n	r	Ti	Tl		n
g	1																			
s	0.90	1																		
a	0.44	0.19	1																	
i	0.49	0.11	0.19	1																
d	0.99	0.49	0.11	0.44	1															
o	0.11	0.44	0.11	0.99	0.44	1														
r	0.00	0.00	0.94	0.41	0.49	0.11	1													
u	0.14	0.91	0.01	0.91	0.00	0.99	0.90	1												
n	0.00	0.00	0.94	0.00	0.40	0.01	0.00	0.19	1											
b	0.44	0.00	0.01	0.01	0.01	0.01	0.01	0.01	0.00	1										
i	0.91	0.44	0.00	0.14	0.14	0.00	0.00	0.19	0.00	0.99	1									
Pb	0.10	0.00	0.11	0.09	0.00	0.10	0.01	0.10	0.19	0.00	0.01	1								
b	0.00	0.04	0.99	0.40	0.00	0.00	0.00	0.14	0.41	0.00	0.01	0.00	1							
b	0.90	0.41	0.00	0.00	0.41	0.10	0.14	0.00	0.91	0.04	0.90	0.01	0.14	1						
n	0.10	0.41	0.40	0.40	0.10	0.90	0.00	0.40	0.00	0.00	0.01	0.10	0.01	0.91	1					
r	0.01	0.90	0.01	0.00	0.00	0.00	0.01	0.00	0.00	0.04	0.00	0.00	0.04	0.00	0.01	1				
Ti	0.09	0.10	0.04	0.10	0.10	0.10	0.10	0.00	0.40	0.01	0.00	0.99	0.11	0.40	0.40	0.09	1			
Tl	0.04	0.00	0.00	0.94	0.41	0.04	0.01	0.19	0.00	0.00	0.10	0.10	0.09	0.00	0.00	0.00	0.01	1		
	0.00	0.04	0.04	0.10	0.90	0.01	0.44	0.01	0.149	0.00	0.90	0.494	0.10	0.09	0.09	0.44	0.00	0.14	1	
n	0.10	0.09	0.00	0.419	0.01	0.10	0.00	0.94	0.40	0.09	0.119	0.40	0.44	0.19	0.00	0.00	0.49	0.19	0.00	1

résumé :

Les objectifs principaux de cette étude étaient d'acquérir une meilleure connaissance des niveaux d'exposition aux particules fines PM_{10} , de leur composition chimique et de leurs sources, dans trois villes situées sur la façade littorale de la région du Nord-Pas-de-Calais. Les particules fines ont été collectées dans le cadre de deux campagnes d'échantillonnage menées entre novembre 2010 et avril 2011 (campagne 'hiver' à Dunkerque et Boulogne-sur-Mer et campagne 'printemps' à Dunkerque et Saint-Omer). La composition chimique des PM_{10} a été déterminée suite à la quantification d'éléments majeurs, d'éléments traces, d'ions hydrosolubles et du carbone total. Pour les deux périodes considérées, les concentrations et la composition chimique en PM_{10} évoluent en suivant les mêmes tendances sur chacun des sites, l'influence de sources locales a été mise en évidence en comparant l'évolution temporelle et les roses de concentration de certains éléments majeurs et éléments traces, d'un site à l'autre. Cette exploitation a permis de proposer des rapports spécifiques entre éléments, qui peuvent être utilisés comme traceurs de certaines sources anthropiques. Enfin, l'application d'un modèle source-récepteur, basé sur la factorisation matricielle non négative (NMF), a permis d'identifier les sources principales des PM_{10} , d'évaluer leur contribution et leur part relative au niveau de chacun des sites étudiés.

abstract :

The main objectives of this study were to acquire a better knowledge on the exposure level to fine PM_{10} particles and on their chemical composition and sources, in three cities located on the littoral facade of the Nord-Pas-de-Calais region. The particles were collected following two sampling campaigns held between November 2010 and April 2011 ("winter" campaign in Dunkerque and Boulogne-sur-Mer; "spring" campaign in Dunkerque and Saint-Omer). The chemical composition of the collected PM_{10} was determined through the quantification of major elements, trace elements, water soluble ions and total carbon. For the two considered sampling periods, PM_{10} concentrations and chemical composition trends followed similar tendencies at each site. Local sources influence was evidenced throughout a comparison of the chronological evolution and concentration roses of some major and trace elements between the sites. This analysis allowed the suggestion of specific elemental ratios, which can be used as tracers of some anthropogenic sources. Finally, the use of a source-receptor model, based on a non-negative matrix factorization (NMF) method, allowed the identification of the main PM_{10} sources as well as the evaluation of their relative contributions in each of the studied sites.